

**ENHANCING THE FIXATION OF MASSIVE
IMPLANTS USING BONE MARROW
STROMAL CELLS**

BY

PRIYA KALIA

**SUBMITTED FOR THE DEGREE OF DOCTOR OF
PHILOSOPHY IN THE UNIVERSITY OF LONDON**

MAY 2007

CENTRE FOR BIOMEDICAL ENGINEERING

**UNIVERSITY COLLEGE LONDON MEDICAL SCHOOL
ROYAL NATIONAL ORTHOPAEDIC HOSPITAL TRUST
BROCKLEY HILL
STANMORE, MIDDLESEX
HA7 4LP
UNITED KINGDOM**

UMI Number: U592070

All rights reserved

INFORMATION TO ALL USERS

The quality of this reproduction is dependent upon the quality of the copy submitted.

In the unlikely event that the author did not send a complete manuscript and there are missing pages, these will be noted. Also, if material had to be removed, a note will indicate the deletion.



UMI U592070

Published by ProQuest LLC 2013. Copyright in the Dissertation held by the Author.
Microform Edition © ProQuest LLC.

All rights reserved. This work is protected against
unauthorized copying under Title 17, United States Code.



ProQuest LLC
789 East Eisenhower Parkway
P.O. Box 1346
Ann Arbor, MI 48106-1346

Table of Contents

ACKNOWLEDGEMENTS	8
LIST OF FIGURES	10
LIST OF TABLES	16
CHAPTER ONE	17
1.1 Aims of Project	18
1.2 Massive Endoprosthetic Replacements	18
1.3 Stem Cells	33
1.3.1 Definition	33
1.3.2 Autologous, Allogeneic and Xenogenic Cells, and the Multipotency of Stem Cells: Definitions	33
1.3.3 Bone Marrow Stromal Cells (BMSCs)	34
1.3.3.1 Previous characterisation of BMSCs	38
1.3.3.2 Proliferation rate of BMSCs	40
1.3.3.3 Immunogenetic properties of BMSCs	40
1.3.4 Haematopoietic Stem Cells (HSCs)	42
1.3.5 Embryonic Stem Cells (ESCs)	43
1.3.6 Other sources of stem cells-Peripheral Blood Stromal-like Cells (PBSCs)	45
1.4 Tissue Engineering	46
1.4.1 Introduction	46
1.4.2 Scaffolds	47
1.4.3 Fibrin Glue	48
1.4.4 The use of BMSCs in the tissue engineering of bone	52
1.4.5 Growth factors: Cytokines to target bone formation and revascularisation	56
1.5 Goals	58
CHAPTER TWO	60
2.1 Introduction	61
2.2 Methods	64
2.2.1 Isolation, Culture, and Expansion of oBMSCs	64
2.2.1.1 Anaesthesia and Pre-Operative Preparation	64
2.2.1.2 Procedure for Bone Marrow Aspiration	65
2.2.1.3 BMSC Isolation and Expansion	65
2.2.2 Characterisation of Ovine Bone Marrow Stromal Cells-Differentiation	67
2.2.2.1 Osteogenic Differentiation	67
2.2.2.2 Adipogenic Differentiation:	68
2.2.2.3 oBMSC Passage Number	69
2.2.2.4 Negative Controls	69
2.2.3 Histology-Osteogenesis	69
2.2.3.1 Von Kossa Assay	69
2.2.3.2 ALP quantitative biochemical assay (Cobas Bio)	70
2.2.3.3 Scanning Electron Microscopy (SEM)	72
2.2.3.4 X-ray detection using Electron Dispersive Analysis of X-Rays (EDAX)	72
2.2.3.5 Alamar Blue Activity Assay	73

2.2.3.6	Thymidine-H ³ Cell Proliferation Assay	74
1.3.7	Histology-Adipogenesis	75
2.2.4	Statistics	75
2.3	Results	76
2.3.1	oBMSCs-Observations	76
2.3.1.1	Colony-forming units-fibroblastic (CFU-Fs)	76
2.3.2	Osteogenesis	77
2.3.2.1	Von Kossa assay-Visual Observation and Qualitative Analysis	77
2.3.2.2	ALP Biochemical Assay	79
2.3.2.3	SEM and EDAX of nodules formed during osteogenesis of oBMSCs and HaCats	82
2.3.2.4	Cell Activity During Osteogenesis – Alamar Blue Assay	87
2.3.2.5	Cell Proliferation During Osteogenesis – Thymidine-H ³ Radioassay	88
2.3.3	Adipogenesis	89
2.3.3.1	Oil Red 'O' Stain	89
2.4	Discussion	90
CHAPTER THREE		101
3.1	Introduction	102
3.2	Materials and Methods	106
3.2.1	Part I: Induced Blood Loss	106
3.2.1.1	Experimental Layout	106
3.2.1.2	Anticoagulants	108
3.2.2	Plating Cells For Counting CFU-Fs	108
3.2.3	Statistics	109
3.2.4	Part II: Effects of G-CSF Treatment	109
3.2.4.1	Experimental Layout	109
3.2.5	Plating for CFU-F Counting and Culture	110
3.2.6	Characterisation of PBSCs	111
3.2.6.1	Chondrogenic differentiation:	111
3.2.6.2	Alician Blue and Sirius Red Histochemistry	112
3.2.7	Statistics	112
3.3	Results	113
3.3.1	Part I: The Effect of Induced Blood Loss on PBSC Mobilisation and Isolation	113
3.3.1.1	Formation of CFU-F	113
3.3.1.2	CFU-F Counts In Blood And Bone Marrow Aspirate Samples	113
3.3.2	Part II: The Effects of G-CSF Treatment on the Isolation and Mobilisation of PBSCs	116
3.3.2.1	CFU-F and Cell Morphology	116
3.3.3	CFU-F Formation At 7 and 14 Days	118
3.3.4	Characterisation of Culture-Expanded PBSCs	122
3.3.4.1	Osteogenesis	122
3.3.4.2	Adipogenesis	125
3.3.4.3	Chondrogenesis	126
3.4	Discussion	127
CHAPTER FOUR		133
4.1	Introduction	134
4.2	Methods and Materials	137
4.2.1	Suspension of oBMSCs in fibrin glue	137
4.2.2	Spraying oBMSCs in fibrin glue and fibrin-cell plug formation	138

4.2.3	The effect of fibrin glue on oBMSC viability, metabolism, proliferation, and morphology when applied using a spray or cannula	139
4.2.3.1	Viability	139
4.2.3.2	Metabolic Activity	140
4.2.3.3	Proliferation	140
4.2.3.4	Morphology and distribution of oBMSCs in fibrin glue plugs	141
4.2.4	The effect of thrombin concentration on oBMSC activity	141
4.2.5	Data analysis	142
4.3	Results	142
4.3.1	The effect of fibrin glue on oBMSC viability, metabolism, proliferation and morphology when applied using a spray or cannula	143
4.3.1.1	Viability	143
4.3.1.2	Cell metabolism	146
4.3.1.3	Proliferation	147
4.3.2	Morphology and distribution of oBMSCs in fibrin glue	149
4.3.3	Testing the effect of thrombin concentration on oBMSC activity using the Alamar Blue assay	150
4.4	Discussion:	151
CHAPTER FIVE		156
5.1	Introduction	157
5.2	Materials and Methods	159
5.2.1	oBMSC Isolation and Expansion	159
5.2.2	Preparation of BMSCs in Fibrin Glue	159
5.2.3	Implant Design and Manufacture	159
5.2.4	Experimental Groups	161
5.2.5	Surgical Procedure	161
5.2.6	Radiography and Radiographic Analysis	165
5.2.7	Undecalcified Hard Resin Histology and Analysis	166
5.2.7.1	Bone Area	167
5.2.7.2	Bone-Implant Contact	167
5.2.7.3	Bone Porosity Measurement	167
5.2.7.4	Fibrous Tissue Measurement	168
5.2.8	Statistics	168
5.3	Results	169
5.3.1	Radiography	169
5.3.1.1	Bone Area	172
5.3.1.2	Pedicle Gap Lengths	173
5.3.2	Histological Analysis	176
5.3.2.1	Bone Area	176
5.3.2.2	Histology: Bone - Implant Contact	184
5.3.2.3	Bone Porosity Measurement	185
5.3.3	Percentage of Fibrous Tissue Adjacent To Implant Collars	186
5.4	Discussion	187
5.5	Conclusion	194
CHAPTER SIX		195
6.1	Introduction	196
6.2	Materials and Methods	198

6.2.1	oBMSC Isolation and Expansion	198
6.2.2	Implant Design and Manufacture	198
6.2.3	Cell Dosages	198
6.2.4	Preparation of BMSCs in Fibrin Glue	199
6.2.5	Surgical Procedure	199
6.2.6	Radiography and Radiographic Analysis	201
6.2.7	Undecalcified Hard Resin Histology and Analysis	202
6.2.8	Statistics	202
6.3	Results	203
6.3.1	Radiographic Analysis	203
6.3.2	Histology	206
6.3.2.1	New Bone Formation	206
6.3.2.2	Bone-Implant Contact	210
6.4	Discussion	211
CHAPTER SEVEN		217
7.1	Future Work	227
REFERENCES		229
APPENDIX		277
Publications & Papers		278

Abstract

Previous studies have shown that increased bone growth over massive prosthesis, promoted by hydroxyapatite (HA)-coated collars, can reduce aseptic loosening. Bone tissue engineering techniques using bone marrow stromal cells (BMSCs) may be able to further enhance bone growth and fixation of implants to host bone. **The hypothesis of this study was that BMSCs could enhance bone growth and bone-implant contact around bone tumour replacements.**

Two sources of bone marrow stem cells were firstly investigated, including those isolated directly from ovine bone marrow (BMSCs), and those isolated from ovine peripheral blood (peripheral blood-derived bone marrow stromal-like cells, or PBSCs). PBSCs were isolated after mobilisation via induced blood loss, or treatment with granulocyte-colony stimulating factor (G-CSF). BMSCs and PBSCs were characterised *in vitro*. A significant increase of fibroblastic colony-forming units (CFU-F) post-G-CSF treatment was observed only after white blood cell counts returned to normal levels, suggesting a possible steady-state balance between haematopoietic stem cells and BMSCs.

Ovine BMSCs (oBMSCs), were found to survive and proliferate in fibrin glue or pressurised spray application.

An *in vivo* mid-shaft tibial replacement model was then used to test the effect of autologous oBMSCs in fibrin glue on bone growth and bone-implant contact, when sprayed onto the HA-coated collars, compared to non-treated implants. Radiography showed that the oBMSCs more than doubled the amount of bone growth around the collars of the implants after six months ($p=0.017$ in the ML view, and $p=0.05$ in the AP view). Using histological techniques

it was shown that bone area was significantly increased ($p=0.02$). Application of oBMSCs also reduced the radiolucent lines present between the new bone and implants, and improved bone-implant contact. This study demonstrated the potential of BMSCs to augment bone growth and bone-implant contact in conjunction with massive implants.

The second *in vivo* study investigated the effect of BMSC cell dosage and use of allogeneic cells on new bone formation and bone-implant contact in a tibial transcortical pin model in sheep. Partially-HA-coated screws were sprayed with varying concentrations of autologous and allogeneic oBMSCs suspended in fibrin glue, and implanted. After six weeks, no significant difference in bone formation around the pins was found between groups ($p>0.05$), although the untreated group with HA coating-only had a significant increase in bone formation ($p=0.03$) compared to the other groups.

In conclusion, this project has shown that ovine multipotent BMSCs and PBSCs can be isolated and expanded. When sprayed onto the HA-coated collars of massive implants, BMSCs can augment bone formation and bone-implant contact. However, another model spraying oBMSCs onto trans-cortical pins did not produce a significant increase in bone growth or bone-implant contact. The findings presented may have important clinical applications in the use of BMSCs to reduce aseptic loosening, which may improve the survival of massive implants.

Acknowledgements

I have been extremely fortunate to be surrounded by a team of very intelligent, dedicated, and caring individuals at the Institute of Orthopaedics and Musculo-Skeletal Science, as well as friends and family, who have all contributed towards the final form of this thesis in some way. “No man is an island” is one of my favourite quotes, and it has been proven to be true many times throughout my PhD.

First, I would like to acknowledge the supervision, guidance and support of my main supervisor, Professor Gordon Blunn, who has been an inspiration to me as a scientist and an engineer, and who has also been very understanding and kind. I would also like to thank Dr. Melanie Coathup, who also patiently helped guide me through my PhD, and has offered many practical words of wisdom, whether in times of enthusiasm or frustration.

Much thanks are due to the staff of the Institute of Orthopaedics and the Centre for Biomedical Engineering, especially Annie Bartram, Josie Marshall, and Rebecca Porter for their priceless assistance, consultation, and support. Thank you also Mark Harrison and Keith Rayner, for your endless help in the workshop, and putting up with my severe lack of technical knowledge. I would also like to give a warm thanks to Gillian Hughes and Lana Capon, who have been a big help to me during my work at the Royal Veterinary College, for the thoughtfulness and organization which has saved me countless times. From “two nations, divided by a language,” we may be, but I believe that homemade flapjacks transcend such differences!

I would like to thank the many friends who have seen me through the ups and downs of a hyperactive Canadian, and have enriched my life with their unique characters. Many thanks

to Michelle, Darren, Alicia, Lisette, Ben, Jen, and Richard for being there and helping an international student have a social life! Thanks also to my sisters, Rohini and Kamini, for always being there, as well as my honorary sister, Novdeep, and my aunt Mala.

Lastly, this thesis is dedicated to my parents, Raji and Ramesh Kalia, who have been my constant (if at times) long-distance, moral, emotional, and academic supports. Thank you very, very much – this is for you.

List of Figures

Figure 1.1. Example of a proximal tibial bone tumour replacement. The implant has proximal (top) and distal (bottom) cemented intramedullary stems (Cannon 1997).	20
Figure 1.2 a) Diagram demonstrating the line of force through the femur, which has a decreasing offset with the axis of the femur as it moves distally; b) illustration of how this offset affects a proximal femoral replacement and c) a distal femoral replacement (adapted from Unwin et al. 1996, p 11).	24
Figure 1.3 Radiograph of the proximal end of a massive implant, illustrating radiolucent lines that indicate aseptic loosening.	25
Figure 1.4 Photographs of hydroxyapatite (HA)-coated collars from a) a proximal tibial replacement and b) a massive implant with an HA-coated collar being implanted.	31
Figure 1.5 Photo of human bone marrow stromal cells (BMSCs; from P. Kalia).	35
Figure 1.6 Photograph showing a colony of H9 human embryonic stem cells (within circle; used with permission from Dr. M. Clements, University of Westminster, 2006).	43
Figure 1.7 a) Components of Tisseel fibrin glue; b) Reflection electron microscopy (REM) image photograph of Tisseel fibrin glue (scale 1:6000, used by permission from Baxter Biosurgery, USA).	50
Figure 1.8 Fibrin glue sprayed using pressurised air (Baxter Biosurgery, USA. Used with permission).	51
Figure 2.1 oMSCs after passage. Cells are flat, spindle-shaped in morphology, with large nuclei that have multiple, prominent nucleoli (see black arrows). The processes of some cells can be seen to be in contact (see white arrows).	76
Figure 2.2 Results of Von Kossa staining (10x magnification). Images d, f, and h are low-passage ovine BMSCs, high-passage ovine BMSCs and HaCats, respectively, that were fixed and stained after being grown in osteogenic culture media for 28 days. Figures c, e, and g are negative controls of low-passage BMSCs, high-passage BMSCs, and HaCats (respectively), grown in non-supplemented DMEM+ for 28 days. Images a and b are low-passage ovine BMSCs that were treated with 5% acetic acid before staining to create a negative calcium control. Nodules of calcium mineral are stained black with the Von Kossa stain, and are indicated with arrows.	78
Figure 2.3 Graphs illustrating ALP biochemical assay results at 7, 14, 21, and 28 days after culture in osteogenic media. The cell lines tested include a) low-passage oBMSCs (P ₃); b) high-passage oBMSCs (P ₁₂); c) goat BMSCs (P ₄); d) HaCats (transformed keratinocytes) and e) LG3 cell line (leukaemic monocytes).	82
Figure 2.4 SEM photographs (1500x magnification) showing the area scanned for EDAX analysis, as well as the EDAX results presented in graphical form, showing peaks for all notable elements, such as carbon, oxygen, phosphate, and calcium. Ca/P ratios are also shown, although some samples did not show calcium or phosphate content. A) shows BMSCs grown in standard DMEM; b) are BMSCs grown in osteogenic media; c) are HaCats grown in standard DMEM+; and d) are HaCats grown in osteogenic media.	84
Figure 2.5 SEM photographs of cell lines after 28 days in osteogenic media. a) and b) are oBMSCs at 230x and 600x magnification, respectively. HaCat cell lines are shown in c) and d), at 200x and 1000x magnification, respectively.	86
Figure 2.6 Chart showing Alamar Blue™ absorbency over a 28-day period in oBMSCs grown in standard (DMEM+) and osteogenic medium.	88

Figure 2.7 ³ H-thymidine incorporation assay results, over 24, 48, and 72 hours. The two groups tested were cells grown in DMEM+, and cells grown in DMEM+ with osteogenic supplement, expressed in Bq/μg DNA.	89
Figure 2.8 a) oBMSCs grown for 14 days in standard DMEM+ medium, fixed and stained with the Oil Red 'O' for lipids and Harris' Haemotoxylin (counterstain) (10x magnification); b) oBMSCs grown for 14 days in osteogenic medium and similarly stained (20x magnification). Arrows point at the positively stained lipids (red).	90
Figure 3.1 Flowchart depicting the experimental layout testing the effects of induced blood loss (7% and 15%) on the mobilisation of BMSCs into the peripheral blood. The experiment consisted of pre-bleeding blood and bone marrow samples being taken, followed by either 7% or 15% blood loss one week later. One week post-blood loss, further blood and bone marrow samples were taken, for cell culture and haematological analysis.	107
Figure 3.2 Flowchart illustrating the experimental design to test the effects of G-CSF on BMSC release into the bloodstream. Firstly, blood samples were taken for haematological analysis. Sheep with normal "within range" results were then administered G-CSF at 5 μg/kg, for five days. Blood samples were then taken 4, 12, 24 and 336 hours after G-CSF treatment, and cultured for CFU-F counting.	110
Figure 3.3 Photo of CFU-F after 14 days of culture, isolated after 7% blood loss (4x magnification).	113
Figure 3.4 Graph illustrating results of CFU-F counting of cells isolated from the peripheral blood under normal conditions (pre-treatment), and after 7% and 15% blood loss. CFU-F counts at 7, 11, and 14 days are shown.	114
Figure 3.5 Means of CFU-F counts of cells isolated from the bone marrow before blood loss, 7 days post-7% blood loss, and 7 days post-15% blood loss.	115
Figure 3.6 Photos of cells isolated from the peripheral blood after G-CSF treatment. a) shows a typical CFU-F observed after 5 days of culture (20x magnification); b) a CFU-F after 7 days of cell culture (20x magnification); c) shows cells at 95% confluence, (20x magnification). D) is a photo of adherent cells that are not fibroblastic in morphology and did not proliferate in CFU-F. These cells appeared spread out and senescent (see arrows, 40x magnification). E) shows non-proliferative, small adherent cells round in morphology (40x magnification); f) is a photograph of proliferative, cuboidal cells that grew to confluence and had a less circular organisation to the observed typical-looking CFU-F (40x magnification).	117
Figure 3.7 Line graph illustrating the number of CFU-F grown from peripheral blood samples before G-CSF treatment, and 4, 12, and 336 hours (2 weeks) after G-CSF treatment.	119
Figure 3.8 Graph comparing the WBC levels to CFU-F counts over 336 hours post-G-CSF treatment. As WBC levels dropped back to normal values, the CFU-F counts significantly increased. When time, WBC levels and CFU-F counts were correlated, this was found not to be significant (p>0.05).	122
Figure 3.9 Photos of cells stained using the Von Kossa method after 28 days in culture in DMEM+, with or without osteogenic supplements (b and a, respectively). Examples of mineralised areas are indicated with arrows.	123
Figure 3.10 SEM images of PBSCs after 28 days in culture with or without osteogenic supplements (b and a, respectively). Nodules can be seen in the osteogenic culture; however, both samples tested positive for the presence of calcium and phosphate. This can be seen in the peak graphs alongside the SEM images. The Ca/P ratios differed between the two groups and have been noted.	124

Figure 3.11 Photos showing results of Oil Red 'O' staining. PBSCs were either cultured in DMEM+ (a) or DMEM+ with adipogenic supplements (b) for 14 days, after which they were stained. A positive reaction, showing the presence of lipid vacuoles, can be seen in b), and is identified by a black arrow. A small positive reaction can be seen in a), indicated by a black arrow.	125
Figure 3.12 PBSC pellet after 21 days of culture in chondrogenic media, stained with Sirius Red (for collagen, red) and Alcian Blue (for GAG expression, blue). GAG-positive cells can be seen at the periphery of the pellet (see black arrows), as well as Sirius Red staining, which has penetrated deeper into the pellet (see white arrow).	126
Figure 4.1 Equipment used for spraying fibrin, including an air compressor and a pressure gauge, which is controlled by a foot pedal (see arrows).	138
Figure 4.2 An example of the sectional images obtained for the live/dead stain using confocal microscopy (20x magnification). In this example, all of the optical sections have been layered so that all cells in the fibrin gel can be visualised. The green cells are those stained positively with calcein AM (live), and is spread throughout the cell cytoplasm. Red cells are those stained with ethidium homodimer (red), which intercalates with nucleic acids and therefore is mostly visualised in the cell nuclei. A double labelled-cell is noted with arrows.	144
Figure 4.3 Chart indicating the percentage of live (Calcein AM positive) oBMSCs in fibrin glue after being ejected from a cannula or using a spray, at 0.5 Atm, 1.0 Atm, and 1.5 Atm. The total number of cells was calculated by dividing the number of live cells by the total number of live and dead (ethidium homodimer positive) cells.	145
Figure 4.4 Graph illustrating results of Alamar Blue™ assay, when oBMSCs in fibrin were either applied with a cannula or spray at 1 Atm. This assay, which is an indicator of cell activity, was tested just after application (Day 0), and at days 1, 2, 4, and 7 after application.	146
Figure 4.5 Bar graph comparing ³ H-thymidine incorporation (indicative of proliferation) between oBMSCs grown on tissue culture plastic, oBMSCs suspended in fibrin glue, and oBMSCs sprayed in fibrin glue, at 0-24 hours (24 hours), 24-48 hours (48 hours) and 48-72 hours (72 hours) after the initiation of culture.	148
Figure 4.6 Images of histological sections of oBMSCs embedded in fibrin glue and cultured for 2 weeks. Photos were taken at 10x magnification. oBMSCs can be seen along the periphery of the fibrin, indicated by arrows. Haemotoxylin (purple) stains cell nuclei, and eosin (pink) is the counterstain (probably fibrin glue). Around cells, the fibrin appears to be stretched or degraded.	149
Figure 4.7 Graph indicating oBMSC metabolic activity when suspended in different concentrations of fibrin, which was achieved by varying the thrombin concentration. Although at a lower density of fibrin (with the lowest thrombin concentration), the Alamar Blue™ absorption is lower than the other groups at day 1, 3 and 9. This difference was not statistically significant.	150
Figure 5.1 a) Photo of an ovine mid-shaft tibial replacement. The implants were made of titanium alloy and were comprised of two components, each of which had a grooved, HA-coated collar at the transection site, and an intramedullary stem. The two pieces were fixed in the centre with screws. b) shows a schematic diagram of the implant, showing the dimensions of the implant and the division between the two components, as well as the location of the thread holes.	160
Figure 5.2 a) After resection of soft tissue from the tibia 50 mm from the tibial tuberosity, an initial cut was made to the tibia; b) A 50 mm tibial segment with an intact periosteum, which was replaced with a massive implant.	162

Figure 5.3 HA-coated collar on distal segment of implant being spray-coated with oBMSCs suspended in fibrin glue, pre-implantation.	163
Figure 5.4 a) Distal implant (from untreated control group) component being cemented into intramedullary canal; b) Implant assembled in centre with screws, with oBMSCs in fibrin glue on HA-coated collars.	164
Figure 5.5 Sample radiograph (2×10^6 BMSCs/collar, ML view) divided into eight regions (A-H) for quantitative analysis of new bone formation adjacent to implants. The pedicle of bone grown along the length of the implant shaft is indicated with a white arrow. A radiolucent line between the pedicle of bone and the implant is shown with a black arrow.	166
Figure 5.6 An example of a photograph of bone adjacent to a control group distal collar with adjacent bone growth, onto which a grid has been overlaid for the quantification of bone porosity. Evaluation of porosity was made at each grid intersection point.	168
Figure 5.7 Radiographs of control (untreated and fibrin-glued treated) implants. (a-d) are radiographs from one untreated control animal, with ML radiographs taken at 2 (a), 3 (b) and 6 (c) months, and an AP radiograph taken at 6 months (d). Bone growth is marked (B), as well as radiolucent lines, which are demarcated with arrows. Photos are shown here at 0.9x of the actual size.	170
Figure 5.8 Radiographs of BMSC-treated implants (0.9x magnification). (a-d) are radiographs taken of the same animal treated with 2×10^6 BMSC/collar at 2 (a), 3 (b), and 6 (c and d) months, with (a-c) being taken in the ML view and (d) taken in the AP view. (e) and (f) are the ML and AP radiographs of another lower-BMSC dose animal, taken at 6 months. A larger cuff of new bone growing over the implants from the transection sites can be seen in these radiographs than with the controls seen in Figure 5.7. An even larger amount of bone can be seen proximally and distally in (g) and (h), which are the ML and AP views of an implant treated with 10×10^6 BMSCs/collar. New bone is marked with a "B," and radiolucent lines are indicated with arrows.	171
Figure 5.9 a) Results of radiological analysis over 2, 3, and 6 months, in the ML aspect. At each time point, there was a significant increase in the area of bone adjacent to the implants in the oBMSC-treated group, when compared to the control group. b) Comparison of bone area adjacent to implants in the ML and AP aspects at 6 months, in all four experimental groups. There was an increase in the amount of bone in the AP aspect when 5 times the number of oBMSCs were applied to the surface of implant collars.	174
Figure 5.10 Radiographic bone area results from the combined oBMSC-treated groups compared to the combined results of the two control (untreated and fibrin-only) groups.	174
Figure 5.11 Graphs showing the percentage of bone pedicle along implants with gaps (seen as radiolucent lines) between the implant and bone. a) shows the results of analysis in the AP view, and b) shows results of the ML view analysis.	175
Figure 5.12 Midsection through the proximal (a, c) and distal (b, d) HA-coated collars of control group specimens, stained with Toluidine Blue and Paragon. Bone formation (B) adjacent to the implant collars can be seen, along with fibrous tissue (F). A fibrous tissue layer was often found between the implant and new bone formation.	177
Figure 5.13 (a-d). Photos of thin, undecalcified, sections from 2.0×10^6 BMSC-treated group stained with Toluidine Blue and Paragon. Bone formation was observed around implant collars (distal and proximal). A larger, thicker, cuff of bone was found	

adjacent to the collars of BMSC-treated implants than in the control groups. Although a fibrous tissue layer was seen around some implant collars, between the bony layer and implant, this was seen less frequently than around control implants. _____	178
Figure 5.14 Lamellar bone (B) grown adjacent to a proximal HA-coated (HA) implant collar (I), which was treated with BMSCs in fibrin glue (2×10^6 BMSCs/collar). Haversian systems can be seen, as well as bone growth into the grooves of the collar and bone-implant contact (4x magnification). _____	179
Figure 5.15 Bone formation (B) around a control (untreated) implant collar (I). This layer of bone is thinner than that often observed with the BMSC-treated implants and is not in contact with the HA-coated implant surface. The HA-coating can be seen as a grey layer as indicated (HA, 4x magnification). _____	179
Figure 5.16 Bone growth into a BMSC-treated collar (2×10^6 BMSCs/collar, 10x magnification). Contact can be seen between the new bone and HA-coating of the implant collar. Haversian systems (H) can be seen surrounding the canals (black spots in photo- see encircled region). _____	180
Figure 5.17 BMSC-treated collar seen in Figure 5.16, at 40x magnification. Bone formation can be seen in contact with the HA-coating of the implant collar. In this photo, there is ingrowth of bone to the HA-coating (HA) and Haversian systems can be seen (H-white circled area). _____	180
Figure 5.18 Porous bone adjacent to implant collar, separated by a fibrous tissue layer. This photograph was taken at 5x magnification and is of a distal collar from the untreated control group. _____	181
Figure 5.19 Resorption pits along the outer edge of a low-BMSC dose treated proximal collar, taken at 10x magnification. Osteoclasts are prominent multinuclear cells, which are indicated with black arrows. _____	181
Figure 5.20 Comparison of bone area around the centre of implant collars, as measured using histological analysis. _____	183
Figure 5.21 A comparison of histological results, comparing proximal and distal collars between groups. _____	183
Figure 5.22 Bone-implant contact around implant collars in the untreated control, fibrin-only, low-concentration oBMSC group, and high-concentration oBMSC group. _____	184
Figure 5.23 Bar graph showing the mean percentage bone porosities in the four experimental groups. _____	186
Figure 5.24 Bar graph illustrating mean fibrous tissue lengths adjacent to implant collars. _____	187
Figure 6.1 Example of a transcortical screw used in study. The top segment was HA-coated and either left untreated, sprayed with fibrin glue-only, or a combination of fibrin glue and varying concentrations of BMSCs (1.0×10^5 - 1.0×10^7 cells/mL). ____	198
Figure 6.2 a) Diagram illustrating insertion of transcortical screw in bone. b) Distance of holes from tibial tuberosity (see top of diagram). _____	201
Figure 6.3 Graph showing normalised bone density in the gaps between the top half of the screws and the surrounding bone. The density was normalised based on the means of the surrounding cortical bone. _____	204
Figure 6.4 Photographs showing typical histological sections through the centre of the partly-threaded screws, taken at 4x magnification. a) shows a sample from an implant-only group specimen; b) shows a specimen from the fibrin-only group; c) shows some new bone formation around an implant treated with 1.0×10^6 cells/mL in fibrin glue; and d) shows a sample from the 10×10^7 cells/mL in fibrin glue. Old bone	

(present pre-operatively) is marked with an 'O', new bone with an 'N', fibrous tissue with an 'F', and HA with 'HA.'	206
Figure 6.5 Images of histological sections around the implants. a), c), d) and e) show new bone formation (N) which is continuous with the older cortical bone (O), but separated from the implant (I) by fibrous tissue layer (F). The threaded portion of the implant seen in b) shows contact with the surrounding older cortical bone.	207
Figure 6.6 Graph outlining the result new bone formation measurement in all six groups. The error bars represent standard error.	210
Figure 7.1 Flowchart outlining thesis – describing questions and methodology for chapters.	219

List of Tables

Table 1.1 Table outlining the Young's Modulus (measure of material stiffness) of biocompatible metals used for massive implants, and cortical and trabecular bone (adapted from "Orthopaedic Prosthesis Fixation," Park 1995, p 542). Note that titanium alloy has approximately 9 times the stiffness of cortical bone in the tangential aspect.	28
Table 1.2 Chart illustrating cells surface markers present and absent on human BMSCs (Baksh et al. 2003; Campagnoli et al. 2001; Pittenger et al. 1999; Watt 2006).	37
Table 2.1 a) Chart showing Alamar Blue™ absorbency over a 28-day period in oBMSCs grown in standard (DMEM+) and osteogenic medium. Cells grown in osteogenic medium had a higher cell activity than those grown in standard medium at all time points, $p < 0.05$ at all time points except day 3.	87
Table 3.1 Chart with results of CFU-F counts of cells isolated from the peripheral blood and bone marrow, before and after blood loss.	115
Table 3.2 Chart displaying CFU-F counts of cells isolated from peripheral blood samples, 7 and 14 days after the initiation of culture.	118
Table 3.3 Results of haematological analysis, of blood samples taken pre-G-CSF (n=6); 4 hours post-G-CSF (n=6); 12 hours post-G-CSF (n=6); 24 hours post-G-CSF (n=6) and 2 weeks post-G-CSF (n=3). Results were compared to normal "range" values, and abnormal results are highlighted (yellow). Blood was also processed for PBSC culture. Abbreviations: WBC = white blood cells; RBC = red blood cells; HGB = haemoglobin; RDW = PLT = platelets.	121
Table 4.1 Table showing the mean percentage and standard error of live cells in each group.	145
Table 4.2 Table showing Alamar Blue™ absorption measurements over the seven days.	147
Table 4.3 Table showing oBMSC proliferation for all groups at the three time points.	148
Table 4.4 Table of P-values between all three groups at each time point.	148
Table 6.1 Groups used in experiment, in the order they were placed in the first sheep.	199
Table 6.2 Mean density in cortical defect, as observed radiographically. Percentage density indicates the mean density of defect divided by the mean cortical density of the surrounding bone.	204
Table 6.3 p-values from the Wilcoxon non-parametric paired statistical test. Auto=autologous; allo=allogeneic.	205
Table 6.4 Results of new bone formation, measured using histology and image analysis, in all six groups.	209

CHAPTER ONE

INTRODUCTION

1.1 Aims of Project

This main goal of my thesis is to enhance the fixation of massive implants, using bone marrow stromal cells (BMSCs) in fibrin glue sprayed onto the surface of orthopaedic implants. In order to realise this goal, my work involved firstly the isolation, expansion, and characterisation of ovine BMSCs, as well as an investigation into stromal-like cells obtained from ovine peripheral blood, with or without blood loss or administration of a cytokine, granulocyte-colony stimulating factor (G-CSF). The viability and proliferation of ovine BMSCs in fibrin (sprayed and un-sprayed) was tested, as well as the ability of this system to enhance bone growth in conjunction with orthopaedic implants to prevent aseptic loosening. **The main hypothesis of this thesis is that viable BMSCs can be applied to orthopaedic implants using a fibrin glue-spray system, and increase bone formation adjacent to the implants and improve bone-implant contact.**

This introduction will first discuss bone tumour replacements and their failure due to aseptic loosening. Secondly an introduction to stem cells will be presented and the advantages of using bone marrow stromal cells (BMSCs), as well as the use of alternative sources to BMSCs, will be discussed. Thirdly, tissue engineering will be reviewed, specifically with regard to bone regeneration.

1.2 Massive Endoprosthetic Replacements

The majority of bone tumours are malignant, including osteosarcoma, Ewing's sarcoma or chondrosarcoma (Grimer et al. 1999; Morris et al. 1995). The main sites of bone tumour development include the humerus, scapula, radius, femur and tibia, with the majority of cases

occurring in the lower extremities (Cannon 1997). Giant cell tumours are often regarded as being benign, but can also potentially become malignant (Jewell and Bush 1964; Lewis et al. 1985). In the past, recurrence was a major issue. However, since the 1970's the survival rate of patients has improved significantly, as a result of early detection of tumours, as well as the increased use of chemotherapy, radiotherapy, and improved techniques of resection of the tumour surgically. (Capanna et al. 1994; Cannon 1997; Grimer et al. 1999; Horowitz et al. 1993). Adjuvant chemotherapy (given post-operatively) has reduced the probability of recurrence and/or metastases (Eckardt et al. 1991; Uchida et al. 1997).

Reconstruction of the segmental defect created during tumour excision, in order to preserve the limb, can use a variety of techniques: arthrodesis with auto/allograft; vascularized fibular graft, resection and reinsertion of bone after sterilization; and arthroplasty using either auto allograft, synthetic graft or massive endoprostheses, including extendible prostheses for growing patients (Schindler et al. 1997; Unwin et al. 1996). Although reconstructions using autograft are preferable, it is frequently difficult to obtain sufficient amounts for bone tumour resection sites. Donor site morbidity can be an issue (Abudu, Carter and Grimer 1996a). Allografts suffer similar problems in terms of supply, disease transfer from donor to patient, graft failure and fracture, as well as issues with non-union of the graft to the host bone (Gebhardt et al. 1991).

At present, the use of endoprosthetic replacements in limb-salvage is the principal alternative to amputation (Cannon 1997). This technique attempts to preserve both the function and aesthetics of the original limb, while allowing immediate post-operative weight bearing (Grimer et al. 1999). Studies have attempted to determine the long-term effects of amputation and endoprosthetic replacement on tumour recurrence, functionality of the limb post-

treatment, and patient satisfaction. Results showed that limb-salvage procedures result in the same rate of disease-free survival as amputations after 10 years, with no significant difference in patient satisfaction in most cases (Rougraff et al. 1994; Sugarbaker et al. 1982; Weddington et al. 1985). Some studies state a patient preference for limb salvage over amputation (Harris et al. 1990), and a study by Grimer et al. (1999) indicated that endoprosthetic reconstructions are more cost effective than amputation.

Massive implants for limb-salvage surgery are either custom-made or modular (Cannon 1997) and generally use stems that are cemented into the intramedullary canals with polymethylmethacrylate (PMMA; see Figure 1.1).

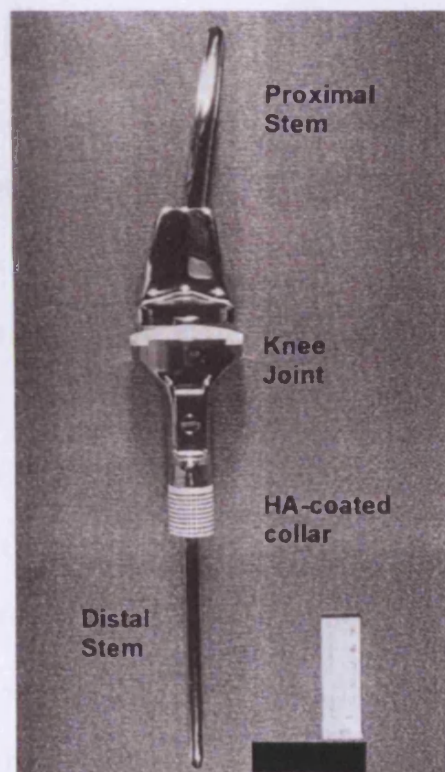


Figure 1.1. Example of a proximal tibial bone tumour replacement. The implant has proximal (top) and distal (bottom) cemented intramedullary stems (Cannon 1997).

Uncemented stems are also used (Blunn et al. 2000; Capanna et al. 1994). An alternative to the use of intramedullary stems is triplate fixation, where extracortical fixation can be used if there has been a large resection, and an insufficient amount of bone remains in which to cement an implant (Coathup et al. 2000; Cobb et al. 2005). Femoral or tibial endoprotheses can also include a knee joint replacement when the bone tumour has spread to the knee or there is possible contamination of the joint or synovium, and *en bloc* resection of the joint is required (Sim 1979a; Walker et al. 1981). However, when compared with the success of joint replacements, massive implants are not as successful (Blunn et al. 2000). The Swedish Hip Registry found that the survival rate of total hip arthroplasties (THAs) over a ten-year period was 92.5% (Malchau et al. 2005). By comparison, a ten-year follow up study of massive implants with cemented intramedullary stems found that 93.8% of proximal femoral, 67.4% of distal femoral and 58% of proximal tibial prostheses survived ten years (Unwin et al. 1996). Scales et al. (1984) investigated the causes of failure for Stanmore cemented massive implants in the 1980's and found that 5.4% of all endoprosthetic reconstructions resulted in infection, 2.7% resulted in implant fracture, and 1.9% failed due to aseptic loosening. Infection was reported to be more common in primary massive endoprosthetic replacements than with conventional joint replacements (Malawer and Chou 1995). Capanna et al. (1994) found that the infection rate of distal femoral replacements, using the Kotz modular femoral and tibial resection system (KMFTR) was highest when most or all of the rectus and vasti muscles had been excised (Capanna et al. 1994). Infection has been a major concern for proximal tibial replacements. Bradish et al. (1987) reported a 7.5% infection rate in distal femoral replacements; whereas Roberts et al. (1991) found that, in 135 distal femoral replacements, 6.8% of all implants suffered from infection, whereas 6% failed due to aseptic loosening. A study from the Royal Orthopaedic Hospital in Birmingham found that up to 33.8% of proximal tibial reconstructions performed between 1977 and 1988 became infected

within the first five years (Grimer et al. 1991). In 1995, Malawer and Chou (1995) reported a 31% rate of infection with proximal tibial replacements. Modern surgical techniques have reduced the overall infection rate suffered previously with this type of procedure. For example, in proximal tibial replacements, retention or replacement of lost musculature around the implant by use of a medial gastrocnemius flap has reduced the above-mentioned infection rate from 33% to 12% (Grimer et al. 1999). Improved surgical techniques that reduce incidences of infection and improved implant design have reduced the rate of implant fracture, so that aseptic loosening is now considered to be the major cause of failure of cemented massive implants (Ward et al. 1991).

As a result of adjuvant chemotherapy, there has been an increase in the number of young limb-salvage patients. This has affected the results of more recent studies, as the methods that were developed for salvaging low-grade lesions in older patients are now routinely used in younger, more active patients with wider resections for larger, more aggressive tumours. A study looking at distal femoral replacements, found that between 1959-1980, the survival of distal femoral replacements was $83 \pm 8\%$, whereas from 1980-1991, the survival was reduced to $64 \pm 27\%$ (Cobb 2002).

A study by Unwin et al. (1996) studied the outcome of 1001 patients with endoprosthetic replacement, mostly as a result of osteosarcoma, osteoclastoma, and chondrosarcoma. This report showed that, over a ten-year period, although 93.8% of proximal femoral replacements survived a ten-year period, only 67.4% of distal femoral replacements and 54.8% of proximal tibial implants survived. Seventy-one of the 1001 patients (7%) required implant revisions for aseptic loosening. The study also found that patients under 20 years of age with more than 60% of bone resected from the distal femur or proximal tibia had the worst prognosis for

implant survival. The amount of bone resected is also associated with failure in proximal tibial replacements (Unwin et al. 1996). The long-term study of implant loosening by Unwin et al. (1996) looking at 493 distal femoral, 263 proximal femoral and 245 proximal tibial replacements, found a high incidence of aseptic loosening.

Failure in the upper humeral prosthesis due to aseptic loosening is rare and is probably due to the lack of heavy weight bearing in that limb (Cannon 1997). Uncemented implants, using the Kotz system, did not appear to show similar levels of aseptic loosening, although there were some cases of implant fracture and infection (Capanna et al. 1994). Horowitz et al. (1993) reported a 25% failure of distal femoral and proximal tibial implants within the first five-years post-operatively in sarcoma patients. Unwin et al. (1991) comparing survival data on 668 Stanmore femoral replacements (221 proximal and 447 distal femoral implants), found that the failure of proximal femoral replacements over ten years was 92%, whereas survival of distal femoral replacements was 72%. When loosening as the only mode of failure was considered. Loosening in this study was defined as when an implant became unstable in the femur, whether it was due to infection, mechanical forces, or bone remodelling, in any replacement that required revision or resulted in amputation of the limb (Unwin et al. 1991).

Diaphyseal femoral and tibial implants also have similar loosening rates. Abudu et al. (1996a) reported approximately one-third of their diaphyseal implants failing due to “symptomatic mechanical loosening”. One mode of failure is thought to result from torsional forces caused by the use of a fixed hinge knee component in certain massive implants (Roberts et al. 1991, Unwin et al. 1996). The use of a rotating hinge has reduced the rate of aseptic loosening (Unwin et al. 1996). However, this is not the only cause of aseptic loosening responsible for implant failure.

Studies by Blunn et al. (2000) and Unwin et al. (1996) have detailed a possible mechanism for aseptic loosening described. In the case of massive implants, an offset exists between the tip of the implant stem and the axis of the femur from the femoral head to the centre of the knee. This offset is thought to cause a bending moment within the cemented fixation. Due to the line of load, this offset is more pronounced proximally on the femur than distally and thus, stems that are cemented more proximally in the bone suffer from greater bending forces within the cement mantle (Figure 1.2).

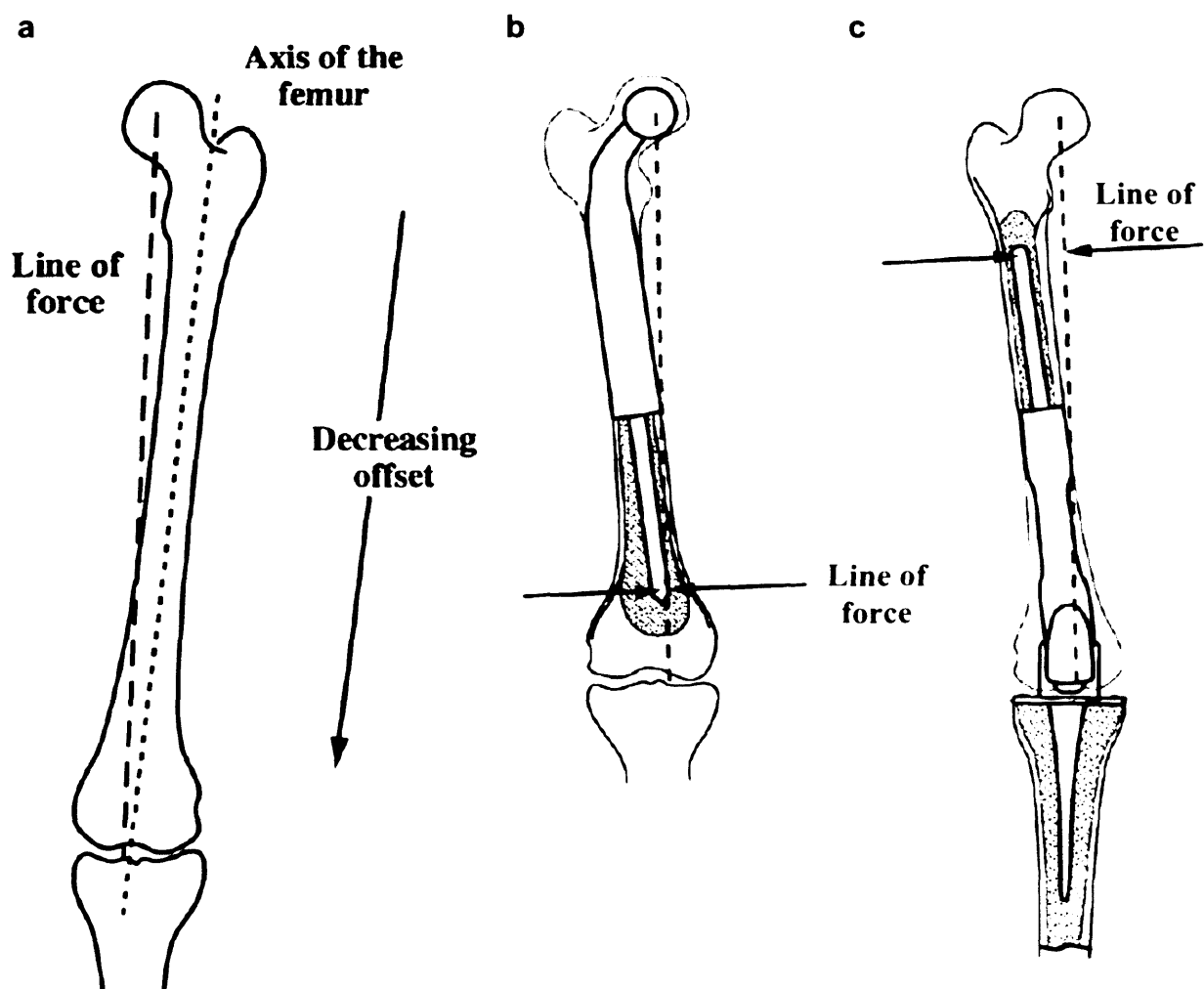


Figure 1.2 a) Diagram demonstrating the line of force through the femur, which has a decreasing offset with the axis of the femur as it moves distally; b) illustration of how this offset affects a proximal femoral replacement and c) a distal femoral replacement (adapted from Unwin et al. 1996, p 11).

As distal femoral replacements have more proximal transection sites and subsequent cemented fixation than proximal femoral implants, they have a greater offset to the axis of the long bone. This is also the case with lengthier tumour resection, where the upper stem may be placed more proximally in the bone. The increased force from the bending caused by this offset eventually causes a deterioration of the bone-cement interface, which slowly progresses from the transection site to the stem tip of the implant (Unwin et al. 1996).

Loosening begins with osteolysis adjacent to the implant shoulder (Blunn and Wait 1991, Ward et al. 1997), which can occur within six months post-operatively. Over time, osteolysis is seen to progress along the bone-cement interface, and radiographically can be viewed as radiolucent lines (seen in Figure 1.3).

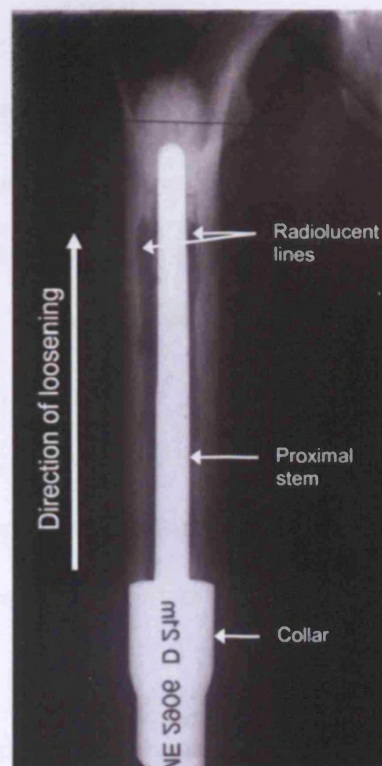


Figure 1.3 Radiograph of the proximal end of a massive implant, illustrating radiolucent lines that indicate aseptic loosening.

Cobb (2002) reported a deterioration of the interface between bone and cement, that was correlated with decreased function of the implant. There was a steady deterioration of the interface, and there was only a 56% probability of a good interface eight years post-operatively. A study investigating telemetric data from a 42-year old patient with a distal femoral replacement compared the forces applied to the stem tip to those on the implant shaft. The data showed an increasing force at the stem tip over time, with an increase in the stem tip-to-shaft force ratio of 25% to 63% over 23 months (Taylor et al. 1997). Supporting histological analysis of growing patients with extendible prostheses shows bone remodelling adjacent to prostheses to porotic bone, and the growth of fibrous tissue under the implant shoulder. However, it must also be noted that the authors mentioned a possible effect on remodelling by the blood supply, which is interrupted during surgery and implantation of a cemented prosthesis. A subsequent ingrowth of blood vessels into necrotic bone from the invading fibrous tissue at the transection site occurs (Blunn and Wait 1991). In addition, poor cement interdigitation, which is affected by the amount of cancellous bone and shape of the intramedullary canal into which the implant stem is inserted, could possibly affect the outcome of these prostheses (Unwin et al. 1996). Nevertheless, various methods have been employed to promote load transfer to the shaft of the prosthesis from the bone at the transection site in an attempt to prevent aseptic loosening. Especially at a time when the survival rate of patients is increasing, the long-term fixation of massive endoprostheses is of even greater importance, and it is possible that bone marrow stromal cells (BMSCs) could play a role in biologically improving the fixation of these implants.

Bone is dynamic, and responds to compressive and tensile forces by bone formation and resorption, respectively. Wolff's law, as first described by Julius Wolff in 1892, is the theory that mechanical stress determines bone structure, and that a change in stress can consequently

result in changes in bone composition (Wolff 1892). Applying this theory to remodelling, in cases of massive implants, means that bone adjacent to massive implants changes as a result of the new compressive and tensile forces being applied. Thus certain trends in bone growth around these implants can be seen.

A common radiographic observation around massive implants, which may reflect the bending effect, is bone growth posteriorly and medially, whereas bone resorption is often seen anteriorly and laterally (Inglis et al. 1991; Unwin et al. 1996). Inglis et al. (1991) reported such a pattern of bone growth around massive proximal femoral replacements. In this survey, which analyzed both lateral and anteroposterior radiographs, it was postulated that cortical thickening in the areas experiencing compressive forces would form a “column” of bone, which would move down the implant with the pressure applied by adjacent muscles.

The metal from which massive implants are manufactured is significantly stiffer than bone. Titanium alloy, such as Ti318, which is Ti-6Al-4Va (also called T₁), is a common alloy used which, in addition to being both strong and biocompatible, has a higher Young’s modulus than natural cortical bone (Table 1.1) (Dobbs and Scales 1983; Park 1995). Young’s modulus is a measure of material stiffness, which is the ratio of the rate of change of stress with strain, or the slope of the curve plotting stress versus strain.

Material	Young's Modulus (GPa)
Stainless Steel (316L)	200
Titanium Alloy (Ti6Al4V)	110
Hydroxyapatite	120
Cortical Bone (Long Axis)	17
Cortical Bone (Tangential)	12
Femoral Trabecular Bone	0.1

Table 1.1 Table outlining the Young's Modulus (measure of material stiffness) of biocompatible metals used for massive implants, and cortical and trabecular bone (adapted from "Orthopaedic Prosthesis Fixation," Park 1995, p 542). Note that titanium alloy has approximately 9 times the stiffness of cortical bone in the tangential aspect.

When prostheses are cemented, the consequence is that the host bone is under a decreased load and the strain is reduced, causing resorption. This phenomenon is known as "stress shielding" (Huiskes 1990). This change in load distribution to the metal implant and reduction of load experienced by surrounding bone, causes strain adaptive remodelling to take place, according to Wolff's law (Wolff 1892).

In some patients, a pedicle of bone grows from the transection site around massive metal implants, often with an intervening fibrous tissue layer between the implant and new bone (Blunn and Wait 1991). Integration of the implant into the host bone by ingrowth and attachment of this new bone is thought to promote better load transfer to the shaft rather than the stem tip, preventing "underloading" (Inglis et al. 1991) of the collar and overloading of the cement mantle (Okada et al. 1988; Sim and Chao 1979). One method that promotes this is the use of a collar on the implant shaft, at the transection site. These collars encourage bone to grow over and attach to the shaft of the prosthesis. Modern implant coatings try to augment this "bony bridge" by using porous titanium beads, bone graft, grooves and/or a

hydroxyapatite coating (Blunn et al. 2000; Chao and Sim 1985; Okada et al. 1988; Ward et al. 1993).

Hydroxyapatite (HA) is a biocompatible, resorbable, osteoconductive material that has been found to greatly enhance bone growth in both patients and animal models (Blunn et al. 2000; Coathup et al. 2000; D'Antonio et al. 1992; Geesink 1993). Osteoconductivity is the ability of a scaffold to promote osteoblast attachment and bone formation. In comparison, an osteoinductive scaffold encourages osteoblast precursor cells, such as BMSCs, to attach and differentiate into active osteoblasts. Natural bone is an example of an osteoinductive material (Datta et al. 2006). Another property of scaffolds, osteogenicity, refers to the presence of osteoblasts or osteoblast precursor cells that deposit bone directly on the scaffold surface (Mizutani et al. 1990).

Synthetic hydroxyapatite is a calcium phosphate ceramic that shares a similar chemical and crystallographic structure to natural hydroxyapatite, which is the main mineral component of bone (Engstrom and Zetterstrom 1951; Jarcho 1981). Although it has poor fatigue properties, which prevents it from being a useful structural implant material, HA can be applied to metal surfaces using a plasma-spray technique. This provides an implant with osteoconductive properties while maintaining the mechanical properties of a metal implant (Geesink et al. 1988). The bonding of bone to HA-coated implants has been investigated previously in canines, and was found to be very strong, which was a result of direct bonding of the material to bone (Geesink et al. 1988). As the HA is resorbed, released calcium and phosphate ions may also promote the formation of a biological apatite layer, and thus promote osteoinduction (Kurioka et al. 1999; Ozawa and Kasugai 1996). However, concerns do exist

about the stability of the metal implant-HA bond, in that it is non-permanent and may lead to wear particle production (Bloebaum et al. 1994).

The use of grooved, porous, hydroxyapatite-coated collars has shown effective results in terms of bone ingrowth to the implant collars (Blunn et al. 2000;

Figure 1.4). In the short-term follow-up reported by the authors (after more than 12 months), only one patient out of forty-four showed any signs of loosening, and a radiographic study showed no signs of radiolucency around the implant. Chao et al. (2004) significantly improved extracortical bone growth around massive implants in patients by using a porous-coated collar augmented with autologous bone graft. Only one out of forty-three patients showed aseptic loosening after a mean of 9.7 years follow-up. The use of cementless fixation with proximal femoral components showed that the use of HA coincided with a more even distribution of bone growth around the implant when compared with control implants (Blunn et al. 2000).

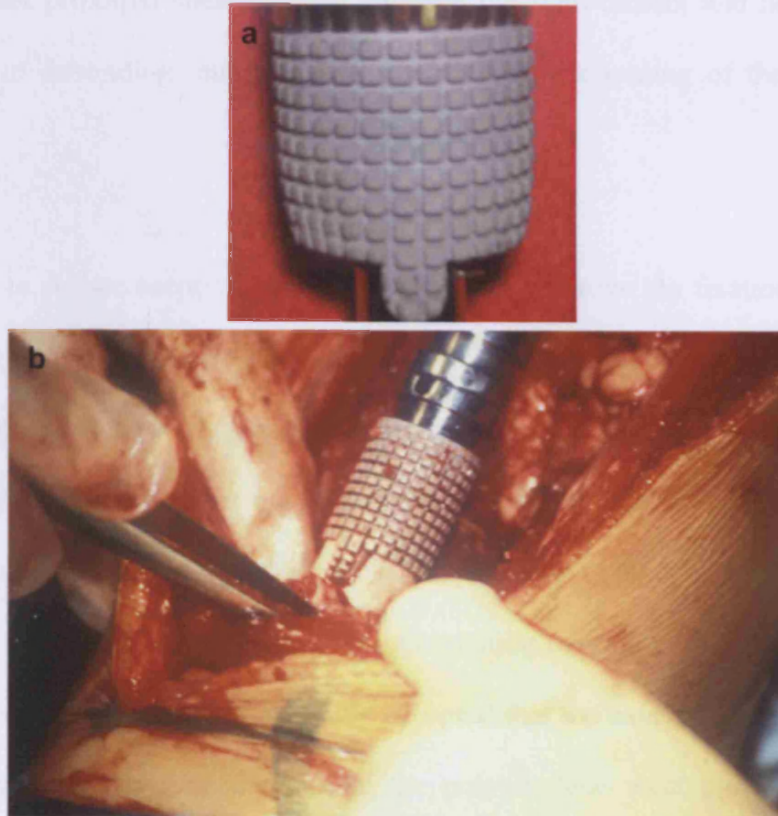


Figure 1.4 Photographs of hydroxyapatite (HA)-coated collars from a) a proximal tibial replacement and b) a massive implant with an HA-coated collar being implanted.

Compared to uncoated porous collars, hydroxyapatite-coated collars on distal femoral replacements appear to promote bone ingrowth in over 70% of cases. This ingrowth is negatively correlated to the extent of radiolucent lines on radiographs. Good bone formation into the HA-coated collars resulted in a decrease in the size and number of radiolucent lines around the intramedullary stem (Cobb 2002; Unwin et al. 2005).

As this uncoupling of load at the implant shoulder to the stem tip ultimately results in debonding and loosening of the implant (Unwin et al. 1996), strategies to prevent this initial uncoupling have been considered. Ideally, the use of a biocompatible material with an elastic

modulus closer to that of cortical bone would prevent overloading of the stem tip. Unfortunately, studies that have investigated more flexible materials have shown them to promote higher proximal shear stresses between the stem/cement and bone interface. This could result in debonding, micro-motion, and eventual loosening of the implant (Huiskes 1990).

One strategy to reduce aseptic loosening has been to improve the fixation of the implant to the bone by improving the osseous integration of the implant. This is thought to prevent the uncoupling of load from the implant shoulder through load transfer. This strategy has focused on promoting bone growth over the implant by developing implant collars at the transection site of the implant. The resultant “bony bridging” is also thought to act as a “purse string,” sealing the bone-implant interface, possibly preventing the migration of wear particles to the site causing osteolysis. However, it should be noted that the existence of these wear particles has not been proved empirically, unlike the polyethylene wear particles generated with traditional arthroplasty.

Another method by which fixation of the implant could be improved is by using osteoblastic precursor cells such as bone marrow stromal cells (BMSCs) in combination with HA-coated collars, to further encourage greater bone growth and attachment into the implant collar. **To augment this beneficial load transfer and reduce the aseptic loosening of massive implants using BMSCs is the goal of my thesis.**

1.3 Stem Cells

1.3.1 Definition

The term “stem cell” refers to an undifferentiated precursor cell that has “the capacity for unlimited or prolonged self-renewal, that can produce at least one type of highly differentiated descendant” (Watt and Hogan 2000). These precursor cells can be induced to differentiate into another cell type, depending on the type of stem cell and the cues given (Jaiswal et al. 1997). Between a fully multipotent stem cell and a terminally differentiated cell type, there are thought to exist a series of “committed progenitors” with a lower proliferative and differentiation potential. These can be referred to as “transit amplifying cells” (Watts and Hogan 2000).

There are many sources of stem cells cited in the literature: the embryo, the adult bone marrow, umbilical cord blood, adipose tissue, as well as neuronal-derived cells (Bacou et al. 2004; Lam et al. 2001; Zvaifler et al. 2000; Zandstra and Nagy 2001), all of which have varying abilities to differentiate down numerous cell lineages. As promising as these cell sources may be, most past and current research concerns the first three types of stem cell. It is becoming increasingly apparent, however, that adult stem cells isolated from the bone marrow have potential regenerative applications (Le Blanc and Pittenger 2005), such as the tissue engineering of bone (Arinzeh et al. 2003; Lee et al. 2005).

1.3.2 Autologous, Allogeneic and Xenogenic Cells, and the Multipotency of Stem Cells: Definitions

In cases where the stem cells from a patient are re-implanted into the same individual, the donor cells are referred to as being autologous. If donor cells are implanted into another individual of the same species, the cells are termed allogeneic, and of another species, xenogenic.

A totipotent cell has the ability to differentiate into any type of cell. Pluripotent cells can differentiate into almost all cell types, but not all. A cell that can only differentiate into a limited number of cell types is termed multipotent (Zandstra and Nagy 2001).

1.3.3 Bone Marrow Stromal Cells (BMSCs)

Bone marrow stromal cells (BMSCs), are a population of plastic-adherent cells derived from the bone marrow, that most often possess a fibroblastic morphology (Figure 1.5). BMSCs, described as “fibroblastic precursor cells,” were first described by Friedenstein, Chailakhjan and Lalykina in 1970. A population of cells within this heterogeneous population (Aubin 1998) are commonly referred to as “mesenchymal” stem cells, referring to their multipotency and/or ability to form mesodermal tissues such as bone (Haynesworth et al. 1992; Jaiswal et al. 1997), cartilage (Johnstone et al. 1998), adipose tissue (Ryden et al. 2003), and stroma (Majumdar et al. 2000). Friedenstein’s seminal works investigated the properties of bone marrow stromal cells, *in vitro*, by observing their ability to mineralise after treatment with osteogenic supplements, and by their ability to form bony tissue in diffusion chambers *in vivo* (Friedenstein, Chailakhjan and Lalykina 1970; Friedenstein 1973; Friedenstein 1976). Bab et al., in 1986, also investigated BMSCs in diffusion chambers, and found that the tissues produced in these chambers originated from a small number of originally implanted cells, with “stem cell-like” characteristics.

Friedenstein proposed a hypotheses leading from his work, that suggested that a single stromal cell could give rise to multiple lines of cells (Friedenstein 1980). From their experimental data of CFU-F derived from the bone marrow, Owen, Cave and Joyner (1987) produced a summarising flow chart which indicated that stromal “stem cells” could

differentiate into committed progenitors, which could then further differentiate into specific cell types such as fibroblasts, reticular cells, adipocytes, and osteoblasts.

Dahir et al., in 2000, isolated a “precursor” cell lines from mouse bone marrow, and was able to show, by labelling cells with the enzyme β -galactosidase (using a non-infections retrovirus containing the lacZ gene), that these cells not only had osteogenic characteristics *in vitro*, and were able to repopulate the bone marrow of host mice, while maintaining their osteogenic capability.

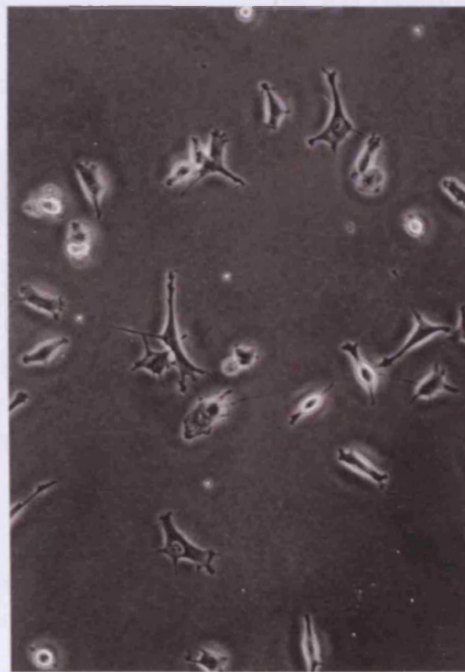


Figure 1.5 Photo of human bone marrow stromal cells (BMSCs; from P. Kalia).

However, there is some controversy as to whether or not BMSCs are actually ‘stem cells,’ as they are only multi-potent or have restricted differentiation potential, as opposed to embryonic stem cells (ESCs) which have the capacity to differentiate into almost any cell type (Heins et al. 2004; Thomson et al. 1998). **For this reason, the population of mononuclear, plastic-adherent, fibroblastic cells isolated from the bone marrow will be**

identified in this thesis as bone marrow stromal cells (BMSCs), a term that refers to the cells' origin and morphology.

In culture, these cells are selected from the marrow based on the following characteristics: their mononuclear phenotype, their capacity for adherence and growth on tissue-culture plastic and their ability to form fibroblastic colony units (colony-forming units-fibroblastic (CFU-F)). BMSCs populations can also be enriched for “multipotent” cells or “stem cells,” by selecting cells based on their surface marker expression pattern using fluorescence-activated cell sorter (FACS) or magnetic-activated cell sorter (MACS) machines. Table 1.2 lists a panel of cell surface markers used in BMSC identification, some of which are expected to be present and others absent.

BMSCs have great promise for tissue repair and regeneration, due to their ease of isolation, high proliferative capacity and ability to retain their multi-potent capacity, as well as their ability to differentiate into various mesenchymal tissues. In addition, the immuno-modulatory effects of BMSCs should also be considered as this may permit the use of allogenic (unrelated cells of the same species) cells in patients (see 1.3.3.3).

Present	Absent
CD29	CD14
CD44	34
CD54	45
CD71	68
CD90	HLA-DR
CD120a	
CD124	
CD105 (Endoglin)	
CD106 (VCAM-1)	
CD164 (Endolyn)	
SH2	
SH3	
SH4	
Stro-1	
P-Zero Protein (PZR)	

Table 1.2 Chart illustrating cells surface markers present and absent on human BMSCs (Baksh et al. 2003; Campagnoli et al. 2001; Pittenger et al. 1999; Watt 2006).

1.3.3.1 Previous characterisation of BMSCs

In current practice, the positive identification of BMSCs as multipotent precursor cells can be achieved through two methods: differentiation of the cells down two or more lineages, and cell surface marker identification. Ideally, both methods should be utilised for complete characterisation.

Upon stimulation in culture with osteogenic reagents, BMSCs change morphology and begin to express osteoblastic characteristics temporally in the following order: *cbfa-1/runx2* and *osterix*, transcription factors involved in osteoblast differentiation; alkaline phosphatase, which is expressed on the cell surface of osteoblasts; osteonectin, which regulates mineral-collagen interactions and calcium binding; osteopontin, involved in calcium deposition; and osteocalcin, which regulates the later stages of mineral deposition (Krishnan et al. 2003; Pittenger et al. 1999). When differentiated towards the chondrogenic lineage, BMSCs seem to upregulate the expression of collagen II (basic matrix molecule of articular cartilage), aggrecan, and *sox-9*, in addition to a chondrocytic phenotype (Lee et al. 2006; Mackay et al. 1998). After treatment with adipogenic reagents, BMSCs appear to accumulate lipid vesicles, and are positive for the expression of genes such as lipoprotein lipase (LPL) and nuclear peroxisome proliferators-activated receptor gamma ($PPAR\gamma 2$) (Pittenger et al. 1999).

There has also been some evidence of neural and hepatocytic (Kang et al. 2005; Lee et al. 2004) phenotypes being derived from BMSCs, although this has also been disputed (Bertani et al. 2005; Wang et al. 2003). Other groups have documented the differentiation of BMSCs into cardiomyocytes and vascular cells (Nagaya et al. 2005). One group tracked cells *in vivo* and found that the implanted BMSCs, in addition to releasing mitogenic, angiogenic, and anti-apoptotic factors *in vitro*, were positive for many cardiac markers once implanted into myocardia *in vivo*.

As mentioned above, human BMSCs (hBMSCs) can also be identified through the presence and absence of a series of cell surface markers, none of which are specific to BMSCs (Baksh et al. 2003; Campagnoli et al. 2001; Pittenger et al. 1999). Recent research has identified the cell surface proteins CD164/endolyn and a specific isoform of P zero-related (PZR) protein as being markers of hBMSCs (Watt 2006), albeit they are not entirely specific. There has been some preliminary work looking at the gene expression of BMSCs that seems to also indicate that the patterns of gene expression of BMSCs are unique (Djouad et al. 2005); however, this is not yet a commonly available tool for most laboratories. Whether or not all of these markers are present or absent from the BMSCs derived from other species is unknown.

BMSCs from other species have been isolated and either partially or fully characterised, such as from mice (Dennis and Charbord 2002; Phinney et al. 1999); rats (Lee et al. 2005); Okamoto et al. 2006), pigs (Bosch et al. 2006; Vacanti et al. 2005), cats (Martin et al. 2002), dogs (Kadiyala et al. 1997; Volk et al. 2005), goats (Kruyt et al. 2003), sheep (Kon et al. 2000; Shang et al. 2001), cows (Troyer et al. 2003) and baboons (Bartholomew 2001).

Although Jiang et al. (2002a; 2002b) were able to isolate a special population of cells from human, mouse and rat BMSCs, called multipotent adult progenitor cells (MAPCs) that appeared to have pluripotency similar to ESCs, some of the FACS analysis for cells surface markers has been called into question (Verfaillie and Jiang 2006; Jiang et al. 2007), challenging the validity of group's results (see general discussion).

1.3.3.2 Proliferation rate of BMSCs

Human BMSCs have been documented as having a high proliferation rate and can undergo as many as 38 population doublings without loss of their proliferative or osteogenic capacity (Bruder et al. 1997). This is almost twice the doubling capacity of other human diploid cell types, such as adult lung fibroblasts, which have a doubling capacity of 20 times (Hayflick 1965). With such prolonged expansion of BMSCs in culture, there are accompanying concerns regarding cell ageing and mutation. Unlike undifferentiated embryonic stem cells (ESCs; Heins et al. 2004), BMSCs do not express high levels of telomerase, the enzyme that lengthens telomeres to prevent their shortening during cell division. As telomere shortening is directly related to cell ageing and senescence, there is a possibility that BMSCs expanded in culture could lose their characteristics and ability to proliferate and differentiate once re-implanted *in vivo* (Baxter et al. 2004). Another factor is an accumulation of mutations by the cells while in culture. It is well documented that not only immortalised tumour cell lines, but also BMSC cell lines could potentially mutate in artificial culture conditions (Devine et al. 2001b). This may result in errors in cell division or DNA repair, which lead to translocations (movement of one segment of a chromosome to another) as well as aneuploidy (Wang et al. 2005), which can be defined as having an abnormal number of chromosomes. In addition, BMSC-like cells have been isolated from giant cell bone tumours (Wulling et al. 2003). The possibility of accumulated cell damage and ageing should therefore be seriously considered when investigating BMSCs and thorough testing should be in place to ensure that such potentially tumorigenic mutations have not occurred before re-implantation or infusion of cells.

1.3.3.3 Immunogenetic properties of BMSCs

Current research suggests that BMSCs have suppressive immunogenetic properties. The first evidence of an immunosuppressive effect of BMSCs was their ability to promote recovery

and engraftment of HSCs in high-dose chemotherapy patients receiving HSC infusions (Koc et al. 2000). A number of *in vitro* experiments have assayed the effects of BMSCs on mixed lymphocyte cultures (Le Blanc et al. 2003; Tse et al. 2003). Le Blanc et al. (2003) added different concentrations of both autologous and allogenic human BMSCs to mixed lymphocyte cultures in an attempt to measure immunoreactivity of the BMSCs. Not only did the group observe a cell-dosage effect of BMSCs on the proliferation of lymphocytes and that BMSCs were able to prevent the formation of activated T-lymphocytes, they also found that this effect was wholly independent of the major histocompatibility complex (MHC). Rasmusson et al. (2003) obtained supporting results in a similar study.

Further work demonstrated that BMSCs retained their immuno-suppressive properties after *in vitro* differentiation into osteogenic, chondrogenic, and adipogenic cells (Le Blanc et al. 2003). What is the mechanism of this immunomodulatory effect? BMSCs express MHC I and lymphocyte function-associated antigen (LFA)-3 antigens as well as MHC II and ICAM-1 antigens after stimulation with γ -interferon treatment (Tse et al. 2003), but the observed effects are independent of the MHC. Evidence by Aggarwal and Pittenger (2005) showed that prostaglandin E₂ (PGE₂) plays a substantial role in mediating anti-inflammatory and immunomodulatory responses by showing a reversal of the immunosuppression after treatment with a known PGE₂ inhibitor. It must be noted, however, that an earlier experiment by Tse et al. (2003) found that inhibiting PGE₂ had no such effect. The mechanism of BMSC-modulated immunosuppression has not been conclusively studied as yet, however this property may explain the acceptance and effectiveness of allogeneic cells in a few bone tissue engineering models (Arinzeh et al. 2003; De Kok et al. 2003; Tsuchida et al. 2003). In these models, allogeneic BMSCs have performed as well as autologous BMSCs in regenerating defects with new bone.

1.3.4 Haematopoietic Stem Cells (HSCs)

HSCs are precursors of the haematopoietic lineage, which are predominantly localised to the bone marrow in their undifferentiated state, and most often derived from this source. In 1980, Till and McCulloch first documented the multipotency of these bone marrow-derived cells after an injection of HSCs into lethally irradiated mice resulted in the formation of donor-derived haematopoietic colonies of various lineages (Till and McCulloch 1980). In comparison to BMSCs, HSCs are well documented in terms of their differentiation pathways and mechanisms, localisation and attachment in the marrow, and the clinical results from transplanting these cells into human patients. Donor HSC infusions have been proved to be clinically effective in the treatment of neutropenia (Reddy 2005). This often involves a selection of cells expressing the cell surface marker CD34 using fluorescence-activated cell sorting (FACS) from a plasma-depleted blood donation, followed by infusion of these cells into the patient. Clinically, HSCs are often mobilised using granulocyte-colony stimulating factor (G-CSF) or granulocyte-macrophage-colony stimulating factor (GM-CSF). The mobilisation of these cells is mediated via the binding of HSCs to the bone marrow stroma. Upon stimulation, the HSC cell surface receptor CXCR4 dissociates from the cytokine stromal-cell derived factor-1 (SDF-1), a factor expressed by BMSCs and other cells of the stromal lineage. A second mechanism involves the release of the HSC adhesion molecule VLA-4 from vascular cell adhesion molecule-1 (VCAM-1), which is expressed on the surface of BMSCs. In both cases, there is liberation of proteases such as elastase, cathepsin G, and matrix metalloproteases (MMPs) such as MMP-9, which result in the degradation of these molecules involved in adhesion as well as a subsequent remodelling of the ECM microenvironment to promote release of cells from the marrow (Lapidot and Petit 2002).

1.3.5 Embryonic Stem Cells (ESCs)

Embryonic stem cells (ESCs) are isolated from the inner cell mass of pre-implantation blastocysts. ESCs were first isolated from mice by Martin Evans in 1981 (Evans and Kaufman 1981). Human embryonic stem cells were first successfully isolated and cultured into cell lines in 1998 (Thomson et al. 1998). A photograph of a human embryonic stem cell colony can be seen in Figure 1.6. ESCs are pluripotent, as they can differentiate into almost any cell type, except a few extra-embryonic cell types such as the yolk sac visceral endoderm, parietal endoderm, and placental trophoblast (Zandstra and Nagy 2001).

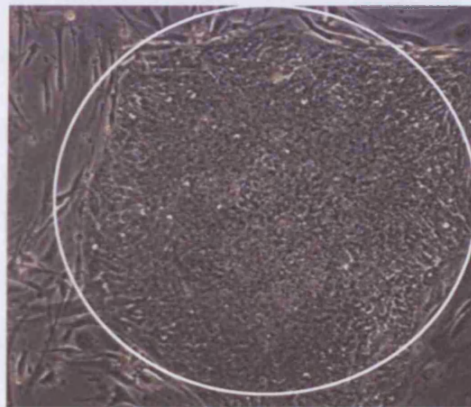


Figure 1.6 Photograph showing a colony of H9 human embryonic stem cells (within circle; used with permission from Dr. M. Clements, University of Westminster, 2006).

The advantage of using ESCs is their ability to differentiate into any tissue derived from the three embryonic lineages (ectoderm, mesoderm, and endoderm) in two or three-dimensional culture. Also, ESCs may hold great promise in the pharmaceutical industry, for drug discovery and toxicity testing. At present, there are insufficient sources of specialised human cell types such as those derived from the liver or heart (hepatocytes or cardiomyocytes). By differentiating the highly proliferative, pluripotent ESCs into these cell types, a new reserve of cells would be available for *in vitro* testing. In fact, as discussed by Améen in 2007, these

cells could even be used to derived cells that could activate and mobilise endogenous cells to organs or tissues in need of repair or improved function.

The potential disadvantages of using ESCs are numerous, and include the difficulties and expense associated with ESCs (Le Blanc and Pittenger 2005). It is impossible to use autologous ESCs, which are derived from embryos, as there are immunoreactivity issues to be considered in transplanting human leukocyte antigen (HLA)-mismatched cells into patients (Heng et al. 2005). When using BMSCs, it is possible to use autologous cells from the patient, expand those cells, and re-implant them without any donor-related risks. Another disadvantage is the difficulty in culturing ESCs. Although ESCs can be grown and expanded *in vitro*, if not maintained under strict control, the cells spontaneously differentiate into different cell types, some of which may not be the desired type (Heng et al. 2005). For example, a study investigating ESCs administered *in vivo* in immuno-compromised mice (Tzukerman et al. 2003) showed that ESCs can give rise to teratomas and are tumourogenic. However, if ESCs were pre-differentiated into specific cell types before implantation, the probability of tertartomic activity could decrease significantly (Améen et al. 2007).

These factors have limited the potential of ESCs for clinical application. The third, and perhaps most controversial consideration in using ESCs, is the ethical and legal dilemma posed by their potential use clinically. An important source of human ESCs are embryos created through *in vitro* fertilisation procedures. The moral idea that embryos have the potential to become human beings and therefore should not be dissected for use in research, and/or clinical practice, has made the use of using human embryos both difficult practically and ethically controversial (Shenfield 2005; Young 2000). When mesenchymal tissues are regenerated in tissue engineering, adult stem cells such as BMSCs have been preferred as

they are readily available, can be isolated from the patient who could be receiving therapy (as autologous cells), and have the potential to differentiate into the tissue of interest.

1.3.6 Other sources of stem cells-Peripheral Blood Stromal-like Cells (PBSCs)

Until recently, the most common source of osteoprogenitor cells has been the bone marrow. However, BMSCs are thought to comprise only 0.0001%-0.001% of the bone marrow cell population (Pittenger et al. 1999). Therefore, other sources of multipotent cells in the body that may require a less invasive procedure than a bone marrow aspirate in order to harvest cells have been considered, such as adipose tissue (Bacou et al. 2004; Rodriguez et al. 2004; Zuk et al. 2002), muscle (Asakura 2003; Sinanan et al. 2004), cord blood (Lam et al. 2001; Lee et al. 2004), and the peripheral blood (Fernandez et al. 1997; Kassis et al. 2006; Mansilla et al. 2006; Wan et al. 2006; Zvaifler et al. 2000). Stimuli that may promote cell mobilisation, such as induced blood loss, have also been investigated. Obtaining a greater number of cells at the time of isolation would expedite the process by which cells are cultured, and potentially used clinically.

In mice, CFU-F progenitors naturally circulate in the peripheral blood, and the possibility of BMSC mobilisation in humans has been debated in the literature. The first published work indicating this possibility was by Fernandez et al. (1997), who isolated a population of cells from the peripheral blood of human patients. The resulting aphaeresis products were density separated and grown in culture. These cells were found to grow fibroblast-like colonies, similar to BMSCs, which were stained positively for the BMSC markers SH2 and SH3, and negative for CD14 and CD34 (monocyte/macrophage and haematopoietic stem cell markers, respectively). Further work by Zvaifler et al. (2000) suggested the existence of a mixed population of cells within the blood, including those with a mesenchymal precursor cell

phenotype, large cells, with adipocytic morphology, as well as those which were multinucleated and stained positively for tartrate-resistant acid phosphatase, a characteristic of osteoclasts. Purton et al. (1998) previously described such CD14⁺ fibroblastic cells as being monocytes, which achieve an osteoclastic phenotype following high-density culture conditions. A similar fibroblastic, CD14⁺ population of cells was termed “fibrocytes” by Bucala et al. (1994) due to their combined features of both fibroblasts and leukocytes. More recently, other groups have obtained and characterised cells from the peripheral blood as having identical surface marker expression and multipotent ability as bone marrow-derived stromal cells (Mansilla et al. 2006, Wan et al. 2006). One of these studies isolated a greater number of PBSCs from patients with major burn injuries, suggesting that these cells are released from the bone marrow into the bloodstream as a natural response to injury (Mansilla et al. 2006). It may be possible to use these cells as an alternative to BMSCs in the tissue engineering or regeneration of bone. A plentiful source of cells can be obtained by taking a blood sample, rather than a painful bone marrow aspiration, which requires anaesthesia, and is more limited in volume.

1.4 Tissue Engineering

1.4.1 Introduction

Organ and tissue transplants have been used for some time in clinical practice, in many areas of medicine, with varying levels of success. Supply and demand, as well as immunocompatibility and disease transmission, are big issues in transplantation that often render them impossible or risky. Immunosuppressive drugs taken to accept these organ transplants can lead to tumour formation (Vacanti and Vacanti 2000). By creating tissues using the basic components of cells, scaffolds, and bioactive factors, tissue engineering attempts to replace, re-construct, or repair tissues. There are two main approaches to this

field, which are *in vitro* (or *ex vivo*) and *in vivo* tissue engineering. *In vitro* tissue engineering strives to create tissue outside the body. This may require the use of tissue culture techniques, in addition to bioreactors, bioactive factors, and specially designed scaffolds and biomaterials.

1.4.2 Scaffolds

One of the important components of tissues in the body, apart from the cells themselves, is the extracellular matrix (ECM) that they lay down. ECM serves a variety of functions, from general structural support of the tissue, to involvement in cell alignment and communication (Martins-Green 2000). This matrix is predominantly collagen-based, although other molecules such as hyaluronic acid, glycoproteins, elastins, fibronectin, vitronectin and laminin are also important components (Pearson et al. 2002). Embedded within the fibrils of these matrix materials can be found various growth factors, cytokines, water molecules and enzymes such as elastases or metalloproteases (Martins-Green 2000). In tissue engineering, scaffolds attempt to simulate a native tissue environment with an artificial extracellular matrix. Ideally, the material should also be biodegradable (Pachence and Kohn 2000). Thus, popular scaffolds used include collagen I, alginate, poly-lactic acid (PLA), poly-glycolic acid (PGA), plasma, as well as fibronectin and fibrin (Andree et al. 2001; Gurevich et al. 2002; King et al. 2006; Kumar and Albala 2001; Pachence and Kohn 2000; Ting et al. 1998; Ye et al. 2000).

In bone tissue engineering, a mechanically supportive, osteoconductive, ceramic scaffold such as natural coral exoskeleton, synthetic hydroxyapatite, beta-calcium triphosphate or Bioglass[®] may be used (Chan et al. 2002; Oonishi et al. 1997), often in combination with one of the above mentioned matrix materials. These scaffolds have inherent osteoinductive

(Ripamonti 1996; Yuan et al. 1998) and/or osteoconductive properties (Geesink and Hoefnagels 1995). Newly developed biomaterials include silk-based scaffolds (Meinel et al. 2005) and chitin-based scaffolds (Di Martino et al. 2005), which appear to be osteoconductive *in vivo*. BMSCs are generally combined with one or a combination of these scaffolds with or without growth factors (see 1.4.5), for bone tissue engineering (Bruder and Caplan 2000).

Porosity and pore sizes have been investigated as to their effects on bone regeneration with scaffolds, with or without cells being added. Various works report that, overall, the minimum pore size of a structure should be great than 300 μm , to allow for cell migration into the pores, nutrient migration, as well as to allow the invasion of capillaries into the site, vasculogenesis being an important first step towards osteogenesis (Kuboki, Jin and Takita 2001; Tsuruga et al. 1997; Gotz et al. 2004). While smaller pores can contribute to hypoxic conditions and the aggregation of cells, resulting in osteochondral ossification, larger pores allow for direct osteogenesis. Although higher scaffold porosity encourages better bone ingrowth, increasing porosity often decreases the mechanical strength of a scaffold, to the point where it is no longer of withstanding the loads seen in orthopaedic applications (Karageorgiou and Kaplan 2005).

1.4.3 Fibrin Glue

Fibrin is a naturally occurring matrix, which has an important role in the final steps of the coagulation cascade in wound healing (Kania et al. 1998), and has been used previously as a tissue engineering scaffold (Grant et al. 2002; Lee et al. 2005). In the body, fibrin is formed by the enzymatic cleavage of the fibrin zymogen fibrinogen by the serine protease thrombin. Fibrin then undergoes a polymerisation reaction with other fibrin molecules, as well as cross-

linking (facilitated through either Factor XIII or endogenous trans-glutaminases) to itself and surrounding tissue, which lends it both haemostatic and adhesive properties (Marx and Mou 2002). Fibrinogen fragments as well as fibrin degradation products are thought to promote the migration of cells such as fibroblasts (Abiraman et al. 2002) and vascular smooth muscle cells to the healing site (Kodama et al. 2002). Fibrinogen-fibroblast interactions have not been thoroughly investigated (Gailit et al. 1997). Fibroblasts are thought to interact with fibrin by the interaction of fibrinogen molecules with the integrins $\alpha_v\beta_1$, $\alpha_v\beta_3$, and $\alpha_{IIb}\beta_3$ (Hubbell 2000). Integrins are a large family of cell surface receptors involved in adhesion by binding to ligands found expressed in the ECM and by other cells (Gailit et al. 1997). Although there is evidence for direct fibroblast-fibrinogen interactions in cell adhesion, evidence shows that indirect interactions with fibronectin are required for cell spreading and migration into fibrin via the crucial integrin $\alpha_1\beta_3$ binding to the sequence RGDS (Gailit et al. 1997; Knox et al. 1986; Pierschbacher and Ruoslahti 1984).

Cells naturally express urokinase plasminogen activator and tissue plasminogen activator, serine proteases that activate the fibrin-degradation enzyme plasmin (Neuss et al. 2004), and this process, in addition to the action of macrophages and multi-nucleated foreign body cells, naturally degrades fibrin over time.

Fibrin glue has been used for many years as a surgical haemostatic agent (Davidson et al. 2000; Spotnitz et al. 1987), as well as other surgical uses, for example, preventing air leaks after pulmonary resection (Belboul et al. 2004). Figure 1.7 shows the components of the commercially available Tisseel[®] fibrin glue, as well as a reflection electron microscopy image of fibrin at high magnification. Fibrin glue can also be sprayed (Figure 1.8). Commercially prepared fibrin glue, such as Tissucol[®] and Tisseel[®] fibrin sealant (Figure 1.7),

have two main components: human fibrinogen reconstituted in a bovine aprotinin solution, and a human thrombin-calcium chloride solution. The availability of fibrin, in addition to its simple application system, makes it easy to obtain and use. Combinations of fibrin and non-resorbable HA have been used throughout Europe for over a decade, in the reconstruction of maxillofacial and dental defects (Bonucci et al. 1997). The fibrin phase has proved effective in moulding the ceramic scaffolds and holding the granules/powder in place as natural mineral deposition occurs.

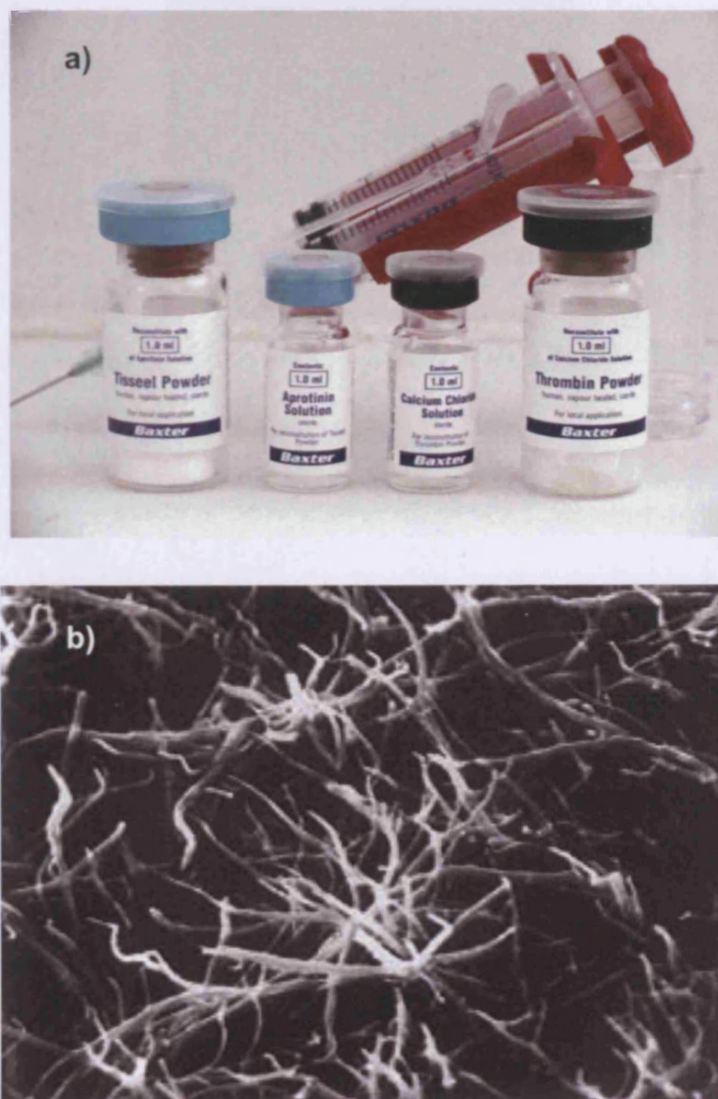


Figure 1.7 a) Components of Tisseel fibrin glue; b) Reflection electron microscopy (REM) image photograph of Tisseel fibrin glue (scale 1:6000, used by permission from Baxter Biosurgery, USA).

At present, fibrin is a promising scaffold for cells for skin regeneration, and when combined with keratinocytes, can be sprayed onto wound sites (Grant et al. 2002). Fibrin has been shown to increase the level of the angiogenic factor VEGF, which could enhance the healing effect of fibrin scaffolds in skin tissue engineering (Hojo et al. 2003).

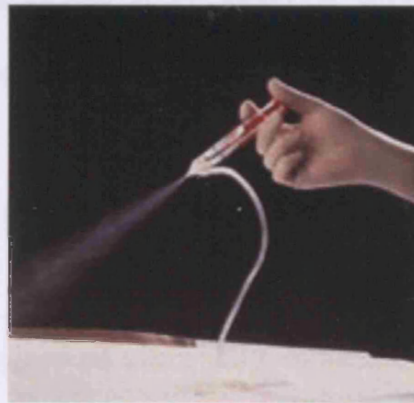


Figure 1.8 Fibrin glue sprayed using pressurised air (Baxter Biosurgery, USA. Used with permission).

The osteoconductive properties of fibrin glue have been reported (Abiraman et al. 2002; Bosch et al. 1980; Kania et al. 1998; Yamada et al. 2003) and disputed (Greco et al. 1988; Lucht et al. 1986; Schwarz et al. 1993). An experiment by Abiraman et al. (2002) showed that fibrin glue had osteoconductive properties at an ectopic site; however, this was only observed when fibrin was combined with hydroxyapatite or bioglass. Similar work in a rat femoral defect model indicated a role for fibrin glue in osteogenesis, when implanted in an orthotopic site. In another study by Schwarz et al. (1993), fibrin glue did not promote osteoinduction at both ectopic and orthotopic locations in rats. Thus, no study has shown fibrin alone to possess osteoinductive properties.

Fibrin may not induce differentiation of osteoblastic precursors into osteoblasts, but may promote neo-vascularisation at the surgical site to promote faster healing and bone formation and organisation (Kania et al. 1998). In the osteoconductive experiments described above, control biomaterials such as bioglass and hydroxyapatite granules did not show reduced bone formation and bone ingrowth to materials when compared to those treated with fibrin, but also lacked neo-angiogenesis (Kania et al. 1998). A study by Abiraman et al. (2002) demonstrated that the ectopic implants coated in fibrin glue had noticeable neo-vascularisation and evidence of intramembranous ossification when compared to controls, which were encapsulated in a thick fibrous layer.

Fibrin's biocompatibility, commercial availability, in addition to its proven effectiveness in bone defects, makes it an ideal cell delivery vehicle *in vivo*, for cells such as BMSCs, in tissue engineering applications.

1.4.4 The use of BMSCs in the tissue engineering of bone

The first evidence indicating the osteoinductive nature of bone marrow cells was the ability of fresh bone marrow to augment bone formation in orthopaedic surgery (Boyne and Yeager 1969; Morris 1969). Following the seminal work of Friedenstein et al. (1968) into the role of BMSCs specifically in bone formation, they have become a major component of bone tissue engineering strategies. One benefit of using BMSCs as opposed to bone marrow is the lack of erythrocytes, which may increase potassium to cytotoxic levels (Street et al. 2000). *In vitro* testing has frequently been used as a pre-indicator of osteogenic capabilities of osteoprogenitor cells and cell-scaffold constructs *in vivo* (Jaiswal et al. 1997, Rust 2004).

BMSCs have been shown to increase bone growth *in vivo*, in small and large animal models, at both orthotopic and ectopic locations (Bruder and Caplan 2000; Haynesworth et al. 1992;

Kalia et al. 2006; Korda et al. 2006; Kruyt et al. 2003). Some of the first experiments investigating the potential of BMSCs in *in vivo*, loaded cubes of calcium phosphate ceramics with or without BMSCs, which were implanted subcutaneously in synergenic or immunocompromised rodents (Haynesworth et al. 1992). These studies found significantly increased bone growth into the cubes loaded with BMSCs when compared to the scaffolds alone. Further work by this group showed that this observation was applicable to cells from many mammalian species, such as goat, sheep, dog, rat, and human. Additionally, it was found that diluting the number BMSCs up to 50% with fibroblasts did not effect bone formation *in vivo* (Bruder and Caplan 2000). In addition to smaller animals such as mice, rats, and rabbits, larger animals, such as dogs, sheep, and goats, are often used for the *in vivo* testing of bone tissue engineering strategies. The results of *in vivo* investigations on the mechanical loading of the hind limbs of large animals indicate similar loading levels to those experienced by humans (Bergmann et al. 1984; Buma et al. 2004; Martini et al. 2001), suggesting that large animals may be a suitable model for the testing of tissue engineering models with BMSCs.

A study investigating ectopic bone growth in a caprine model showed a significant effect of BMSCs loaded seven days pre-operatively or per-operatively onto porous ceramic cubes, suspended in autologous plasma, and implanted into the bilateral paraspinal muscles of goats (Kruyt et al. 2004). This biphasic calcium phosphate (BCP) scaffold has previously been shown to be osteoinductive, in that it promotes bone growth in an ectopic site, without the aid of osteoinductive growth factors or osteoprogenitor cells (Yuan et al. 2002). In the 2004 ectopic study by Kruyt et al. (2004), a comparison was made between cryopreserved and fresh cells to see if cells could be obtained in advance of surgery and preserved for future use. These groups were also compared to control, untreated scaffolds as well as devitalised scaffolds. These are scaffolds which have cells grown onto them for seven days, after which

the construct is devitalised to remove live cells, leaving behind an extracellular matrix coating. In this study, it was found that these ceramic blocks had significantly more bone growth when seeded pre-operatively or per-operatively with BMSCs compared to the scaffold only or a devitalised cell matrix/scaffold combination.

Kon et al. (2000) preceded their orthotopic, large animal work with a small animal study demonstrating the osteoinductive effects of ovine BMSCs when loaded into fibrin-coated HA blocks, and implanted subcutaneously in nude mice. Interestingly, it has been suggested that an ectopic intramuscular site, which is extremely vascular, could be an effective *in vivo* bioreactor for bone tissue (Stevens et al. 2005; Warnke et al. 2006).

Bone tissue engineering can also be applied to cases where bone has been resected to treat tumours such as high-grade osteosarcomas, Ewing's sarcoma, or malignant fibrous histiocytoma (Kenan et al. 1987). The patients are given pre-operative and post-operative chemotherapy to prevent the spread of the tumour and the possibility of metastases. One study demonstrated an improvement of the five-year survival of stage IIB osteosarcoma patients from 32% without chemotherapy to 57% with this treatment (Eckardt et al. 1991). Lee et al. (2005) showed a negative effect of a neoadjuvant chemotherapy regime on BMSCs proliferation on osteogenesis *in vitro* and new bone formation in a rat osteotomy model, by using a combination of doxorubicin and cisplatin. However, he was also able to demonstrate in a rat femoral defect model with external fixation, that the application of fibrin glue and BMSCs to the defect site resulted in similar amounts of bone formation, whether or not the rats had been given chemotherapy. These studies therefore both indicate a role for BMSCs in bone regeneration after chemotherapy, as well as the effectiveness of BMSCs in combination with fibrin glue for augmenting new bone formation at an orthotopic site.

In 1998, Bruder et al. demonstrated the effectiveness of autologous BMSCs in the healing of canine segmental bone defects, when the cells were loaded onto a fibronectin-coated, β -TCP cylindrical construct. The femoral implants were supported by a lengthening plate and left *in situ* for 16 weeks (Bruder et al. 1998). In this case, the BMSCs resulted in a noticeable bony callus around the implant, as well as significantly more bone formation than the controls (untreated with fibronectin and cell-free). Untreated defects (with no implant or treatment) resulted in non-unions after sixteen weeks, and those ceramic implants that were not cell-loaded began to show signs of cracking at twelve weeks, in contrast to the cell-loaded implants. This same group showed similar results after 16 weeks in the same canine defect model, but this time substituting allogeneic BMSCs that were dog leukocyte antigen (DLA, analogous to HLA)-mismatched as opposed to autologous cells (Arinzeh et al. 2003). Petite et al. (2000) attempted critical-sized defect bone regeneration, with the goal of preventing non-union. As an alternative to autograft, the group created a BMSC-coral “biohybrid,” and compared bone formation and union of the scaffold to host bone in an ovine model. The group first established the minimum length for non-union in sheep by creating a series of metatarsal defects and observing their ability to achieve union, that is, ability to heal and form new bone to bridge the gap rather than become scarred (Petite et al. 2000). They then created a “biohybrid” to fit the critical-size defect and tested BMSC-loaded coral constructs and fresh bone marrow-loaded constructs to cell-free scaffold controls and untreated defects. They found that while the untreated defects did not heal after 16 weeks, cell-free scaffolds achieved some bone growth, although they did not integrate into the host bone. Those constructs containing fresh bone marrow were filled with fibrous tissue more akin to scar tissue than bone formation, whereas BMSC-loaded constructs demonstrated mostly new bone formation and union with the host bone (Petite et al. 2000).

In another large animal model, a BMSC-loaded construct was implanted into critically sized defects of sheep. BMSCs were loaded into HA cylinders by coating them with fibrin and absorbing a cell solution into the fibrin-ceramic scaffold. This cell-loaded group had noticeably more bone growth into the construct, as well as greater callus formation around the implant, bridging it to the host bone (Kon et al. 2000). However, it must be noted that the group size was too small for meaningful statistical analysis.

Similarly for other types of tissue engineering of mesenchymal tissues, such as articular cartilage and craniofacial tissue (Frosch et al. 2006; Shang et al. 2001), ceramic or metal implants have been used as a scaffold for BMSCs, and tested in large animal models. In these cases it has been shown that BMSCs can be used to restore other tissues that provide important functional and or aesthetic roles.

1.4.5 Growth factors: Cytokines to target bone formation and revascularisation

In an effort to stimulate natural molecular mechanisms that trigger bone formation, one can implant growth factors at a site where bone regeneration or formation is required, or incorporate them into a scaffold in the presence or absence of osteoprogenitor or osteoinductive cells. These factors can be used to target the temporal mechanism of bone growth. In this case, bone morphogenetic proteins such as BMP-2, BMP-4, BMP-7, or BMP-9, can be used to promote fracture healing, or healing of critical-sized defects (Lin et al. 2005; Mistry and Mikos 2005). Genes that also have been demonstrated to promote bone formation include sonic hedgehog (Edwards et al. 2005) and Runx2 (Byers et al. 2006). Vascularisation can be promoted by using growth factors such as VEGF, whether by direct protein or gene (DNA) injection into a site of bone repair (Geiger et al. 2005; Huang et al.

2005). There are, however, some disadvantages to using growth factors, such as their great expense, which makes their regular use exorbitant. For example, a study by Dimitriou et al. (2005) found that the average cost of treating a fracture non-union with BMP-7 cost approximately £7,338. In an American study by the Washington State Department of Labour and Industries (2003), treating a tibial non-union with BMP-2 cost approximately \$12,468 (about £6,764), which was about the same cost as treatment with autograft. Also, the effectiveness of growth factors is not completely predictable, and in some cases is comparative to the use of autograft (Friedlaender et al. 2001; Maniscalco et al. 2002). Autograft in this scenario refers to bone graft harvested from another site on the patient, such as the iliac crest (Burkus et al. 2003).

Similarly, osteoprogenitor cells or other cell types used for tissue engineering purposes can be genetically modified to express these growth factors. Use of a temporary vector, such as replication-incompetent adenovirus, which will insert its DNA into host cells and express the protein for a limited period of time, has its advantages (Lieberman et al. 1999; Tsuchida et al. 2003). These advantages include the targeted temporal expression of the genes of interest, as well as preventing over-expression of the gene, and not using a virus prevents the risk of adverse immune reactions or the formation of recombination-competent virus. In some cases the adenoviral vector has been injected directly into a site of repair (Kang et al. 2004). However, long-term expression of growth factors by cells can be achieved by using retroviral vectors. Replication incompetent retroviruses have been used to insert genes into the host genome of cells being implanted for use in bone tissue engineering (Breitbart et al. 1999; Mason et al. 2000).

1.5 Goals

The main hypothesis of this thesis is that viable BMSCs can be applied to implants using a fibrin glue-spray system, and increase bone formation adjacent to the implants and improve bone-implant contact.

This work aimed to improve fixation of orthopaedic implants to host bone in an attempt to reduce rates of aseptic loosening, and can be divided into five aims:

- 1) To isolate, grow and characterise BMSCs from the bone marrow using standard tissue culture methods, as well as differentiating the cells down different mesenchymal lineages.**
- 2) To investigate the behaviour of BMSCs in a fibrin glue scaffold, and determine if this therapy could potentially be applied as a spray by analysing the morphology of the cells using histological techniques, and measuring cell viability, metabolism, and proliferation using enzymatic and DNA-labelling assays.**
- 3) To determine if bone marrow stromal-like cells (peripheral blood stromal cells-PBSCs) can be isolated and grown from the peripheral blood as an alternative to bone marrow aspirates, and measure the influences of blood loss or G-CSF on circulating PBSC number.**
- 4) To test the system of sprayed, autologous BMSCs in fibrin in a large animal massive implant model, and measure the amount of bone growth around the implant when compared to an untreated implant, with the goal of improving fixation of the implant to reduce aseptic loosening, with the outcome determined in terms of radiological and histological measurements.**

- 5) To apply this same system in an *in vivo* model of implant loosening, and to compare the effects that different cell dosages have on new bone formation by assessing the amount of bone growth around the implant.**

CHAPTER TWO

THE ISOLATION, EXPANSION, AND CHARACTERISATION OF OVINE BONE MARROW STROMAL CELLS (OBMSCS)

2.1 Introduction

First identified by Friedenstein as being “fibroblast precursors” in 1976 (Friedenstein et al. 1976), bone marrow stromal cells (BMSCs) have been extensively studied, and their potential use in bone tissue engineering investigated. The primary characteristics of BMSCs were originally identified by their adherence to tissue culture plastic, fibroblastic morphology and their ability to form colonies, derived from a single cell, called colony-forming units-fibroblastic (CFU-F). When the cells were transplanted in porous ceramic cubes into the backs of nude mice, significantly more bone was produced than blocks alone, indicating the bone-forming potential of these cells (Friedenstein et al. 1970; Castro-Malaspina et al. 1980; Owen et al. 1988). There are two main methods used to characterise BMSCs. The first is to demonstrate the multipotency of the BMSCs by differentiation down two or more lineages (Pittenger et al. 1999), the second is to use cell surface marker identification (Bruder et al. 1997).

When cultured with dexamethasone, ascorbic acid, and β -glycerophosphate, or BMPs (Friedman, Long and Hankenson 2006; Chaudhary, Hofmeister and Hruska 2004) BMSCs have been observed to change morphology to a cuboidal, osteoblastic shape; express genes related to osteoblastic differentiation (Krishnan et al. 2003; Pittenger et al. 1999), and produce nodules that stain positively for calcium (Jaiswal et al. 1997; Gronthos et al. 1994). BMSCs have been stimulated to differentiate into other mesodermal cell types such as adipocytes, chondrocytes, and even neuronal cells.

In vitro mineralisation can be tested by using a substitution reaction that allows visualisation of the nodules with light microscopy (Von Kossa assay). This stain has been used for many

years to indicate regions where calcium is deposited, which contain both phosphate and carbon salts. Following exposure to bright light, the Ag⁺ ion in silver nitrate replaces the calcium ion in these salts and stains the calcium deposit brown-black. This stain has also been used to show osteogenic differentiation of BMSCs (Schecroun and Delloye 2003; Gronthos et al. 1994).

Use of energy dispersive analysis of X-rays (EDAX) to identify and quantify the elemental composition of these nodules can be used to identify the presence of hydroxyapatite crystals (Best et al. 2004). Additionally, osteoblasts are known to express alkaline phosphatase (ALP) on their cell surface in order to create an alkaline environment in which bone mineral is laid down. An ALP assay determines the activity of alkaline phosphatase (ALP) expressed by the differentiating cell. As stromal cells differentiate into osteoblasts, an increase in ALP has been observed in many studies (Rust PA 2005; Oreffo et al. 1998). In these studies, differentiated cells were compared to undifferentiated BMSCs that had not been exposed to the same chemical cues (dexamethasone, ascorbic acid and β -glycerophosphate). ALP cleaves the phosphate group found in p-nitrophenol phosphate to produce p-nitrophenol, which is alkaline, and can be spectroscopically detected at 405 nm. This increase in coloured product created by the enzymatic reaction is compared to the reaction time to produce a reaction rate, or enzyme activity rate. Oreffo et al. (1998) used this reading to indicate differentiation of bone marrow osteoprogenitors into osteoblasts.

After culture with dexamethasone, indomethacin, 1-methyl-3-isobutylxanthine, and insulin (Pittenger et al. 1999), BMSC-derived adipocytes collect lipids that can be detected using stains such as Oil Red 'O' and Sudan Black IV (Sotiropoulou et al. 2005). Oil Red O is a

lipid-soluble dye used as a histochemical stain to indicate the presence of neutral lipids, triglycerides, cholesterol esters, markers of adipocytic cells (Preece 1972).

The second method used to identify BMSCs is to determine cell surface marker expression. A panel of positive and negative reactions for various markers has been extensively used to isolate and identify BMSCs, and this expression is often used for fluorescence or magnetic-activated cell sorting techniques (FACS and MACS, respectively). Cells are subjected to such a panel of markers in order to ensure positive identification. A number of studies have identified both positive and negative markers for BMSCs; however, there is no single positive marker for these cells (due to their plasticity and often unpredictable reaction to these markers). Even Stro-1, a commonly-used hBMSC marker, reacts positively with some glycophorin-A-positive nucleated red cells and B-lymphocytes that are often isolated from the bone marrow along with hBMSCs (Gronthos 2003) - emphasising the need to test for multiple cell surface markers.

Previous work has attempted to characterise ovine BMSCs, however, these cells not been as well documented as the BMSCs from other species. In this chapter, a protocol for the isolation, expansion, and characterisation for ovine BMSCs is presented and discussed.

Hypothesis: Multipotential ovine BMSCs (oBMSCs) can be isolated from ovine bone marrow and expanded in culture, and differentiated down three different cell lineages: the osteoblastic, chondrogenic and adipogenic lineages.

The aims and objectives of this chapter are to:

1. To isolate BMSCs from ovine bone marrow aspirates.

2. To expand ovine BMSCs cells in culture using two-dimensional cell culture methods.
3. To differentiate oBMSCs down mesenchymal cell lineages: osteoblastic and adipogenic; using specific chemical cues for differentiation.
4. To confirm the differentiation of oBMSCs down mesenchymal lineages using standard histological and immunohistochemical techniques.

2.2 Methods

2.2.1 Isolation, Culture, and Expansion of oBMSCs

English mule ewes were selected for use in this study. These animals were skeletally mature (two to five years in age), and weighed between 65-90 kg. All procedures were carried out according to the Home Office Animals Scientific Procedures Act of 1986. Bone marrow aspirates were taken from sheep iliac crests using an aseptic technique, as follows.

2.2.1.1 Anaesthesia and Pre-Operative Preparation

Sheep were premedicated with an intramuscular (IM) injection of Xylazine (0.1 mg/kg, Rompun, Bayer Health Care, Newbury, Berkshire, UK), 10-30 minutes prior to induction of anaesthesia. Sheep were then administered Ketamine (2 mg/kg, Ketaset, Fort Dodge Animal Health Ltd, Southampton, UK) and Midazolam (2.5 mg, Hypnovel, Roche Products Ltd., Welwyn Garden City, Hertfordshire, UK) intravenously (IV) into the jugular vein to induce anaesthesia. An endotracheal tube was then inserted and connected to an anaesthetic machine. Anaesthesia was maintained using a 2% halothane (Merial Animal Health Ltd., Harlow, Essex, UK) and oxygen mixture, which was adjusted as required. A stomach tube was inserted. A 10 cm² area of skin overlying the iliac crest was then prepared, first by shaving,

then by treatment with Povidine, a Povidone-iodine scrub and antiseptic solution (C-Vet, Bury St. Edmunds, UK). The area was then covered with a fenestrated drape.

2.2.1.2 Procedure for Bone Marrow Aspiration

A 0.5% w/v chlorhexidine gluconate solution in spirit (Adams Healthcare, Leeds, UK) was then applied to the skin as a sterilising agent, before a small incision directly positioned on top of the iliac crest was made. A Jamshidi biopsy needle (R56780, Rocket Medical, Washington, UK) was used to penetrate into the intramedullary cavity of the iliac crest. A minimum of 8 mL of bone marrow was aspirated, in 4 mL aliquots (Rust P et al 2004). Clotting was prevented by drawing up aspirates in syringes containing 0.5 mL heparin (1000 units/mL) (Monoparin, CP Pharmaceuticals, Barnstable, UK). Post-operatively, animals were given 0.6 mg Buprenorphine as an analgesic (Vetergesic, Alstoe Animal Health, Melton, Mowbray, UK), as well as a long-acting antibiotic (15 mg/kg Amoxillicin, Betamox LA, Norbrook Laboratories (GB) Ltd., Great Corby, Carlisle, UK).

2.2.1.3 BMSC Isolation and Expansion

Manipulation of aspirates and cells took place in a lamellar flow hood. Each 4 mL aliquot of ovine bone marrow was carefully layered on top of a 3 mL layer of Ficoll-Paque™ PLUS sucrose gradient (17-1440-02, Amersham Biosciences, Chalfont St. Giles, UK). This gradient was used to separate the bone marrow components by density centrifugation. After layering, samples were spun in a refrigerated centrifuge at 1500 rpm, at 4°C, for 30 mins. After this time, layers became apparent in the sample, with a bottom layer that included an upper buffy layer, containing the mononuclear cells of the bone marrow (Ficoll® users guide). This buffy layer was carefully removed and washed with 10 mL of DMEM media (DMEM+, or control

media), supplemented with 10% fetal calf serum (FCS, First Link, UK) and 100 units/mL penicillin/streptomycin (P/S, 0082, Invitrogen, Paisley, UK). The cell suspension was then centrifuged for 5 minutes at 2000 rpm at room temperature. The supernatant was discarded and the remaining pellet resuspended in 1 mL DMEM+ using a 21 gauge needle and 1 mL syringe, before being transferred to a T25 polystyrene cell culture flask (Corning, Corning, NY, USA) with 4 mL of media. This flask has a surface area of 25 cm² for cell expansion, and a treated surface for cell adhesion (Ramsey WS 1984, Amstein CF 1975).

Flasks were kept in a humidified incubator at 37°C, with 5% CO₂. Within 7-14 days, colony-forming units (CFU-Fs) became apparent in the flask. Once these cells had expanded to cover 70% of the cell culture surface (70% confluent), cells were “passaged,” or expanded further (approximately 10-14 days).

DMEM+ in the cell culture flasks was removed and discarded, using a pipette. The cells were then washed with cold phosphate buffered saline (PBS), which was also discarded. The cell culture surface was incubated at 37°C for 5 minutes with a 0.5% trypsin- 5.3 mM EDTA·4Na solution (15400-054, Invitrogen, Paisley, UK), diluted from a 10x stock solution with PBS. After 5 minutes, the cells lifted off the surface, and the trypsin was neutralised by adding a 1:1 volume of DMEM+. In order to determine cell viability, a 0.4% Trypan Blue solution (T8154, Sigma-Aldrich, Dorset, UK) was then used in a 1:1 ratio with a small quantity of the cell suspension. A haemocytometer was used to quantify the concentration of cells under a phase-contrast light microscope. Trypan Blue is a dye with two azo chromophores. The chromophore is negatively charged, and thus only reacts with cells when the membrane is damaged. Thus it is assumed that the (blue) stained cells are dead and the unstained (clear) cells are alive (Biosource AlamarBlue™ manual). The cell suspension was then centrifuged

for 5 minutes at 2000 rpm at room temperature, to obtain a cell pellet. The supernatant was discarded, and the cell pellet then resuspended in 1 mL of DMEM+ (control media) using a 21 gauge needle and syringe. Approximately 3,000 – 4,000 cells were seeded per cm² of cell culture area, and cells cultured in 0.1333 mL of DMEM+ (control media) per cm² of surface area. DMEM+ (control media) media was changed every 3-5 days. This technique was used to expand cells when they reached 70-80% confluence on the cell culture flasks, until passage 3-4, at which time they were used in *in vitro* and *in vivo* experiments.

2.2.2 Characterisation of Ovine Bone Marrow Stromal Cells-Differentiation

2.2.2.1 Osteogenic Differentiation

Osteogenic Media (from Rust 2005 and Kostura et al. 2004):

	Dulbecco's Modified Eagle's Medium (DMEM) (4500 mg/L glucose, D6429, Sigma-Aldrich, Dorset, UK)
10%	Fetal calf serum (FCS; First Link, UK)
1.0%	Penicillin/streptomycin (P/S; 0082, Invitrogen, Paisley, UK)
1.0×10^{-7} M	Dexamethasone, water-soluble (D2915, Sigma-Aldrich, Dorset, UK)
5.0×10^{-4} M	Ascorbic Acid (255564, Sigma-Aldrich-Aldrich, Dorset UK)
1.0×10^{-2} M	β -glycerophosphate (G9891, Sigma-Aldrich, Dorset, UK)
For both the osteogenic and adipogenic supplemented media, FCS and P/S were added to the	

DMEM. The differentiating reagents were dissolved in 10 mL of this solution, then added back to the bottle of DMEM using a 0.2 μ m filter with a sterile 10 mL syringe.

Dexamethasone is a common glucocorticoid used in all of the differentiation media. Used on its own as a cell culture media supplement, it has been shown to promote adipogenic and myogenic differentiation of hBMSCs (Grigoriadis, Heersche and Aubin 1988; Yin, Li and Wang 2006) and has been suggested that it decreases the expression of bone matrix protein

mRNA transcripts (Cheng, Zhang and Avioli 1996), although a study by Igarashi et al. (2004) disputes this evidence.

oBMSCs were isolated, expanded, and trypsinised as described above. For histochemical staining (Von Kossa), 6×10^4 cells were plated out onto Thermanox[®] coverslips (Nalge Nunc International, Rochester, NY, USA), which had been placed at the bottom of the wells of 12-well plates (Corning, NY, USA). 1 mL of supplemented osteogenic media was added to each well. Cells were grown in a standard humidified incubator, and media was changed every 3-5 days. Cell morphology was observed every 5-7 days, up to 28 days after the initiation of culture.

For the alkaline phosphatase (ALP) assay, 6.0×10^4 cells were plated into 6-well plates (Nunc, NJ, USA) and grown for 7, 14, 21 and 28 days. For each cell line, there were two groups: cells grown in standard supplemented media, and cells grown in osteogenic media. Each group was repeated in triplicate for each time point.

2.2.2.2 Adipogenic Differentiation:

Adipogenic Media (from Rust 2005):

	Dulbecco's Modified Eagle's Medium (DMEM) (4500 mg/L glucose, D6429, Sigma-Aldrich, Dorset, UK)
10%	FCS (First Link, UK)
1.0%	P/S (0082, Invitrogen, Paisley, UK)
1.0×10^{-6} M	Dexamethasone, water-soluble (D2915, Sigma-Aldrich, Dorset, UK)
200 μ M	Indomethacin (I7378, Sigma-Aldrich, Dorset, UK)
500 μ M	1-methyl-3-isobutylxanthine (I5879, Sigma-Aldrich, Dorset, UK)
10 μ g/mL	Insulin (I0516, Sigma-Aldrich, Dorset, UK)

For adipogenesis, 1×10^5 cells were cultured per well in 12-well plates, on Thermanox coverslips. Cells were cultured in adipogenic media for 21 days, with media being changed every 3-5 days. After 21 days, cells were fixed in 10% neutral buffered saline (NBS).

2.2.2.3 oBMSC Passage Number

For adipogenic and chondrogenic differentiation, cells of passage four were used. For osteogenesis, however, cells of both passage 4 and passage 12 were used. As a direct comparison for sheep BMSCs, goat BMSCs were also differentiated as described above, and Von Kossa and ALP biochemical assays were performed.

2.2.2.4 Negative Controls

As negative controls, the HaCat (human transformed keratinocyte) and LG3 (human leukaemia monocytic) cell lines were used. HaCat cells are a transformed keratinocyte cell line, which means that they can continuously proliferate. The LG3 cell line is a lung fibroblast-derived cell line.

2.2.3 Histology-Osteogenesis

2.2.3.1 Von Kossa Assay

Cells were cultured on coverslips in osteogenic media for 28 days, after which the coverslips were washed with PBS after discarding the cell culture media. The coverslips were then fixed in methanol for 10 minutes. The coverslips were then gently washed with distilled water three times, after which they were incubated in 1.5% silver nitrate (762000, Hopkin & Williams, UK) under a lamp for one hour. The light promotes the reduction of Ca^{2+} ions in the presence of silver nitrate. After incubation, the silver nitrate was discarded and the coverslips were gently washed 3 times with distilled water. At this point, samples were covered with 2.5% thiosulphate (Fisions Scientific Apparatus, Loughborough, UK) for 5 minutes, after which

samples were gently washed once with distilled water. Coverslips were counterstained for 5 minutes with Neutral Red (x634, Sigma-Aldrich, Dorset, UK), which stains cell nuclei red, and afterwards rinsed gently in distilled water until clear. A negative control was prepared prior to staining by pretreating a coverslip with 5% acetic acid for 2 minutes. Photos were taken using an Olympus BH2 photographic microscope and a JVC KY F55B Colour Video Camera using Zeiss KS300 software (Imaging Associates, Thame, UK).

2.2.3.2 ALP quantitative biochemical assay (Cobas Bio)

For the assay, a kit was used (AP307, Randox Laboratories, Antrim, UK). Pre-weighed p-nitrophenol powder was mixed with 10 mL of diethanolamine buffer and pre-heated to 37°C to produce the working reagent. Cell culture samples, either treated with DMEM+ or osteogenic DMEM+, were washed in PBS, then cells were lysed by adding autoclaved, distilled water at 37°C (a hypotonic solution). Samples were frozen and thawed three times, then transferred to Eppendorf tubes and spun in an ultracentrifuge at 10,000 rpm for 10 minutes. 50 µL of the resultant supernatant was loaded into Cobas Bio® blue sample cups (AS Diagnostics, Blackpool, UK). 0.25 mL of the p-nitrophenol phosphate working solution was used for each sample. The reagent and samples were loaded into the Cobas Bio® analyser (Roche, Lewes, UK) to run the assay. ALP activity measurements were calculated as U/L.

To compare results within groups, ALP activity readings were normalised for the number of cells, by measuring the amount of DNA in each sample. This was done using the fluorometric dye Hoechst 33258, which binds specifically to the adenine-thymidine base pairs of DNA (Rago, Mitchen and Wilding 1990, Rao and Otto 1992). For the assay, lysed samples were transferred from cell culture dishes to Eppendorf tubes, which were spun in an ultracentrifuge

at 10,000 rpm for 10 minutes, and the supernatant transferred to fresh tubes. A standard curve was prepared in a Fluoronunc® 96-well plate (Nunc, Roskilde, Denmark), by diluting a stock, 1 mg/mL DNA standard (from calf thymus, D3664, Sigma-Aldrich, Dorset, UK) in saline sodium citrate (SSC) buffer, to 20, 10, 5, 2.5, 1.25, 0.625 and 0.3125 µg/mL, and loading 100 µL of the standards into the 96-well plate in triplicate. To prepare 500 mL of a 20x stock SSC buffer (20x the working concentration), 87.65 g of sodium chloride and 44.1 g of trisodium citrate was dissolved in distilled water and the pH was adjusted to 7.0 with 1M HCl or 1M NaOH.

A map of the 96-well plate was made to record the standard/sample order. 100 µL of each sample was loaded into the plate in duplicate. The Hoechst 33258 dye (B2883, Sigma-Aldrich, Dorset, UK) was diluted from 1.0 mg/mL to 1.0 µg/mL in SSC and 100 µL added to each standard or sample well in the Fluoronunc® plate. Samples were run in a Fluoroskan Ascent® fluorimeter (Labsystems, Finland), using Genesis version 2.19 (Life Sciences UK Ltd.) and Ascent Research Edition version 1.1.1 software (Labsystems, Finland). The adenine-thymidine-Hoechst 33258-specific fluorescence was read at 460 nm. From the standard curve, the DNA concentrations could be calculated. For this, Microsoft Excel was used to plot the known concentration of the standards versus their absorbance at 460 nm, and a linear equation fitted to the resulting line. Equations having a correlation coefficient of 0.95 or above were acceptable for calculating the DNA concentrations of the samples.

ALP activity (U) per µg DNA was calculated as follows:

$$\frac{\text{ALP activity (U/L)}}{\text{Sample DNA concentration} \times 0.05 \text{ mL (volume of each sample used for ALP assay)}} = \frac{[\text{ALP activity (U/mL)} / 1000]}{1}$$

2.2.3.3 Scanning Electron Microscopy (SEM)

Cells attached to coverslips were fixed in 1.5% glutaraldehyde (SEM grade, Agar Scientific, Stansted, UK) diluted in 0.1M sodium cacodylate (Na Cac, Agar Scientific, Stansted, UK) buffer for at least six hours. After this, samples were washed in 0.1M Na Cac buffer for 10 minutes, then treated for two hours in 1% osmium tetroxide (Agar Scientific, Stansted, UK) in 0.1M Na Cac buffer. After this period of time, samples were washed in 0.1M Na Cac buffer three times for five minutes. Samples were then covered with 1% tannic acid in 0.05M Na Cac buffer for one hour. After this, samples were washed for 5 minutes in 0.1M Na Cac buffer, then dehydrated with decreasing dilutions of industrial methylated spirit (IMS) in distilled water, from 20% IMS to 96% IMS, for 5 minutes each. The samples were then dehydrated in 100% ethanol dried with sodium sulphate for 10 minutes and 15 minutes. Samples were then treated with hexamethyldisilazane (H.M.D.S., H4875, Sigma-Aldrich, Dorset, UK) three times for 2 minutes each, then air-dried. Dried coverslips were then mounted onto titanium discs and sputter-coated using an Emitech K550 Sputter Coater (Emitech, Ashford, Kent, UK). Samples were then visualized using a Jeol JSM-5500LV Scanning Electron Microscope (SEM) using the corresponding Jeol User Interface version 4.04 (Jeol Technics, Welwyn Garden City, UK), at 5kV.

2.2.3.4 X-ray detection using Electron Dispersive Analysis of X-Rays (EDAX)

Electron probe X-ray microanalysis characterises elements present in a sample using x-ray detection. It has been used previously to determine a calcium-phosphate ratio in mineralised tissues, as would be found in bone containing hydroxyapatite ($\text{Ca}_{10}(\text{PO}_4)_6(\text{OH})_2$). This uses the SEM-prepared samples in the SEM machine, in combination with the EDAX PV9830 Genesis X-Ray Microanalysis System (XMS), with EDAX Genesis[®] software (EDAX UK, Cambs. UK) at 1500x magnification, and 15.0 kV. The percentage (%) weight of calcium

content of samples was divided by the percentage weight of phosphate to give a calcium to phosphate (Ca/P) ratio. The stoichiometric ratio of calcium to phosphate naturally found in hydroxyapatite is 1.67 (Nayar et al. 2006).

2.2.3.5 Alamar Blue Activity Assay

To observe the effect of osteogenic media on cell activity and viability, the AlamarBlue™ assay was used. AlamarBlue™ is a redox indicator; it changes colour from blue/non-fluorescent to red/fluorescent after being reduced from an oxidised state. This redox reaction is related to metabolic activity and cell growth, where a reductive environment indicates cell growth. It is reduced as a result of acting as an intermediate in the electron transport chain of the cells. This is in contrast to other assays, such as the MTT assay (Korda et al. 2006), which interrupt the flow of electrons throughout the chain, causing a shutdown of the electron transport chain and eventually cell death (AlamarBlue™ manual). For this assay, 6.0×10^4 cells were plated out per well in a 12-well plate (Corning, Corning, NY, USA), 1 mL of standard DMEM+ added, and cells incubated for 24 hours in standard conditions to permit cell attachment. The following day, the media was changed, so that half of the samples were cultured in DMEM+ and half cultured in DMEM+ with osteogenic supplements. After 24 hours, AlamarBlue™ was diluted in PBS to make a 10% working solution. This solution (1 mL) was added to each well and the plates incubated under standard conditions for 4 hours. After 4 hours, 100 μ L from each AlamarBlue™-reacted sample was loaded in duplicate into a FlurorNunc™ white fluorometric 96-well plate, and absorbance read in a fluorometer. The excitation frequency was 560 nm and the absorbance frequency was 590 nm. Results are expressed as absorbance at each time point.

2.2.3.6 Thymidine- H^3 Cell Proliferation Assay

This assay measures the rate of cell proliferation by measuring the rate of DNA synthesis. Radioactive thymidine- H^3 (thy- H^3 , GE Healthcare, Giles, Buckinghamshire, UK) is added to the culture media of cells and incorporated into nascently synthesised DNA (Maurer 1981, Millipore 1991). For this assay, 1.0×10^5 cells were added to each well of 3 6-well plates (Orange Plastics, Triple Red Laboratory Technology, Long Crendon, Buckinghamshire, UK), covered with 2.0 mL of standard DMEM+ and left overnight to allow cell attachment under standard conditions. Afterwards, the media was changed in all wells, half of the wells receiving 2.0 mL of standard media and half receiving 2.0 mL osteogenic media. At this point, in one plate, 1.0 μ L of thy- H^3 was added for each 1.0 mL of media, and placed in a designated standard humidified incubator for 24 hours. After this time, the media was removed and cells washed with PBS. Autoclaved, distilled water (1mL) was added to each well, and the cells left to lyse at 37°C for one hour, after which they were frozen at -20°C. The above steps were repeated between 24-48 and 48-72 hours after adding osteogenic supplements to cells. After the 72-hour period, all cell lysates were freeze-thawed 3 times. The samples were transferred to 1.0 mL Eppendorf tubes and centrifuged at 10,000 rpm for 10 minutes. For the scintillation assay, 200 μ L of 20% trichloroacetic acid (TCA, T6399, Sigma-Aldrich, Dorset, UK), at 4°C was added to all the wells of 96-well Millipore Multiscreen[®] filter plates (Millipore U.K. Ltd, Watford, UK). This TCA was aspirated off using a Millipore Multiscreen[®] vacuum manifold (Millipore, Watford, UK). 100 μ L of the cell lysate was then loaded into the wells of these plates, a plate map being used to track samples. Following the samples, a further 100 μ L of 20% TCA at 4°C was added to all wells. The plates were incubated at 4°C for 30 minutes, on a shaker, after which the plates were aspirated again. Wells were washed with 200 μ L 10% TCA, aspirating the wells after each wash. The plastic underside of the plates were then removed and the filters left to dry

overnight at room temperature. The 96-well filters were then punched out into scintillation vials and 500 μ L 0.01M potassium hydroxide were added to vials, which were then mixed on a R100/TW Rotatest shaker (Luckham, Burgess Hill, Sussex, UK) for 2 hours. After this, 4.0 mL of scintillant (6013119, Ultima Gold™ XR, PerkinElmer, Boston, USA) was added to each vial. Vials were then capped, vortexed and read on a β -counter (Tri-Carb 2900TR Liquid Scintillation Analyzer, PerkinElmer, Boston, USA). Results were read using Quanta Smart 1.31 software (Packard Instrument Co.) for Windows NT.

1.3.7 Histology-Adipogenesis

Oil Red 'O' Stain

A stock Oil Red 'O' solution was prepared by dissolving 0.5 g of oil red O in 500 mL isopropanol and warming the bottle for 30-60 minutes at 56°C. A working solution was made by diluting 30 mL of the stock solution in 20 mL distilled water. After 14 days in adipogenic media, cells were fixed in neutral buffered formalin for 10 minutes, after which they were washed with distilled water and then stained in Oil Red 'O' for 10 minutes. After staining, cells were washed in distilled water and then counterstained using Harris' haematoxylin for 1 minute.

2.2.4 Statistics

For the ALP biochemical assay, activity and proliferation assay results, normality was determined with the Kolmogorov-Smirnov and Shapiro-Wilk tests, using SPSS 12. For non-parametric data, a comparison between groups was made using the Mann Whitney U test, where a p-value ≤ 0.5 was considered a significant result.

2.3 Results

2.3.1 oBMSCs-Observations

2.3.1.1 Colony-forming units-fibroblastic (CFU-Fs)

Within 5-7 days, fibroblastic colony-forming units (CFU-Fs) were observed in the cultures. These consist of a colony of fibroblastic-shaped cells originating from a single cell. After the first passage, cells took on a flat, fibroblastic morphology (Figure 2.1).

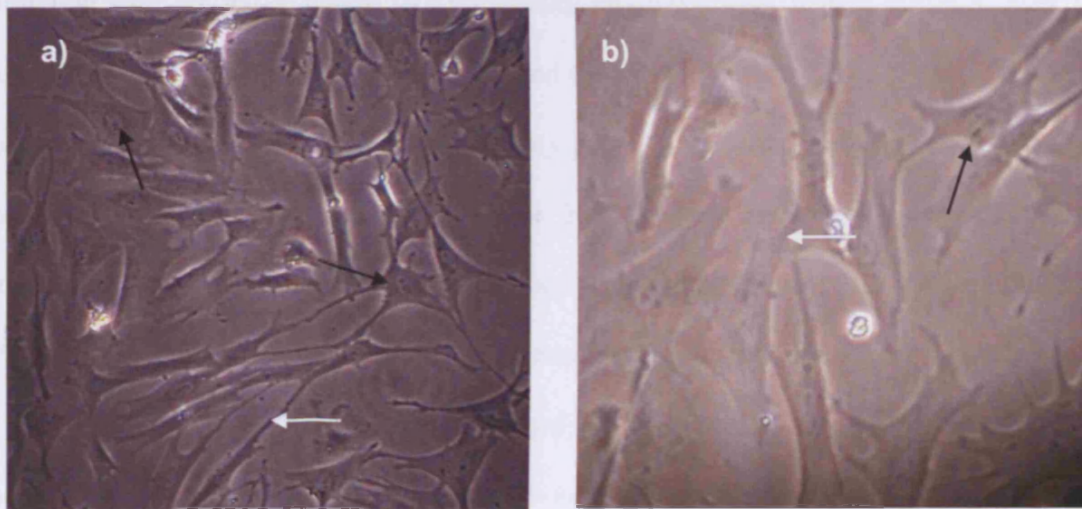


Figure 2.1 oMSCs after passage. Cells are flat, spindle-shaped in morphology, with large nuclei that have multiple, prominent nucleoli (see black arrows). The processes of some cells can be seen to be in contact (see white arrows).

2.3.2 Osteogenesis

2.3.2.1 Von Kossa assay-Visual Observation and Qualitative Analysis

After 28 days, those oBMSCs treated with osteogenic media had a greater positive reaction than those oBMSCs grown in normal media, with black deposits indicating sites of mineralisation. This included oBMSCs of a low passage, and high passage oBMSCs (Figure 2.2c-f). Interestingly, the untreated oBMSCs also stained positively to the Von Kossa assay, although to a far lesser extent. As previously described with human BMSCs, over the 28 days, a multilayer of cells eventually formed three-dimensional folds, resulting in retraction of cells on the plastic surface and thus empty pockets of culture plastic became available for cell proliferation (Schecroun and Delloye 2003). There was no distinct change in cell morphology over the 28 days. Negative controls samples (Figure 2.2a-b) were low-passage BMSCs that were negative for the Von Kossa stain after treatment with 5% acetic acid. It should also be noted that the immortalised keratinocyte cell line (HaCats) also reacted positively to the Von Kossa stain when treated with osteogenic media for 28 days, with a minimal reaction when grown in normal media. Figure 2.2 shows photographs taken of Von Kossa stain samples for the different cell lines.

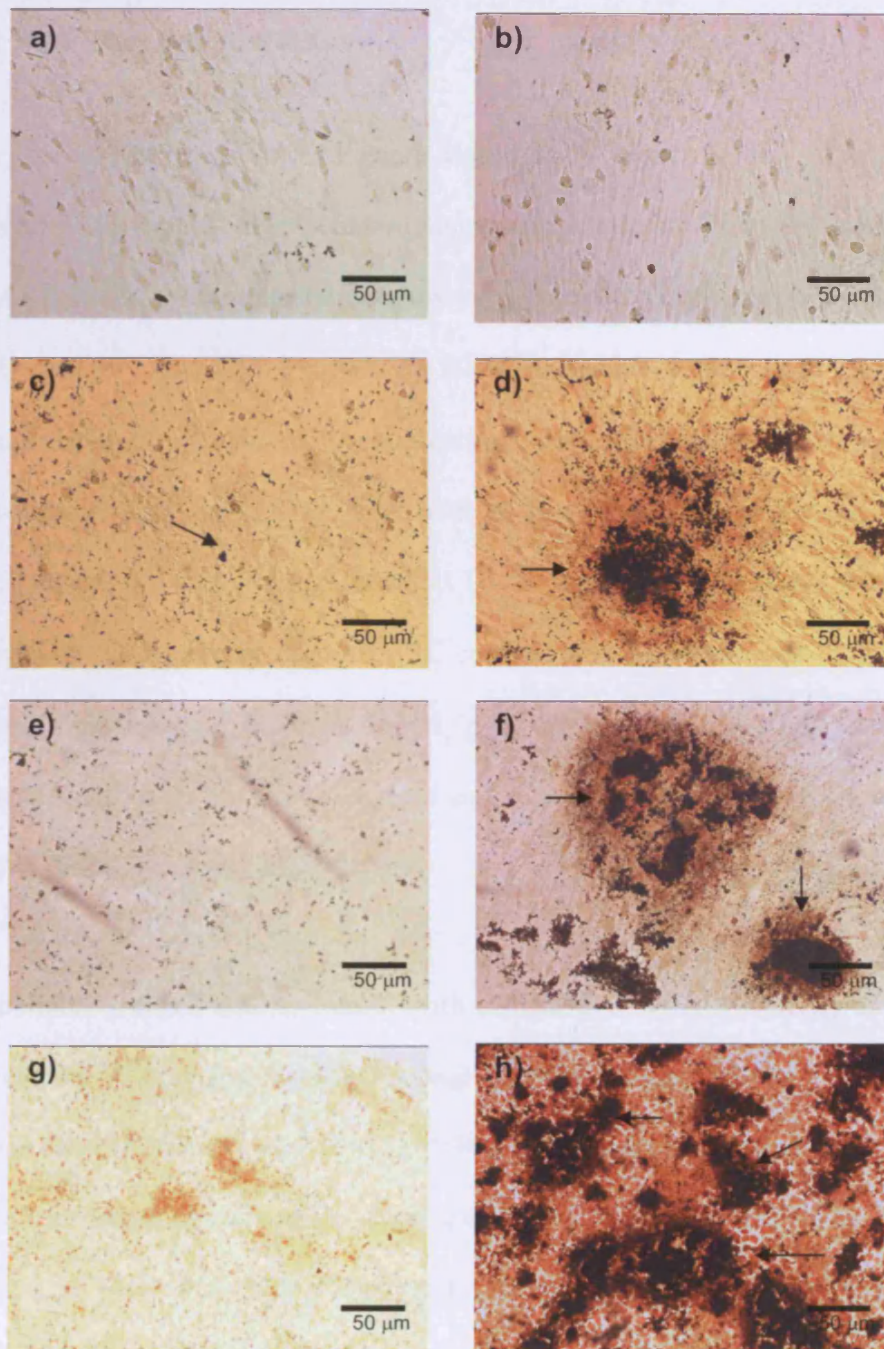


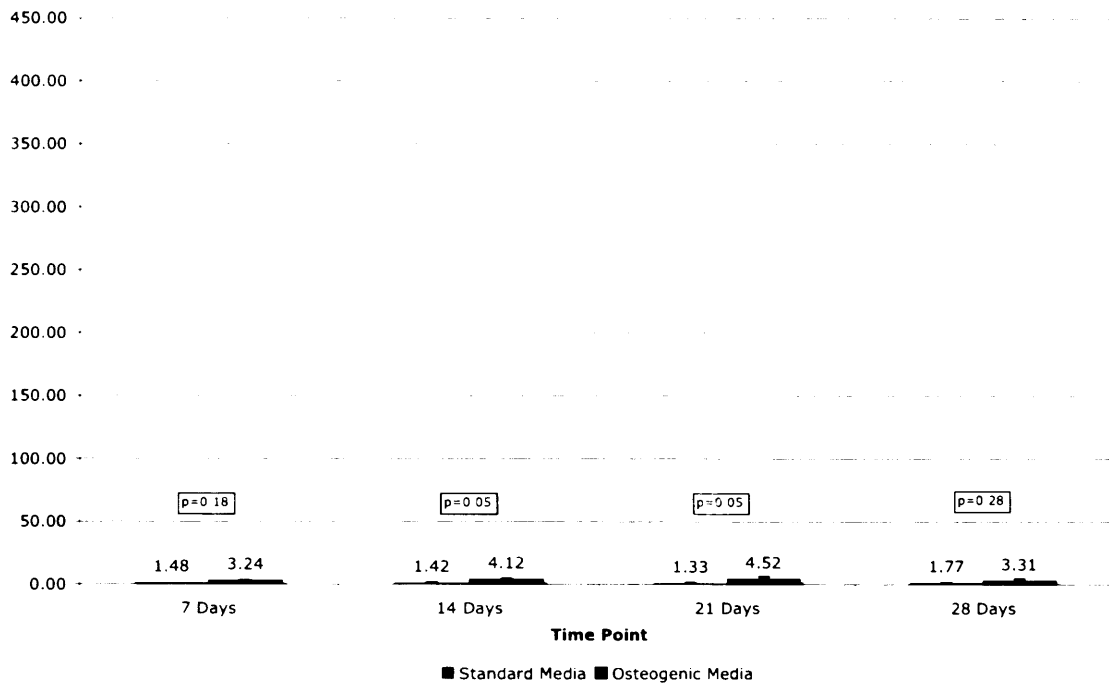
Figure 2.2 Results of Von Kossa staining (10x magnification). Images d, f, and h are low-passage ovine BMSCs, high-passage ovine BMSCs and HaCats, respectively, that were fixed and stained after being grown in osteogenic culture media for 28 days. Figures c, e, and g are negative controls of low-passage BMSCs, high-passage BMSCs, and HaCats (respectively), grown in non-supplemented DMEM+ for 28 days. Images a and b are low-passage ovine BMSCs that were treated with 5% acetic acid before staining to create a negative calcium control. Nodules of calcium mineral are stained black with the Von Kossa stain, and are indicated with arrows.

2.3.2.2 ALP Biochemical Assay

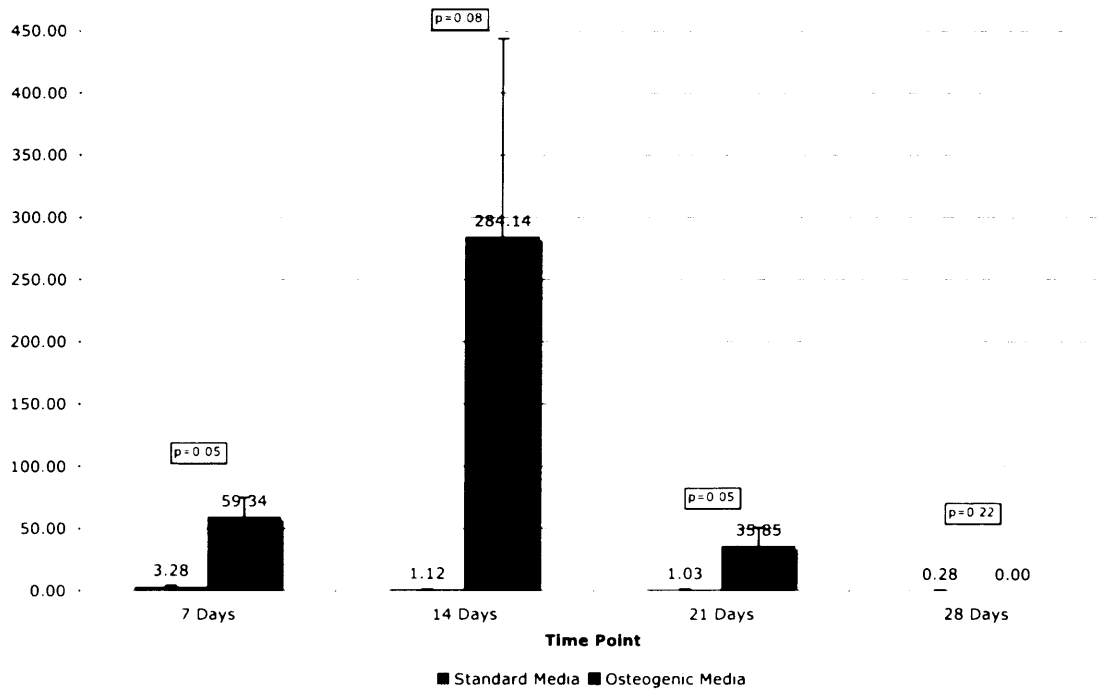
In all cultures, the levels of ALP were significantly higher at day 14 when cultured in osteogenic media compared to standard supplemented media. With treatment in osteogenic media, ALP activity was highest in the low-passage oBMSC cultures at days 14 and 21 (1.42 ± 0.53 U/ μ g DNA, and 1.33 ± 0.10 U/ μ g DNA, respectively; see Figure 2.3). There was no significant difference within each group (normal and osteogenic) at each time point in the low-passage oBMSC group. The ALP activity in osteogenic cultures was higher than in oBMSC cultures grown in normal media at 14, 21 ($p=0.05$ at both days 14 and 21), whereas the activity in the higher-passage oBMSC cultures was highest at day 14 (2.84×10^2 U/ μ g DNA), and significantly different at day 21 ($p=0.05$). Between days 7 and 14, and 7 and 28 in the control group, and between 21-28 days and 7-28 days in the osteogenic group, there was a significant difference in the ALP activity.

HaCat cultures showed similar trends, with a high level of ALP activity at all time points when treated with osteogenic media, and significantly different ALP activity when compared to normal oBMSC cultures at day 14 ($p=0.05$). Between time points in both the control and osteogenic groups, there was only a statistical significant difference between 7-14, 14-21, 21-28, 7-28, and 14-28 days in the osteogenic group. LG3-osteogenic supplemented cultures showed a significant difference in ALP activity at 7, 21, and 28 days ($p=0.05$ at all three time points). Looking at statistically significant differences between time points in LG3 cultures found a significant change in ALP activity between 21-28 days, 7-28 days, and 14-28 days in the control group, and between 7-14, 14-21, 7-21, 7-28, and 14-28 days in the osteogenic group.

a) Low-Passage oBMSCs (P₃)



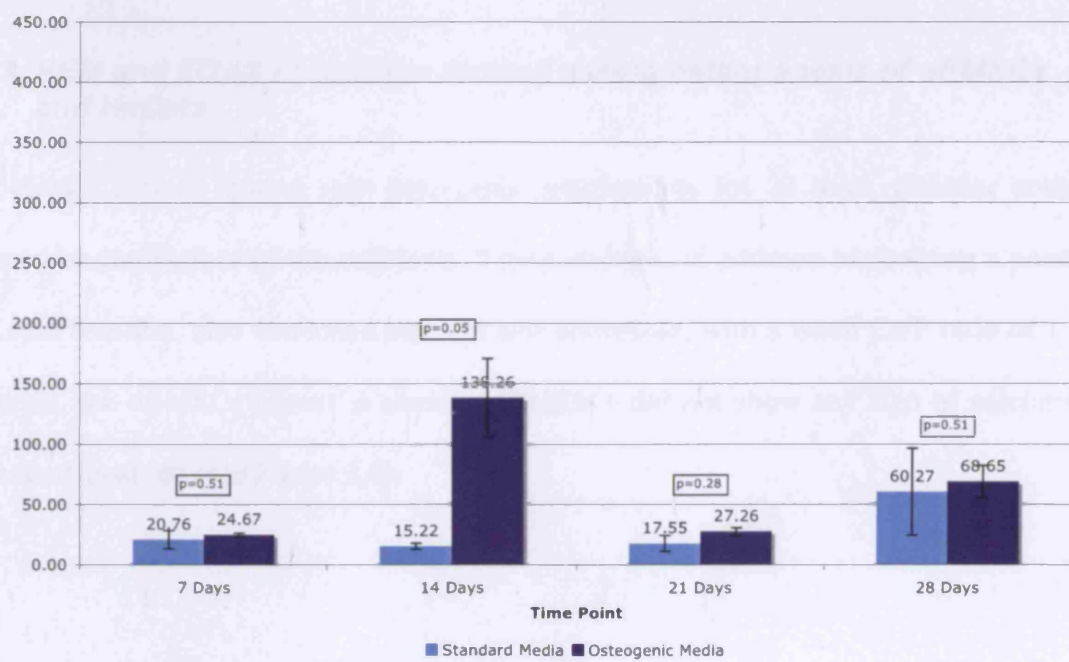
b) High-Passage oBMSCs (P₁₂)



c) gBMSCs (P₄)



d) HaCats



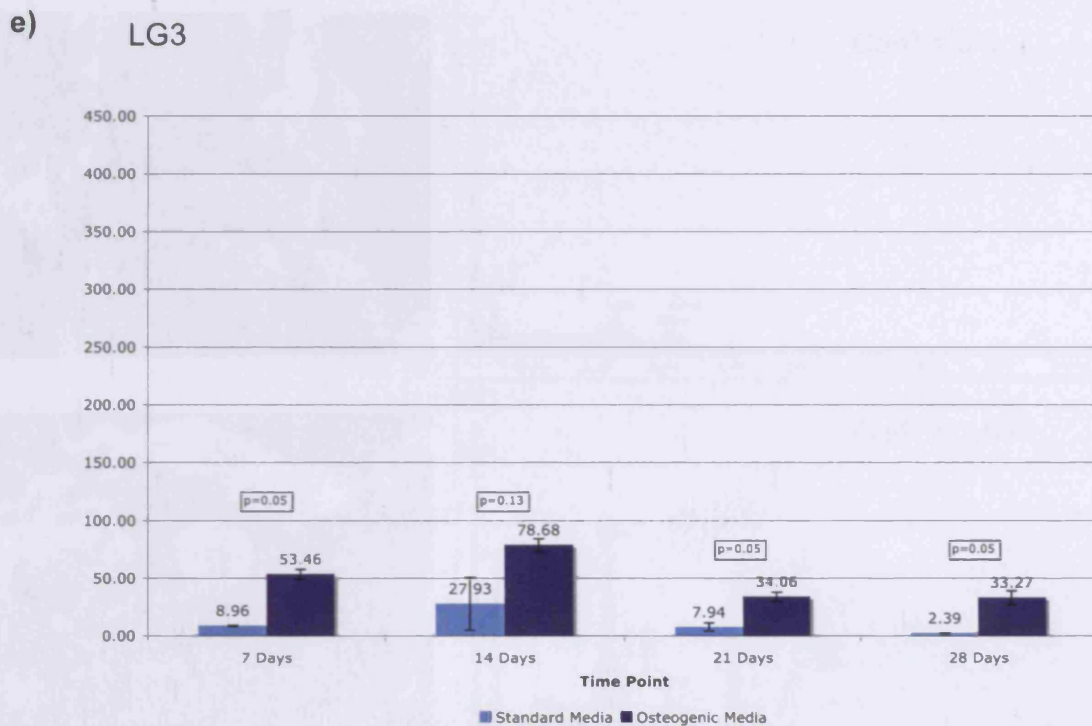


Figure 2.3 Graphs illustrating ALP biochemical assay results at 7, 14, 21, and 28 days after culture in osteogenic media. The cell lines tested include a) low-passage oBMSCs (P₃); b) high-passage oBMSCs (P₁₂); c) goat BMSCs (P₄); d) HaCats (transformed keratinocytes) and e) LG3 cell line (leukaemic monocytes).

2.3.2.3 SEM and EDAX of nodules formed during osteogenesis of oBMSCs and HaCats

When oBMSCs were treated with osteogenic supplements for 28 days, globular nodules developed on the surface of the cell layer. These nodules, in addition to showing a positive Von Kossa reaction, also contained calcium and phosphate, with a mean Ca/P ratio of 1.69. In contrast, the oBMSCs grown in standard DMEM+ did not show any sign of calcium or phosphate deposition (see Figure 2.4).

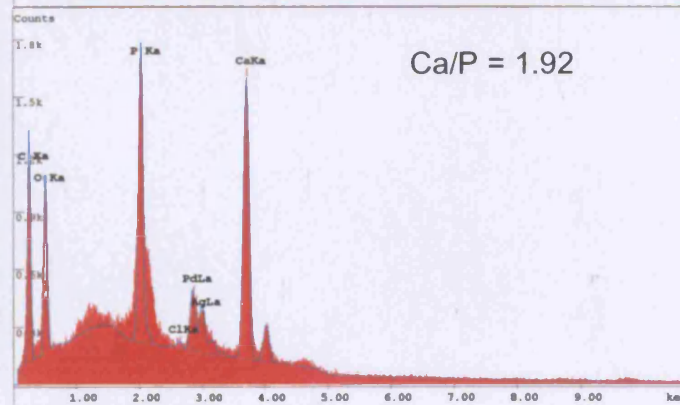
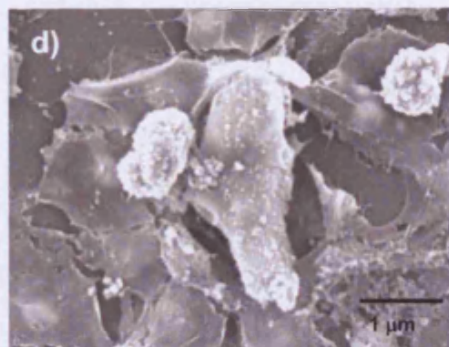
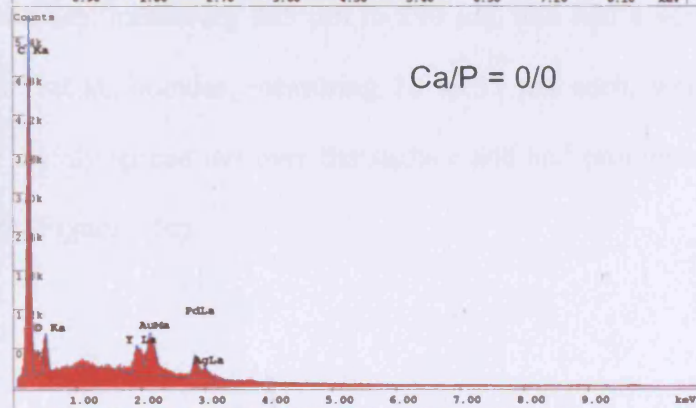
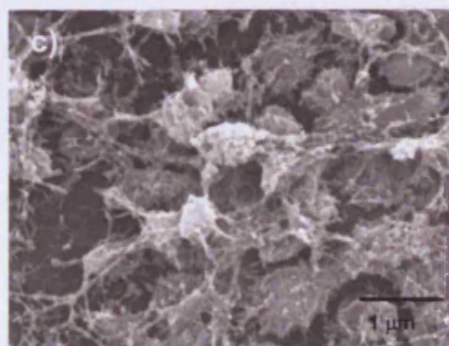
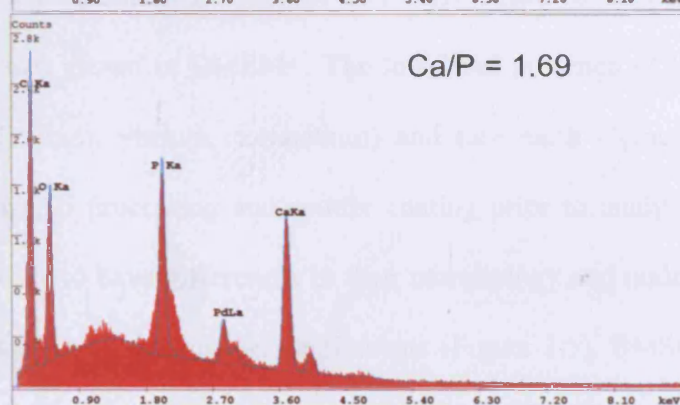
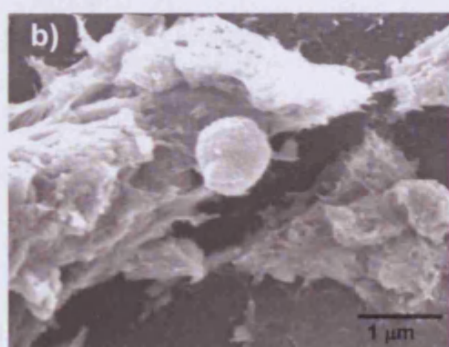
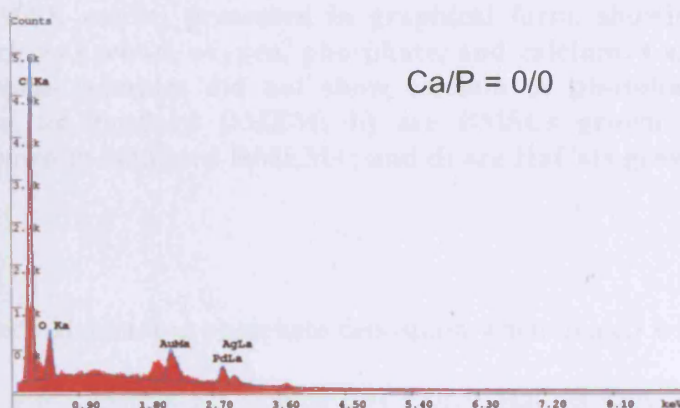
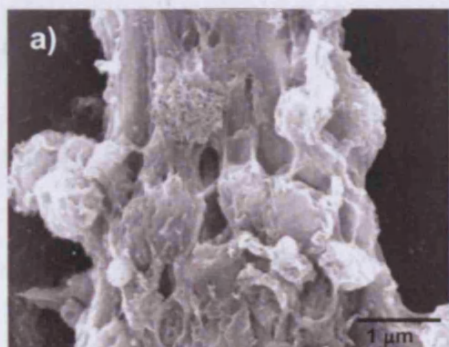


Figure 2.4 SEM photographs (1500x magnification) showing the area scanned for EDAX analysis, as well as the EDAX results presented in graphical form, showing peaks for all notable elements, such as carbon, oxygen, phosphate, and calcium. Ca/P ratios are also shown, although some samples did not show calcium or phosphate content. A) shows BMSCs grown in standard DMEM; b) are BMSCs grown in osteogenic media; c) are HaCats grown in standard DMEM+; and d) are HaCats grown in osteogenic media.

The HaCat cell line also demonstrated calcium and phosphate deposition when treated with osteogenic supplements for 28 days, with a mean Ca/P ratio of 1.91 ± 0.70 . HaCats were not positive for calcium or phosphate when grown in DMEM+. The low-level presence of the inorganic metallic (gold, silver, palladium, yttrium, technetium) and rare earth elements (lanthanum), have resulted from sample processing and sputter coating prior to analysis. SEM images show oBMSCs and HaCats to have differences in their morphology and nodule formation, even after 28 days in culture with osteogenic supplements (Figure 2.5). BMSCs appeared to form distinct globular nodules, measuring 265 μm to 290 μm , and had a very organised structure, whereas smaller HaCats nodules, measuring 10 to 35 μm each, were sometimes clustered, appeared more evenly spread out over the surface and had prominent cell processes extending between cells (Figure 2.5c).

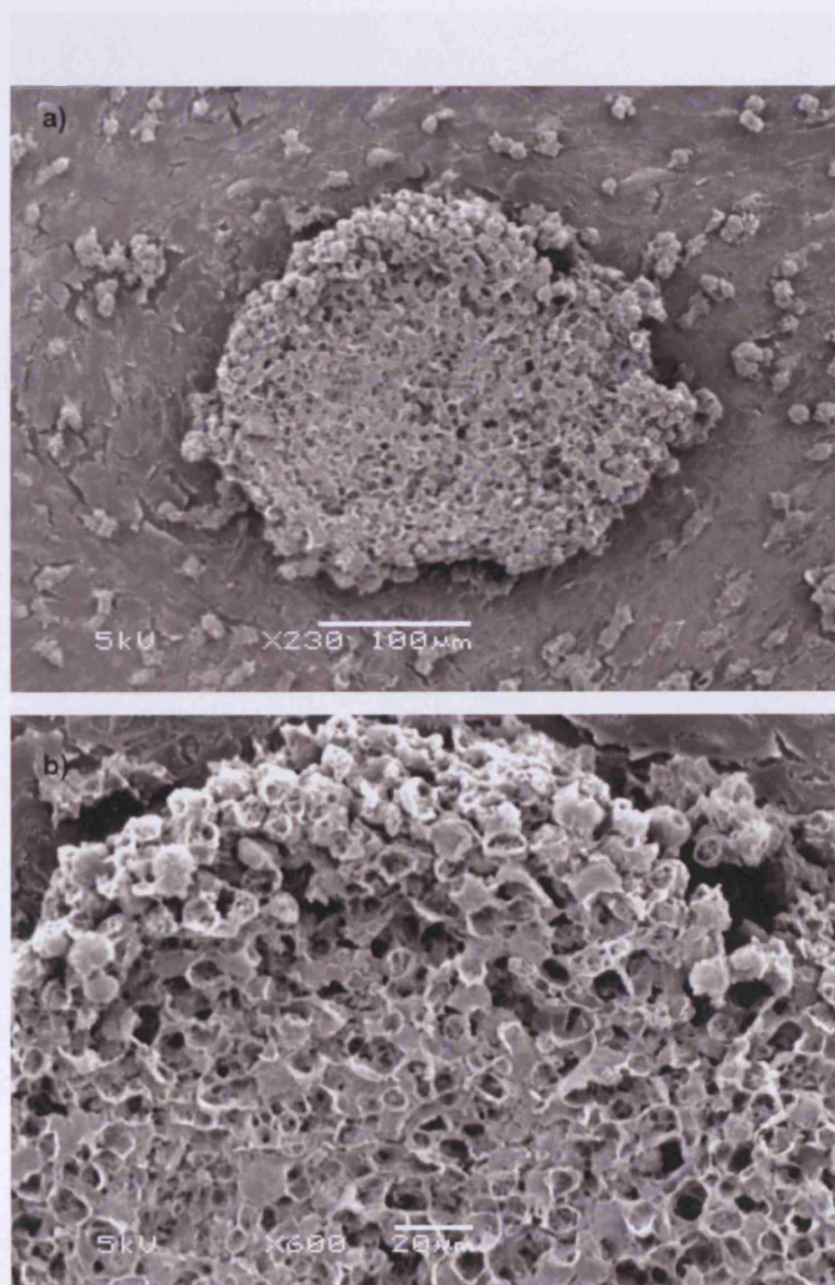


Figure 2.5 Scanning electron micrographs of the surface of the material after 22 days of incubation in medium. (a) and (b) are the surface of the cells and cells after 22 days, respectively. The scale bars show the magnification of 100x and 1000x, respectively.

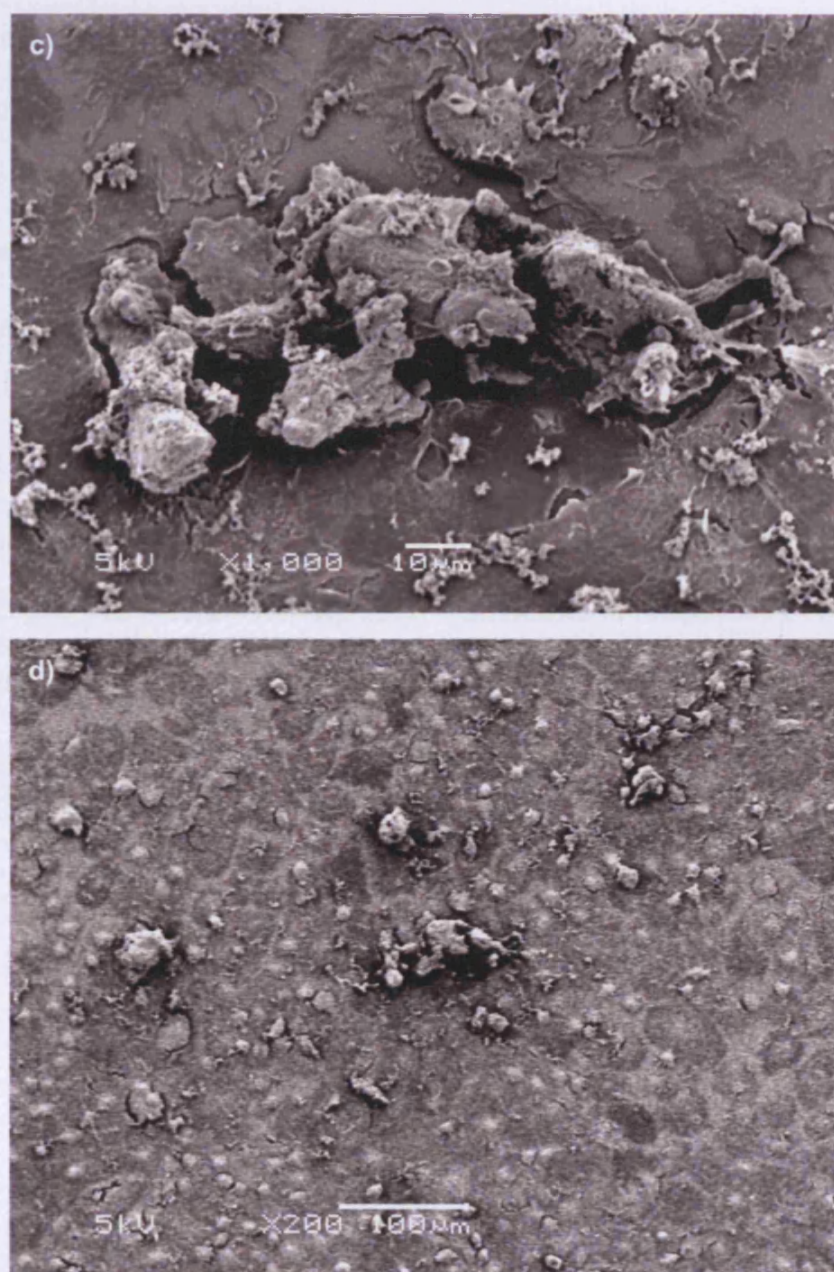


Figure 2.5 SEM photographs of cell lines after 28 days in osteogenic media. a) and b) are oBMSCs at 230x and 600x magnification, respectively. HaCat cell lines are shown in c) and d), at 200x and 1000x magnification, respectively.

2.3.2.4 Cell Activity During Osteogenesis – Alamar Blue Assay

Observations made using Alamar Blue™ absorbency as a measure of cell activity showed a significant increase in cell activity after treatment with osteogenic supplements when compared to normal (DMEM+) oBMSC cultures, except at day 3 ($p=0.01$, $p=0.01$ and $p=0.20$ after 1, 2, and 3 days in culture, and $p=0.000$ at days 7, 10, 14, 21, and 28.). The lowest Alamar Blue™ reading was made at day 1, with an absorbance of 130.53 ± 4.23 and 152.44 ± 4.46 for the DMEM+ and osteogenic medium groups, respectively. The highest values were observed after the cells had been growing for 28 days, when the absorbencies were 383.45 ± 6.89 and 581.26 ± 3.48 for the DMEM+ and osteogenic groups, respectively (Table 2.1 and Figure 2.6). Looking between all time points in each group (DMEM+ and osteogenic), there was a statistically significant differences in absorbency except between 3-7, 21-28, 10-21, and 10-28 days in the DMEM+ group, and between 10-21 days in the osteogenic group.

	DMEM+	Osteogenic
Day 1	130.53 ± 4.23	152.44 ± 4.46
Day 2	161.90 ± 7.81	209.80 ± 12.81
Day 3	197.00 ± 13.72	301.70 ± 26.42
Day 7	266.32 ± 13.36	414.98 ± 21.31
Day 10	350.39 ± 10.61	521.07 ± 6.77
Day 14	354.91 ± 8.55	576.54 ± 7.31
Day 21	359.20 ± 11.46	530.37 ± 4.87
Day 28	383.45 ± 6.89	581.26 ± 3.48

Table 2.1 a) Chart showing Alamar Blue™ absorbency over a 28-day period in oBMSCs grown in standard (DMEM+) and osteogenic medium. Cells grown in osteogenic medium had a higher cell activity than those grown in standard medium at all time points, $p<0.05$ at all time points except day 3.

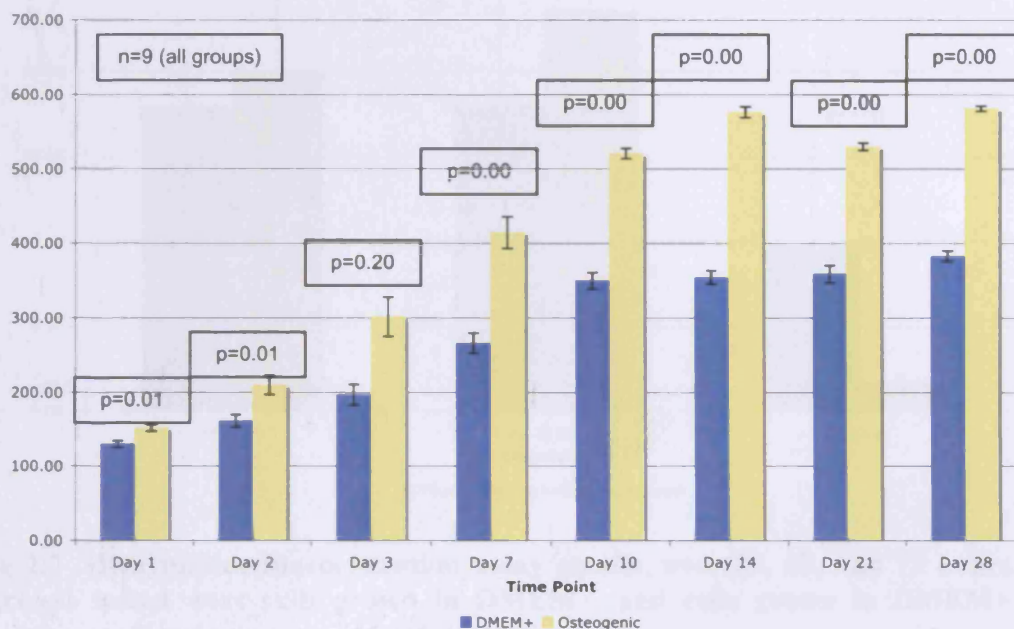


Figure 2.6 Chart showing Alamar Blue™ absorbency over a 28-day period in oBMSCs grown in standard (DMEM+) and osteogenic medium.

2.3.2.5 Cell Proliferation During Osteogenesis – Thymidine- H^3 Radioassay

There was no significant difference in the proliferation rate of oBMSCs, with or without osteogenic supplements over the first 72-hour period ($p>0.05$). There was, however, a significant decrease in overall cell proliferation observed during the 48-72 hour period, after cells had been cultured in osteogenic media (47.20 ± 4.70 Bq/ μ g DNA \cdot hour and 3.37 ± 0.95 Bq/ μ g DNA \cdot hour, respectively, $p=0.01$). Figure 2.7 illustrates the results of this assay. In the osteogenic group, between 48-72 hours and between 24-72 hours there was a statistically significant decrease in proliferation in the osteogenic group ($p=0.004$). There was no statistical significance between time points in the control group.

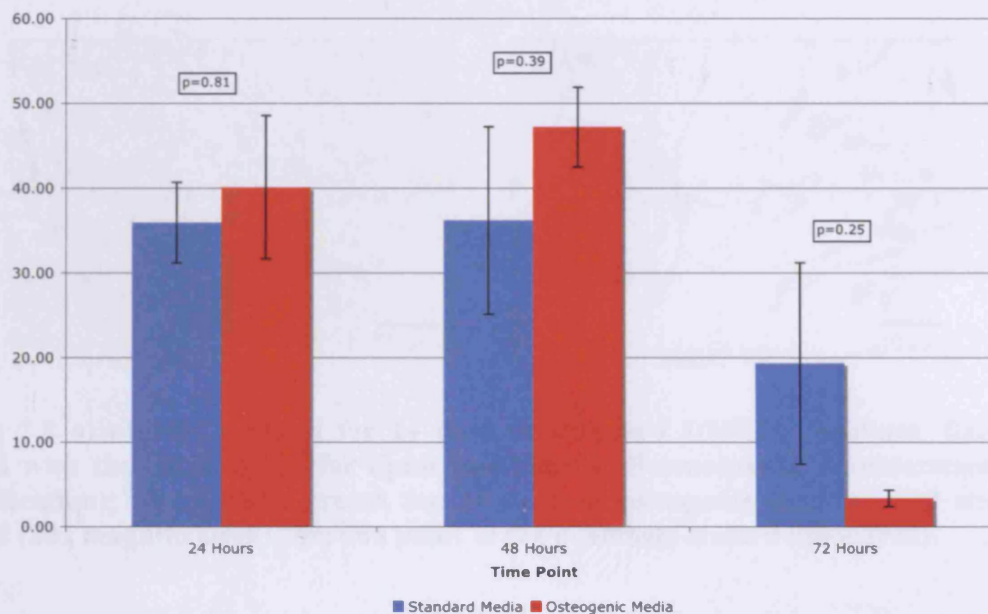


Figure 2.7 ^3H -thymidine incorporation assay results, over 24, 48, and 72 hours. The two groups tested were cells grown in DMEM+, and cells grown in DMEM+ with osteogenic supplement, expressed in Bq/μg DNA.

2.3.3 Adipogenesis

2.3.3.1 Oil Red 'O' Stain

Over the 14 days, cells changed morphology, becoming less spindle-shaped and shorter with long extensions (Figure 2.8). The Oil Red 'O' stain indicated the increased presence of lipids after oBMSCs were treated for 14 days in adipogenic media, when compared to those that were cultured in standard media. Although it must be noted that there were some cells staining positively for this lipid stain in the untreated oBMSCs cultures, it was to a much lesser extent than the 'adipogenic' cultures.

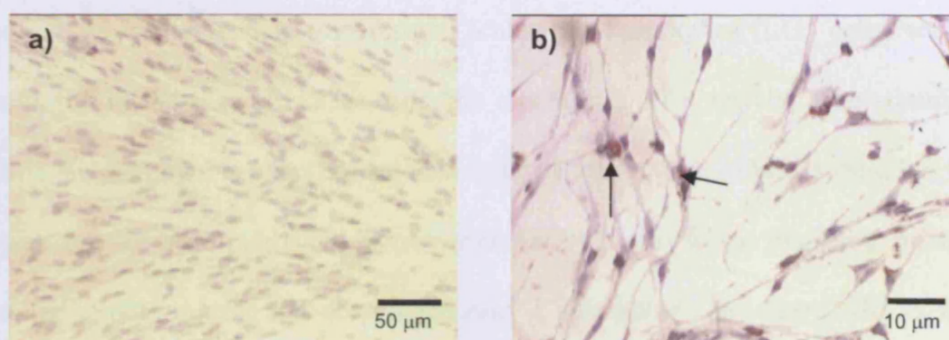


Figure 2.8 a) oBMSCs grown for 14 days in standard DMEM+ medium, fixed and stained with the Oil Red 'O' for lipids and Harris' Haematoxylin (counterstain) (10x magnification); b) oBMSCs grown for 14 days in osteogenic medium and similarly stained (20x magnification). Arrows point at the positively stained lipids (red).

2.4 Discussion

According to conventional BMSC differentiation, from the results observed in this chapter, the oBMSCs isolated here contain progenitor cells, capable of differentiating down three different cell lineages. The oBMSCs were derived from the bone marrow, were plastic-adherent cells that formed characteristic CFU-Fs and had a fibroblastic morphology. When treated with osteogenic media for 28 days, these oBMSCs produced mineral-like nodules and had a significant increase in ALP activity. When differentiated down the adipocytic lineage for 21 days, lipids were detected using the conventional stain and when treated in a pellet with chondrogenic supplements, cells appeared to express markers of hyaline (collagen II, GAGs) and fibrocartilage (collagen I, GAGs). Cells appeared to slow down their proliferation and increase their cellular activity, as found with the thymidine- H^3 and Alamar Blue assays. However, by including a few cell controls, from lineages unrelated to oBMSCs, I have shown evidence that could be used to prove oBMSCs contain progenitor cells using these techniques is insufficient. It is possible that these assays may only be demonstrating cell plasticity, rather than BMSC identity.

Regarding osteogenic differentiation, it appears that transformed keratinocytes (HaCat cell line) as well as spontaneously transformed leukaemic monocytes (LG3 cells) seem to react very similarly. In the case of HaCat cells, the increase in ALP activity after stimulation with osteogenic supplements is even higher than with oBMSCs and gBMSCs. Similar, unspecific ALP assay results were published by Almeida (2001), who found that after treatment with nacre water-soluble matrix and dexamethasone, a non-BMSC cell line (MRC-5 fibroblasts, derived from human fetal lung tissue), also expressed ALP similarly to BMSCs (Almeida 2001).

It is possible that the ALP assay, first used by Oreffo et al. (1998) to show osteoblastic differentiation of hBMSCs, is not specific enough. There exist a few different isoforms of ALP, which are expressed in various tissues, such as the kidneys, liver and bone (Nakayama et al. 1998). ALP on osteoblasts is expressed on the cell membrane, whereas this assay looks at ALP activity of a cell lysate. However, specific ALP antibodies have been used to show cell surface expression of ALP (Rust 2004, Gronthos et al. 1994), although it has been suggested that the post-translational modifications to the carbohydrate side chains of the different ALP isoforms may not be easily detectable by commercially available antibodies (Nakayama et al. 1998). It would be useful to test if the ALP proteins expressed by the oBMSCs and HaCat cell lines were of the same isoform, by either using more specific monoclonal antibodies that differentiate between isoforms (Martin et al. 1997, Masuhara et al. 1991) or affinity chromatography (Nakayama et al. 1998). Additionally, to ensure that the observed positive osteogenic-like reaction of the immortalised HaCat and LG3 cell lines is not due to changes in gene expression as a result of transformation-related chromosomal or aneuploidic aberrations (Phillips et al. 2001), it would be useful to repeat this experiment in a

primary, terminally differentiated and/or non-mesenchymal cell line, such as primary keratinocytes or epithelial cells.

Like other studies (Janssen et al. 2006; Gorustovich, Rosenbusch and Guglielmotti 2002), I was able to show calcium phosphate production in BMSCs undergoing osteogenic differentiation. However, the HaCat cell line also produces calcium and phosphate results. The non-cell-specific formation of these nodules is a cause for concern, considering that it is widely used, although the nodules have a distinct morphology when grown from the oBMSC cell lines or the HaCat cell line. Positive Von Kossa staining has previously been encountered in cases of acute phosphate nephropathy, where phosphate-based cathartic agents caused the formation of calcium phosphate deposits in the kidney, with a calcium to phosphate ratio of 1.67, which is the ratio for pure hydroxyapatite (Desmeules, Bergeron and Isenring 2003). These results are in accordance with the positive Von Kossa stains.

Interestingly, some nodules could be detected in those samples cultured in standard media for the 28-day period. Although spontaneous differentiation of the cells is a possibility, it has been suggested that phenol red, used as a pH indicator in normal cell culture media, may be responsible for this differentiation. Still et al, attempted to culture human BMSCs in phenol red-free medium, but did not see an osteogenic stimulatory effect of the media on the cells until a significant concentration of phenol red was present (Still, Reading and Scutt 2003).

The surfaces used to to culture the cells described in this chapter, and well as the surfaces used during differentiation, were slightly different in some cases. For example, Thermanox[®] coverslips were used to culture oBMSCs in osteogenic media to show mineralisation after 28 days using the Von Kossa stain, whereas 6-well plates were used to culture cells for the ALP

assay, at 7, 14, 21 and 28 days. Each plastic surface is fabricated from different materials, and uses different techniques to treat the surface, whether it is by using an electrostatic charge, or etching methods (EMS Catalog 2007; Scholz 2007). This may, in turn have resulted in varying conditions and reactivity to the differentiating supplements.

In this chapter, all cell lines stained positively for Von Kossa (mineralisation) after 28 days. A study by Declercq et al. (2005) found that cell lines derived from the rat bone marrow, calvarial and early passage periosteal cells formed positively staining nodules after about 12 days in osteogenic media containing dexamethasone and β -glycerophosphate. In contrast, late-passage periosteal cells and the osteoblast-like cell line UMR-106 showed a much more diffuse pattern of positive Von Kossa staining. These samples were tested using x-ray diffraction and Fourier transform infrared spectrometry to investigate the properties of these crystals, and found that all samples had similar results (Declercq et al. 2005). In this chapter, a similar lack of nodule formation was observed when HaCat cells were treated in osteogenic supplements, despite their positive Von Kossa results. In contrast, the oBMSC-derived nodules had an intricate, matrix-like structure. The nodule formation suggests a cell-mediated process of mineralisation as opposed to a nucleation-type process (Schecroun and Delloye 2003; Bellows et al. 1986). In future, one method that may be useful in the detection of mineralised and non-mineralised nodules is the use of the two-colour image analysis used by Purpura, Aubin and Zandstra (2003), where bone nodule number, size and type can be distinguished.

There were two oBMSC lines investigated in this chapter. It is possible that the difference in passage might have affected the reactivity of the cells to differentiation medium. With increasing passage, the properties of the cells may have changed (Devine et al. 2001b) such

that they react differently with the osteogenic media. We did not perform karyotyping on the cells, so it is also possible that aneuploidy may have spontaneously occurred during cell division in my cell lines (Wang et al. 2005), affecting gene expression accordingly, thereby affecting the differentiation and growth of the cells. This is one reason why the different passages of the various cell lines used may have also influenced the results, as well as a potential change in cell phenotype as the cells were passaged and expanded in *in vitro* culture (for example, low-passage oBMSCs were passage 3, whereas gBMSCs were passage 4).

It is possible that the reason for the HaCat and LG3 responses to osteogenic media are due to transdifferentiation, or cell plasticity. Transdifferentiation involves the “conversion” of one cell type to another cell type (Burke and Tosh 2005). The gene for Core-binding factor A1 (Cbfa-1) is the first transcription factor gene to be expressed after stimulation with osteogenic supplements. This gene is thought to be a “master gene” that instigates osteogenic differentiation of cells by triggering a cascade of gene expression that promotes osteogenesis, including binding of the protein product, CBF β) to Runt-related gene 2 (Runx-2) (Mori et al. 2006; Dennis and Charbord 2002). Osterix is another downstream transcription factor involved in activating a gene expression cascade including bone sialoprotein, osteocalcin, and collagen I (Mori et al. 2006). Wu et al. (2002) identified a molecular stimulator of Cbfa-1, 2,6,9-trisubstituted purine compound, purmorphamine, which upregulated members of the hedgehog (Hh) signalling pathway such as Gli1 and Patched. It is possible that either this molecule, produced as a breakdown product of osteogenic supplements, or the original chemical stimuli in osteogenic media, is responsible for a strong effect on the gene regulation of many cell types, and that this Cbfa-1 activation may cause “reprogramming” of the cell. Looking for these “osteoblastic” genes in the different cell lines after treatment with osteogenic supplements, using a quantitative method such as real-time polymerase chain

reaction (RT-PCR) would be useful in determining the specificity of gene regulation in adult cell lines.

Another point regarding ALP expression after treatment with osteogenic media is that dexamethasone is a potent up regulator of ALP expression in BMSCs (Yin, Li and Wang 2006; Yang et al. 2003; Cheng, Zhang and Avioli 1996; Kim, Cheng and Kim 1999) or a rat calvarial cell line (Grigoriadis, Heersche and Aubin 1988). It may also be possible that ALP expression is elevated after BMSC treatment with other differentiating supplements. Diefenderfer et al. (2003) showed that dexamethasone triggered ALP expression in hBMSCs *in vitro*, whereas BMP-2, BMP-4, or BMP-7 failed to induce such an effect.

Few other groups have attempted characterisation of oBMSCs, the purpose of the tests having been mainly to validate the oBMSCs used in large animal orthopaedic models (Kon et al. 2000; Shang et al. 2000). One study detected ALP activity using a similar p-nitrophenol phosphate to p-nitrophenol assay, and found very low levels of ALP in the ovine BMSCs when cells were grown in standard medium, when compared to human BMSCs (Kon et al. 2000). This study also applied oBMSCs in fibrin glue into ceramic cubes to test the *in vivo* osteogenic capacity of oBMSCs, and found that they had a much more significant bone growth into the ceramic cubes when compared to human BMSCs. Another study, by Shang et al. (2000), showed a significant difference in the ALP activity of oBMSCs when compared to sheep dermal fibroblasts, with oBMSCs having ten times the activity of the fibroblast cultures. In my experiment, I was able to show different levels of ALP activity by different cell lines and from different species, such as sheep and goat BMSCs. The goat BMSCs were found to have approximately two-and-a-half times the ALP activity of the low-passage sheep BMSCs. It may be possible that different species have different levels of ALP or differences

in ALP activity. Shang et al. (2000) also looked at osteocalcin expression using a radioimmunoassay over a 17-day period, and found that osteocalcin expression was much greater in those oBMSC samples treated with osteogenic supplements than those grown in standard culture medium. This paper also showed collagen I expression by the oBMSCs after four weeks and positive Von Kossa staining after 21 days, although no controls were shown for these stains. Work by Cheng et al. (1996) showed only positive Von Kossa staining for oBMSC osteogenesis and Sudan Black IV for adipogenesis (Muraglia, Cancedda and Quarto 2000). Appropriate controls are obviously critical determinants of validity for these various stains and assays regarding differentiation. As yet, adipogenic and chondrogenic differentiation have not been attempted using the HaCat and LG3 cell lines. It is possible that with the normal differentiation supplements these cells may show signs of “differentiation” as well. Is this a sign of transdifferentiation or are these assays any indication of an oBMSC’s identity? In addition, BMSCs are often regarded as being a heterogeneous population of cells, having varying degrees of multipotency (Aubin 1998; Purpura, Aubin and Zandstra 2003). In order to determine the actual ‘multipotency’ of the oBMSCs isolated in this chapter, that is, the ability of the cells in the population to differentiate down all lineages, one would have to use a cell lines derived from a single cell (using serial dilutions), and test the ability of these cells to differentiate down all three lineages, as well as testing the cell surface marker expression. The population I have reported on is heterogeneous, and therefore most probably contains cells with varying capacities for differentiation down different cell lineages or levels of ‘multipotency,’ as suggested for human BMSCs by Jane Aubin in 1998. I have not shown that the entire population of oBMSCs used in this chapter can differentiate down all three cell lineages, however I have been able to show that some cells in the population have the capacity to differentiate down at least one cell lineage.

In future, other useful tests that could be used to characterise oBMSCs are a surface marker profile, as well as to look for mRNA expression of genes involved in the different differentiation pathways, such as osteocalcin, osteopontin, ostrom, PPAR γ 2, and collagen type II and X, and aggrecan (Lisignoli et al. 2006). One method that has been used to a smaller extent in the characterisation of BMSCs is analysis of many different genes using a gene chip (Bourne et al. 2004; Hishikawa et al. 2004). I previously attempted to react ovine BMSCs with the human Stro-1 marker, with negative results (not shown), as well as other human CD markers such as CD105 and CD44. More surface marker profiling using oBMSCs is a very important task that should be carried out promptly, following from the results presented in this chapter.

There was no significant difference in the proliferation of cells over a 72-hour period. However, these results conflict with other studies, which detected a significant decrease in thymidine-H³ incorporation after treatment with osteogenic media for as little as 24 hours (Kim, Cheng and Kim 1999). This may be in part due to the fact that 24 hours is too distant a time-point. Some cells may have already been undergoing S-phase when the tritiated thymidine was added to the cell culture media, so the results could reflect a combination of proliferation that was already occurring before the thymidine was added, plus any proliferation that occurred afterwards. The same idea could be applied to the 48- and 72-hour time points.

Additionally, although the Alamar Blue[®] observations in this chapter have been attributable to metabolic activity, cell numbers were not accounted for in this assay. As the cells were proliferating during the time course of the assay, the cell number would have changed, and this would have contributed to the rise in absorbency of the samples at later time points. In

future, the results of this assay should be standardised to cell number, by either measuring DNA content using the Hoerscht assay, performing cell counts using Trypan Blue staining and a haemocytometer, or by treating the cells with a fluorescent stain, followed by flow cytometry for cell counting.

It has been suggested in the literature, that, although dexamethasone is required for the initial differentiation of BMSCs, it may hinder the formation of bone nodules (Schecroun and Delloye 2003; Chang et al. 1998), as cellular proliferation is reduced by cells exposed to dexamethasone, reducing collagen I expression, vital for the formation of nodules. Additionally, it has been suggested that prolonged steroid intake in humans could be one probable cause of osteonecrosis (Yin, Li and Wang 2006; Wang et al. 2003). It could be that steroids such as dexamethasone have detrimental effects on the mineralisation and nodule-forming activity of osteoblasts.

There was no observable change in morphology of the oBMSCs over the maximum of 28 days cells were cultured with osteogenic supplements. This is in contrast to many studies, which observe a marked change in cell morphology, from a fibroblastic shape to a cuboidal, round cell shape (Jaiswal et al. 1997, Grigoriadis, Heersche and Aubin 1988).

It is unknown as to whether or not the anaesthetic regime used during bone marrow aspiration affected the isolation, viability, or phenotype of the BMSC isolated from sheep. Halothane does not immediately clear out of the body, staying dissolved in fat and other tissues for up to x to x hours after the cessation of the anaesthetic regime. Also, the bone marrow was treated with 500 IU of heparin per sample, in order to prevent clotting. The effects of heparin on BMSCs or bone marrow cells has not been extensively reported in the literature, although it

has been suggested that heparin-binding domains found in various elements of the extracellular matrix and the cell surface composition might affect cells signalling (Beauvais and Rapraeger 2004; Lopes, Dietrich and Nader 2006). Also, the animals were under general anaesthesia with an inhaled anaesthetic (halothane) while bone marrow aspirates were taken. Bone marrow contains fatty tissue, which can accumulate hydrophobic halothane molecules (Martin 2004), which may in turn affect the BMSCs. However, studies show that the first tissues to be exposed to halothane are those that receive a high fraction of cardiac output. The bone marrow is well vascularised, so a certain percentage of halothane probably did reach those cavities in the short term, even though the animals were not under anaesthetic for extended periods of time (time ranging from 10-45 minutes). Halothane has been shown to be carcinogenic *in vitro*, although one report did describe an increase in cancer cases in anaestheticians who had been repeatedly exposed to waste anaesthetic gas, as well as a rise in congenital abnormalities and spontaneous abortion (Martin 2004). It is therefore possible that halothane could cause mutagenesis in the BMSCs, or be accumulated in liposomes or any other lipid-containing structure in the cell for some length of time, before breaking down into its metabolic derivatives.

In conclusion, the results presented in this chapter suggest that standard histochemical and enzymatic detection of cell type after osteogenic differentiation of BMSCs may not be specific to BMSCs. Thus, a thorough characterisation of oBMSCs would be the most conclusive identification of a multipotent bone marrow stromal cell. This could be done using cell surface marker identification, using FACS or MACS and via the detection of mRNA transcripts of osteoblastic genes, in addition to the standard histochemical tests. Also, *in vivo* tests of BMSCs, showing their differentiation into osteoblasts after seeding onto ceramic cubes and implanting ectopically would be useful, and may show species-specific differences

in the osteopotential of BMSCs. In the case of human BMSC-derived osteoblasts, the expression of osteoblastic mRNA transcripts such as *cbfa1*, *c-fos*, *osterix*, *osteocalcin*, and *osteopontin* (Marom et al. 2005, Igarashi et al. 2004, Jaiswal et al. 1997) are tested and should be repeated with oBMSCs. Gene analysis using microarrays may also differentiate cell types, for example, work by Brendel et al. (2005) which showed unique gene expression between BMSCs and skin fibroblasts when compared in over 9600 genes. The presence of chondrocyte and adipocyte differentiation-related mRNA transcripts should also be tested with BMSC-derived chondrocytes and adipocytes. This future work will be very important in determining the effectiveness of *in vitro* tests in proving BMSC identity.

CHAPTER THREE

THE EFFECTS OF GRANULOCYTE-COLONY STIMULATING FACTOR (G-CSF) AND BLOOD LOSS ON THE ISOLATION OF PERIPHERAL BLOOD-DERIVED STROMAL-LIKE CELLS

3.1 Introduction

Bone marrow stromal cells (BMSCs) are a heterogeneous population of non-haematopoietic cells derived from the adult bone marrow. The stroma, from which these cells are derived, is the connective tissue of the bone marrow that supports haematopoiesis via the expression of cytokines and cell-cell interactions. Much of the recent literature supports evidence that MSC-like cells are present in many other tissues in the body, such as fat, skin, muscle, and umbilical cord blood. Many of these cell lines, derived from these other sources, have been shown to demonstrate a similar multipotency to BMSCs (Kern et al. 2006; Lee et al. 2004; Bartsch et al. 2005). One recent source of BMSCs that was previously debated in the literature is the peripheral blood. Kucia et al. (2004) showed the presence of muscle, neural and liver stem cells in the bone marrow that responded to a stromal-derived factor-1 (SDF-1) gradient and were mobilised to the peripheral blood after tissue injury and stress.

In terms of bone tissue engineering, it would be advantageous to have an alternative source of BMSCs other than the bone marrow, which requires a painful aspiration step and provides varied results in terms of isolated cell number. Over the past five years, evidence has been growing that BMSC-like cells have the capacity to migrate or “home” to adult bone and bone marrow when infused into the bloodstream (Devine et al. 2001), with or without stimulus. These stimuli include chronic hypoxia in rats (Rochefort et al. 2006) and G-CSF administration following breast cancer treatment in humans (Fernandez et al. 1997). This paper reported that peripheral blood-derived stromal-like cells (PBSCs) were isolated from eleven out of fourteen patients tested. It has also been demonstrated that BMSCs have the capacity for engraftment and site-specific differentiation in sheep when implanted *in utero* (Liechty et al. 2000). Another study has isolated peripheral blood-derived stromal-like cells (PBSCs) using fibrin microbeads. Paget, in 1854, described matrix-producing cells in the

peripheral circulation. Kuznetsov et al. (2001) were able to consistently isolate peripheral blood from normal individuals as well as small animals such as mice, rabbits and guinea pigs. Wan, He and Li (2006) were also able to isolate peripheral blood stromal-like cells in one out of two human cases.

High levels of haematopoietic stem cell (HSC) mobilisation from the bone marrow to the circulating bloodstream occurs during leukocyte recovery following chemotherapy, and can also be induced using granulocyte colony stimulating cytokines. The harvest, purification and transplantation of these cells back into patients undergoing high-dose cytotoxic chemotherapy to repopulate their bone marrow are successful procedures.

The very late antigen 4 (VLA4) adhesion molecule expressed by HSCs, binds in the marrow compartment to VCAM-1, expressed by stromal cells, endothelial cells, and BMSCs. Additionally, the molecule stromal-derived factor (SDF-1/CXCL12), expressed by BMSCs and stromal cells, attracts and localises HSCs by interacting with the receptor CXCR4. These interactions may be interrupted when HSC release from the bone marrow is required, or stimulated by mobilising factors such as G-CSF. Cleavage of VCAM-1 and the degradation of SDF-1 by proteases, neutrophil elastases and cathepsin G are implicated in this mechanism and are released upon G-CSF administration (Levesque et al. 2001; Levesque et al. 2003; Velders and Fibbe 2005; Kronenwett, Martin and Haas 2000). Cell-specific splice variants of the mucin receptor CD164, also with varying glycosylation patterns, have also been implicated in HSC-endothelial cell/BMSC interactions (Zannettino et al. 1998; Watt et al. 1998).

The matrix metalloprotease (MMP)-7 has been implicated in the remodelling of the bone marrow microenvironment by degrading extracellular matrix interactions and structure. MMP-7 is increased upon G-CSF administration and is also known as type VI collagenase (Sugimoto et al. 2001). Collagen IV is another molecule thought to be involved in HSC-BMSC interactions in the bone marrow, and G-CSF has been shown to modulate collagen IV expression in BMSCs (Fernandez et al. 1997).

Possible multipotent stromal cell mobilisation into the peripheral blood system concurrent to HSC mobilisation has been debated (Fernandez et al. 1997; Lazarus et al. 1997; Purton, Mielcarek and Torok-Storb 1997). However an *in vitro* study in 2003 by Baksh, Davies and Zandstra proposed that the increased BMSC growth observed when co-cultured with CD45⁺ haematopoietic was due to positive interactions between the two cell types in terms of survival and proliferation, and a possible steady-state balance. This group was able to show the sustained growth of HSCs in the presence of BMSCs, in a non-adherent culture system, without growth factors normally required to propagate HSC growth and proliferation *in vitro*. One HSC transplantation study also showed an increase in successful haematopoiesis with the co-infusion of HSCs with cultured BMSCs (Koc et al. 2000). I postulated that it may be possible that a smaller volume of blood loss, such as that experienced in blood donation, may induce stromal cell release into the peripheral blood, and that mobilised cells from the bone marrow may contain BMSC-like precursor cells. In my thesis, I investigated this possibility in an ovine animal model by quantifying the number of fibroblastic colony-forming units isolated from blood and bone marrow after blood loss or cytokine therapy. The peripheral blood could be an alternative source to bone marrow for multipotent stromal-like cells, which unlike the latter two sources, would be simpler to obtain and could follow a similar protocol to the current practice for mobilised HSC therapy (Reddy 2005).

The first hypothesis is that peripheral blood-derived stromal-like cells (PBSCs) could be isolated from an ovine model, expanded and characterised to be multipotent.

The second hypothesis is that induced stress, such as blood loss or cytokine-induced mobilisation of HSCs, would also result in the co-mobilisation of PBSCs into the peripheral blood in greater numbers and that these mobilised cells would have the same multipotent identity as those isolated from untreated peripheral blood.

The aims and objectives of this chapter were to:

1. Show that the isolated ovine PBSCs have the same multipotent characteristics as BMSCs.
2. Demonstrate that induced blood loss (7 and 15% blood loss) would increase PBSC release into the bloodstream alongside HSC release in both the marrow and the blood in an ovine model.
3. Test if cytokine stimulation using G-CSF (Filgrastim) would increase PBSC circulation in an ovine model.
4. Investigate if there exists a change in the number of PBSCs isolated from the blood in relation to the amount of time post-G-CSF administration.

3.2 Materials and Methods

3.2.1 Part I: Induced Blood Loss

3.2.1.1 Experimental Layout

To determine baseline levels of CFU-F forming stromal cells in the bone marrow and blood, iliac crest bone marrow aspirates (two 4 ml samples) and venous blood samples (two 5 ml samples) were taken from 8 Mule ewes for haematological analysis and cell culture. Bone marrow was aspirated from the iliac crest and processed on Ficoll[®] for BMSC culture as described in Chapter 2.

Those sheep that did not have normal haematological results were not used any further for this investigation (2 sheep), leaving 6 sheep in total that were used for the experiment. Blood cell counts (concentrations of white blood cells, neutrophils, lymphocytes, monocytes, eosinophils, basophils, red blood cells and platelets) from these initial samples were taken as being the “baseline” result for cells from the blood and marrow, with which all other results were compared. Seven sheep samples were used to create the baseline mean CFU-F counts and three sheep underwent 7% bleeding, and 15% bleeding one month afterwards. Blood and bone marrow samples were then taken, and respective CFU-Fs counted.

The estimated blood volume of each sheep was calculated using the assumption that each animal’s total blood volume was approximately 70 ml/kg body mass. All sheep used in this study ranged in mass from 80-87 kg and therefore 7% of the blood volume (5 ml/kg) ranged from 392 – 426 ml.

Seven days post-aspiration, 7.0% of each sheep’s blood was removed from the internal jugular vein, using a syringe and canula. Of this blood, 10 ml was taken back to the

laboratory for cell culture. Further aspirates (two 4 ml samples) and small blood samples (two 5 ml samples, one for culture and one for haematology) were taken seven days after bleeding for haematological analysis and cell culture. Animals were then allowed to recover for a period of three weeks.

After the three week recovery period, 15% of the animals' blood volume (10.5 ml/kg) was then taken over two days from the internal jugular vein. On the second day, 10 ml of blood was taken for cell culture and counting. A week after the 15% bleeding, aspirates (two 4 ml samples) and small blood samples were taken (two 5 ml samples, one for culture and one for haematology). Figure 3.1

Figure 3.1 illustrates the experimental layout using a flowchart.

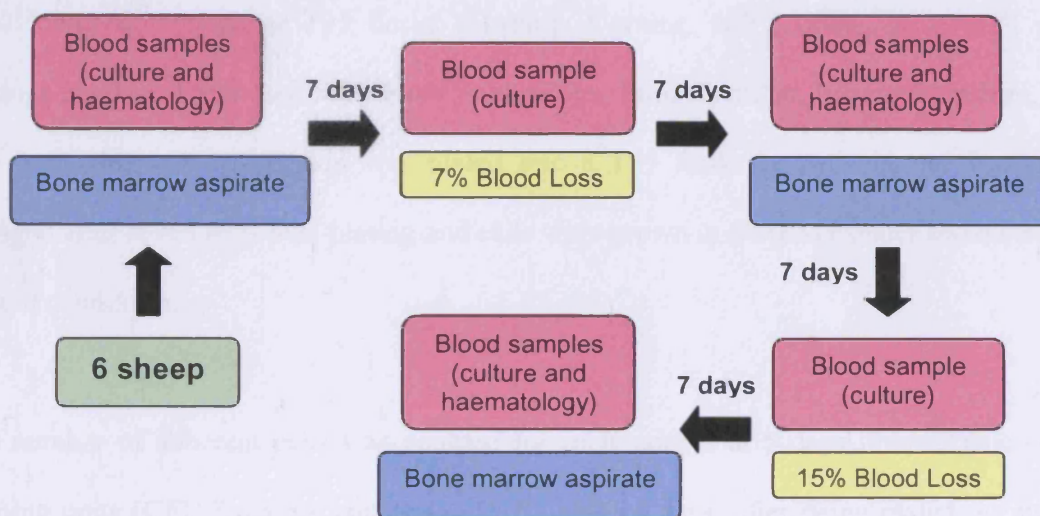


Figure 3.1 Flowchart depicting the experimental layout testing the effects of induced blood loss (7% and 15%) on the mobilisation of BMSCs into the peripheral blood. The experiment consisted of pre-bleeding blood and bone marrow samples being taken, followed by either 7% or 15% blood loss one week later. One week post-blood loss, further blood and bone marrow samples were taken, for cell culture and haematological analysis.

3.2.1.2 Anticoagulants

For aspirates and blood being used for cell culture, 500 units/5 ml of heparin was used for each sample. For those samples used for haematological analysis, 15% EDTA was used as an anticoagulant.

3.2.2 Plating Cells For Counting CFU-Fs

After being processed on Ficoll and the buffy layer removed, washed and pelleted (see Chapter 2), cells were resuspended in 5 ml of DMEM+. 2 ml of this suspension was diluted in 15 ml of media, and counted using a haemocytometer. Cells were plated in triplicate at 4.0×10^5 cells/cm², on either T25 flasks (Corning, Corning, N.Y., USA), or 12-well plates (Orange Plastics, Triple Red Laboratory Technology, Long Crendon, Buckinghamshire, UK). The remaining cell suspension was plated into a T25 flask for cell culture. Media was changed after seven days post-plating and cells were grown in DMEM+ under standard tissue culture conditions.

The number of adherent cells was counted for each sample at 5 days. Fibroblastic colony forming units (CFU-Fs) were counted at 7, 11, and 14 days, after being plated out using a light microscope. As each clonal colony is derived from a single cell (Friedenstein AJ 1976), CFU-F counting gave an approximate number of BMSC-like cells in the initial cell culture. Counts were expressed as CFU-F/cm², from both the blood and bone marrow.

3.2.3 Statistics

Non-parametric data from all three groups was compared using Friedman's ANOVA. Data from the first two groups (Pre-treatment and 7% blood loss) were tested using the Wilcoxon test for related samples.

3.2.4 Part II: Effects of G-CSF Treatment

3.2.4.1 Experimental Layout

Eight Mule ewes had 1 ml venous blood samples taken for haematological analysis, as described above. Six of these sheep, which displayed "normal" results, were used in this study. Sheep were estimated to be approximately 4-5 years old, as identified from coloured ear tags demarcating year of birth.

Before G-CSF treatment, two 20 ml blood samples were taken from the internal jugular vein of one sheep with 0.5 units of heparin /10 ml, for pre-G-CSF cell culture.

Filgrastim[®] (G-CSF) was given to sheep subcutaneously at the same time each day, at a daily dose of 5 µg/kg, for five days. This is based on a protocol for human administration of G-CSF described by Cottler-Fox et al. (2003). Sheep were observed for any sign of side effects during this time.

After G-CSF treatment, 16 ml of blood was taken as described above, 4, 12, and 24 hours after the last G-CSF dose was given, for cell culture. For three sheep, 16 ml blood samples were taken 14 days post-G-CSF treatment. At each of these time points, 1 ml of blood was taken for haematological analysis. Figure 3.2 is a diagram depicting the experimental design.



Figure 3.2 Flowchart illustrating the experimental design to test the effects of G-CSF on BMSC release into the bloodstream. Firstly, blood samples were taken for haematological analysis. Sheep with normal “within range” results were then administered G-CSF at 5 µg/kg, for five days. Blood samples were then taken 4, 12, 24 and 336 hours after G-CSF treatment, and cultured for CFU-F counting.

3.2.5 Plating for CFU-F Counting and Culture

Cells were processed as described in 7.2.1.2, except that for cell counting, red blood cells were first burst using 2.5% acetic acid. Nucleated cells were then counted using Trypan blue (to exclude dead cells from counting) and a haemocytometer and plated out in vented T25 culture flasks (Corning cellBIND[®], Corning, Corning, N.Y., U.S.A.) at a cell density of 4.0×10^4 nucleated cells/cm², and cultured according to standard cell culture methods (see Chapter 2) in 4 ml of DMEM with 20% FCS (First Link, UK) and 1% penicillin/streptomycin (0082, Invitrogen, Paisley, UK). Media was changed seven days afterwards.

CFU-F were counted 7 and 14 days after initial culture under a phase-contrast light microscope and expressed as CFU-F/cm². Cell morphology and behaviour was also observed. Photographs were also taken using an Olympus Camedia C2020Z digital camera (Olympus UK Ltd, London, UK), and Olympus 1x70 microscope (Olympus UK Ltd, Middlesex, UK).

3.2.6 Characterisation of PBSCs

For osteogenic and adipogenic histochemical stains, ovine PBSCs obtained post-bleeding (see 3.2.2) were plated out at 4.0×10^4 cells/Thermonox[®] coverslip, onto six coverslips, and grown in osteogenic media for 28 days or adipogenic media for 14 days, using the defined media outlined in Chapter 2. Following osteogenic differentiation, the Von Kossa stain, SEM and energy dispersive analysis of X-rays (EDAX) was performed as described in Chapter 2. For adipogenic differentiation, the Oil Red 'O' stain was performed as described in Chapter 2. Chondrogenic differentiation is outlined below. Samples were compared to oBMSC and HACAT cell lines, as differentiated in Chapter 2.

3.2.6.1 Chondrogenic differentiation:

Chondrogenic Media (modified from Rust 2005):

	High-glucose DMEM (4500 mg/L, D6429, Sigma-Aldrich, Dorset, UK)
1.0%	P/S (0082, Invitrogen, Paisley, UK))
1.0×10^{-7} M	Dexamethasone, water-soluble (D2915, Sigma-Aldrich, Dorset, UK)
50 ng/mL	Ascorbic Acid (A4544, Sigma-Aldrich, Dorset, UK)
1.0 nM	Sodium Pyruvate (P5280, Sigma-Aldrich, Dorset, UK)
10 ng/mL	Recombinant Human TGF- β_3 (#100-36, PeproTech EC Ltd., London, UK)

A control media was prepared as above, but without TGF- β_3 . For differentiation into chondrocytes, oBMSCs were isolated, expanded, and trypsinised as described above, and counted using a haemocytometer. Approximately 5.0×10^5 oBMSCs were transferred to universal containers, where they were then centrifuged at 2000 rpm for 5 mins. These pellets were left at the bottom of the universal containers, and 10 mL chondrogenic media added. The lids of the containers were left loosely screwed onto the containers to permit gas exchange. The pellets were cultured in a standard humidified incubator, at 37°C with 5% CO₂ (Nuair DH Autoflow, Triple Red Laboratory Technologies, Long Crendon,

Buckinghamshire, UK). After 24 hours, the pellets rounded up into small spheroid-shaped pellets. These pellets were cultured for 21 days, with media changes every 3-5 days, using supplemented chondrogenic media. Both control and chondrogenic pellets were 3-dimensional (3D). After this time, the pellets were frozen in Tissue Tek[®] OCT compound (Sakura Finetek, Zoeterwoude, Netherlands), and stored at -20°C. 10 µm Cryosections were made of the pellets, using a cryosectioning machine (Bright Instrument Company, Huntingdon, UK) at -20°C, and mounted onto 1.0 - 1.5 mm thick glass slides (BDH, UK) and stored at -20°C.

3.2.6.2 *Alician Blue and Sirius Red Histochemistry*

To prepare the Alcian Blue stain. 1 g of Alcian Blue powder was dissolved in 100 mL of 3% acetic acid, and the solution filtered. The Sirius Red stain was prepared by dissolving 0.5 g of Sirius red F3B in 45 mL of distilled water. Absolute ethanol (50 mL) was then added, followed by 1.0 mL 1% sodium hydroxide. The solution was mixed vigorously, adding 4.0 mL of 20% sodium chloride, and the solution left to stand overnight before being filtered. Slide-mounted cryosectioned samples were fixed with methanol, after which they were washed in distilled water. They were then incubated with the Alcian Blue stain for 5 minutes, washed with distilled water, and then incubated in the Sirius Red stain for 1 hour.

3.2.7 Statistics

SPSS 11.0 for Mac was used for all statistical tests. Normality was calculated using the Kolmogorov-Smirnov test. Non-parametric data comparing pre- and post-G-CSF treatment groups, at 7 and 14 days, was calculated using the Friedman for multiple, related groups. Bivariate correlation co-efficients were calculated with Pearson's correlation co-efficient, and

partial correlation co-efficients were also calculated. FACS data was analysed as described in Chapter 2.

3.3 Results

3.3.1 Part I: The Effect of Induced Blood Loss on PBSC Mobilisation and Isolation

3.3.1.1 Formation of CFU-F

CFU-Fs were obtained from all pre-bleeding, and post-7% bleeding bone marrow aspirate samples, and from some of the post-7% and 15% bleeding venous blood samples. CFU-Fs from both sources had a similar morphology: spindle or fibroblastic-shaped cells growing outwards in a circular colony (Figure 3.3).

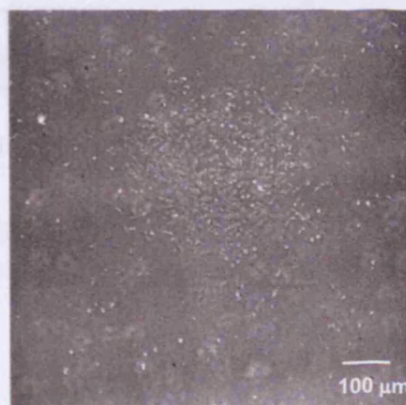


Figure 3.3 Photo of CFU-F after 14 days of culture, isolated after 7% blood loss (4x magnification).

3.2.1.2 CFU-F Counts In Blood And Bone Marrow Aspirate Samples

No PBSC/CFU-F were isolated from the blood before 7 and 15% bleeding (i.e. initial samples and samples taken at time of bleeding). After 7% blood loss, 0.0150 ± 0.015 CFU-F/cm² were counted at 7 days, 0.0300 ± 0.02058 CFU-F/cm² at 11 days, and 0.1211 ± 0.1063 CFU-F/cm² at 14 days. Using Friedman's ANOVA, differences were not found to be significant ($p = 0.368$, $p = 0.135$, and $p = 0.135$ at 7, 11, and 14 days). After 15% blood loss,

0.0078 ± 0.005490 CFU-F/cm² were counted at 7 days (Table 3.1). Out of three sheep, PBSCs were isolated from two sheep after 7% bleeding. Figure 3.4 and Table 3.1 graphically illustrate these results. In the pre-bleeding group, there was a statically significant increase in the number of CFU-Fs between 7-14 days, 7-11 days, and 11-14 days. There were no significant differences observed between time points in the other groups.

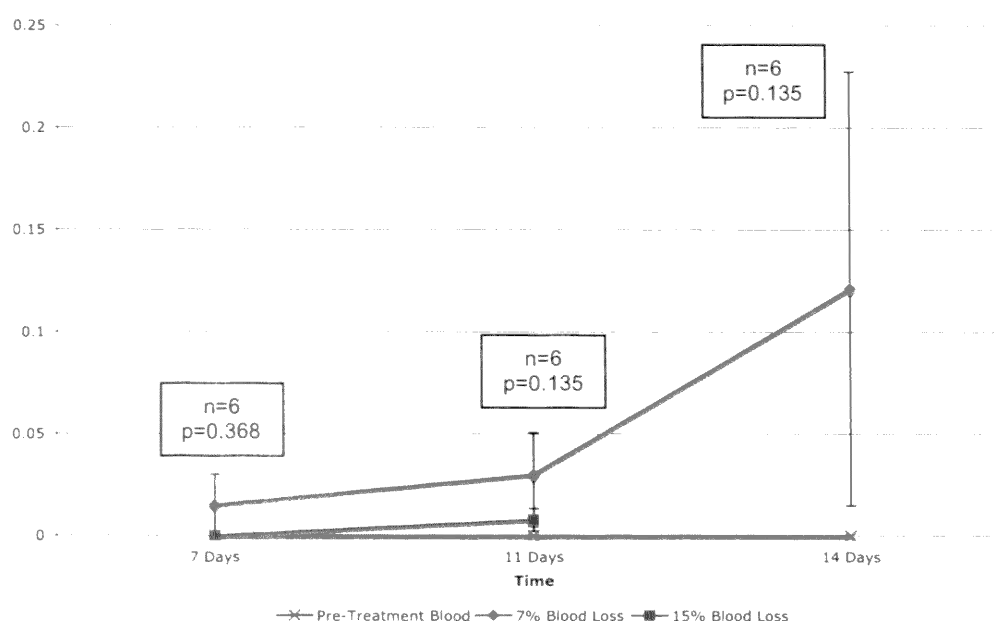


Figure 3.4 Graph illustrating results of CFU-F counting of cells isolated from the peripheral blood under normal conditions (pre-treatment), and after 7% and 15% blood loss. CFU-F counts at 7, 11, and 14 days are shown.

Looking at bone marrow samples, after 7% blood loss, there was a significant increase in the number of CFU-Fs. Pre-treatment, there were 0.2711 ± 0.09035 CFU-F/cm², 0.3425 ± 0.09035 CFU-F/cm² and 0.4259 ± 0.1479 CFU-F/cm² counted at 7, 11, and 14 days; whereas after 7% blood loss, 0.9644 ± 0.2183 , 1.653 ± 0.3913 CFU-F/cm², and 1.851 ± 0.6193 CFU-F/cm² were counted at 7, 11 and 14 days respectively (see Figure 3.5 and Table 3.1). Using Friedman's ANOVA at 7 days, this difference is significant ($p = 0.023$). Using Wilcoxon's test at 11 and 14 days, comparing the pre-treatment and post-7%-blood loss groups, the difference was also significant ($p = 0.012$ and $p = 0.012$, respectively). Once again, only a

fraction of these initial, adherent cells grew into CFU-F. There were no statically significant differences in the CFU-F counts between time points in the two groups.

	7 Days (CFU-F/cm ²)	11 Days (CFU-F/cm ²)	14 Days (CFU-F/cm ²)
Blood			
Pre-Treatment	0	0	0
7% Loss	0.0150 ± 0.0150	0.0300 ± 0.02058	0.1211 ± 0.1063
15% Loss	0	0.0078 ± 0.005490	0
Marrow			
Pre-Treatment	0.2711 ± 0.09035	0.3425 ± 0.1075	0.4259 ± 0.1479
7% Loss	0.9644 ± 0.2183	1.653 ± 0.3913	1.851 ± 0.6193
15% Loss	0.3178 ± 0.1040	-	-

Table 3.1 Chart with results of CFU-F counts of cells isolated from the peripheral blood and bone marrow, before and after blood loss.

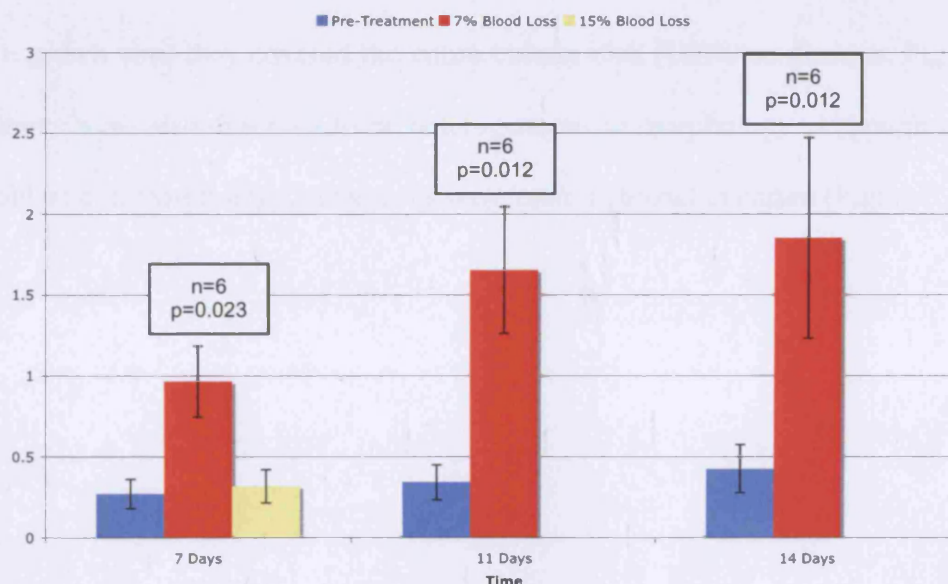


Figure 3.5 Means of CFU-F counts of cells isolated from the bone marrow before blood loss, 7 days post-7% blood loss, and 7 days post-15% blood loss.

3.3.2 Part II: The Effects of G-CSF Treatment on the Isolation and Mobilisation of PBSCs

3.3.2.1 CFU-F and Cell Morphology

At seven days, a noticeably heterogeneous population was observed in the G-CSF treated cell cultures. Spindle-shaped, fibroblastic cells formed CFU-F in a circular pattern (Figure 3.6a is an early CFU-F, Figure 3.6b after 10 days) in addition to macrophage colony forming units (CFU-M) and dendritic colony forming units (CFU-D), were noted. CFU-M consisted of highly reflective, round cells that were in association with bipolar cells with a pinched appearance, in addition to polygonal-shaped cells (Figure 3.6d, Figure 3.6e). CFU-D consisted of colonies of cells with spiked protoplasmic processes. Distributed throughout all cultures were small, round, adherent cells, akin to lymphocytic cells, which did not form colonies or appear to proliferate *in vitro* (Figure 3.6d, Figure 3.6e). In control cultures, large, multi-nucleated, senescent-looking cells were seen, nearby to the small, round, cells described above (Figure 3.6d, Figure 3.6e). These cells did not proliferate.

Cells were grown until they covered the entire culture dish (100% confluence, Figure 3.6c). These cultures were also observed to be heterogeneous in morphology. Although most cells were fibroblastic in morphology, some cells were more cuboidal in nature (Figure 3.6f).

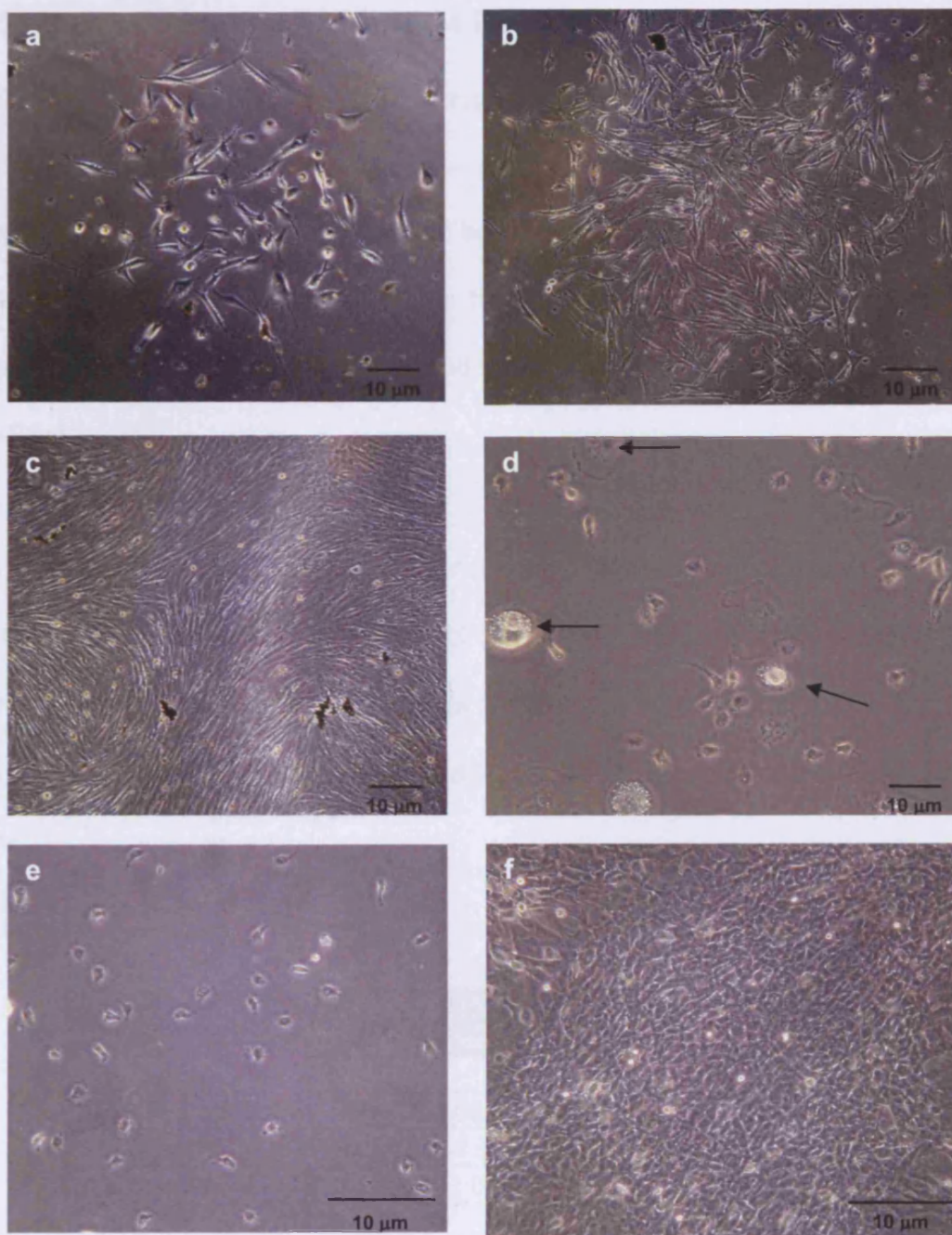


Figure 3.6 Photos of cells isolated from the peripheral blood after G-CSF treatment. a) shows a typical CFU-F observed after 5 days of culture (20x magnification); b) a CFU-F after 7 days of cell culture (20x magnification); c) shows cells at 95% confluence, (20x magnification). D) is a photo of adherent cells that are not fibroblastic in morphology and did not proliferate in CFU-F. These cells appeared spread out and senescent (see arrows, 40x magnification). E) shows non-proliferative, small adherent cells round in morphology (40x magnification); f) is a photograph of proliferative, cuboidal cells that grew to confluence and had a less circular organisation to the observed typical-looking CFU-F (40x magnification).

3.3.3 CFU-F Formation At 7 and 14 Days

All blood samples taken before G-CSF therapy did not show any signs of CFU-F formation (0 CFU-F), after both 7 and 14 days *in vitro*. However, after G-CSF treatment, CFU-Fs were observed in blood samples taken 4 and 12 hours, and 2 weeks after treatment. The CFU-F count was highest at 7 days of culture, in the blood samples taken 12 hours post-G-CSF treatment (0.1467 ± 0.1388 CFU-F/cm²), and lowest 4 hours post-G-CSF (0.02668 ± 0.01978 CFU-F/cm²).

After 14 days in culture, CFU-F counts were highest in the blood samples obtained 2 weeks post-G-CSF administration (1.027 ± 30.1353 CFU-F/cm²), compared to the lowest count which was at 12 hours post-G-CSF treatment (0.064 ± 0.064 CFU-F/cm²). Table 3.2 is a chart containing the quantitative observations, and Figure 3.7 is a graphical representation of the results.

	CFU-F/cm ² at 7 Days	CFU-F/cm ² at 14 Days
Pre-G-CSF (n=1)	0	0
4 Hours Post-G-CSF	0.02668 ± 0.01978	0.09332 ± 0.05992
12 Hours Post-G-CSF	0.1467 ± 0.1388	0.064 ± 0.0064
2 Weeks Post-G-CSF	0.04 ± 0.02310	1.027 ± 0.1353

Table 3.2 Chart displaying CFU-F counts of cells isolated from peripheral blood samples, 7 and 14 days after the initiation of culture.

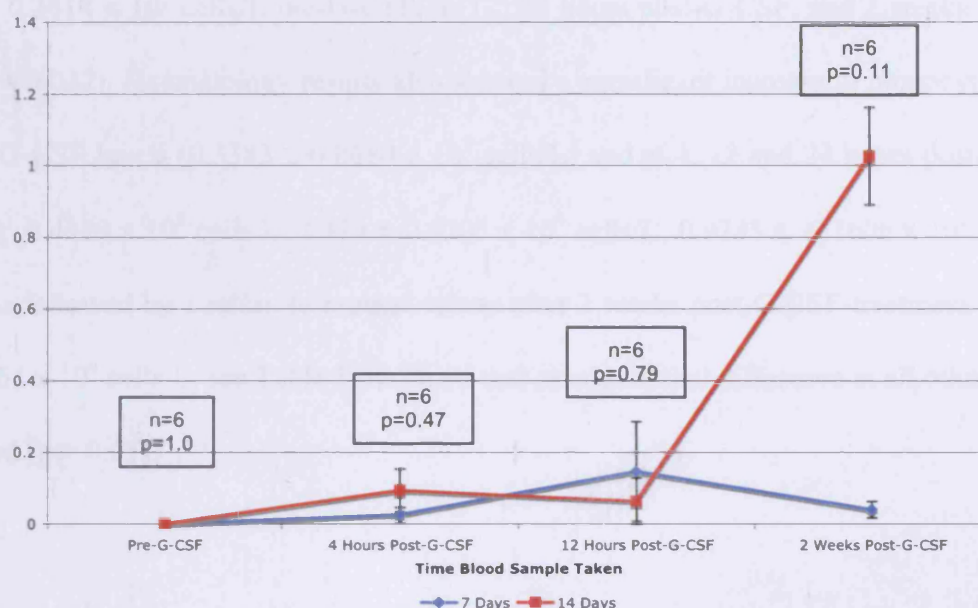


Figure 3.7 Line graph illustrating the number of CFU-F grown from peripheral blood samples before G-CSF treatment, and 4, 12, and 336 hours (2 weeks) after G-CSF treatment.

Haematology results showed an increase in white blood cell, neutrophil, and monocyte counts over the two week period after G-CSF administration. After five days of G-CSF administration, the white blood cell (WBC) count increased from $7.610 \pm 0.7988 \times 10^9$ cells/L to $26.90 \pm 1.909 \times 10^9$ cells/L. This count remained out of range 12 and 24 hours after the last dose of G-CSF ($29.25 \pm 2.501 \times 10^9$ cells/L and $27.70 \pm 1.381 \times 10^9$ cells/L, respectively), and returned to normal levels after two weeks ($10.57 \pm 0.4065 \times 10^9$ cells/L). These changes in WBC levels were significant (compared to pre-G-CSF values) over all time points ($p = 0.031$). This trend was also seen with neutrophils ($1.828 \pm 0.2220 \times 10^9$ cells/L, $14.81 \pm 1.322 \times 10^9$ cells/L, $22.11 \pm 2.098 \times 10^9$ cells/L, $17.15 \pm 1.657 \times 10^9$ cells/L, and $2.413 \pm 0.1519 \times 10^9$ cells/L pre-G-CSF, 4, 12, 24 hours post-G-CSF, and 2 weeks post-G-CSF, respectively; $p = 0.038$). Also there were significant differences observed in lymphocyte counts in pre- and post-G-CSF blood samples ($5.100 \pm 0.7179 \times 10^9$ cells/L,

$8.388 \pm 1.635 \times 10^9$ cells/L, $3.650 \pm 0.7765 \times 10^9$ cells/L, $8.833 \pm 1.630 \times 10^9$ cells/L, and $6.950 \pm 0.3614 \times 10^9$ cells/L pre-G-CSF, 4, 12, 24 hours post-G-CSF, and 2 weeks post-G-CSF; $p = 0.022$). Haematology results also showed a significant increase in monocytes from the pre-G-CSF levels ($0.3383 \pm 0.0680 \times 10^9$ cells/L) and at 4, 12 and 24 hours post-G-CSF ($2.470 \pm 0.4329 \times 10^9$ cells/L, $2.373 \pm 0.5205 \times 10^9$ cells/L, $0.9783 \pm 0.1606 \times 10^9$ cells/L). This was followed by a return to normal values after 2 weeks post-G-CSF-treatment ($0.1067 \pm 0.06064 \times 10^9$ cells/L, see Table 3.3). There was no significant difference in all other values measured ($p > 0.05$).

Full Blood Count	Normal Range	Pre-G-CSF	4 Hours Post-G-CSF	12 Hours Post-G-CSF	24 Hours Post-G-CSF	2 Weeks Post-G-CSF
WBC ($10^9/L$)	4.0-12	7.610 \pm 0.7988	26.90 \pm 1.909	29.25 \pm 2.501	27.70 \pm 1.381	10.57 \pm 0.4065
Neutrophils ($10^9/L$)	0.7-6.0	1.828 \pm 0.2220	14.81 \pm 1.322	22.11 \pm 2.098	17.15 \pm 1.657	2.413 \pm 0.1519
Lymphocytes ($10^9/L$)	2.0-9.0	5.100 \pm 0.7179	8.388 \pm 1.635	3.650 \pm 0.7765	8.833 \pm 1.630	6.950 \pm 0.3614
Monocytes ($10^9/L$)	0-1.5	0.3383 \pm 0.0680	2.470 \pm 0.4329	2.373 \pm 0.5205	0.9783 \pm 0.1606	0.1067 \pm 0.06064
Eosinophils ($10^9/L$)	0-1.0	0.2683 \pm 0.0788	0.7760 \pm 0.2607	0.5400 \pm 0.2474	0.6033 \pm 0.09790	1.063 \pm 0.1617
Basophils ($10^9/L$)	0-0.4	0.0467 \pm 0.03461	0.0660 \pm 0.06600	0.1400 \pm 0.1038	0.0483 \pm 0.0483	0.1333 \pm 0.08452
RBC ($10^{12}/L$)	8.0-16	12.03 \pm 0.5149	11.85 \pm 0.6915	12.50 \pm 0.6792	11.48 \pm 0.5491	11.00 \pm 0.6110
HGB (g/dL)	8.0-16	12.80 \pm 0.4412	12.54 \pm 0.4946	13.27 \pm 0.5420	12.38 \pm 0.4110	11.73 \pm 0.5239
RDW (%)	-	22.00 \pm 0.5177	22.68 \pm 0.4984	24.18 \pm 0.7696	21.70 \pm 0.7563	21.67 \pm 0.7356
PLT ($10^9/L$)	200-800	396.0 \pm 92.66	603.8 \pm 84.98	537.3 \pm 140.0	352.2 \pm 40.55	502.0 \pm 72.75

Table 3.3 Results of haematological analysis, of blood samples taken pre-G-CSF (n=6); 4 hours post-G-CSF (n=6); 12 hours post-G-CSF (n=6); 24 hours post-G-CSF (n=6) and 2 weeks post-G-CSF (n=3). Results were compared to normal “range” values, and abnormal results are highlighted (yellow). Blood was also processed for PBSC culture. Abbreviations: WBC = white blood cells; RBC = red blood cells; HGB = haemoglobin; RDW = PLT = platelets.

It was at two weeks post-G-CSF, when WBC, neutrophil, lymphocyte, and monocyte counts reduced to normal values, that the highest number of CFU-F/cm² were observed after 14 days of cell culture (Figure 3.8). When WBC numbers were correlated with CFU-F counts, the Pearson’s correlation co-efficient, the co-efficient was -0.523, which was significant (p=0.023), indicating that 27.4% of the WBC counts were inversely related to CFU-F counts and vice versa. However, once the time variable was accounted for and controlled using the

test for partial correlation coefficients, the correlation co-efficient was found to be -0.0063, and was not significant ($p=0.492$).

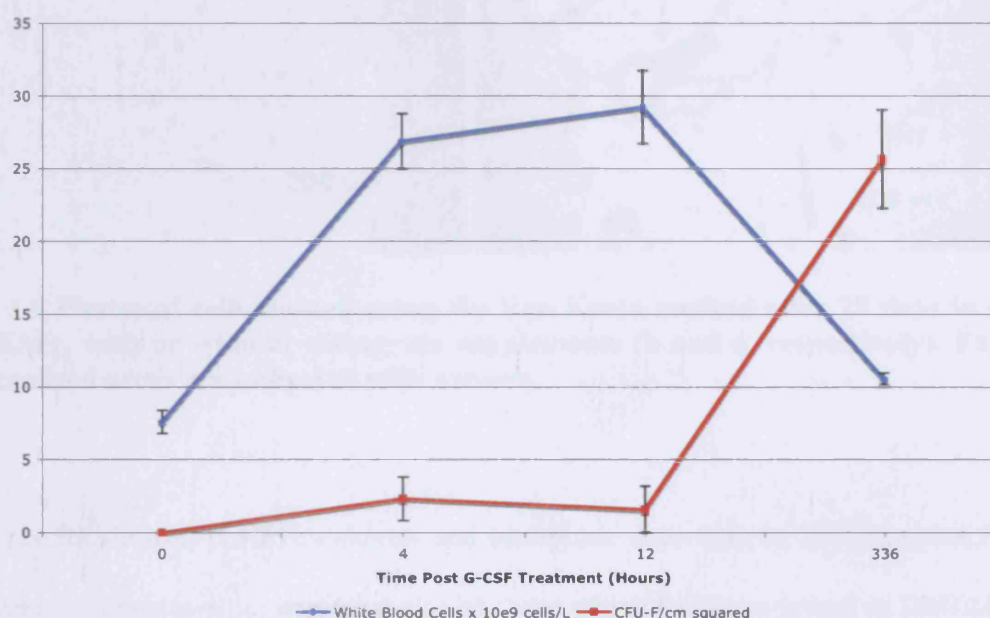


Figure 3.8 Graph comparing the WBC levels to CFU-F counts over 336 hours post-G-CSF treatment. As WBC levels dropped back to normal values, the CFU-F counts significantly increased. When time, WBC levels and CFU-F counts were correlated, this was found not to be significant ($p>0.05$).

3.3.4 Characterisation of Culture-Expanded PBSCs

3.3.4.1 Osteogenesis

After 28 days in culture, cells were stained for mineralisation using the Von Kossa method. PBSCs (cultured from peripheral blood CFU-Fs) treated with osteogenic supplements stained positively, with large regions 50 μm in width and 100 μm in length showing evidence of mineralisation. PBSCs grown in normal DMEM+, showed small flecks (5-20 μm^2) that stained positively for the Von Kossa stain, but to a much smaller extent to the osteogenic cells (Figure 3.9). The morphology of cells treated with osteogenic supplements was not observed to change and remained fibroblastic in appearance.

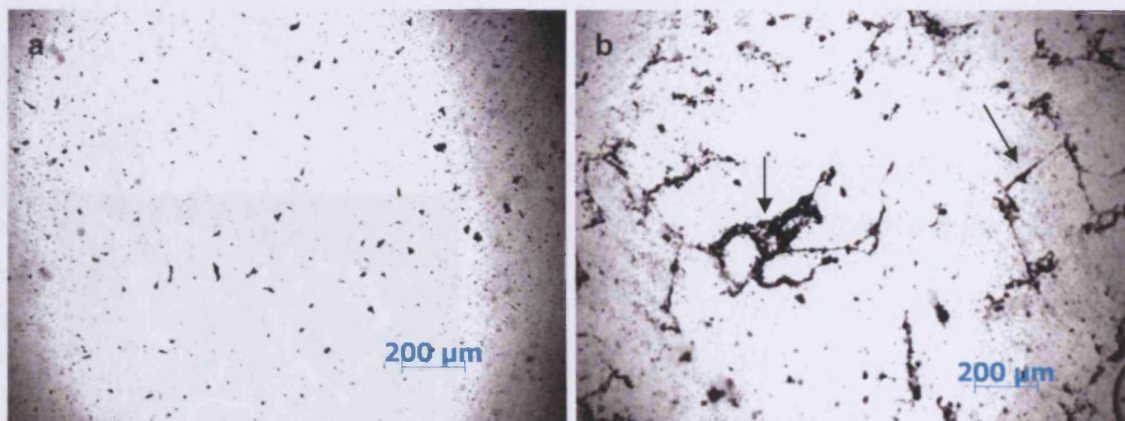


Figure 3.9 Photos of cells stained using the Von Kossa method after 28 days in culture in DMEM+, with or without osteogenic supplements (b and a, respectively). Examples of mineralised areas are indicated with arrows.

EDAX results showed positive calcium and phosphate detection, in both samples that had been treated with osteogenic supplements and those which had been grown in DMEM+ only. In the SEM photos, nodules can be seen in the sample treated with osteogenic supplements. These were positive for calcium and phosphate using EDAX. In terms of calcium phosphate ratios, the untreated sample had a Ca/P ratio of 1.96 ± 0.037 , whereas the sample treated with osteogenic supplements had a ratio of 2.14 ± 0.072 , slightly higher than the untreated sample ratio.

Figure 3.10 shows the SEM photos and EDAX peak graphs for the two groups. Like the samples in Chapter 2, there were peaks for other elements that were present as a result of processing and sputter coating. Also, these samples were run alongside HaCat cell lines, which produced calcium and phosphate nodules upon culture with osteogenic supplements, as described in Chapter 2. However, the PBSCs produced nodules with a different Ca/P ratio (the HaCat ratio was 1.92 with osteogenic supplements) with or without osteogenic medium and did not require supplements in order to produce these nodules.

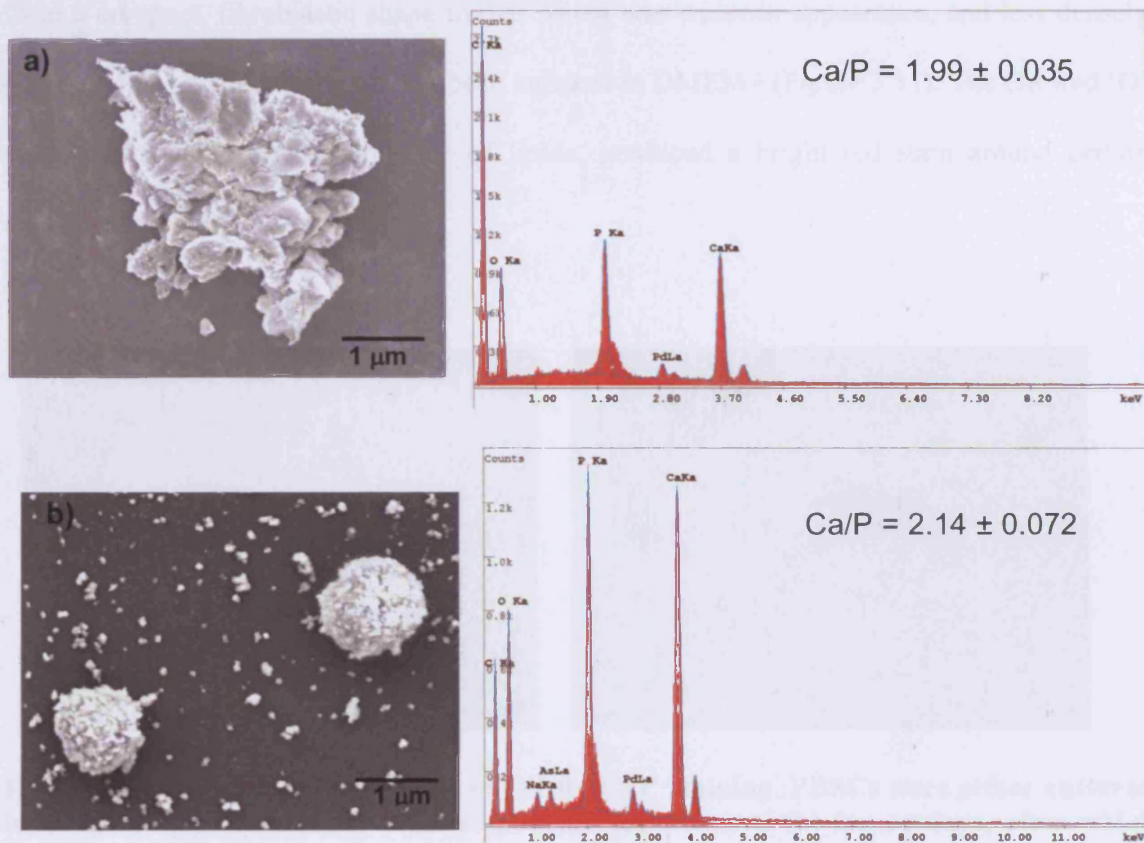


Figure 3.10 SEM images of PBSCs after 28 days in culture with or without osteogenic supplements (b and a, respectively). Nodules can be seen in the osteogenic culture; however, both samples tested positive for the presence of calcium and phosphate. This can be seen in the peak graphs alongside the SEM images. The Ca/P ratios differed between the two groups and have been noted.

3.3.4.2 Adipogenesis

PBSCs were observed to change morphology after 14 days of culture in adipogenic media from a compact, fibroblastic shape to that which was wider in appearance, and less densely populated than the controls that had been cultured in DMEM+ (Figure 3.11). The Oil Red 'O' stain, which indicates the presence of lipids, produced a bright red stain around certain clusters of cells (see arrows).

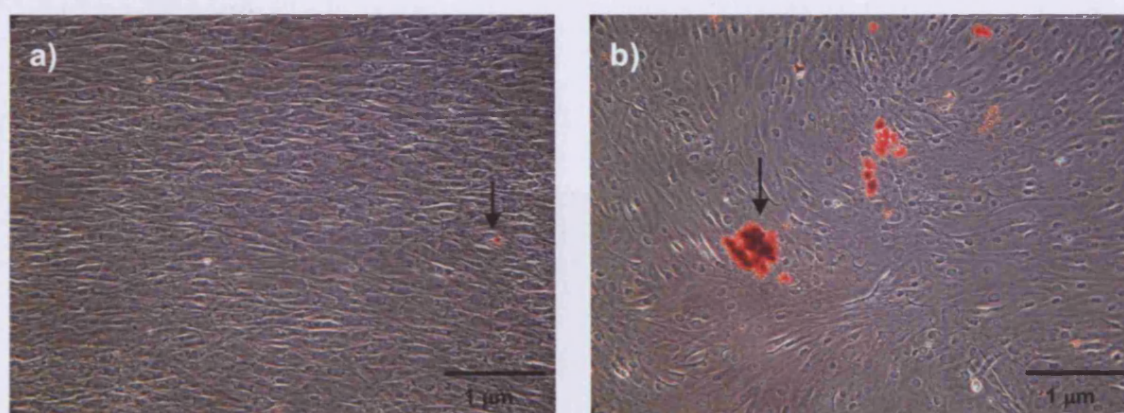


Figure 3.11 Photos showing results of Oil Red 'O' staining. PBSCs were either cultured in DMEM+ (a) or DMEM+ with adipogenic supplements (b) for 14 days, after which they were stained. A positive reaction, showing the presence of lipid vacuoles, can be seen in b), and is identified by a black arrow. A small positive reaction can be seen in a), indicated by a black arrow.

3.3.4.3 Chondrogenesis

After 21 days in chondrogenic media, PBSC pellets showed positive staining with Sirius Red and Alcian Blue (see Figure 3.12). Both stained more noticeably at the periphery of the pellet, although the Sirius Red stain was seen to stain a larger area around the pellet. The inside of the pellet was not as well stained and look necrotic under light microscopy. There were not enough cells available to run a negative control of PBSCs grown in a pellet, in normal DMEM+.

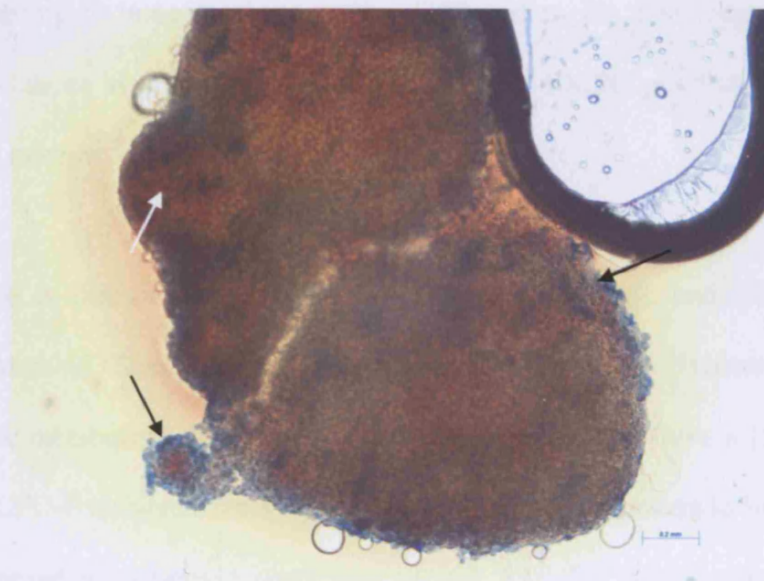


Figure 3.12 PBSC pellet after 21 days of culture in chondrogenic media, stained with Sirius Red (for collagen, red) and Alcian Blue (for GAG expression, blue). GAG-positive cells can be seen at the periphery of the pellet (see black arrows), as well as Sirius Red staining, which has penetrated deeper into the pellet (see white arrow).

3.4 Discussion

Due to injury (bone marrow aspiration), the results from the first part of this study may have been affected, in addition to the effects of blood loss. Future experiments require a group of animals that only have induced blood loss, with no bone marrow aspirates. However, studies analysing the amount of time required for the bone marrow to regenerate after bone marrow donation found that, in two patients, the turnover of CD34⁺ ranged between 20-25% per day (Sinclair et al. 2000). However, from the bone marrow CFU-F counts, a significant difference was found between periods of blood loss. The aspiration taken after 15% bleeding had much lower CFU-F than the previous aspirate, which had been taken 3-4 weeks previously. Although, according to bone marrow regeneration studies, the HSC population may have recovered (Sinclair et al. 2000), it is possible that the BMSC population has not as yet repopulated the marrow.

A 7% blood loss is akin to Class I, or minor haemorrhagic shock, and 15% blood loss can result in symptoms of Class II shock (Wilson and Baskett 1992). Haemorrhagic shock can result in hypoxic metabolism. Rochefort et al. (2006) were able to show a 15-fold increase in the number of CFU-F isolated from the peripheral blood after exposure to hypoxia conditions (50 kPa as opposed to normoxic conditions of 101 kPa) for three weeks in a rat model. However, differences between this study and the one reported in this chapter are the different species used and the method of inducing hypoxia, as well as the amount of time before blood and bone marrow was retrieved. Interestingly, this increase in PBSCs did not relate to a change in the number CFU-Fs obtained from the bone marrow. Also, this change did not affect HSC levels in the bloodstream, as measured by counting the colony-forming units of granulocyte-macrophages (GM), macrophages (M), erythroid (E), mixed (Mix) and burst-forming units-erythroid (BFU-E). In this chapter, bone marrow aspirates showed a significant

decrease in CFU-F number after the different levels of blood loss. This may be due to repeated aspirations (as mentioned above), whereas in the rat study by Rochefort et al. (2006) bone marrow was taken from femurs retrieved after sacrifice.

In one sample post-15% blood loss, CFU-F were observed after 7 days of culture. However, at 14 days, these cells ceased proliferation and the display of CFU-F-like characteristics, disputing the identity of this CFU-F as a true stromal population. In future studies, it would be useful to retain these cells and characterise their cell surface marker expression to see if they may be terminal cells of the mesenchymal lineage.

The differentiation of these cells down the osteogenic, adipogenic, and chondrogenic lineages suggests that these cells are multipotent. However, results from Chapter 2 showing a similar response of HaCat (transformed keratinocytes) after stimulation with osteogenic supplements, brings into light questions regarding the effectiveness of these methods for proving BMSC identity. The Ca/P ratio obtained in this chapter with the PBSCs was 2.14, whereas the normal ratio for hydroxyapatite is 1.67. This ratio is based on the formula for pure hydroxyapatite, $\text{Ca}_{10}(\text{PO}_4)_6(\text{OH})_2$ (Posner 1969). Variations in the hydroxyapatite that was present, as well as the formulation of different molecules such as calcium phosphates, could have altered the standard ratio, increasing it to 2.14. This could be investigated further, in future, by using techniques such as X-ray diffraction, in order to approximate the material structure (Posner 1969, Calafiori et al. 2007).

With regards to the adipogenic and chondrogenic differentiation, although some positive staining was seen (Oil Red 'O' in the case of adipogenesis, and Sirius Red/Alcian Blue in the case of Chondrogenesis), it was not completely widespread or evenly distributed in the

samples. Therefore only some of the cells differentiated can be said to be phenotypically adipocytic or chondrogenic. Use of techniques such as RT-PCR for genes involved in BMSC differentiation, as well as cell surface marker analysis, may prove to be more useful and/or specific tools for confirming BMSC/PBSC identity. It should also be noted that no proper negative or positive controls were run alongside the PBSCs, unlike in Chapter 2, in order to check the efficacy of staining for the osteogenic, adipogenic, and chondrogenic cell lines. This would be important for future work, in order to confirm the identity of the differentiated cell lines.

Blood loss from the peripheral blood circulation did not appear to have as dramatic an effect on the numbers of CFU-F obtained from the blood, as with the use of G-CSF. It is possible that the repetitive aspirations in part I of this study may have confounded the results, being an invasive procedure removing bone marrow from the animal. However, only one iliac crest was aspirated in the animals, which is only one source of bone marrow out of many. The hypothesis therefore has proved to be false. The theory behind this experiment was that physically removing blood from the circulation would cause mobilisation of HSCs from the bone marrow to repopulate the blood cell population (via cell signalling due to blood loss and/or a change in oxygen pressure in the systemic environment (Antoniou et al. 2004)), and the remodelling of the bone marrow microenvironment involving such proteins involved in HSC mobilisation, such as MMP-9 and elastases, might result in a drive to restore a HSC-MSC equilibrium, and subsequent BMSC mobilisation (Levesque et al. 2001; Sugimoto et al. 2001; Baksh, Davies and Zandstra 2003). The fact that BMSCs can increase erythrocyte formation also provokes a look at the HSC-BMSC balance (DeGowin and Gibson 1981). This experiment took blood samples seven days post-bleeding, when in Part II of this experiment, a large increase in CFU-F counts took place at 10 and 14 days post-G-CSF

treatment, after haematological results had returned to pre-G-CSF values. It is possible that BMSCs were only released from the bone marrow or detectable at a later time point than was investigated.

Regarding G-CSF-induced bone marrow cell mobilisation, the rise in WBC, neutrophil, lymphocyte, and monocyte counts (HSCs and cell types originating from CD34⁺ HSCs) after the 5 days of G-CSF treatment has been observed in many studies (Fischmeister and Gardner 2000; Takeyama and Ohto 2004). After two weeks, the levels of these cell counts returned to normal. In 3/3 animals, this return to normal levels coincided with a significant increase in CFU-F counts and the growth of PBSCs with a fibroblastic morphology. A significant bivariate correlation between WBC levels and CFU-F counts was demonstrated, which was not significant when time was a constant. The results for two weeks post-G-CSF have a lower number of samples in the group. Therefore, it is important to repeat this experiment to increase the sample size to comparable levels (a minimum of $N=6$). This may result in the partial correlation becoming significant. Clinically, blood is collected for HSC donation 4 hours after the full G-CSF treatment (Watts et al. 1998), however the number of PBSCs isolated did not appear highest at this time.

It is possible that, after mobilisation of HSCs into the peripheral bloodstream, the remodelling of the extracellular matrix associated with G-CSF-mobilised HSC release eventually caused a shedding of the bone marrow stroma, and subsequent release of BMSC-like cells. Interestingly, it has been shown that constant treatment with G-CSF can cause osteopenia in patients with congenital neutropenia (Sekhar et al. 2001). In a mouse model of sustained HSC mobilisation for 3 weeks, mice showed a significantly increased osteoclast/endosteum ratio. In these cases, an increase in osteoclast activity due to the release

of monocytes into the peripheral blood has been indicated as a possible mechanism. However, work by Semerad et al. (2005) showed that upon constant G-CSF stimulation, mice with a mutation in their G-CSF receptor displayed a reduction in CXCL12/SDF-1 expression after treatment with G-CSF for 5 days, which was related to a decrease in osteoblast number, rather than a decrease in CXCL12 expression. G-CSF was administered at a much higher concentration than used in this study (100-250 µg/kg per day, or a 20-50 times the dose given clinically). This corresponded with histomorphometry and osteocalcin results, which indicated a noticeable reduction in osteoblasts lining the endosteum 3 to 4 hours after the last dose of G-CSF. Osteoblasts are considered to be a critical factor in the bone marrow microenvironment (Calvi et al. 2003; Taichman and Emerson 1998). These authors suggested that through an indirect mechanism, osteoblast activity and/or CXCL12 expression is downregulated following G-CSF administration, which in turn would promote HSC release. It is possible that, with constant HSC mobilisation, a readjustment in the HSC-BMSC equilibrium in the bone marrow causes a release of BMSCs that no longer interact with HSCs via adhesion molecules and growth factors. There is experimental evidence to suggest that HSCs influence BMSC growth *in vitro*, and that cross talk exists between the two cell types (Baksh, Davies and Zandstra 2003). BMSCs could possibly be attracted out of the bone marrow into the circulation via interactions with HSCs, or shed as a result of the lack of interactions with HSCs. Future work should further investigate the relationship between HSC and BMSC release into the peripheral blood, by looking at cell levels at different time points, as well as their proliferative and differentiation potential. Another interesting point of investigation could be to try to reverse this mobilisation process, for example, to observe any changes in the HSC-BMSC steady-state balance after an intravenous infusion of BMSCs or HSCs, by quantifying the numbers of these cells over time, from the peripheral blood or bone marrow. This could possibly answer questions as to whether or not it is the presence of HSCs

in the bone marrow, or the process of bone marrow remodelling, or both events, that are responsible for the delayed detection of PBSCs after HSC mobilisation. Investigating the microenvironment of the bone marrow after G-CSF treatment compared to untreated sheep, looking at the morphology, and HSC and BMSC levels may also give some insight.

CHAPTER FOUR

THE SURVIVAL AND PROLIFERATION OF BMSCS IN FIBRIN GLUE AND THE USE OF A SPRAY SYSTEM FOR THE APPLICATION OF CELLS TO IMPLANT SURFACES

4.1 Introduction

In Chapters 2 and 3 of my thesis, ovine bone marrow stromal cells (oBMSCs) and peripheral-blood derived stromal-like cells (PBSCs) were isolated, expanded, and characterised, with the purpose of using these cells to augment bone growth around orthopaedic implants. For effective application of these cells to an implant surface, a sprayable, biodegradable matrix would be best.

As introduced in Chapter 1, fibrin glue is a natural scaffold that is derived from human plasma and is biodegradable, with a half-life of 21 days (Baxter Healthcare Corporation 2006). Baxter's Tisseel[®] is a fibrin matrix that has been previously applied in combination with stem cells in a femoral defect model in rats undergoing chemotherapy (Lee et al. 2005). In this study, filling the defect with only fibrin using a cannula promoted less bone growth than a combination of BMSCs and fibrin. Another application in orthopaedics would be to spray cells within fibrin directly onto implant surfaces. Sprayed fibrin is used routinely, without cells, in surgery adjunct to haemostasis or in other surgical situations where sutures or cautery should not be used. A previous study using keratinocytes sprayed in cell culture medium found no negative effects on cell viability following spraying (Grant et al. 2002). The effect of spraying BMSCs in fibrin on viability, proliferation and metabolic activity has not previously been determined. Additionally, although human BMSC activity has been previously shown to vary according to different thrombin and fibrinogen concentrations (Bensaid et al. 2003), this has not been tested with oBMSCs. This is an essential first step before oBMSCs can be used in a fibrin glue spray for bone tissue engineering in a large animal model.

There are a variety of assays that can be used to test the viability, metabolic activity and proliferation of cells after suspension in fibrin glue or after spraying in fibrin glue. To test viability in a gel scaffold, the most appropriate method to use is the fluorescent Live/Dead stain with confocal microscopy, which can be used to quantify the number of live and dead cells in fibrin glue after spraying. Confocal microscopy allows the visualisation throughout many optical sections, in contrast to normal microscopy. This feature makes it suitable for scanning three-dimensional samples.

The Live/Dead assay uses two molecules, calcein AM and ethidium homodimer. These two dyes stain live or dead cells, respectively (Molecular Probes 2001). Calcein AM is a nonfluorescent, cell-permeable molecule, which is metabolised by live cells to the fluorescent molecule calcein, visible in the FITC range (excitation wavelength 495 nm; emission wavelength 515 nm). Ethidium homodimer can enter cells with damaged membranes, whereas it cannot enter live cells with undamaged plasma membranes, and can bind to nucleic acids within the cell, where its fluorescence is then enhanced forty times (excitation wavelength 495 nm; emission wavelength 635 nm, Molecular Probes 2001; L3224, Invitrogen, Paisley, UK). These stains can also be visualised in three-dimensional (3D) constructs using confocal microscopy (Kauth and Kapperich 2005).

To measure cell metabolism, a “redox” indicator, such as Alamar Blue™, can be used. Alamar Blue™ changes colour from blue/non-fluorescent to red/fluorescent after being reduced from an oxidised state (Fields and Lancaster 1993). This “redox” reaction is related to metabolic activity and cell growth, where a reductive environment indicates cell growth. It is reduced as a result of it acting as an intermediate in the electron transport chain (ETC) of the cells. This is in contrast to other assays, such as the MTT assay (Korda et al. 2006), which

interrupts the flow of electrons through the chain, resulting in a shutdown of the ETC and eventually, cell death (Biosource™ International Inc.).

To test for differences in cell proliferation, measuring the rate of new DNA synthesis can be accomplished by quantifying the rate of radioactive thymidine incorporation in a certain period of time (Lee et al. 2005). Radioactive thymidine- H^3 is added to the culture media of cells, and incorporated into nascently synthesised DNA (Maurer 1981) during the S phase of the eukaryotic cell cycle (Voet and Voet 1995).

The hypothesis of this study is that oBMSCs would still be viable and retain the ability to proliferate following suspension in Tisseel® fibrin glue, and after application by cannula or by spraying.

The aims and objectives of this chapter are to:

- 1) To observe the viability, metabolic activity, proliferation, and morphology of oBMSCs in fibrin glue when applied using a cannula or a pressurised spray, using *in vitro* assays.
- 2) To determine the best pressure at which to spray oBMSCs in fibrin glue onto surfaces by making observations on the ability of fibrin to coat surfaces, and by measuring the survival of cells with the Live/Dead assay.
- 3) To investigate the effects of different thrombin concentrations (500 IU², 250 IU², and 100 IU²) on oBMSC metabolic activity, when suspended in fibrin glue, using the *in vitro* Alamar Blue™ assay.

4.2 Methods and Materials

4.2.1 Suspension of oBMSCs in fibrin glue

Ovine BMSCs were isolated and expanded in culture as previously described in Chapter 2. To test the proliferation of the cells in fibrin, cells were trypsinised off tissue culture plastic after three passages (P_3), centrifuged to form a pellet and were resuspended in the thrombin component of fibrin glue at a concentration of 1.0×10^6 cells/mL.

The fibrin glue used in this study was Tisseel[®] fibrin glue (Baxter Health Care Ltd., Newbury, Berkshire, UK). This glue consisted of four components in their commercial concentrations: a vapour-heated Tisseel[®] powder component (100-130 mg protein, of which approximately 75-115 mg is human fibrinogen); a bovine aprotinin solution; a vapour-heated human thrombin powder (45-55 mg protein containing about 500 IU² active bovine thrombin); a calcium chloride solution. The Tisseel[®] fibrinogen component was reconstituted in the aprotinin solution after a 10-minute incubation at 37°C in a device specifically created to heat fibrin components (Fibrinotherm[®], Baxter Health Care Ltd., Newbury, Berkshire, UK). Ovine BMSCs were put in a universal container and spun in a centrifuge at 2000 rpm for 5 minutes. The supernatant was then discarded and the pellet at the bottom of the universal resuspended in the 1.0 mL of reconstituted thrombin. Each component was then loaded into a 1.0 – 2.0 mL syringe (included in the Tisseel[®] package) and snapped into a dual-syringe holder with attached plunger device.

To make plugs, a cannula was fixed to the end of the dual-syringe system and the oBMSC-fibrin combination ejected to produce 0.1 mL plugs of fibrin. These were transferred to 12-well plates (Corning, Corning, N.Y., USA), covered with 1 mL of standard DMEM+ and cultured using standard tissue culture techniques.

4.2.2 Spraying oBMSCs in fibrin glue and fibrin-cell plug formation

To spray the fibrin glue using this system, a Duploject[®] (Baxter Health Care Ltd., Newbury, Berkshire, UK) spray set was used, which consisted of sterile plastic tubing which connected to the a dual-syringe tip, which allowed air to come into contact with the fibrin components as they came out of the syringe. The other end of the tubing was connected to a Fibrijet[®] (Micromedics, Inc., St. Paul, Minnesota, USA) pressure gauge, which was connected to a pressure pump (Figure 4.1). The Fibrijet was set to 0.5, 1.0, or 1.5 Atm, and the plungers of the fibrin system pressed to allow release of sprayed fibrin onto the dry tissue culture surface (6-well plates; Orange Plastics, Triple Red Laboratory Technology, Long Crendon, Buckinghamshire, UK), without any tissue culture media present. The area of each well was 9.03 cm². 2 ml of DMEM+ (control media) was added to each well afterwards.

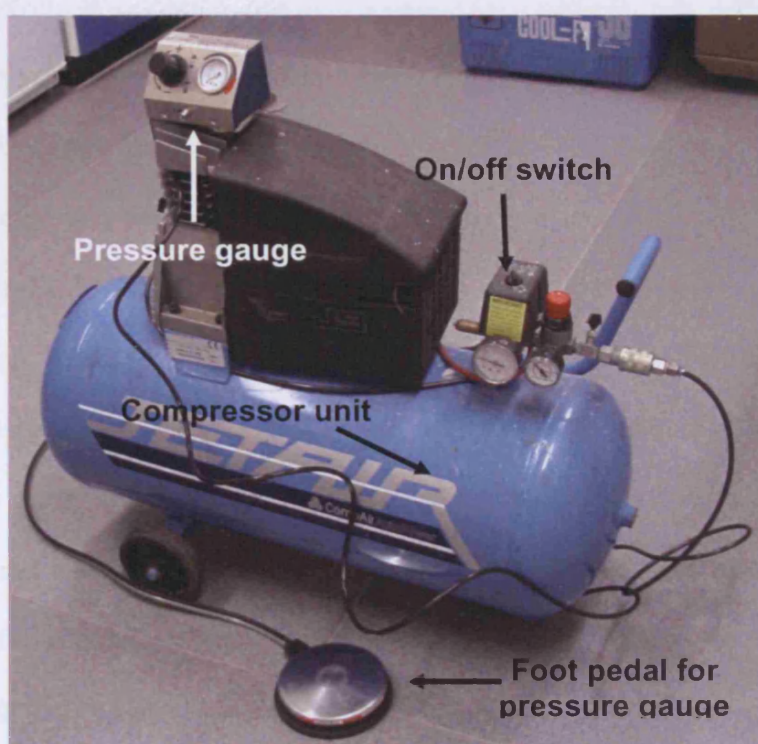


Figure 4.1 Equipment used for spraying fibrin, including an air compressor and a pressure gauge, which is controlled by a foot pedal (see arrows).

4.2.3 The effect of fibrin glue on oBMSC viability, metabolism, proliferation, and morphology when applied using a spray or cannula

4.2.3.1 Viability

To assess the viability or death of cells after spraying the Live/Dead assay was used. For this experiment, 2.0×10^6 cells/mL were suspended in thrombin and combined with fibrinogen, as described above, and 0.05 mL of each component was applied using a cannula, or with a pressurised spray, onto the tissue culture surface of 6-well plates (6-well plates (Orange Plastics, Triple Red Laboratory Technology, Long Crendon, Buckinghamshire, UK),. Cells were then incubated with DMEM+ with 1.0 μ M calcein and ethidium homodimer each, for one hour. After this time, samples were rinsed in PBS and viewed under a confocal microscope (Leica SP2 AOBS system, Leica Microsystems UK Ltd., Milton Keynes, Buckinghamshire, UK), using Leica Confocal Software (LCS version 2.61, Leica Microsystems UK Ltd., Milton Keynes, Buckinghamshire, UK) in 200 μ m-thick sections, and were reconstructed in a 3D overlay using LCS Lite (version 2.61, Leica Microsystems UK Ltd., Milton Keynes, Buckinghamshire, UK) software. Six samples were analysed per group. The four groups were: 1) oBMSCs suspended in fibrin glue, applied with a cannula; 2) oBMSCs suspended in fibrin glue, which was sprayed at 0.5 Atm; 3) oBMSCs sprayed in fibrin glue at 1 Atm; and 4) oBMSCs in fibrin glue, sprayed at 1.5 Atm. The percentage of live cells was calculated by dividing the number of live (calcein AM positive) cells by the total number of live and dead (ethidium homodimer-positive) cells. Results were compared to oBMSCs initially plated at the same concentration, but on tissue culture plastic and without fibrin glue.

4.2.3.2 Metabolic Activity

To observe the effect of fibrin glue on the cells' metabolic activity, the Alamar Blue™ assay was used on oBMSCs in fibrin glue applied with a cannula or sprayed at 0.5, 1.0 or 1.5 Atm of pressure. After 4 hours of sample incubation with Alamar Blue™, 100 µL from each Alamar Blue™-reacted sample was used and analysed as described in 2.2.3.5. These results were compared to oBMSCs applied at the same concentration without fibrin glue.

4.2.3.3 Proliferation

A thymidine- H^3 incorporation assay was used to determine the proliferation of oBMSCs in fibrin glue when applied via a cannula or sprayed at different pressures. For this assay, either 0.1 mL of fibrin was cannulated onto the surface or sprayed at 1 Atm onto the well surface of 6-well plates (Orange Plastics, Triple Red Laboratory Technology, Long Crendon, Buckinghamshire, UK), and covered with 2 mL of standard DMEM+. Proliferation was measured from 0-24 hours, 24-48 hours and 48-72 hours. For the 0 - 24 hours group, 1.0 µL of thymidine- H^3 (GE Healthcare, Giles, Buckinghamshire, UK) was added for each 1.0 mL of media, and placed in a designated standard humidified incubator for 24 hours. The assay was repeated in triplicate for each treatment and results were compared to oBMSCs seeded at the same cell numbers as the cells suspended in fibrin, but cultured without fibrin glue.

After each 24-hour time point, cells were lysed and processed as outlined in 2.2.3.6, with an additional step: to break down the fibrin, samples were then freeze-dried overnight, resuspended in 0.5 mL of 1% papain in PBS and incubated at room temperature overnight on a gentle shaker.

4.2.3.4 Morphology and distribution of oBMSCs in fibrin glue plugs

To observe the morphology and distribution of oBMSCs in fibrin glue, six plugs were formed using the commercial concentrations of thrombin and fibrinogen (see 4.2.1) and cultured for 2 weeks, then fixed for wax histology in 10% formal saline. Samples were dehydrated in increasing concentrations of industrial methylated spirit (IMS), from 30% to 100% IMS, cleared in xylene, infiltrated with paraffin wax and embedded. Wax-embedded samples were mounted on a sledge microtome and thin (4-5 μm) sections cut, which were then mounted onto glass slides. Specimens were de-waxed in xylene and stained with haematoxylin (a nuclear stain) and eosin (counterstain).

4.2.4 The effect of thrombin concentration on oBMSC activity

Different concentrations of thrombin were tested for their effects on cell proliferation. Thrombin was either used undiluted (500 IU^2 - Tisseel[®]'s commercially available concentration) diluted with phosphate buffered saline (PBS) to half (250 IU^2) and one-fifth the original concentration of thrombin (100 IU^2). Ovine BMSCs were isolated and expanded in culture as previously described in Chapter 1. For this assay, 2.0×10^6 oBMSCs/mL were suspended in thrombin. Using the cannula-ended dual syringe, 0.05 mL of each component was ejected to produce 0.1 mL plugs of fibrin glue. These plugs were cultured in 12-well tissue culture plates with 1.0 mL of DMEM+. An Alamar Blue assay was carried out at 1, 3, and 9 days to assess cell activity. For each time point and each concentration of thrombin, six samples were tested.

4.2.5 Data analysis

Raw data was entered into SPSS 11 for statistical analysis. Data normality was determined with the Kolmogorov-Smirnov test. Parametric data for two groups was tested with the student t-test and non-parametric data from two groups were compared using the Mann-Whitney U test for independent samples. The one-way analysis of variance (ANOVA) test was used to compare parametric results from more than 2 independent groups. Results were considered significant when $P \leq 0.05$.

4.3 Results

Fibrin application at 1.0 and 1.5 Atm was visibly easier, smoother and more evenly distributed when compared to spraying fibrin at 0.5 Atm, where the fibrin did not have enough pressure to properly form an aerosol.

4.3.1 The effect of fibrin glue on oBMSC viability, metabolism, proliferation and morphology when applied using a spray or cannula

4.3.1.1 Viability

There was no significant difference in the viability of cells after spraying at 0.5 Atm, 1.0 Atm, or 1.5 Atm in fibrin glue. Calcein was spread intracellularly, while the ethidium was visualised in the nucleus/nucleolar region of the cell. In all samples, some cells were seen to stain positively for both calcein AM and ethidium homodimer, suggesting plasma membrane damage that allowed ethidium penetration or cell death within minutes after spraying (Figure 4.2). The mean percentage of live cells in the groups sprayed at 1.5 Atm was $52.26 \pm 5.08 \%$, while for the cells applied by a cannula, the mean percentage of live cells was $59.82 \pm 13.36 \%$ (Figure 4.3, Table 4.1). There was no significant difference between all groups ($p > 0.05$ in all comparisons).

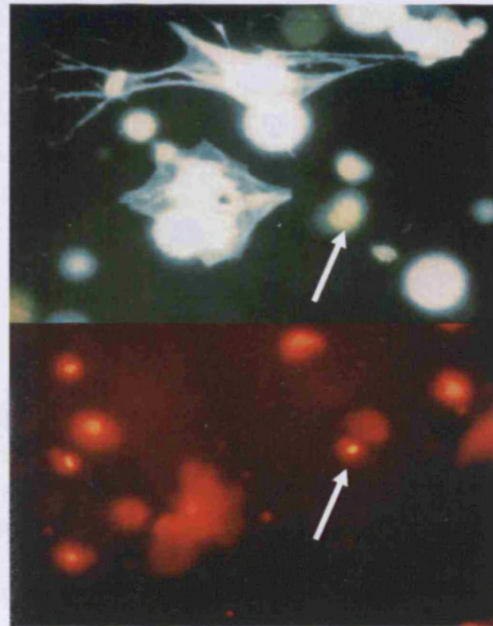


Figure 4.2 An example of the sectional images obtained for the live/dead stain using confocal microscopy (20x magnification). In this example, all of the optical sections have been layered so that all cells in the fibrin gel can be visualised. The green cells are those stained positively with calcein AM (live), and is spread throughout the cell cytoplasm. Red cells are those stained with ethidium homodimer (red), which intercalates with nucleic acids and therefore is mostly visualised in the cell nuclei. A double labelled-cell is noted with arrows.

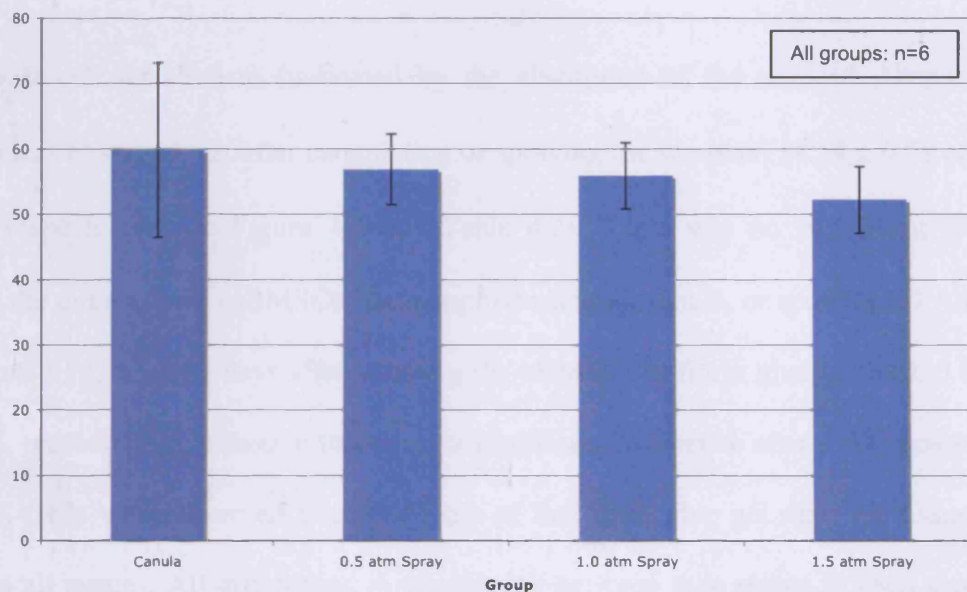


Figure 4.3 Chart indicating the percentage of live (Calcein AM positive) oBMSCs in fibrin glue after being ejected from a cannula or using a spray, at 0.5 Atm, 1.0 Atm, and 1.5 Atm. The total number of cells was calculated by dividing the number of live cells by the total number of live and dead (ethidium homodimer positive) cells.

Group	% Live oBMSCs ± Standard Error
Cannula	59.82 ± 13.36
0.5 Atm Spray	56.89 ± 5.37
1.0 Atm Spray	55.91 ± 5.05
1.5 Atm Spray	52.26 ± 5.08

Table 4.1 Table showing the mean percentage and standard error of live cells in each group.

4.3.1.2 Cell metabolism

The lowest cell metabolism (indicated by the absorption of the reduced Alamar Blue™ product) was observed just after cannulating or spraying the samples (14.54 ± 0.58 and 14.40 ± 0.27 , respectively, see Figure 4.4 and Table 4.2). There was no significant difference between the three groups (oBMSCs fibrin applied using a cannula, or spray at 1.0 Atm) at all time points 0, 2, 4, and 7 days after spraying the oBMSCs in fibrin glue ($p=1.00$, 0.87 , 0.15 , and 0.55 , respectively), although there was a significant difference after 1 day post-spraying ($p=0.00$). Cells were observed to migrate out of the fibrin glue gel onto the tissue culture plastic in all groups. All differences in absorbency between time points in each group were significant ($p<0.03$) except between days 2-4, 4-7, and 1-7 in the canula group, and between 2-4, 4-7, 1-4, 1-7 and 2-7 in the 1.0 atm spray group, where $p>0.05$.

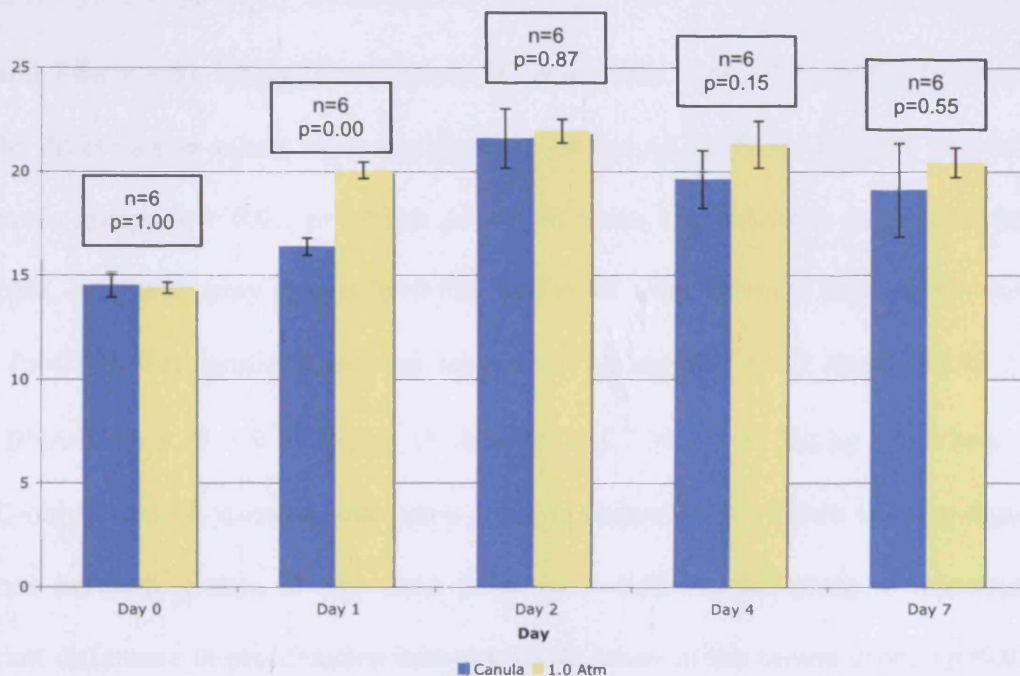


Figure 4.4 Graph illustrating results of Alamar Blue™ assay, when oBMSCs in fibrin were either applied with a cannula or spray at 1 Atm. This assay, which is an indicator of cell activity, was tested just after application (Day 0), and at days 1, 2, 4, and 7 after application.

	Day 0	Day 1	Day 2	Day 4	Day 7
Cannula	14.54 ± 0.58	16.39 ± 0.41	21.61 ± 1.43	19.63 ± 1.38	19.13 ± 2.25
1.0 Atm	14.40 ± 0.27	20.06 ± 0.39	21.96 ± 0.56	21.32 ± 1.13	20.44 ± 0.71

Table 4.2 Table showing Alamar Blue™ absorption measurements over the seven days.

4.3.1.3 Proliferation

Samples grown without fibrin glue (oBMSCs only) appeared to have less proliferation than those samples in fibrin glue applied with a cannula at 24 and 48 hours (35.95 ± 4.74 Bq/ μ g DNA/hour and 36.20 ± 11.06 Bq/ μ g DNA/hour in the oBMSC-only group; 79.33 ± 8.61 Bq/ μ g DNA/hour and 70.66 ± 7.73 Bq/ μ g DNA/hour in the cannula group). Cell proliferation was reduced after 24 hours in samples that had been sprayed, compared to cannula-applied controls (63.93 ± 6.00 Bq/ μ g DNA/hour at 24 hours, 6.61 ± 0.90 Bq/ μ g DNA/hour at 48 hours and 7.56 ± 1.81 Bq/ μ g DNA/hour at 72 hours; see Figure 4.5, Table 4.3, and Table 4.4). The difference in values were significant at 24 and 48 hours between the oBMSC-only and cannula groups ($p = 0.01$, $p=0.03$ at 24 and 48 hours, respectively), at 24 hours between the oBMSC-only and spray groups ($p=0.02$), and at 48 hours between the cannula and spray groups ($p=0.03$). Cell proliferation was reduced in all samples at 72 hours (19.32 ± 11.89 Bq/ μ g DNA/hour; 3.78 ± 0.66 Bq/ μ g DNA/hour; and 7.56 ± 1.81 Bq/ μ g DNA/hour, in the oBMSC-only (control, cannula and spray groups, respectively). There was no significant difference between groups at this time point ($p > 0.05$ for all group comparisons). A significant difference in proliferation between 48-72 hours in the cannula group ($p=0.02$) and between 24-72 hours in the spray group ($p<0.01$) was observed.

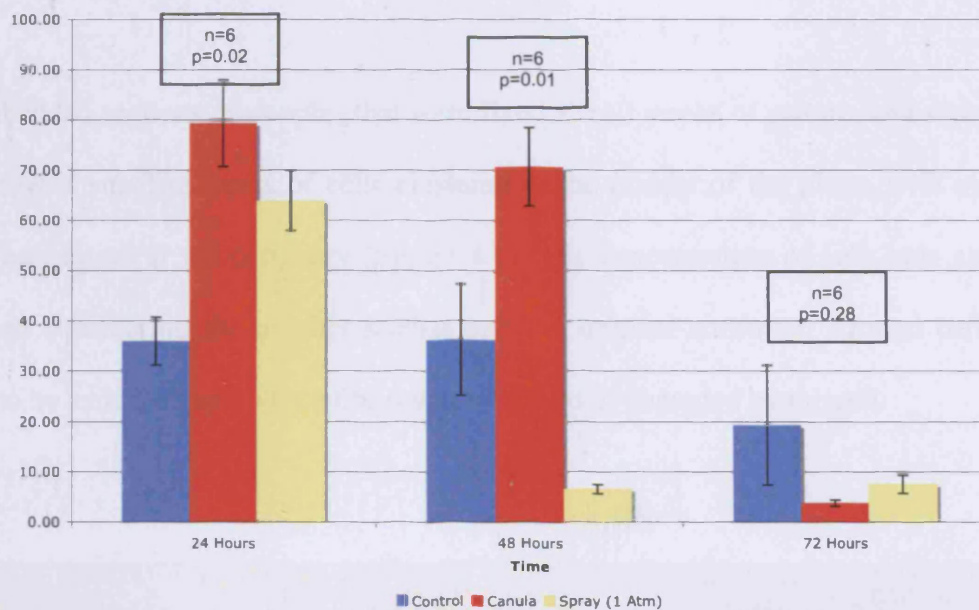


Figure 4.5 Bar graph comparing ³H-thymidine incorporation (indicative of proliferation) between oBMSCs grown on tissue culture plastic, oBMSCs suspended in fibrin glue, and oBMSCs sprayed in fibrin glue, at 0-24 hours (24 hours), 24-48 hours (48 hours) and 48-72 hours (72 hours) after the initiation of culture.

Group	0 - 24 Hours (Bq/μg DNA/hour)	24 - 48 Hours (Bq/μg DNA/hour)	48 - 72 Hours (Bq/μg DNA/hour)
oBMSC-only	35.95 ± 4.74	36.20 ± 11.06	19.32 ± 11.89
Cannula	79.33 ± 8.61	70.66 ± 7.73	3.78 ± 0.66
Spray	63.93 ± 6.00	6.61 ± 0.90	7.56 ± 1.81

Table 4.3 Table showing oBMSC proliferation for all groups at the three time points.

Group	Day 1 p-value	Day 2 p-value	Day 3 p-value
oBMSC-only-Cannula	0.01	0.03	0.48
oBMSC-only-Spray	0.02	0.22	0.66
Cannula-Spray	0.22	0.03	0.14

Table 4.4 Table of P-values between all three groups at each time point.

4.3.2 Morphology and distribution of oBMSCs in fibrin glue

Wax-embedded sections of samples that were fixed after 2 weeks of culture, and stained with H&E, showed small numbers of cells clustered in the middle of the plugs, with elongated cells being present at the periphery (Figure 4.6). The concentration of cells was extremely low, when considering the number seeded into the original construct. Around cells, there appears to be a cleared area where fibrin was stretched or degraded by the cell.

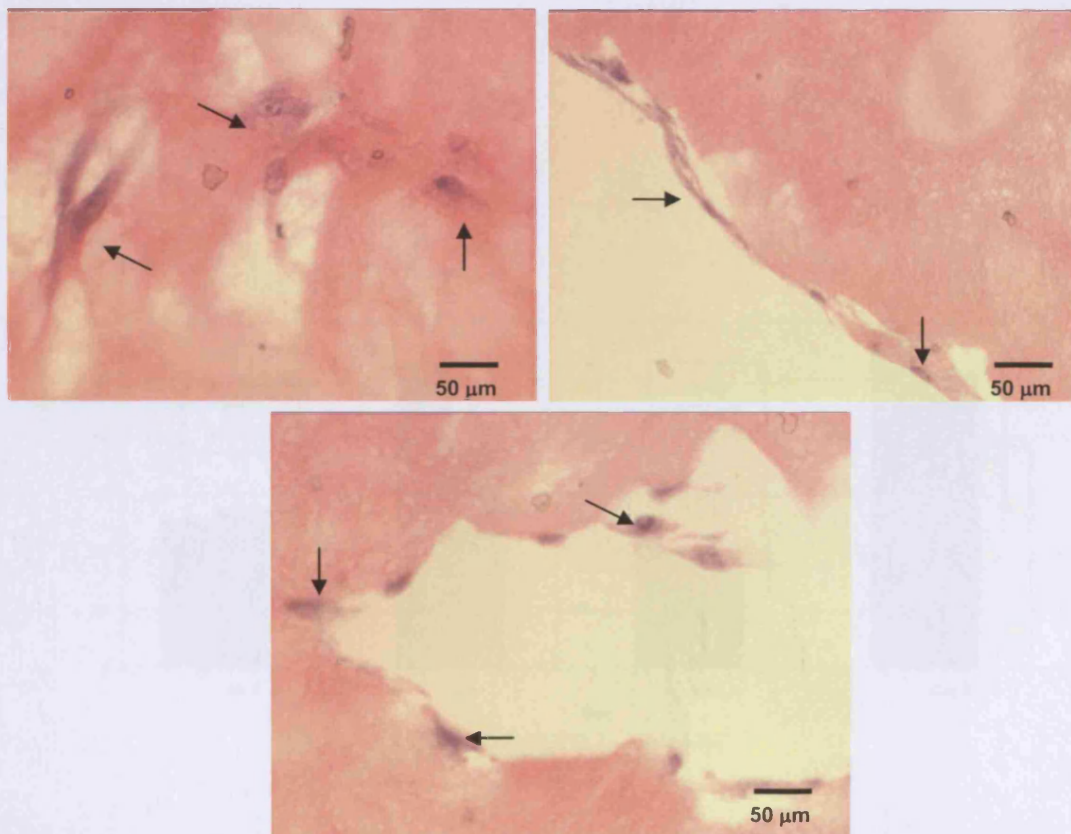


Figure 4.6 Images of histological sections of oBMSCs embedded in fibrin glue and cultured for 2 weeks. Photos were taken at 10x magnification. oBMSCs can be seen along the periphery of the fibrin, indicated by arrows. Haemotoxylin (purple) stains cell nuclei, and eosin (pink) is the counterstain (probably fibrin glue). Around cells, the fibrin appears to be stretched or degraded.

4.3.3 Testing the effect of thrombin concentration on oBMSC activity using the Alamar Blue assay

Ovine BMSCs were metabolically active in the fibrin plugs for the 9-day period of the experiment. The mean absorption of the ovine BMSCs at different thrombin concentrations at day 1 were: 41.80 ± 8.41 (standard error) with no thrombin dilution (500 IU^2), 33.50 ± 5.91 with at 250 IU^2 (half thrombin dilution), and 27.94 ± 5.68 at 100 IU^2 (a fifth dilution). On day 3, the readings were 46.53 ± 15.01 with no dilution, 40.72 ± 8.41 at 250 IU^2 , and 30.45 ± 5.86 at 100 IU^2 . On day 9, the mean absorption were 48.71 ± 14.88 in the plugs with undiluted thrombin, 54.73 ± 11.89 at 250 IU^2 of thrombin, and 39.18 ± 10.52 at a fifth dilution. Figure 4.7 illustrates these results in a bar graph.

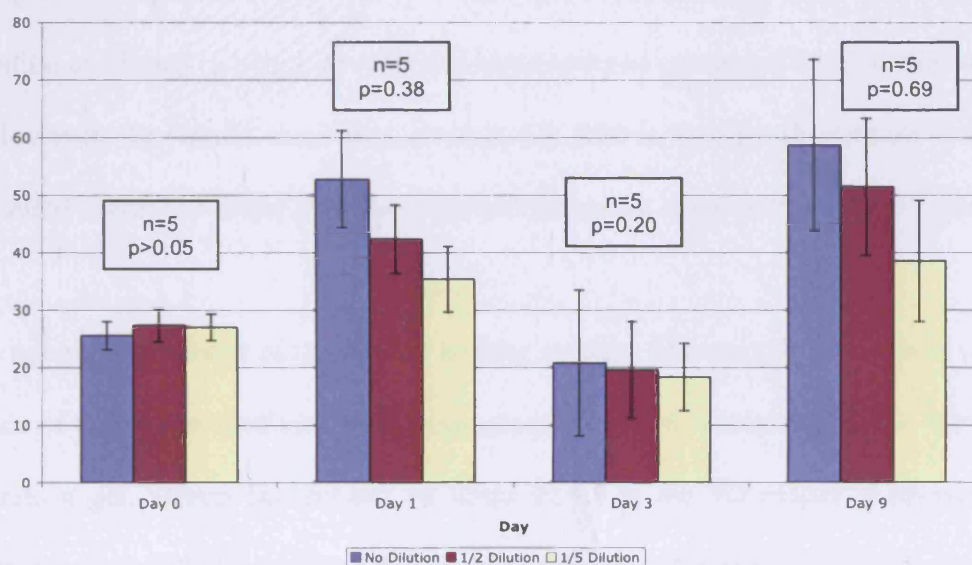


Figure 4.7 Graph indicating oBMSC metabolic activity when suspended in different concentrations of fibrin, which was achieved by varying the thrombin concentration. Although at a lower density of fibrin (with the lowest thrombin concentration), the Alamar Blue™ absorption is lower than the other groups at day 1, 3 and 9. This difference was not statistically significant.

Comparing the different dilutions of thrombin using one-way ANOVA, there was no significant difference in the proliferation of the cells in the plugs (day 1, $p=0.38$; day 3, $p=0.30$; day 9, $p=0.69$). Cells were observed to migrate out of the fibrin onto the tissue culture plastic, and although there appeared to be no difference in the migration between groups, this was not quantified. Within each group, there were no significant differences between time points ($p>0.05$ in all cases).

4.4 Discussion:

This chapter has shown that after the spraying of oBMSCs in fibrin glue at 1 Atm of pressure, cells are still viable, active and proliferative. There was no significant difference observed in the spraying of fibrin glue at 0.5, 1.0 or 1.5 Atm of pressure, although there was a difference in proliferation at 48 and 72 hours, in cells that were sprayed compared to those that were not sprayed. However, the results show that, overall, 1.0 Atm is the lowest pressure at which a well-distributed coating of fibrin glue can be achieved and so is the best pressure to be used.

Fibrin is a natural component of the wound healing system. The enzyme, thrombin, which in the presence of Ca^{2+} ions catalyses the fibrinogen precursor to fibrin molecules, which then assemble into a gel, affects the density of fibrin fibres in the 3D matrix. Although ovine BMSCs appear to proliferate in fibrin (at the commercial concentration) for 14 days, there was a possibility that different densities of gel would be more beneficial to cell growth than others. However, in this study no differences were found in cell proliferation with cells grown in fibrin with no diluted thrombin or in fibrin with thrombin diluted by a half or by a fifth. This is similar to results found by Catelas, Sese and Helgersson (2004), which showed that the concentration of thrombin did not effect the proliferation of hBMSCs to the same extent as the fibrinogen concentration. This is despite the fact that a lower thrombin

concentration results in a fibrin mesh structure with fibrils of a larger diameter and larger pore size ($>5\ \mu\text{m}$ at a 5 IU thrombin), and that Tisseel™ contains significantly more fibrinogen than human plasma (75-115 mg/mL versus 2-4 mg/mL in plasma; Exner et al. 1979). The thrombin concentrations used in this experiment was at the commercial concentration of 500 IU, where the mesh structure would develop with thinner fibrils and smaller pores ($<1\ \mu\text{m}$, (Baxter Tissue Engineering Guide). This is in contrast to a study by Bensaid et al. (2003), which found that a thrombin concentration of 100 μm was more optimal than a concentration of 500 μm . This experiment also found that fibrin, *in vitro*, was optimal for hMSC growth at 20% of the normal fibrinogen levels used commercially. However, it should be noted that a much smaller concentration of cells was used in this study (5×10^4 cells/mL) when compared to our study (1×10^6 cells/mL).

Cells were observed to migrate out of the fibrin glue scaffold at all thrombin concentrations and when samples had been sprayed as well. Promoting cell proliferation and migration is an observed property of fibrin glue (Becker, Domschke and Pohle 2004; Cox, Cole and Tawil 2004; Brown 1993). However, from the thymidine- H^3 incorporation assay results, it appeared that proliferation in both fibrin groups was lower than in the group that was grown directly on tissue culture plastic. The effects of nutrient gradients, from the supplemented media, and oxygen diffusion through the gel could have influenced the results, as sprayed fibrin applied as a thinner finely applied layer, may differ in these properties from cells grown in a monolayer, or those cells applied to the cell surface in fibrin using a cannula. Migration of cells, as well as differences in proliferation may have resulted. Despite the differences in proliferation, however, the cells were always metabolically active in fibrin glue, according to my Alamar Blue[®] data, and the activity levels were not shown to greatly increase over 7 days. The unaccounted cell proliferation in the thymidine assay, as discussed in Chapter 2,

due to S-phase cells already being present when the thymidine- H^3 had been added to cell culture media, may also have affected the results. In addition, cell number was not accounted for in the Alamar Blue[®] assays, meaning that the results, which were reported in this chapter to reflect cell metabolism, may have been confounded by the increase in cell numbers over time, as the cells proliferated (see Chapter 2 Discussion).

A quantitative measure of cell migration out of gels from these various groups (different concentrations of thrombin, sprayed fibrin) could be visualised using time-lapse video microscopy (Knapp, Helou and Tranquillo 1999). This migration is the likely explanation for the lack of cells viewed in the histological specimens. Modifying the fibrin with integrin-binding molecules such as RGD peptides could possibly modify cell migration from the gels (Meinhart 2005; Yang et al. 2004). In future, scanning electron microscopy (SEM) of oBMSCs in varying fibrin densities may also give a visual perspective on cell survival, spreading, and morphology.

In future experiments, it would be interesting to grow oBMSCs in fibrin glue on non-treated tissue culture plastic, or tissue culture plastic that has been specially treated such as Ultra Low Attachment coated polystyrene, produced by Corning, Corning, N.Y., U.S.A.), which is coated with a hydrogel layer that prevents cell attachment. Using the Alamar Blue assay, we have shown that the spraying of BMSCs does not affect its viability or proliferation. One dermal tissue engineering study using this system with epidermal cells had similar Trypan Blue results (Cohen, Bahoric and Clarke 2001). However they did not attempt a viability assay within fibrin glue itself (their spray technique was tested on cells in culture media).

In order to make more detailed observations of the effects and viability of BMSCs suspended and sprayed in fibrin, it would be useful to look at the histology of the cells in fibrin, sprayed or unsprayed, as well as electron microscopy, 1) initially after spraying the cells in fibrin glue, as well as 2) making more macroscopic observations of the different plugs after culture, at different thrombin concentrations, and after being sprayed at different concentrations. Lee et al. (2005) showed that rat BMSCs were viable and healthy in morphology after being suspended in fibrin glue, using histology, scanning electron microscopy (SEM) and transmission electron microscopy (TEM); however such work has not been repeated using ovine BMSCs.

Whether or not the shear stress and fluid flow experienced by the cells in fibrin instigates an effect on the cells differentiation or programmed cell death (apoptotic) pathways is not known. Shear stress has been shown to induce osteocalcin expression in rat BMSCs (Kreke and Goldstein 2005) and may aid in the osteogenic differentiation of cells. In the Live/Dead experiment presented in this chapter, some cells appeared to undergo cell death minutes after spraying, having first reacted with the “live” cell marker calcein AM to produce fluorescent calcein molecules. Whether or not this is apoptosis or necrosis due to irreversible cell damage could be determined by using apoptosis assays such as the terminal transferase dUTP nick end labelling (TUNEL) assay, which detects the DNA degradation step in apoptotic cells (Gavrieli, Sherman, and Ben-Sasson 1992), or protein detection methods like immunohistochemical staining or western blotting for apoptotic markers such as Annexin V, Bax or p53 (Loewe et al. 2006; Basu and Haldar 1998). Also, as cell death due to apoptosis often takes longer than 1 hour to initiate and progress, the 1 hour time point for the Live/Dead assay might not have been sensitive enough to detect apoptosing cells. Therefore, there may have been unrecorded cell loss after spraying, which should be taken into account

in the future. However, those oBMSCs that do survive actively metabolise and proliferate, as shown using Alamar Blue and Thymidine- H^3 incorporation. Spraying did affect cell metabolism after the first 24 hours post-spraying (Results- 4.3.2.3), but cells appear to have recovered by Day 2 of the experiment. To look at the effects of spraying in fibrin glue on oBMSC osteogenic differentiation, one could perform RT-PCR detection of early osteoblastic genes such as cbfa-1 or osterix.

Currie et al. (2003) found no significant difference between spraying keratinocytes onto freshly debrided porcine wound sites in fibrin glue or without (cells suspended in culture medium) on the epithelial areas after three weeks *in vivo*.

In conclusion, oBMSCs were viable and were able to metabolise and proliferate in fibrin glue. Spraying at 1.0 Atm gave the best result in terms of control and even distribution of fibrin onto surfaces, and did not significantly affect cell viability or metabolism. In the next two chapters, the oBMSC-fibrin spray system described in this chapter is used in an attempt to encourage new bone formation around orthopaedic implants *in vivo*, by spraying oBMSCs onto implant surfaces.

CHAPTER FIVE

AUGMENTING THE FIXATION OF MASSIVE IMPLANTS USING BONE MARROW STROMAL CELLS

5.1 Introduction

For treatment of bone tumours of the extremities, endoprosthetic replacements are a viable alternative to amputation and the preferable option in modern surgery. As described in Chapter 1, bone tumour replacements have a significantly lower survival rate when compared to total hip replacements (Blunn et al. 2000). The main cause of this high failure is aseptic loosening. In the case of massive bone tumour implants fixed within the femoral cavity using cemented intramedullary stems, excessive bending and torsion within the fixation causes loosening and failure of the implant (Unwin et al. 1996; Roberts et al. 1991). Revisions are not as successful as a primary replacement and sometimes an amputation is required.

Previous chapters of my thesis showed that cultured oBMSCs can be isolated from ovine bone marrow and are viable and proliferate within fibrin glue, with or without spraying at 1 atm. Earlier work has showed that rat BMSCs, when implanted *in vivo*, can significantly increase bone formation within a femoral defect in chemotherapy-treated and non-chemotherapy-treated rats. The aim of this chapter is to investigate whether or not spraying oBMSCs in fibrin glue will increase bone formation and attachment to the HA-coated collars of a massive bone tumour replacement in an ovine model.

The hypotheses of this chapter are that:

- 1) By applying BMSCs to the surface of massive implant HA-coated collars, bone growth and bone-implant contact will be increased, compared to untreated and fibrin glue-treated controls.**
- 2) Increasing the number of BMSCs will result in greater new bone formation around the collars.**

The aims and objectives of this chapter are to:

1. Spray oBMSCs at two different concentrations (2×10^6 cells and 10×10^6 cells) in fibrin glue onto the HA-coated collars of tibial midshaft replacements in an ovine *in vivo* model;
2. Measure the area of new bone growth around the implants using radiography, and compare these results to untreated implant controls and those implants treated with fibrin glue only;
3. Observe and measure the area of bone growth around the centre of each implant collar using histological techniques;
4. Measure the bone-implant contact at the centre of each implant collar;
5. Measure the percentage porosity of the new bone growth adjacent to implant collars as an indicator of bone loading; and
6. Measure the amount of fibrous tissue adjacent to the implant collars.

5.2 Materials and Methods

5.2.1 oBMSC Isolation and Expansion

OBMSCs were isolated as previously described (See Chapter 2 Materials and Methods). Cells were expanded to passages 3 and 4 for use in this study.

5.2.2 Preparation of BMSCs in Fibrin Glue

The fibrin glue used was Tisseel[®] fibrin glue (Baxter Health Care Ltd., Newbury, Berkshire, UK). This glue consisted of four components, a vapour-heated Tisseel[®] powder component (100-130 mg protein, of which approximately 75-115 mg is fibrinogen); a bovine aprotinin solution; a vapour-heated thrombin powder (45-55 mg protein containing about 500 IU² active thrombin), and a calcium chloride solution (see Chapter 1 for a detailed description about fibrin's properties). The Tisseel[®] fibrinogen component was reconstituted in the aprotinin solution after a 10-minute incubation at 37°C in a heater manufactured by Baxter Health Care (Fibrinotherm[®], Baxter Health Care Ltd., Newbury, Berkshire, UK). Pre-operatively, for cell-loaded implants, 2×10^6 or 10×10^6 oBMSCs were centrifuged at 2000 rpm for 5 minutes. The supernatant was discarded and the pellet at the bottom of the universal was re-suspended in the 1 mL of reconstituted thrombin and injected back into the manufacturer's vial for transport to the operating theatre.

5.2.3 Implant Design and Manufacture

The implant used was a mid-shaft tibial replacement, which was a design that had previously been used in a goat *in vivo* study by Coathup et al. (2000). Implants were made from titanium alloy (Ti6Al4V). The implant shaft was 50 mm long and 10 mm in diameter. HA-coated collars were used at each transection site. HA coatings were highly crystalline and were

around 50 μm thick (Plasma Biotol, Tideswell, North Derbyshire, UK). The collars were 15 mm in length, with 1 mm grooves (Figure 5.1). The implant consisted of proximal and distal parts that were joined together during surgery by two juxtapositioned screws. Each stem was fixed within the intramedullary canal using cement. A long groove was present along each stem to promote the interlocking of cement.

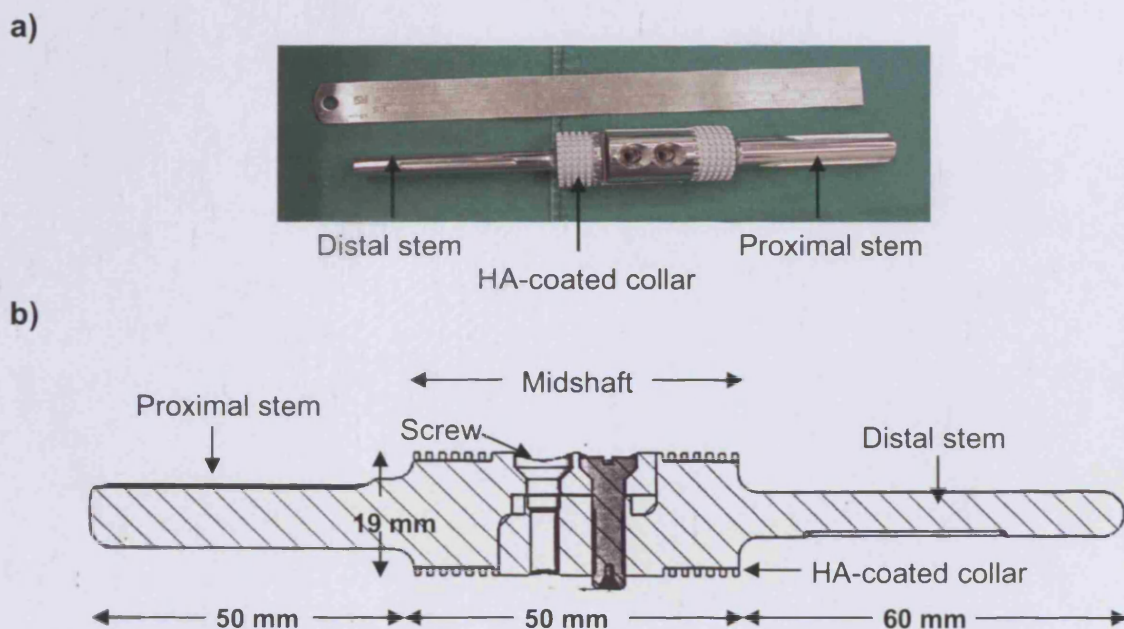


Figure 5.1 a) Photo of an ovine mid-shaft tibial replacement. The implants were made of titanium alloy and were comprised of two components, each of which had a grooved, HA-coated collar at the transection site, and an intramedullary stem. The two pieces were fixed in the centre with screws. b) shows a schematic diagram of the implant, showing the dimensions of the implant and the division between the two components, as well as the location of the thread holes.

5.2.4 Experimental Groups

There were four experimental groups, with six animals randomly assigned to each:

Group 1: Untreated implants (n=6);

Group 2: Implants sprayed with 2 mL fibrin glue/collar (n=3);

Group 3: Implants sprayed with 2×10^6 autologous oBMSCs/collar in 2 mL fibrin glue (n=6);

Group 4: Implants sprayed with 5×10^6 autologous oBMSCs/collar in 2 mL fibrin glue (n=2).

5.2.5 Surgical Procedure

All animals were handled and cared for as described in Chapter 2 (Materials and Methods) and the site of surgery was prepared as previously described. Approximately six weeks prior to surgery, bone marrow aspirates were taken from skeletally mature mule ewes, from the appropriate experimental animals and oBMSCs isolated as outlined in Chapter 2 of this thesis. Tibiae were first clipped to expose the skin, after which the area was washed with an iodine solution (as described in Chapter 2). The operation was carried out under sterile conditions. The animal's right leg was draped to expose the medial anterior aspect of the right tibia. This area was rinsed with a chlorhexidine solution and then a proximal-distal incision 60 mm in length was made, starting 50 mm distal to the tibial tuberosity. A 50 mm section of the tibial midshaft was excised 60 mm from the tibial tuberosity using an air-saw (Figure 5.2a). The periosteum from this section was removed intact (Figure 5.2b).

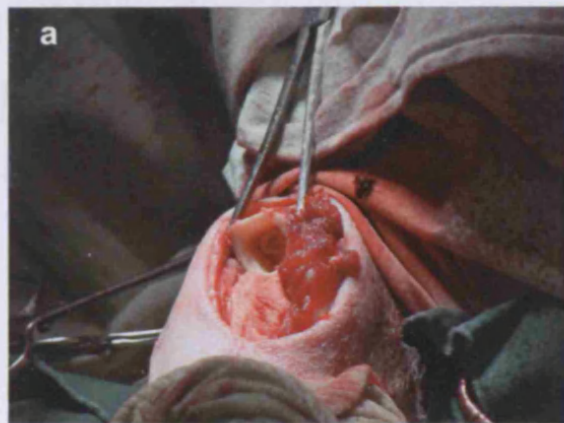


Figure 5.2 a) After resection of soft tissue from the tibia 50 mm from the tibial tuberosity, an initial cut was made to the tibia; b) A 50 mm tibial segment with an intact periosteum, which was replaced with a massive implant.

The intramedullary canals were prepared for implantation by first removing the bone marrow, then by repeated washing with saline (a sterile, 0.9% sodium chloride solution). Where necessary, canal diameters were increased to ensure a minimum cement mantle thickness of approximately 1.5 - 2.0 mm. In experimental group animals, 2 mL of autologous oBMSCs in fibrin glue was sprayed onto the HA-coated surface of the implant collars (proximal and distal) at 1.0 atm of pressure. To do this, the fibrinogen and thrombin components of the fibrin glue were transported to the operating theatre with or without oBMSCs (see 4.2.1) and maintained at 37° C in a Baxter Fibrinotherm[®] device (Baxter Health Care Ltd., Newbury, Berkshire, UK) until used. Each component was loaded into a 1.0 mL syringe (included in the Tisseel[®] package) and snapped into a dual-syringe holder with attached plunger device. To spray the fibrin glue using this system, a Duploject[®] (Baxter Health Care Ltd., Newbury, Berkshire, UK) spray set was used, which consisted of sterile plastic tubing which connected to a dual-syringe tip, which allowed air to come into contact with the fibrin components as they came out of the syringe. The other end of the tubing was connected to a Fibrijet[®] (Micromedics, Inc., St. Paul, Minnesota, USA) pressure gauge, which was connected to a pressure pump (see 4.2.2). The Fibrijet was set to 1 atm and the plungers of the fibrin system

pressed to allow release of aerolised fibrin onto the surface of the HA-coated implant collars. The implants were slowly turned as the fibrin was applied, to allow an even distribution of fibrin around the collar (Figure 5.3). Either two million or ten million cells were applied to each collar (proximal and distal) of every implant in the oBMSC group.



Figure 5.3 HA-coated collar on distal segment of implant being spray-coated with oBMSCs suspended in fibrin glue, pre-implantation.

Control animals recieved fibrin glue only or no treatment to the collar at all. Implants were cemented in place using Palacos R with Gentamicin (Biomet Europe, South Wales, UK, Figure 5.4a). The two halves of the prosthesis were joined centrally (Figure 5.4b), and the surrounding fasica, muscle and skin were closed.

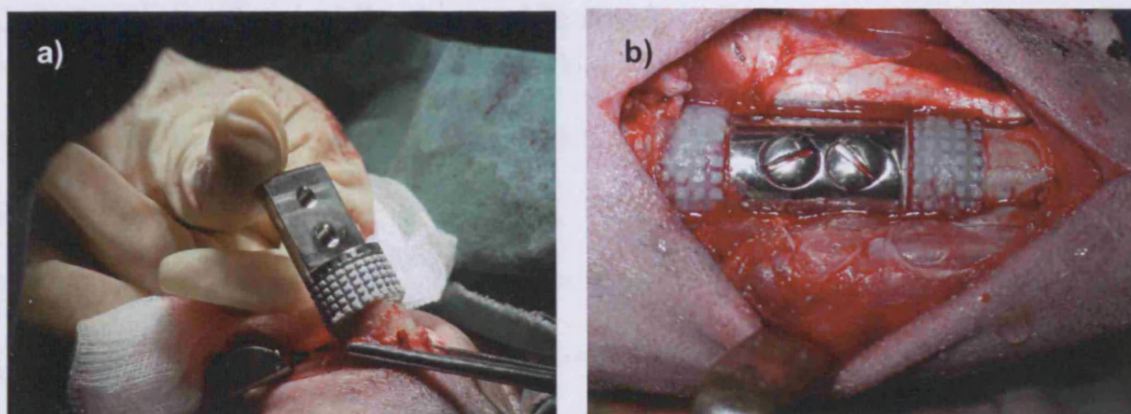


Figure 5.4 a) Distal implant (from untreated control group) component being cemented into intramedullary canal; b) Implant assembled in centre with screws, with oBMSCs in fibrin glue on HA-coated collars.

A spray bandage (OpSite[®], Smith & Nephew, Gallows Hill, Warwick, UK) was applied prior to recovery. Animals were allowed immediate postoperative mobilisation and weight-bearing as tolerated. Antibiotic and analgesic prophylaxis was administered daily with subcutaneous injections of Exenel[™] (ceftiofur hydrochloride, 1 mL/50 kg, Pfizer Animal Health, Tadworth, Surrey, UK) and IM injections of Vetergesic[™] (buprenorphine, 0.6 mg/animal, Reckitt and Colman Products Ltd., Hull, UK) for three days post-operatively. Animals were kept in individual pens until fully weight-bearing and were then grouped together in large pens.

Animals were euthanised 6 months post-operatively by an intravenous overdose of 0.7 mg/kg pentobarbitone (20%, J.M. Loveridge Ltd., Southampton, UK).

5.2.6 Radiography and Radiographic Analysis

Medio-lateral (ML) radiographs of the right tibiae were taken at two and three months post-operatively for the control (untreated) and 2.0×10^6 oBMSC groups, using an MX4 X-ray machine (PLH Medical Ltd., Watford, UK). For the fibrin-only and 2.0×10^7 oBMSC groups, radiographs were taken at six months only, as part of two pilot groups. At six months, both ML and anterior-posterior (AP) radiographs were taken after animal sacrifice and removal of the right tibia, in all four groups. For analysis of new bone formation, digital images of the radiographs were captured using a JVC KY F55B Colour Video Camera using Zeiss KS300 software (Imaging Associates, Thame, UK). The radiographed area adjacent to the implants was divided into eight regions of equal size, and labelled from A-H (Figure 5.6). Images were captured using a JVC KY F55B Colour Video Camera along with Zeiss KS300 software (Imaging Associates, Thame, UK). Bone area in these regions was then quantified using the KS300 image analysis software.

The osseointegration of the pedical bone was measured by determining the length of radiolucent lines found between the pedicle of bone and the implant surface (see Figure 5.5), using image analysis software. The lengths of the radiolucent lines were expressed as a percentage of the length of pedicle-implant interface, as measured using image analysis software.

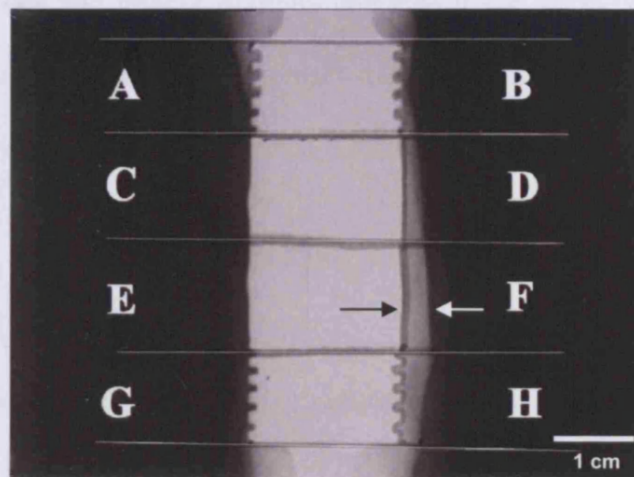


Figure 5.5 Sample radiograph (2×10^6 BMSCs/collar, ML view) divided into eight regions (A-H) for quantitative analysis of new bone formation adjacent to implants. The pedicle of bone grown along the length of the implant shaft is indicated with a white arrow. A radiolucent line between the pedicle of bone and the implant is shown with a black arrow.

5.2.7 Undecalcified Hard Resin Histology and Analysis

Following sacrifice, all right tibiae were prepared for histology by stripping excess soft tissue and fixing in 10% neutral buffered formalin (NBF) for a minimum period of one week. Specimens were dehydrated in increasing concentrations of industrial methylated spirit (IMS). Samples were de-fatted in chloroform and immersed in a 50% IMS, 50% resin mixture (LR White Resin, London Resin Company Ltd., Reading, Berkshire, UK), followed by immersion in 100% resin. Samples were then cast using a polymerisation accelerator (LR White Accelerator, London Resin Company Ltd., Reading, Berkshire, UK). Specimen blocks were sectioned at four sites, using a water-cooled band saw with a diamond-edged blade (Exact saw, Germany). One section was made through the centre of the proximal collar and one through the centre of the distal collar. Thin sections (approximately 80 μ m thick) were prepared (Exact grinding machine, Germany; and Exact Polishing machine, Germany) and stained with Toluidine Blue (Bancroft and Stevens 1986) and Paragon (Tanzer et al. 2003) to stain soft tissue and bone, respectively. Stained slides were then viewed under an Olympus

BH2 light microscope and images digitally captured using a JVC KY F55B Colour Video Camera. Bone area and bone-implant contact was quantified using image analysis software (Zeiss KS300 software, Imaging Associates, Thame, UK).

5.2.7.1 Bone Area

To measure bone area using image analysis software, the area of bone was 'encircled' using freeform polygons and the area within it calculated by the software in mm² (see Figure 5.14 and Figure 5.15 for sample photographs of sections).

5.2.7.2 Bone-Implant Contact

To measure bone-implant contact, 48 equi-distant points spanning the entire surface of the implant collar were analysed at 2.5x magnification for the presence of bone-implant contact. The results were recorded as yes or no (0 or 1) at all points and the percentage of contact calculated out of 48.

5.2.7.3 Bone Porosity Measurement

To measure bone porosity around the centre of each implant collar, photographs were taken at 2.5x magnification around the implant collar. A 17x13 line grid was then overlaid onto these photographs, with lines approximately 1.0 cm apart from one another (Figure 5.6). At each intersection point within an area of bone, the number of porous regions was quantified. To calculate a percentage, the number of intersections with pores was totalled and divided by the total number of intersections within the bone area adjacent to the implant collars. The same grid was used for all photographs.



Figure 5.6 An example of a photograph of bone adjacent to a control group distal collar with adjacent bone growth, onto which a grid has been overlaid for the quantification of bone porosity. Evaluation of porosity was made at each grid intersection point.

5.2.7.4 Fibrous Tissue Measurement

The percentage of fibrous tissue adjacent to implant collars was quantified at 48 points along the implant surface, at 2.5x magnification. The width of the layer was quantified from its contact with the implant outwards, within a 2.0 mm distance. The percentage of fibrous tissue within this distance was then calculated and results analysed using the Mann Whitney U non-parametric comparison of means.

5.2.8 Statistics

To test the normality of the distribution of the data, the Kolmogorov-Smirnov test was used, using SPSS 11.0 for Mac OSX. Parametric data was analysed using an independent-samples T test; non-parametric data was analysed using the Mann-Whitney U test. Where there were more than two groups (radiographic analysis) being analysed, the non-parametric Kruskal-Wallis test was used. Bivariate (Pearson's) and partial correlations were used to analyse any correlations between the percentage porosity of bone adjacent to implant collars (Point 00)

and bone-implant contact (Point 0) to observe if bone-implant contact affected the porosity of the bone observed. Results were considered significant when $p \leq 0.05$.

5.3 Results

Sheep fully recovered within a few days post-operatively and were weight-bearing on all four limbs for the duration of the experiment.

5.3.1 Radiography

There were distinct patterns of growth observed around the implants. The largest amount of bone was observed posteriorly and medially along the implants. A greater amount of bone growth adjacent to the implants was observed at the proximal transection site than distally. Figure 5.7 and Figure 5.8 show typical radiographs for all 4 groups. A greater amount of new bone formation could be seen in the two BMSC-treated groups (2×10^6 and 10×10^6 BMSCs/collar) than in the control (untreated and fibrin glue-treated) groups, as well as a lower frequency of radiolucent lines between the implant and bone pedicles.

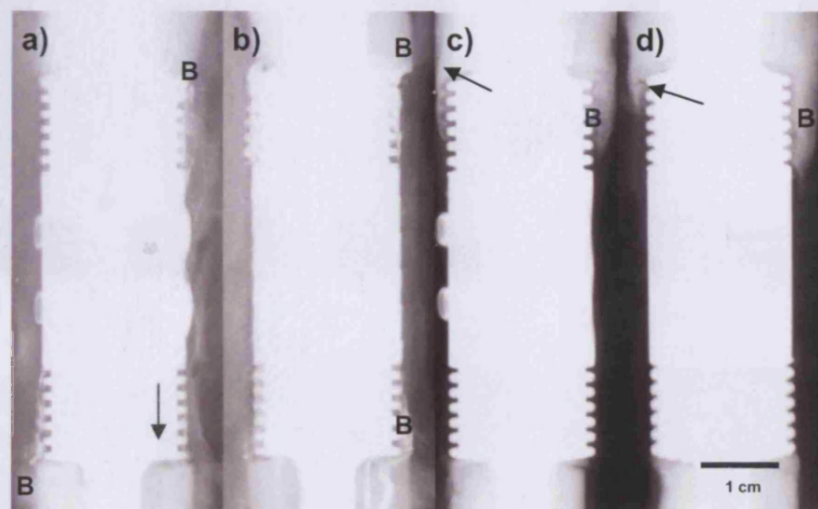


Figure 5.7 Radiographs of control (untreated and fibrin-glued treated) implants. (a-d) are radiographs from one untreated control animal, with ML radiographs taken at 2 (a), 3 (b) and 6 (c) months, and an AP radiograph taken at 6 months (d). Bone growth is marked (B), as well as radiolucent lines, which are demarcated with arrows. Photos are shown here at 0.9x of the actual size.

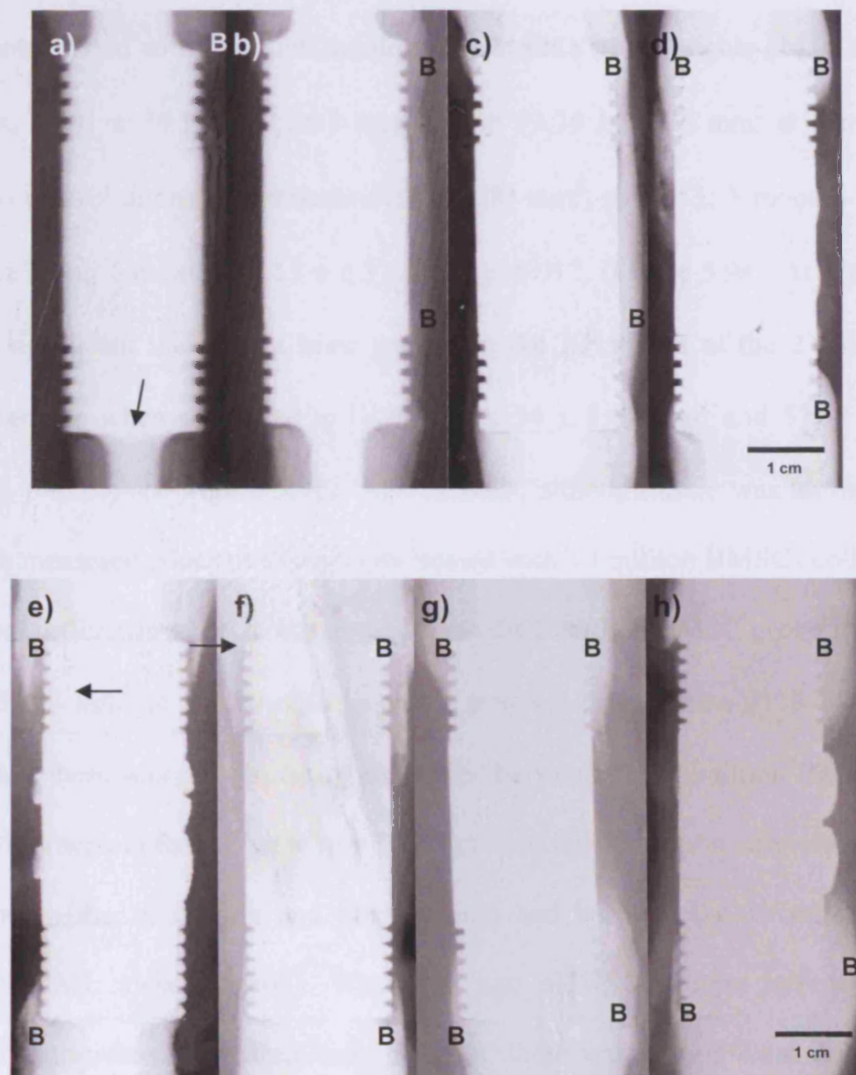


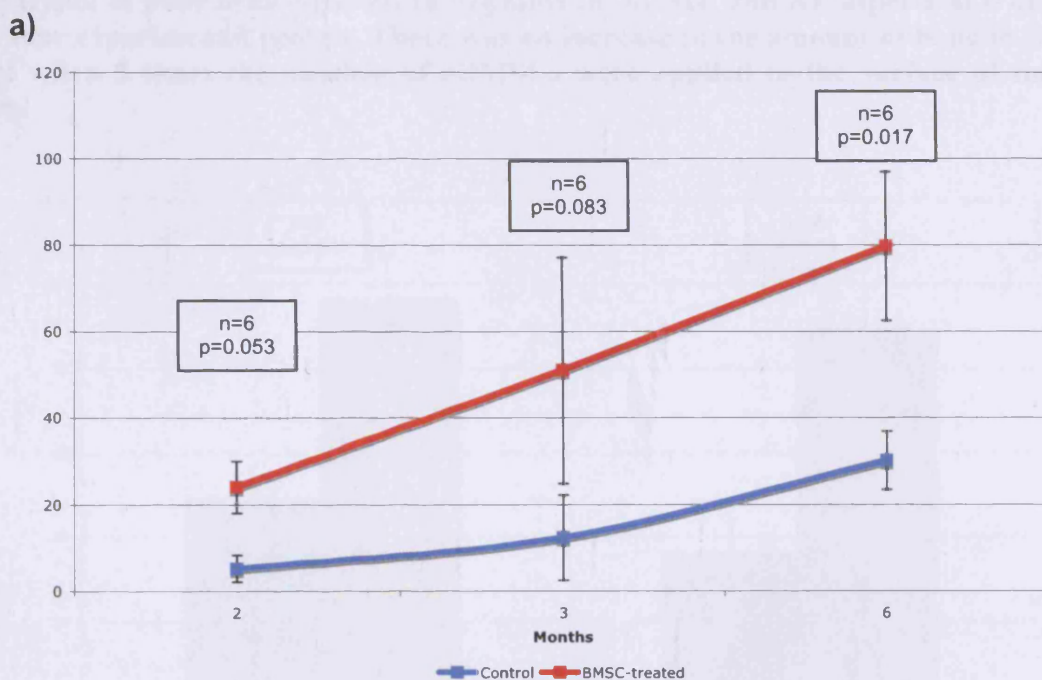
Figure 5.8 Radiographs of BMSC-treated implants (0.9x magnification). (a-d) are radiographs taken of the same animal treated with 2×10^6 BMSC/collar at 2 (a), 3 (b), and 6 (c and d) months, with (a-c) being taken in the ML view and (d) taken in the AP view. (e) and (f) are the ML and AP radiographs of another lower-BMSC dose animal, taken at 6 months. A larger cuff of new bone growing over the implants from the transection sites can be seen in these radiographs than with the controls seen in Figure 5.7. An even larger amount of bone can be seen proximally and distally in (g) and (h), which are the ML and AP views of an implant treated with 10×10^6 BMSCs/collar. New bone is marked with a "B," and radiolucent lines are indicated with arrows.

5.3.1.1 Bone Area

Analysis of new bone adjacent to tibial implants using ML radiographs showed that at each of the time points investigated, there was a significant increase in bone formation around those implants treated with 2 million autologous oBMSCs in fibrin glue ($24.07 \pm 5.988 \text{ mm}^2$ at 2 months, $51.01 \pm 26.13 \text{ mm}^2$ at 3 months and $79.74 \pm 17.25 \text{ mm}^2$ at 6 months, when compared to control animals (2 months- $5.24 \pm 3.09 \text{ mm}^2$, $p=0.053$; 3 months- $12.37 \pm 9.87 \text{ mm}^2$, $p=0.083$; and 6 months- $30.13 \pm 6.72 \text{ mm}^2$, $p=0.017$, (Figure 5.9a). At 6 months, there was also a significant increase in bone growth in the AP aspect of the 2 million-oBMSC group radiographs when compared to controls ($90.34 \pm 8.66 \text{ mm}^2$ and $57.38 \pm 9.04 \text{ mm}^2$ respectively, $p=0.05$, see Figure 5.9b). At 6 months, although there was an increase in the area of bone measured adjacent to implants treated with 10 million BMSCs/collar, there was no significant difference when it was compared to the 2 million BMSC group in the AP view ($112.29 \pm 33.03 \text{ mm}^2$ in the 10 million group, $p=0.44$) or ML view ($138.74 \pm 9.30 \text{ mm}^2$, $p=0.18$). Also, there was no significant difference between the 10 million BMSC group and the other two groups in the AP view ($p = 0.06$ between the 10 million and control groups and $p=0.08$ between the 10 million and fibrin group) and between the 10 million and fibrin groups in the ML view ($p=0.08$). When the two oBMSC groups were combined and compared to non-treated and fibrin-only controls, there was a significant difference in the amount of bone observed in the AP and ML views ($p < 0.01$, Figure 5.10). Within each group, there were statistical significant differences observed between 2 and 6 months in the control and low-dose oBMSC groups ($p=0.05$ and $p=0.01$, respectively).

5.3.1.2 Pedicle Gap Lengths

Radiolucent pedicle gap lengths were found to be longest in the control group, with a mean percentage gap length of $76.65 \pm 10.19\%$ in the AP view, and $52.67 \pm 14.97\%$ in the ML view. The smallest percentage gap lengths were found in the high-dose BMSC group (1.0×10^7 cells/collar) in the AP view ($25.02 \pm 18.9\%$), and the fibrin glue-only group in the ML view, with a $23.05 \pm 11.23\%$ pedicle gap length (Figure 5.11). A Kruskal-Wallis non-parametric test for multiple groups found a significant difference between all four groups in the length of pedicle gaps adjacent to distal collars in the AP view ($p=0.03$). Comparing the control (untreated) group and the low-dose BMSC group (2.0×10^6 cells/collar) using the Mann Whitney U test, a significant difference was found ($p=0.01$).



b)

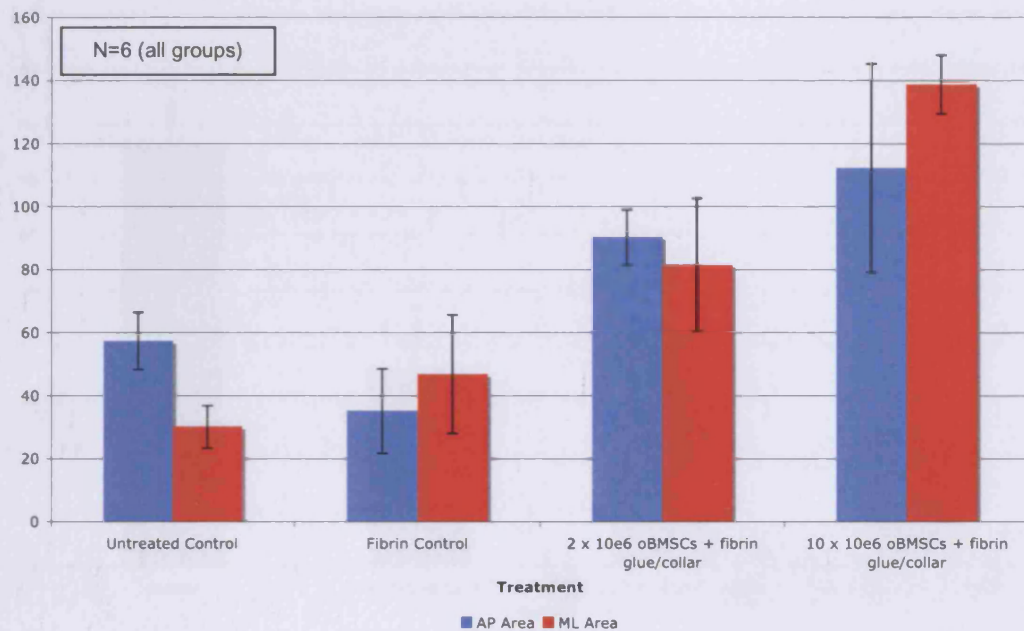


Figure 5.9 a) Results of radiological analysis over 2, 3, and 6 months, in the ML aspect. At each time point, there was a significant increase in the area of bone adjacent to the implants in the oBMSC-treated group, when compared to the control group. b) Comparison of bone area adjacent to implants in the ML and AP aspects at 6 months, in all four experimental groups. There was an increase in the amount of bone in the AP aspect when 5 times the number of oBMSCs were applied to the surface of implant collars.

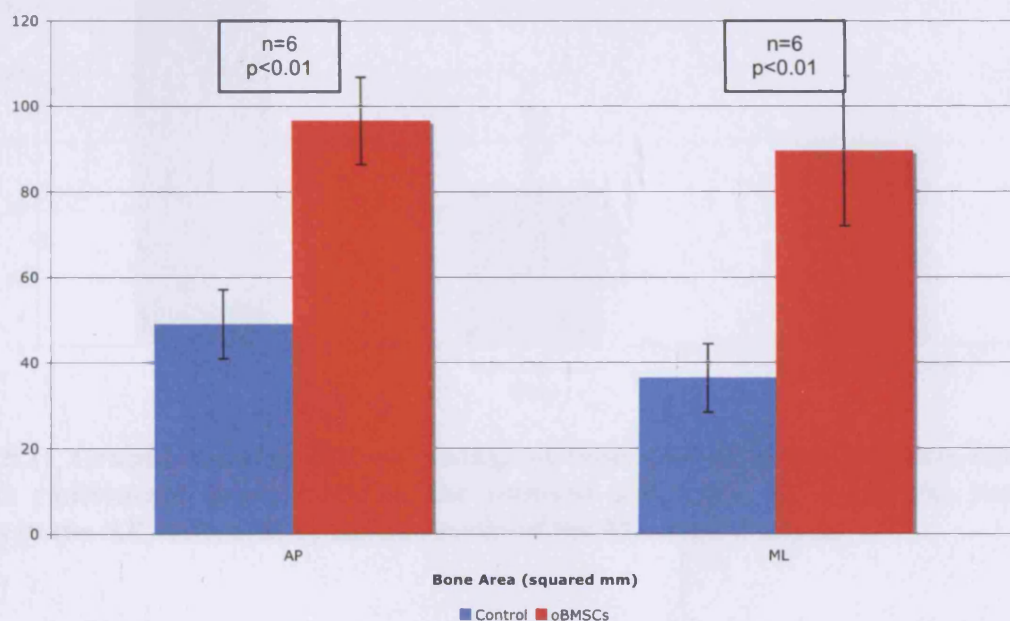
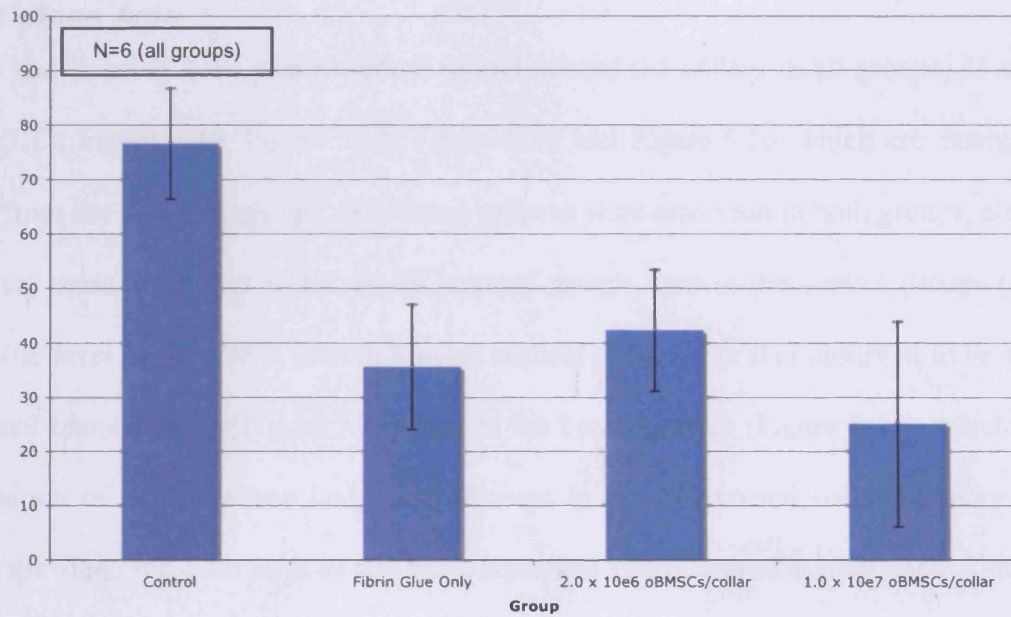


Figure 5.10 Radiographic bone area results from the combined oBMSC-treated groups compared to the combined results of the two control (untreated and fibrin-only) groups.

a)



b)

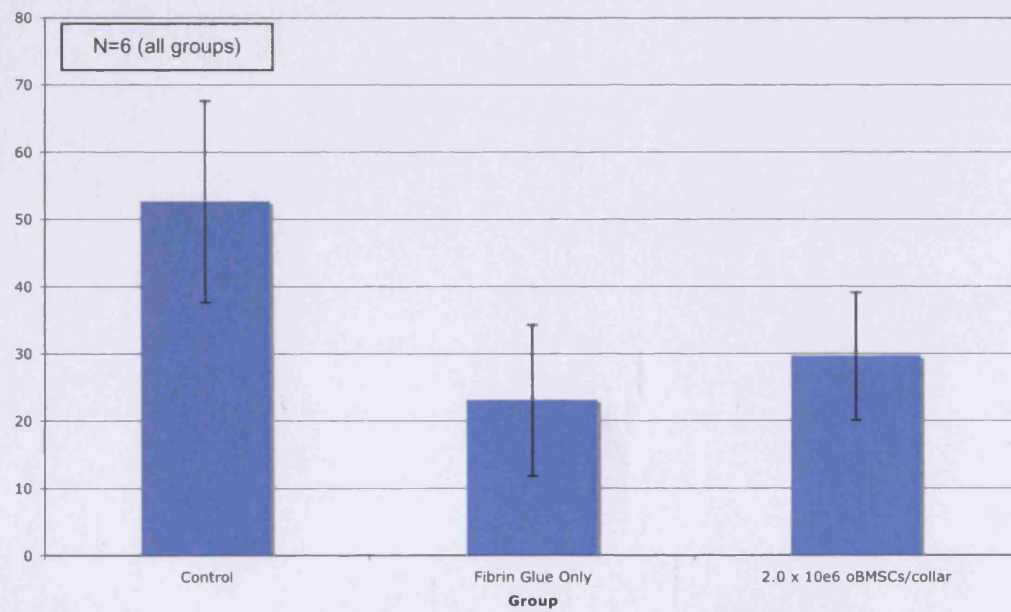


Figure 5.11 Graphs showing the percentage of bone pedicle along implants with gaps (seen as radiolucent lines) between the implant and bone. a) shows the results of analysis in the AP view, and b) shows results of the ML view analysis.

5.3.2 Histological Analysis

5.3.2.1 Bone Area

Woven and lamellar bone was observed in and around the collars in all groups, as seen in Figure 5.12, Figure 5.13, Figure 5.14, Figure 5.15 and Figure 5.16, which are examples of collars from the different groups. Haversian systems were also seen in both groups, although they were more prominent in the BMSC-treated groups than in the control groups (Figure 5.17). The layer of new bone growth around implant collars was also observed to be thicker in the cell-treated group (Figure 5.14) than in the control group (Figure 5.15), which had a combination of fibrous tissue and bone adjacent to the HA-coated collars (Figure 5.18). Resorption along the outer edge of this bony layer was also observed in both control and low-dose BMSC samples (Figure 5.19), as the bone surface appeared ‘scalloped’ following recent osteoclast activity.

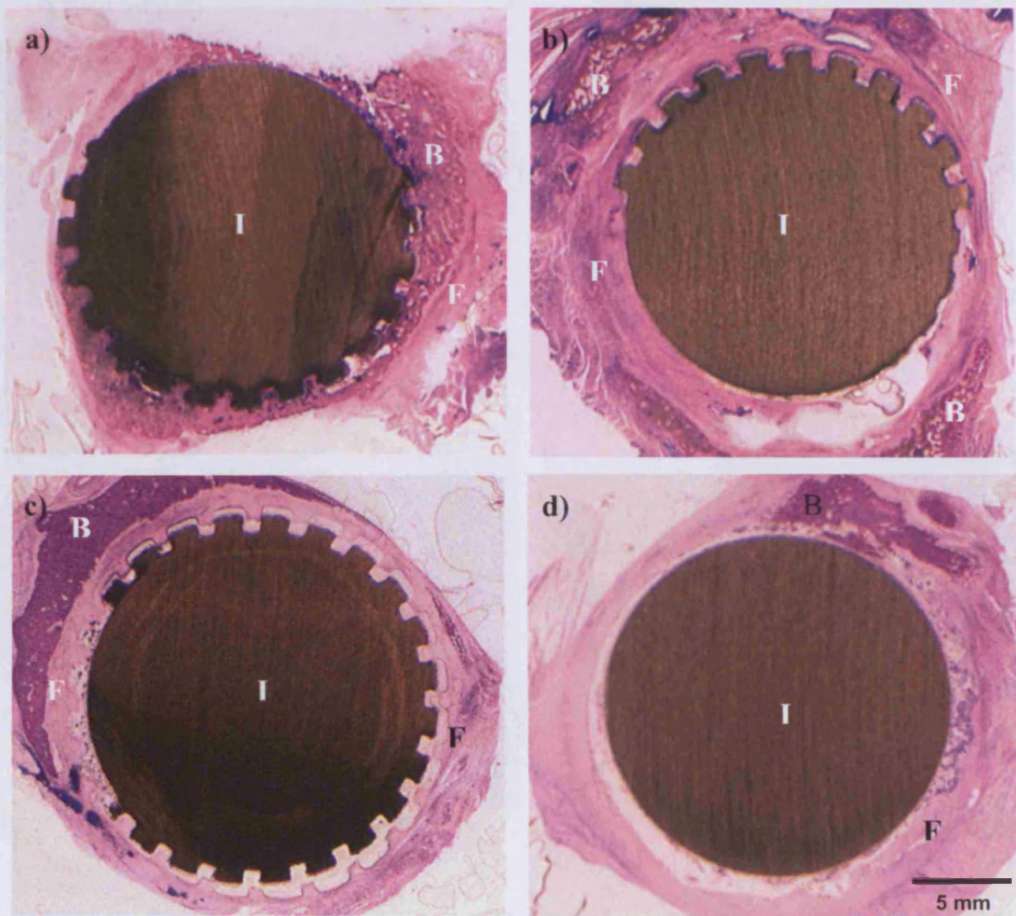


Figure 5.12 Midsection through the proximal (a, c) and distal (b, d) HA-coated collars of control group specimens, stained with Toluidine Blue and Paragon. Bone formation (B) adjacent to the implant collars can be seen, along with fibrous tissue (F). A fibrous tissue layer was often found between the implant and new bone formation.

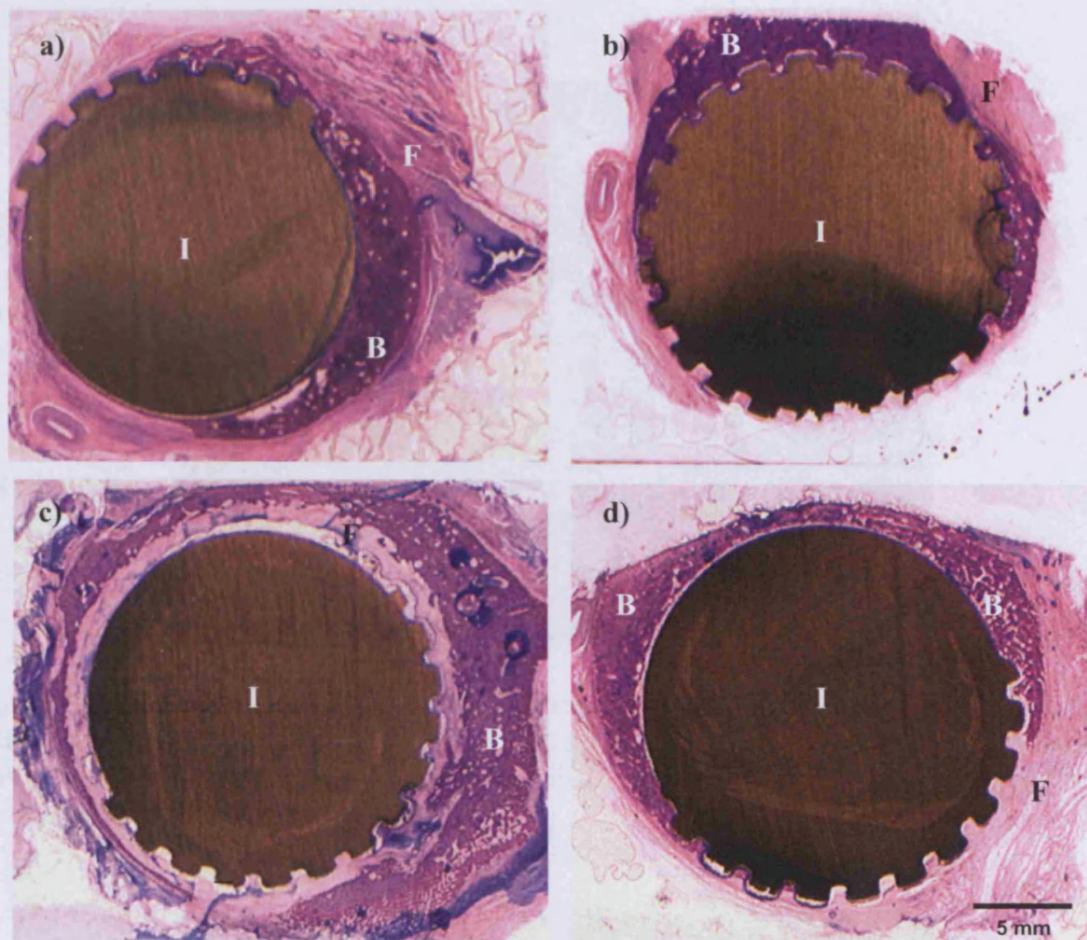


Figure 5.13 (a-d). Photos of thin, undecalcified, sections from 2.0×10^6 BMSC-treated group stained with Toluidine Blue and Paragon. Bone formation was observed around implant collars (distal and proximal). A larger, thicker, cuff of bone was found adjacent to the collars of BMSC-treated implants than in the control groups. Although a fibrous tissue layer was seen around some implant collars, between the bony layer and implant, this was seen less frequently than around control implants.

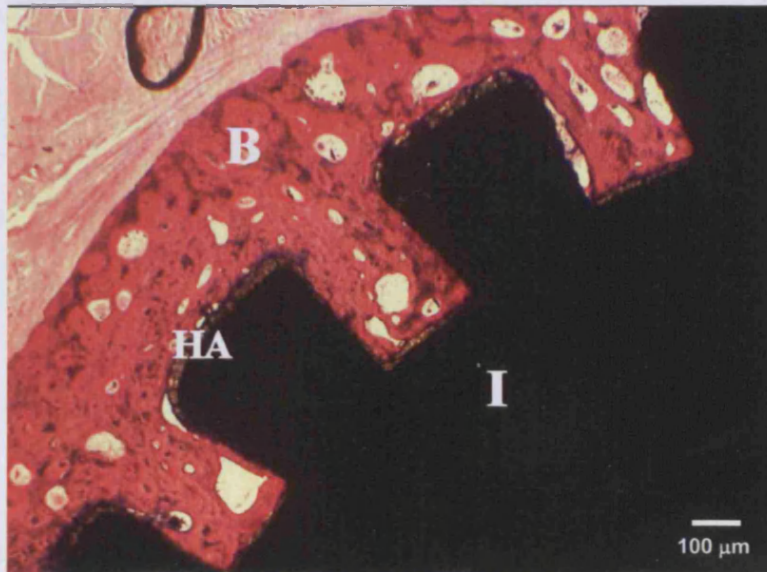


Figure 5.14 Lamellar bone (B) grown adjacent to a proximal HA-coated (HA) implant collar (I), which was treated with BMSCs in fibrin glue (2×10^6 BMSCs/collar). Haversian systems can be seen, as well as bone growth into the grooves of the collar and bone-implant contact (4x magnification).

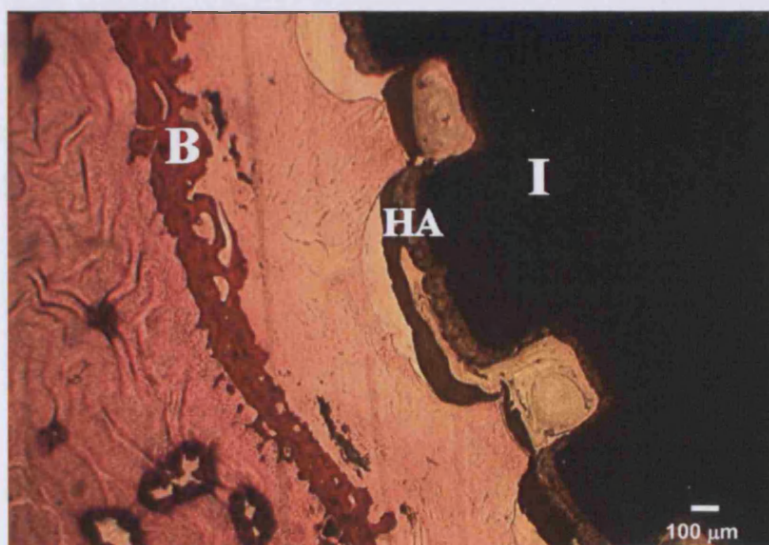


Figure 5.15 Bone formation (B) around a control (untreated) implant collar (I). This layer of bone is thinner than that often observed with the BMSC-treated implants and is not in contact with the HA-coated implant surface. The HA-coating can be seen as a grey layer as indicated (HA, 4x magnification).

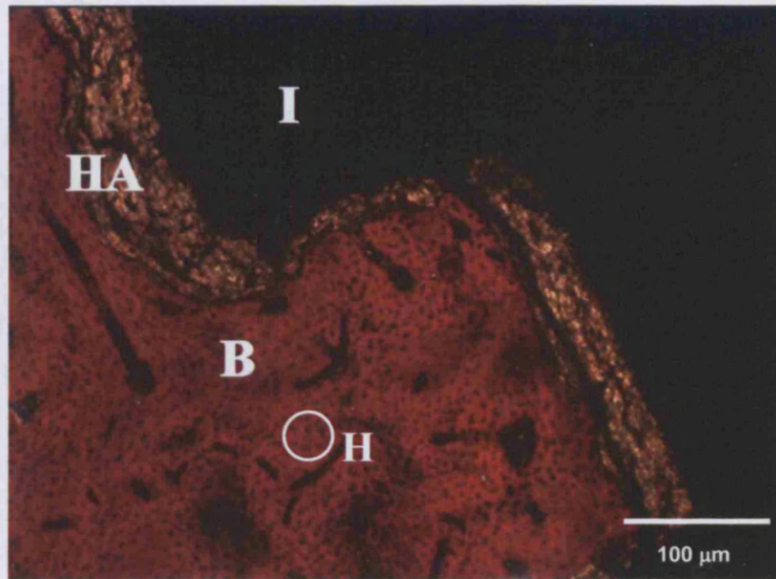


Figure 5.16 Bone growth into a BMSC-treated collar (2×10^6 BMSCs/collar, 10x magnification). Contact can be seen between the new bone and HA-coating of the implant collar. Haversian systems (H) can be seen surrounding the canals (black spots in photo- see encircled region).



Figure 5.17 BMSC-treated collar seen in Figure 5.16, at 40x magnification. Bone formation can be seen in contact with the HA-coating of the implant collar. In this photo, there is ingrowth of bone to the HA-coating (HA) and Haversian systems can be seen (H-white circled area).

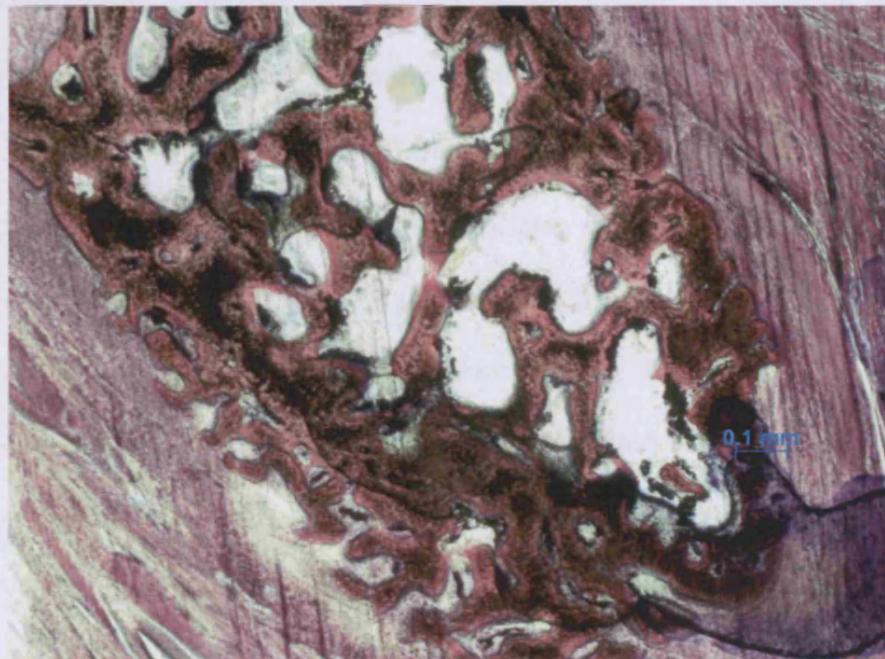


Figure 5.18 Porous bone adjacent to implant collar, separated by a fibrous tissue layer. This photograph was taken at 5x magnification and is of a distal collar from the untreated control group.

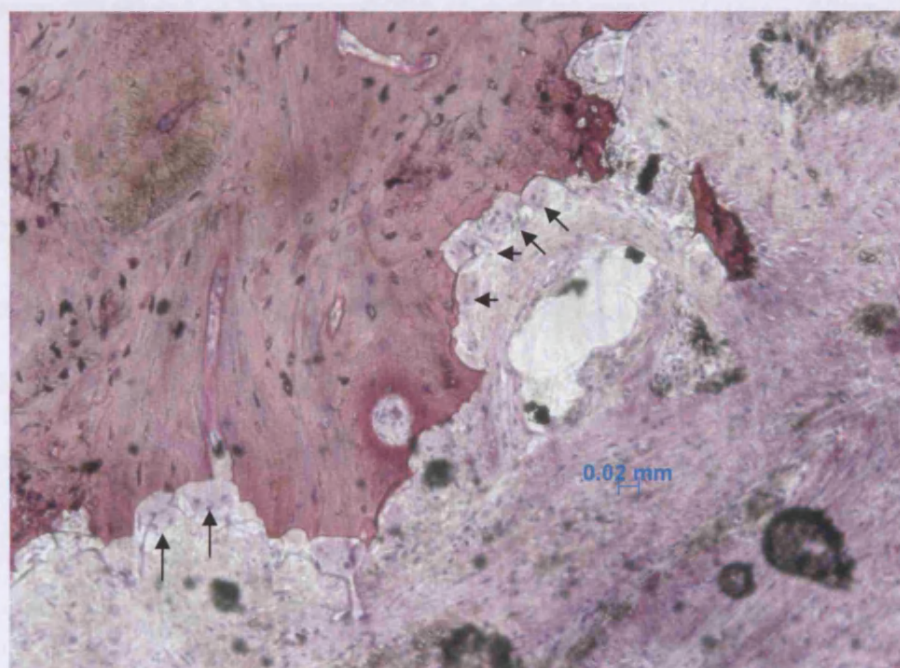


Figure 5.19 Resorption pits along the outer edge of a low-BMSC dose treated proximal collar, taken at 10x magnification. Osteoclasts are prominent multinuclear cells, which are indicated with black arrows.

A significantly greater amount of fibrous tissue was quantified adjacent to the untreated, control collars when compared to the cell-treated groups. As seen in Figure 5.20, significantly increased bone area was demonstrated adjacent to the mid-point of the collars in the oBMSC groups when compared with the control implants (mean $46.50 \pm 8.35 \text{ mm}^2$ in the low dose group, $127.63 \pm 36.94 \text{ mm}^2$ in the high dose group and $21.07 \pm 7.03 \text{ mm}^2$ in the untreated control group; $p=0.02$ between the low-dose group and controls, $p=0.01$ between the high-dose group and controls and $p=0.05$ between the high and low oBMSC doses). The fibrin glue-only group had a higher amount of new bone formation around implant collars than the low-oBMSC dose group ($64.49 \pm 23.59 \text{ mm}^2$), although this difference was not significantly different when compared to each of the other three groups. Looking at the proximal and distal collars separately (Figure 5.21), there was no significant difference between all groups, except between the distal collars in the control and high-oBMSC group ($15.93 \pm 8.90 \text{ mm}^2$ and $220.16 \pm 58.60 \text{ mm}^2$, $p=0.05$), and low-oBMSC group and high oBMSC group ($35.60 \pm 12.62 \text{ mm}^2$ and $220.16 \pm 58.60 \text{ mm}^2$, $p=0.044$). Although there was more bone observed around the proximal collars in the control and low-dose oBMSC groups (control group $27.49 \pm 11.83 \text{ mm}^2$; fibrin-only group $53.94 \pm 37.68 \text{ mm}^2$, low-dose oBMSC group $50.27 \pm 12.00 \text{ mm}^2$, high-dose BMSC group 81.36 ± 26.43) than the distal collars (control group 15.93 ± 8.90 , fibrin-only group $71.52 \pm 36.33 \text{ mm}^2$; low-dose oBMSC group $35.61 \pm 12.62 \text{ mm}^2$, high-dose oBMSC group 220.16 ± 58.60), this was the opposite in the other two groups, and these differences were not statistically significant.

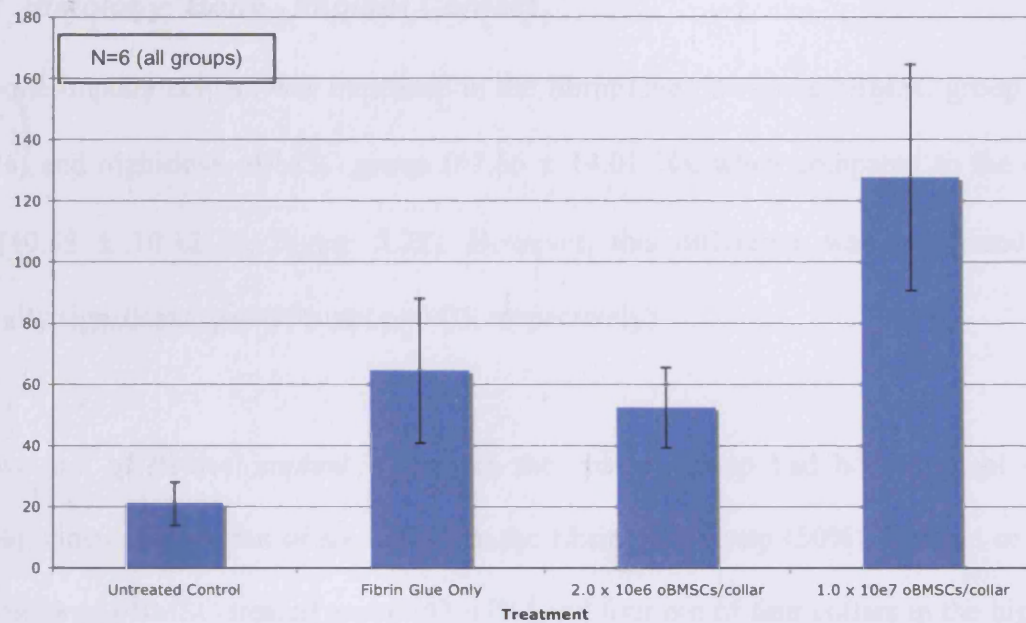


Figure 5.20 Comparison of bone area around the centre of implant collars, as measured using histological analysis.

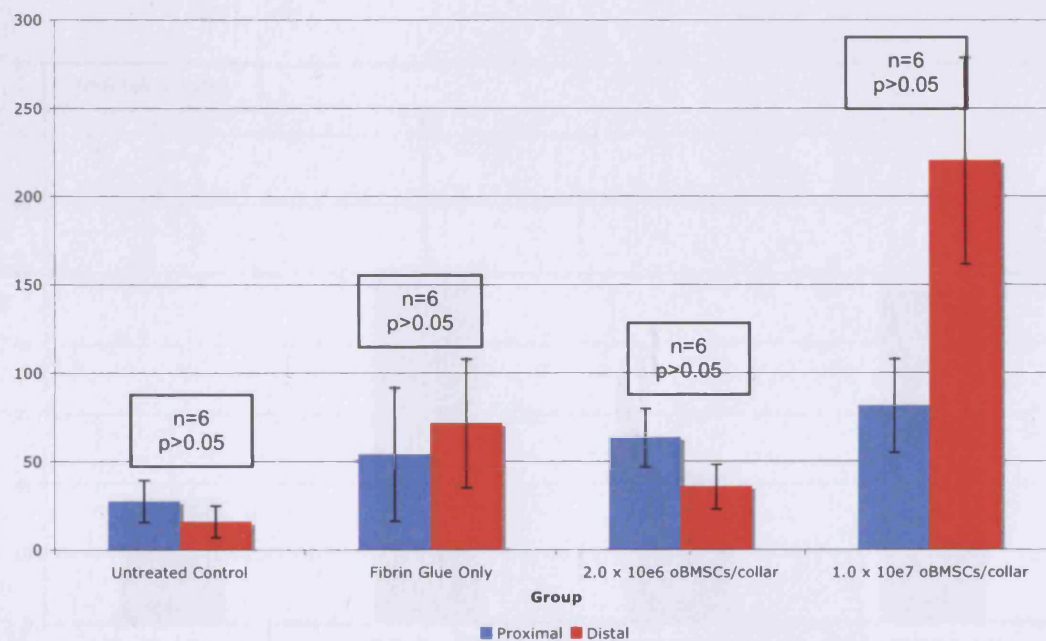


Figure 5.21 A comparison of histological results, comparing proximal and distal collars between groups.

5.3.2.2 Histology: Bone - Implant Contact

Mean bone-implant contact was increased in the fibrin glue, low-dose oBMSC group ($21.35 \pm 9.84\%$) and high-dose oBMSC group ($47.66 \pm 14.01\%$), when compared to the control group ($10.88 \pm 10.12\%$, Figure 5.22). However, this difference was not found to be statistically significant ($p=0.936$ and $p=0.05$, respectively).

Only two out of twelve implant collars in the control group had bone-implant contact (16.67%), whereas three out of six collars in the fibrin glue group (50%), five out of twelve in the low-dose oBMSC-treated group (41.67%) and four out of four collars in the high-dose oBMSC group (100%) had bone-implant contact. Bone-implant contact was observed at both proximal and distal collars.

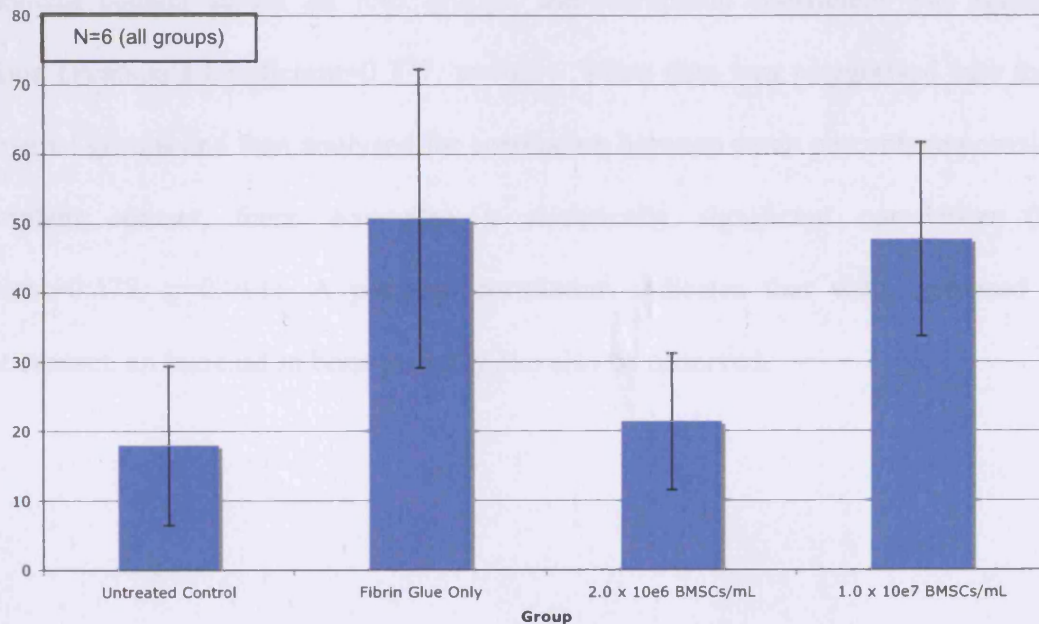


Figure 5.22 Bone-implant contact around implant collars in the untreated control, fibrin-only, low-concentration oBMSC group, and high-concentration oBMSC group.

5.3.2.3 Bone Porosity Measurement

Looking at bone porosity in the bone adjacent to implant collars in the four groups, the control group had the highest mean percentage porosity ($24.37 \pm 4.13\%$), followed by the fibrin-only group ($17.41 \pm 4.11\%$), the low-dose oBMSC group ($14.91 \pm 1.80\%$) and the high-dose oBMSC group ($11.76 \pm 1.68\%$), with the lowest mean porosity. The difference between the untreated control group and the high-dose oBMSC group was significant ($p=0.018$) and although the untreated control group had almost double the mean percentage porosity compared to the low-dose oBMSC-treated group, the difference was not statistically significant ($p=0.064$). Figure 5.23 summarises these results in a bar graph. Implants with no bone present adjacent to the implant collars were excluded from the above analysis.

When bivariate correlations were made between the percentage bone porosity and percentage bone-implant contact across all four groups, the correlation coefficient was statistically significant (Pearson's coefficient=0.377, $p=0.05$). When data was categorised into the four experimental groups and then analysed for correlation between mean percentage porosity and bone-implant contact, there was also a statistically significant correlation (Partial coefficient=0.478, $p=0.013$). A positive correlation indicates that with increased bone-implant contact, an increase in bone porosity can also be observed.

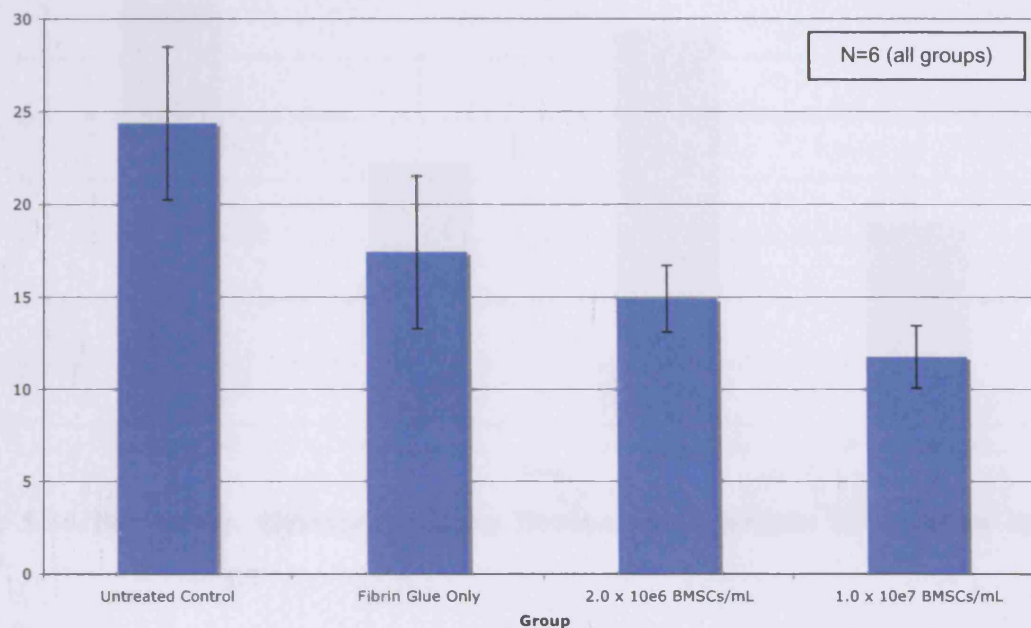


Figure 5.23 Bar graph showing the mean percentage bone porosities in the four experimental groups.

5.3.3 Percentage of Fibrous Tissue Adjacent To Implant Collars

Measurement of fibrous tissue layers adjacent to implant collars within 2 mm of the implant found a mean fibrous tissue percentage of $70.72 \pm 10.23\%$ in the control group, $42.63 \pm 17.70\%$ in the fibrin-only group, $64.30 \pm 10.18\%$ in the low-dose oBMSC group and $32.90 \pm 11.14\%$ in the high-dose oBMSC group. There was a significant difference between the untreated control group and the high-dose oBMSC group ($p=0.048$). Figure 5.24 shows these results graphically.

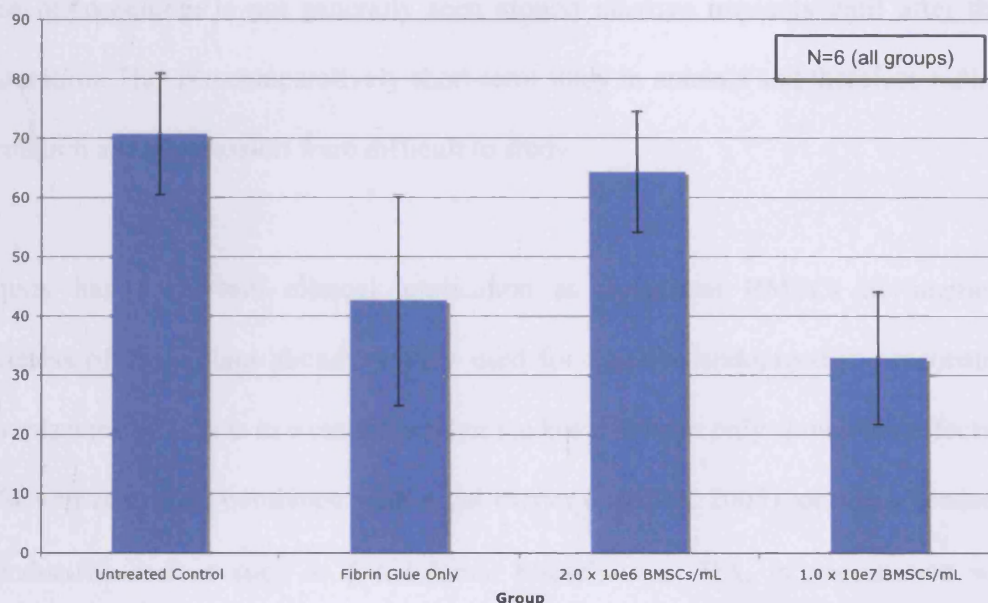


Figure 5.24 Bar graph illustrating mean fibrous tissue lengths adjacent to implant collars.

5.4 Discussion

The study described in this chapter demonstrated that BMSCs, when sprayed onto the surface of HA-coated implant collars, significantly increased bone formation around the collars and improved bone-implant contact to massive segmental bone tumour implants when compared to untreated implants with HA-coated collars. By promoting the growth of a “bony bridge” across the transection site from the host bone to the implant collar, load transfer to the implant at the transection site may be improved. This in turn, may improve the failure rates experienced by massive endoprostheses. Further radiographic analysis looking at the effects of applying BMSCs in fibrin glue onto HA collars of the massive implants on radiolucent line formation around the stem would be useful, as this is the mode of aseptic loosening of these implants in humans. In this PhD, the focus was to determine whether or not applying BMSCs to orthopaedic implants would augment bone growth adjacent to the implants and improve bone-implant contact. Therefore, analysis of radiolucent lines and loosening around the stem was not investigated. Radiolucent line formation and progression, which is considered to be

evidence of loosening, is not generally seen around massive implants until after the first year's duration. This is a comparatively short-term study in animals and therefore radiolucent line formation and progression were difficult to study.

This study has a relevant clinical application as it utilises BMSCs to augment the effectiveness of an implant already widely used for massive endoprosthetic reconstruction and/or replacement. This is in contrast to other studies that have only shown the effectiveness of BMSCs in rats when combined with a gel carrier (Lee OK 2005), or when seeded in an osteoconductive surface such as β -tricalcium phosphate or HA, in conjunction with an internal plate (Arinzeh et al. 2003), external distraction (Richards et al. 1999) or external fixation (Lee et al. 2005). Although these models have clinical relevance in demonstrating bone tissue engineering with BMSCs, the model I used is also immediately weight bearing and was tested in sheep, which have been shown to have loading patterns running through their hind limbs as compared to humans (Bergmann et al. 1984). Fibrin glue is a convenient vector for BMSCs as it is commercially available and simple to reconstitute and assemble. This fibrin-oBMSC system has been shown in this study to significantly augment bone regeneration. Fibrin glue is already widely used in many different areas of surgery and is familiar to surgeons worldwide. It is possible that osteoinduction could be further encouraged by using a scaffold that promotes the proliferation of cells and their differentiation into osteoblasts, as well as retaining them in the structure. An example of this could be fibrin combined with BMPs, HA or β -tri-calcium phosphate, or all of these combined (Hong et al. 2006; Han et al. 2005; Schmoekel et al. 2005). One potentially negative aspect to using autologous BMSCs in patients who have bone tumour replacements is the possibility of metastatic cells in the bone marrow that may be isolated with autologous BMSCs (Wakasugi

et al. 2002; Bruland et al. 2005), which may justify the use of allogeneic cells in these patients (see General Discussion - Chapter 7).

Radiographic analysis of bone growth in all groups indicated a similar pattern, whereby there was more new bone formation medially and posteriorly around the implants and less new bone formation laterally and anteriorly. This pattern is similar to that observed in the clinical scenario of femoral endoprosthetic replacements, where a medial and posterior increase in bone mineral density (BMD) was found, as well as a BMD decrease laterally and anteriorly (Inglis and Walker 1991). This reflects the pattern of stress and strain around proximal femoral replacements measured telemetrically (Taylor et al. 1997) and a study using photoelastic coatings to measure shear strain (Hua and Walker 1992), where the strain measured medially was 53% of normal on the medial side, but only 35% on the lateral side of the implant.

The purpose of quantifying bone porosity of bone adjacent to implant collars was to observe any difference in bone quality between groups. Bone is known to be responsive to load, therefore, it was thought that, if BMSCs were promoting fixation of the massive implants in this model, one might see, in addition to an increase in bone area and bone-implant contact, a lower porosity of bone. Also, it was thought that, with the addition of osteoblast precursor cells, the quality or type of bone observed may be different to bone found adjacent to control group implants. There was a significant difference between the porosity of the untreated control group and that of the high-dose oBMSC-treated group, although the N-number of the latter group was only 2, as opposed to 6 in the former. It must also be noted that there was an increase in the amount of bone-implant contact in all treated groups when compared to the control group, although this difference was only statistically significant between the control

group and the high-dose oBMSC group. Although the bone-implant contact in the fibrin-only group is comparatively high compared to the control group, the N-number is half of the control group and therefore the results may change when the other samples are taken into account.

Interestingly, when percentage bone porosity was correlated with bone-implant contact over both control and low-dose BMSC groups, there was a positive correlation, indicating that with increased bone-implant contact, there is increased bone porosity. This result is contradictory to Wolff's law (Wolff 1892), which states that bone responds to load. A greater degree of bone-implant contact would indicate a higher amount of load being transmitted from the implant to the surrounding bone, requiring a denser bone formation. However, with increased bone-implant contact there is less of a fibrous tissue layer between bone pedicles and implants. This fibrous tissue layer could possibly have a role in transmitting load from connecting soft tissue (such as muscle) to the bone, thus causing denser bone formation, and without such a force, the bone could be more porous (Blunn 2007). Current outcomes of HA-coated collars show that, while in some patients there is bone growth over the implant collars and along the shaft of the prosthesis (70% of cases, Unwin, Walker and Blunn 1995), others have little or no bone growth (30% of cases). This result can be unpredictable. However, with the application of BMSCs in fibrin glue to the implant collar, there may be a more predictable outcome with regards to bone growth over HA-coated collars, with an increase in bone-implant contact and corresponding bone quality. The results of the radiographic bone pedicle gap analysis support this claim, as there was a significant decrease in the pedicle gap found between bone adjacent to implants in the high-dose BMSC-treated group when compared to control groups. The fibrin glue group also had a positive outcome, although it must be noted that the N-number for this group and group 4 was half of groups 1 and 3 (n=3).

The study by Unwin, Walker, and Blunn (2005) found that when plasma-sprayed, HA collars were used in massive implants in human patients, there was a qualitative difference observed in the radiolucent lines (pedicle gap) found between new bone growth and the implant, when compared to untreated and bead-coated collars. It may be possible that the use of BMSCs furthers this effect.

My analysis of percentage fibrous tissue adjacent to implant collars found statistically significant differences between the untreated control and high-dose oBMSC group, and between the low-dose oBMSC group and high-dose oBMSC group. These results indicate that treating implant collars with a high concentration ($1.0 \times 10^7/\text{mL}$) of BMSCs in fibrin glue reduced the percentage of fibrous tissue adjacent to the implant, which may reduce loosening in the longer term. It may be interesting to investigate how such a fibrous tissue layer between implant and bone may affect loading of bone, and if fibrous tissue lengths differ over a larger sample size. Demarcating implant orientation (anterior, posterior, medial, and lateral) when processing histological specimens may also show trends with regards to fibrous tissue lengths, bone porosity and bone area around implant collars. The data reported in this chapter showed a substantial difference in the bone area found adjacent to proximal collars, when compared to distal collars (over twice the amount of bone), however, no observable difference in bone morphology (porosity, type of bone) was seen between the proximal and distal collars. Therefore the difference in bone area between the two collars may be attributable to differential loading of the proximal and distal collars in ovine tibiae, influencing different levels of bone growth according to Wolff's law (Wolff 1892). Although fibrin glue increased new bone formation and bone-implant contact around implants, its influence is not as substantial as when oBMSCs were applied. Fibrin glue does appear to have some effect on bone formation. Once again, it should be noted that the fibrin-only and

high-dose oBMSC groups had a much lower sample size (N=3 and N=2, respectively), when compared to the other two groups.

Fibrin has a natural role in the wound-healing pathway. It is one of the first matrix molecules present at wound sites, providing a physical barrier and temporary strength to the wound site. As discussed in the introduction to this thesis (Chapter 1), fibrin glue has been shown to encourage osteoconduction when applied with HA (Abiraman et al. 2002). However it has also been shown to induce significantly less bone growth *in vivo* when compared to fibrin glue combined with BMSCs with or without a ceramic scaffold (Lee et al. 2005; Yamada et al. 2003). A study by Kadiyala et al showed an increase in bone formation when the β -TCP scaffold was impregnated with fibronectin before cells were seeded onto the scaffold (Bruder et al. 1998; Arinzech et al. 2003). One study by Roy et al. (1993) actually showed a decrease in new bone formation around a titanium femoral endoprosthesis in canines when fibrin glue was used to pack bone graft around the implant, when compared to fibrin-free implants. An *in vivo* study in rats by Lee et al. in 2005 showed that there was no significant difference between untreated femoral gaps and those treated with fibrin glue only. However, bone growth was significantly increased with the addition of allogenic BMSCs, up to 20% more bone. This effect was even more pronounced in those rats treated with chemotherapy. Those rats treated with fibrin and BMSCs compared to those with chemotherapy only, had a 220% increase in bone formation.

It has been suggested that fibrin glue can have a pro-angiogenic effect, which may promote new bone growth or repair (Kania et al. 1998). Based on experimental results presented in the literature, it is unlikely that the fibrin glue is completely responsible for the observed increase

in bone growth when compared to implants with untreated, HA-only collars. Increasing the sample size may alter the pilot results presented in this chapter.

HA has already been well documented in the literature as being osteoconductive (Blunn et al. 2000; Coathup et al. 2000; D'Antonio, Capello and Jaffe 1992; Geesink 1993). Possible mechanisms of this bone-promoting effect have been suggested. One theory is that as HA slowly degrades in the body, the degradation products released from the implant surface, such as calcium and phosphate, or the change in pH (Ozawa and Kasugai 1996; Kurioka et al. 1999), may promote differentiation of the BMSCs to osteoblasts, or even improve bone formation by host osteoblasts which have migrated to the implant site, or the BMSC-derived osteoblasts (Datta et al. 2006). Kilpadi, Chang and Bellis (2001) have also shown that HA has the capacity to bind proteins such as important integrins (for example $\alpha 5 \beta 1$ and $\alpha v \beta 3$), as well as fibronectin, vitronectin and osteoblast precursor cells, when compared to metals.

Another question that my chapter aimed to answer was the question of cell dosages. In the radiographical results, there was no significant difference found between the groups with 10×10^7 BMSCs/collar, and all other groups. This is probably due in part to the small sample size, which may have contributed to the high standard error (almost equivalent to a third of the measured new bone area). In the histological results, the high dose of oBMSCs resulted in a significantly higher bone area, bone-implant contact and lower percentages of fibrous tissue and bone porosity adjacent to the collars. Of course, increasing the N-number could potentially make the addition of more cells to the collars significant. However, this group was essentially a small pilot group and cell dosages will be investigated in more detail in future projects, with the right number of specimens to produce a result with the appropriate statistical power. This sort of work has not previously been published in the literature for *in*

vivo bone tissue engineering. It is possible that cell dosage does not affect the amount of new bone formation around collars. This may be possible if there is some sort of threshold or upper limit on the effects of cells, so that beyond a certain number of cells there is possibly no difference in the results. A clinical study by Gu, Zhang and Qi (2006) looking at the treatment of lower limb ischemia with autologous BMSCs found that the BMSC dosage (1×10^5 cells versus 1×10^8 cells) significantly affected the outcome, which was the development of collateral blood vessels and a decrease in amputation rates. This group found that for an effective dosage, one must use a minimum of 1×10^8 cells. However, cell dosages may have a different effect in cases of hard (bone) tissue engineering, and result in different amounts of trophic factors being released into the environment by implanted BMSCs, which may indirectly facilitate bone growth (Caplan and Dennis 2006).

5.5 Conclusion

BMSCs can be used in a fibrin glue spray system to augment bone growth around massive implants. Bone growth around BMSC-treated implants was significantly increased when compared to controls. Bone-implant contact was also improved and the length of radiolucent gaps between the new bone and implants was reduced. The quality of bone (porosity) was also observed to be different between untreated and BMSC-treated implants. Fibrin-treated implants also showed a similar effect, although much lower than when a high concentration of BMSCs was applied to implant collars. The enhancement of bone growth and quality observed when BMSCs in fibrin glue are applied to HA-coated collars may improve the fixation of massive implants. This could potentially reduce incidences of aseptic loosening.

CHAPTER SIX

THE EFFECT OF BMSC DOSAGES AND GUIDED BONE REGENERATION ON THE FIXATION OF REVISION IMPLANTS.

6.1 Introduction

The previous chapter showed that the application of autologous BMSCs to massive implants resulted in improved new bone formation and bone-implant contact. However, in that experiment, only two cell dosages (2.0×10^6 and 10.0×10^6 BMSCs) were investigated. Two important questions that arose from that study were: 1) Whether or not a higher or lower concentration would result in more or less new bone formation; and 2) Whether allogeneic BMSCs will stimulate equal or increased amounts of bone when compared with autologous BMSCs.

The use of autologous BMSCs is advantageous, as it uses the patients' own cells at the site of implantation, reducing the risk of disease transmission. Bone marrow aspiration, which is required for the isolation of BMSCs, is an invasive procedure. In contrast, if allogeneic cells were to be used, an immediately available product could be made possible. Allogeneic cells have been shown to produce bone in many *in vivo* models (Arinzeh et al. 2003; De Kok et al. 2003; Tsuchida et al. 2003).

Guided bone regeneration using an e-polytetrafluoroethylene (e-PTFE, Gore-Tex™) membrane promotes new bone formation by sealing the defect site from the surrounding tissue (Bhumbra et al. 1998). E-PTFE is a biocompatible, non-resorbable, synthetic membrane that has previously been used in guided bone regeneration. Its inner layer, which has 1 mm pores, prevents the ingrowth of cellular material such as fibrous tissue, whereas water and various macromolecules and growth factors can pass through freely. In a small rabbit tibial defect model, e-PTFE was shown to significantly improve new bone formation compared to uncovered controls (Bhumbra et al. 1998). E-PTFE has also been shown, in a large animal model, to effectively prevent wear-particle induced osteolysis at the acetabular

cup implant-bone interface created by total hip replacements, significantly reducing the aseptic loosening of these implants (Bhumbra et al. 2000). Guided bone regeneration techniques have previously been applied to bone tissue engineering techniques, where a non-porous poly-DL-lactide chamber was used in combination with BMSCs and demineralised bone matrix (DBM) to promote new bone formation in rabbit radii (Giardino et al. 2002). However, use of PTFE to cover orthotopic defects or implants treated with BMSCs has not been previously investigated. The use of a membrane in this model may prevent the migration of cells out of the defects into the surrounding tissues or from one site to another, as well as promote new bone formation.

The hypothesis of this chapter is that a larger cell dosage would result in greater new bone formation in cortical defects and improve bone-implant contact in an *in vivo* revision implant model, when compared to lower cell dosages. Also, allogeneic BMSCs would be as effective as healing a bone defect as autologous BMSCs.

The aims and objectives of this chapter were:

1. To use an ovine tibial transcortical pin model to investigate the effects of varying cell dosage (1.0×10^5 , 1.0×10^6 , and 1.0×10^7 BMSCs/mL), as well as fibrin alone, on the amount of new bone formation, within a 1.5 mm 'gap' defect, in an *in vivo* ovine model.
2. To investigate the effect of using allogeneic cells on the amount of new bone formation in the same model.
3. To evaluate new bone density in the gaps created in this model using radiological techniques.
4. To prepare histological sections and measure the amount of new bone formation adjacent to the implants and within the gaps.
5. To quantify the amount of bone-implant contact.

6.2 Materials and Methods

6.2.1 oBMSC Isolation and Expansion

Ovine BMSCs were isolated as previously described (See Chapter 2, Materials and Methods).

Cells were expanded to passages 3 and 4 for use in this study.

6.2.2 Implant Design and Manufacture

The implants were small partially-threaded transcortical screws similar to that used by Bhumbra et al. (1998) and manufactured from titanium alloy (Ti6Al4V, Figure 6.1). The screws were 25 mm in length, and the distal M5 threaded region was 5.0 mm in diameter. A cutting flute was located at the bottom, for ease of insertion into the cortical bone. The top half of the screw was 3.0 mm in diameter and was plasma sprayed with a highly crystalline, thin (<50 μm thick) HA-coating (Plasma Biotol, Tideswell, North Derbyshire, UK).

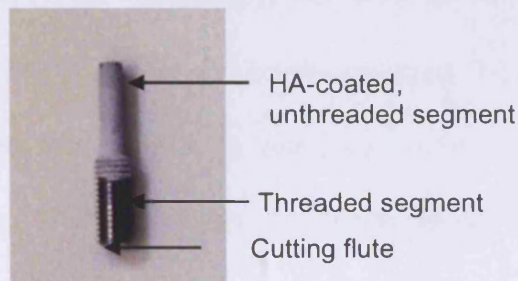


Figure 6.1 Example of a transcortical screw used in study. The top segment was HA-coated and either left untreated, sprayed with fibrin glue-only, or a combination of fibrin glue and varying concentrations of BMSCs (1.0×10^5 - 1.0×10^7 cells/mL).

6.2.3 Cell Dosages

Three implants were inserted into the left and right tibia of each sheep, with a total of six implant groups per sheep.

Table 6.1 outlines the treatment and position of the six groups investigated, which were rotated clockwise in each successive animal. Cells were administered via incorporation within fibrin glue and sprayed onto the surface of the unthreaded, HA-coated segment of the implant at 1.0 atm of pressure.

Left	Right
1. No treatment	4. 1×10^6 autologous oBMSCs/mL in fibrin
2. Fibrin only	5. 1×10^7 autologous oBMSCs/mL in fibrin
3. 1×10^5 autologous oBMSCs/mL in fibrin	6. 1×10^6 allogeneic oBMSCs/mL in fibrin

Table 6.1 Groups used in experiment, in the order they were placed in the first sheep.

6.2.4 Preparation of BMSCs in Fibrin Glue

Tisseel[®] fibrin glue (Baxter Health Care Ltd., Newbury, Berkshire, UK) was reconstituted at 37°C as described in Chapter 4. Pre-operatively, for cell-loaded implants, 5.0×10^4 , 5.0×10^5 , or 5.0×10^6 oBMSCs were counted and put into a universal container and spun in a centrifuge at 2000 rpm for 5 minutes. The supernatant was discarded and the pellet at the bottom of the universal resuspended into 0.25 mL of reconstituted thrombin. This was mixed with 0.25 of the Tisseel[®] fibrinogen component preoperatively when the fibrin-cell mixture was sprayed onto the implants. The fibrin control group consisted of fibrin glue only, without cells.

6.2.5 Surgical Procedure

All animals were handled and cared for as described in Chapter 2 (Materials and Methods), and the site of surgery prepared as previously described. Six skeletally mature mule ewes were used in this experiment. All methods were completed under sterile conditions.

Approximately six weeks prior to surgery, bone marrow aspirates were taken from sheep in the BMSC group and oBMSCs isolated as outlined in Chapter 2 of this thesis. The animal was draped to expose the medial anterior aspect of the right tibia. This area was rinsed with a chlorhexidine solution and a small (10.0 mm) incision was made 30.0 mm distal to the tibial tuberosity. The tibia was exposed by blunt dissection. A small section of the periosteum was scraped at the approximate vertical centre of the bone. A 6.0 mm hole was then drilled into the near cortex. A drill guide was inserted to centralise drilling. A 4.0 mm hole was drilled through the far cortex and tapped with an M5 tap and corresponding tap guide. The site was then washed with saline. At this point, implants in the treated groups were sprayed with fibrin with or without oBMSCs, according to the experimental group, onto the HA coated section of the implant with 1.0 atm of pressurised air. The implant was then inserted into the tibia, and the threaded section screwed into the far cortex. As the implant was only 3.0 mm in diameter at the near cortex, there was a 1.5 mm gap between the implant and bone, which was bridged by fibrin in groups 2-6. The top of the implant at the near cortex was then sealed with a square piece of e-polytetrafluoroethylene membrane (e-PTFE, Gore-Tex[®], Gore, Flagstaff, Arizona, USA) measuring approximately 5.0 mm x 5.0 mm, and glued onto the bone using butyl-cyanoacrylate glue (Figure 6.2a, Vetbond[™], National Veterinary Supplies, Talke Pits, Stoke-on-Trent, UK), after which, the fascia, muscle, and skin were sutured. Two more implants were similarly inserted in each tibia, with each implant 30 mm apart (see Figure 6.2b).

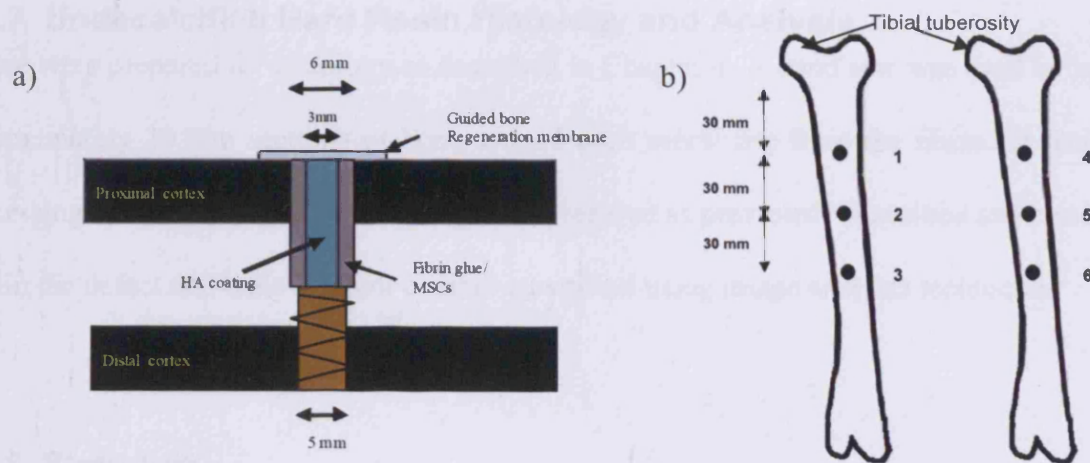


Figure 6.2 a) Diagram illustrating insertion of transcortical screw in bone. b) Distance of holes from tibial tuberosity (see top of diagram).

A spray bandage (OpSite, Smith & Nephew, Gallows Hill, Warwick, UK) was applied, before the animal was brought out of anaesthesia. Animals were kept for a period of 6 weeks, after which they were sacrificed, by intravenous injection of 0.7 mg/kg pentobarbitone (20%, J.M. Loveridge Ltd., Southampton, UK). Both tibiae were harvested immediately and fixed in 10% neutral buffered formalin (NBF) and processed for histology.

6.2.6 Radiography and Radiographic Analysis

Medio-lateral (ML) radiographs of each tibia were taken using an MX4 X-ray machine (PLH Medical Ltd., Watford, UK) at 66 kV and 50 mA, for 0.6 seconds, at 0.8 m from the specimen. Images of the radiographs were captured using a JVC KY F55B Colour Video Camera, and the density within the defects were analysed using Zeiss KS300 software (Imaging Associates, Thame, UK). Results were normalised for each sheep according to the mean bone density of surrounding cortical bone.

6.2.7 Undecalcified Hard Resin Histology and Analysis

Tibiae were prepared for histology as described in Chapter 4. A band saw was used to cut out approximately 20 mm sections of bone around each screw site from the tibiae, to facilitate processing and sectioning. Thin sections were prepared as previously described and bone area within the defect and bone-implant contact quantified using image analysis techniques.

6.2.8 Statistics

The sample size was calculated to a power of 80% with a p-value of 0.05 using data from Chapter 4. This resulted in a sample size of 6.

To test the normality of the distribution of the data, the Kolmogorov-Smirnov test was used, using SPSS 11.0 for Mac OSX. Non-parametric data was analysed using an analysis of variance (Friedman's test) for non-parametric related samples. Data from the different groups were compared in pairs using the Mann Whitney U test. Results were considered significant when $p < 0.05$.

6.3 Results

Sheep fully recovered within a few days post-operatively, and were weight-bearing on all four limbs.

6.3.1 Radiographic Analysis

Mean density values were calculated for bone within cortical defects (Table 6.2, Figure 6.3). The highest mean density was found in the group with the highest concentration of BMSCs in fibrin (1×10^7 BMSCs/mL, 136.2 ± 3.31) and the lowest mean density in the group with the lowest concentration of BMSCs (1.0×10^5 BMSCs/mL, 132.96 ± 5.51). Using Friedman's paired non-parametric test for multiple groups, there was no statistical difference in the mean bone density between groups, ($p = 0.86$). When all groups were compared to one another using the Wilcoxon test to compare two paired groups, there was no significant difference between groups ($p > 0.05$ for all pairings, see Table 6.3).

Number	Group	Mean Density
1	Control (No Treatment)	132.96 \pm 5.51
2	Fibrin Glue Control	133.9 \pm 4.51
3	1.0x10 ⁵ auto BMSCs/mL	134.19 \pm 4.88
4	1.0x10 ⁶ auto BMSCs/mL	133.02 \pm 3.99
5	1.0x10 ⁷ auto BMSCs/mL	136.2 \pm 3.31
6	1.0x10 ⁶ allo BMSCs/mL	135.73 \pm 4.75

Table 6.2 Mean density in cortical defect, as observed radiographically. Percentage density indicates the mean density of defect divided by the mean cortical density of the surrounding bone.

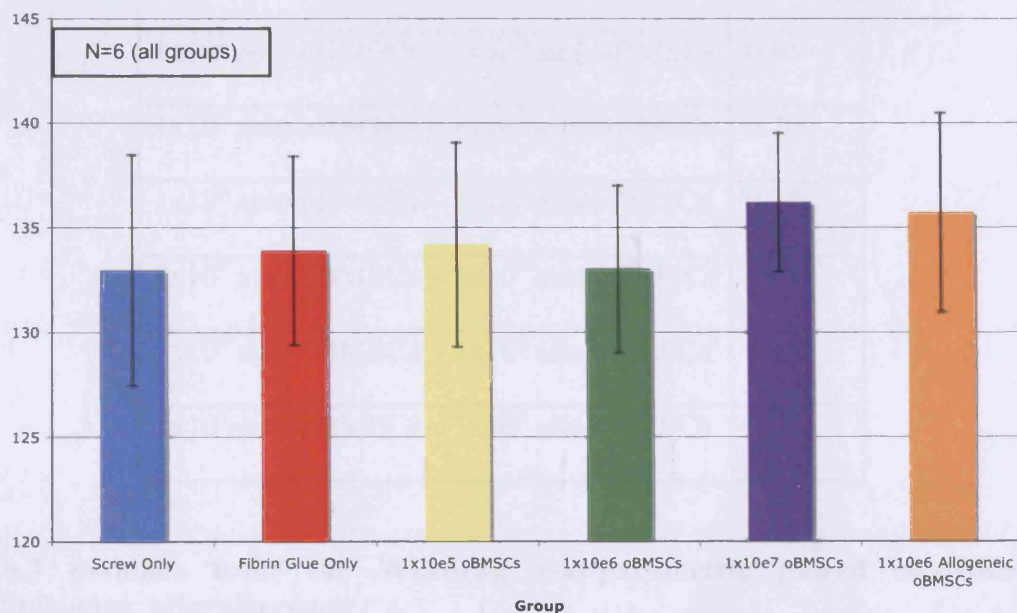


Figure 6.3 Graph showing normalised bone density in the gaps between the top half of the screws and the surrounding bone. The density was normalised based on the means of the surrounding cortical bone.

Paired Group	P-value
Screw Only – Fibrin Glue Only	0.88
Screw Only – 1×10^5 auto oBMSCs	0.70
Screw Only – 1×10^6 auto oBMSCs	0.94
Screw Only – 1×10^7 auto oBMSCs	0.88
Screw Only – 1×10^6 allo oBMSCs	0.88
Fibrin Glue Only – 1×10^5 auto oBMSCs	0.81
Fibrin Glue Only – 1×10^6 auto oBMSCs	0.75
Fibrin Glue Only – 1×10^7 auto oBMSCs	0.43
Fibrin Glue Only – 1×10^6 allo oBMSCs	0.64
1×10^5 auto oBMSCs – 1×10^6 auto oBMSCs	0.94
1×10^5 auto oBMSCs – 1×10^7 auto oBMSCs	0.70
1×10^5 auto oBMSCs – 1×10^6 allo oBMSCs	0.35
1×10^6 auto oBMSCs – 1×10^7 auto oBMSCs	0.18
1×10^6 auto oBMSCs – 1×10^6 allo oBMSCs	0.48
1×10^7 auto oBMSCs – 1×10^6 allo oBMSCs	0.81

Table 6.3 p-values from the Wilcoxon non-parametric paired statistical test. Auto=autologous; allo=allogeneic.

6.3.2 Histology

6.3.2.1 New Bone Formation

New bone in the defects was continuous with the surrounding cortical bone when observed, in all groups, and was often separated from the implant and PTFE membrane by a fibrous tissue layer (Figure 6.4). The threaded portion of the implants was in contact with the surrounding cortical bone (Figure 6.5). The highest average new bone formation was found in the untreated control group ($67.33 \pm 6.83 \text{ mm}^2$) and the least in the BMSC group with the lowest concentration of cells ($1.0 \times 10^5 \text{ BMSCs/mL}$, $39.24 \pm 1.28 \text{ mm}^2$, mean new bone formation).

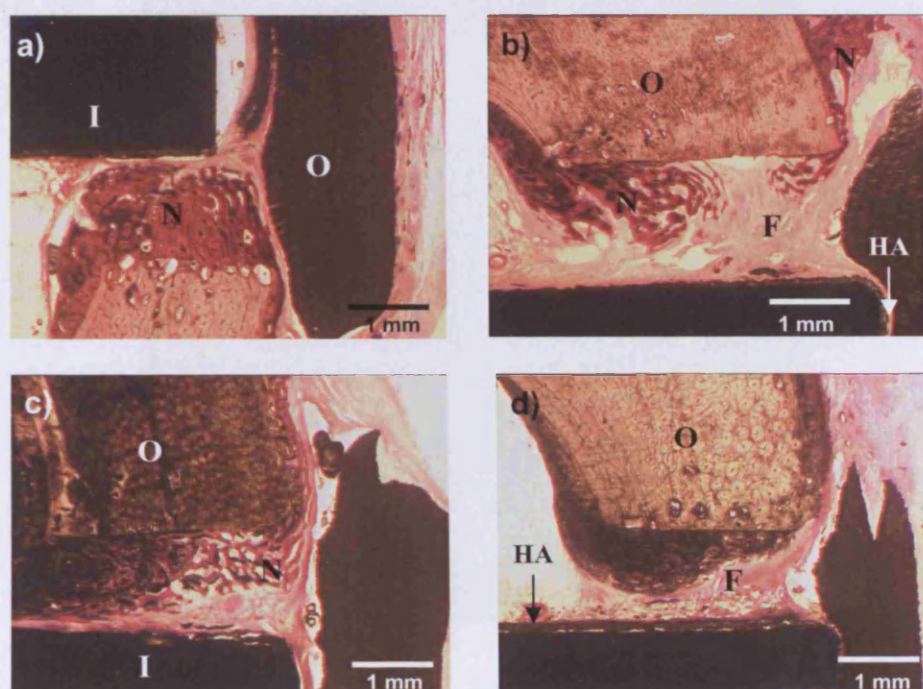
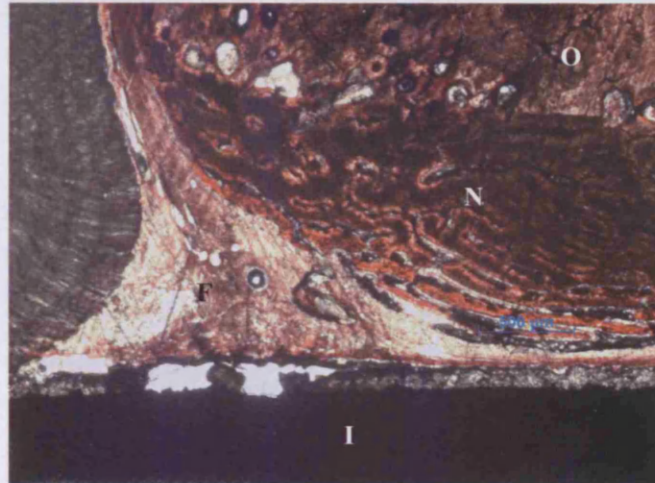


Figure 6.4 Photographs showing typical histological sections through the centre of the partly-threaded screws, taken at 4x magnification. a) shows a sample from an implant-only group specimen; b) shows a specimen from the fibrin-only group; c) shows some new bone formation around an implant treated with 1.0×10^6 cells/mL in fibrin glue; and d) shows a sample from the 10×10^7 cells/mL in fibrin glue. Old bone (present pre-operatively) is marked with an 'O', new bone with an 'N', fibrous tissue with an 'F', and HA with 'HA.'

a)



b)

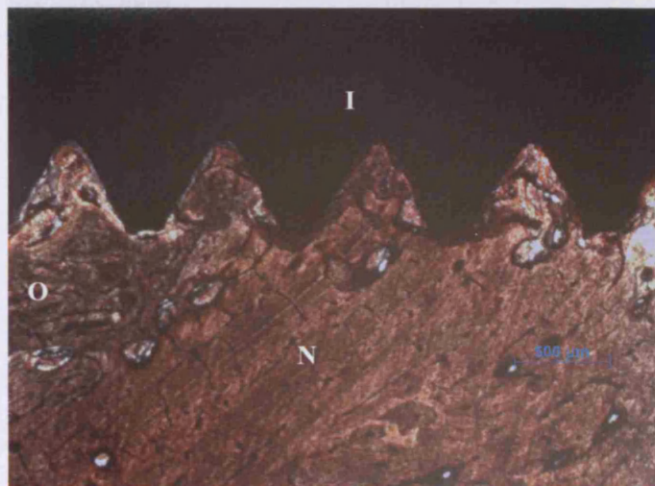
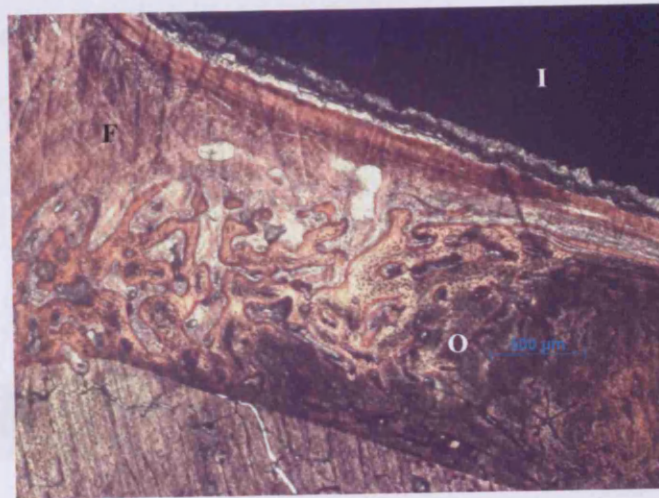
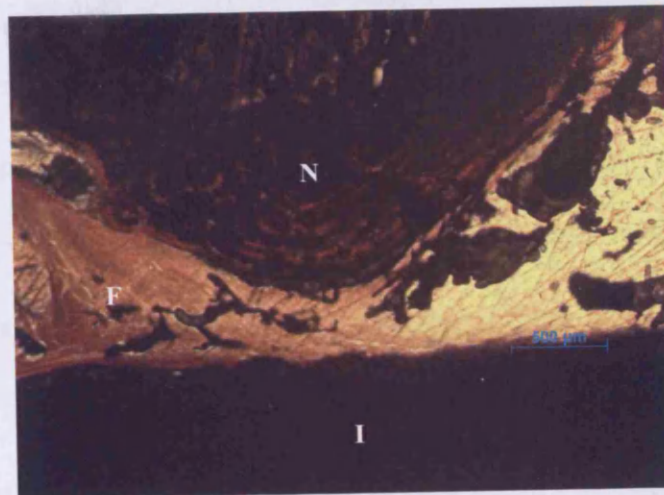


Figure 6.5 Images of histological sections around the implants. a), c), d) and e) show new bone formation (N) which is continuous with the older cortical bone (O), but separated from the implant (I) by fibrous tissue layer (F). The threaded portion of the implant seen in b) shows contact with the surrounding older cortical bone.

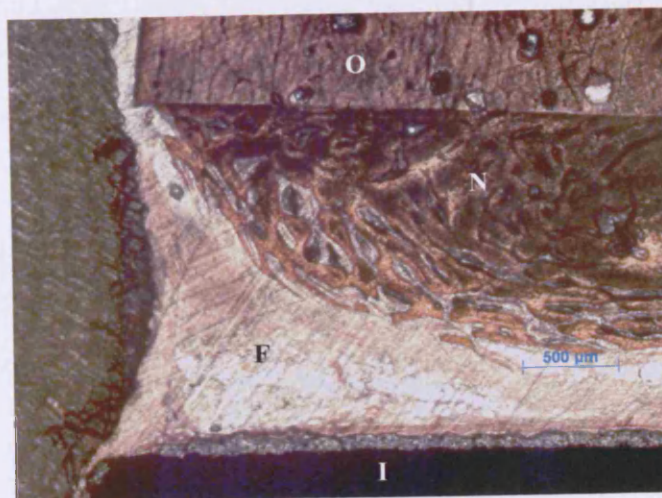
c)



d)



e)



When all fibrin and BMSC-treated groups were compared (see Table 6.4 and Figure 6.6), no significant differences were demonstrated ($p=0.25$). However, a significant difference was found between the autologous and allogeneic BMSC-fibrin-treated groups and the untreated control group ($p = 0.03$).

Group	New Bone Formation (mm ²)
Control	67.33 ± 6.83
Fibrin Only	40.53 ± 1.28
1.0 x 10 ⁵ autologous BMSCs/mL	39.24 ± 9.95
1.0 x 10 ⁶ autologous BMSCs/mL	48.03 ± 10.90
1.0 x 10 ⁷ autologous BMSCs/mL	43.69 ± 10.70
1.0 x 10 ⁶ allogeneic BMSCs/mL	43.93 ± 9.98

Table 6.4 Results of new bone formation, measured using histology and image analysis, in all six groups.

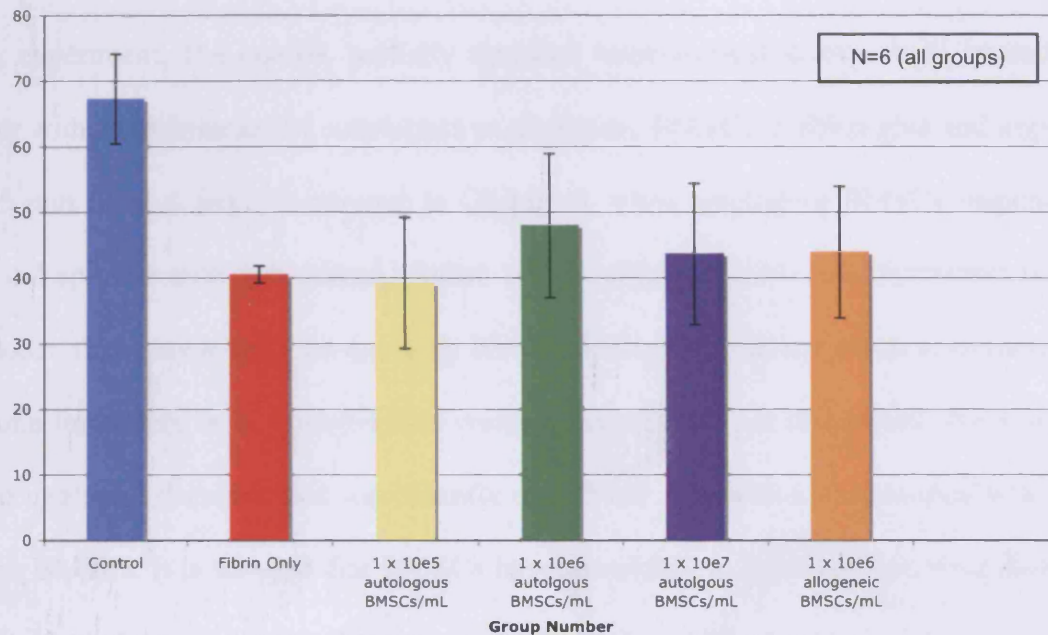


Figure 6.6 Graph outlining the result new bone formation measurement in all six groups. The error bars represent standard error.

6.3.2.2 Bone-Implant Contact

Woven bone was found along both the endosteal and periosteal surfaces of the tibial defects, in contact with the surrounding cortical bone. However, in all samples bone-implant contact was observed on only two occasions in the untreated control group. In these two specimens, the percentage bone-implant contact was 37.85% and 20.50% each. In all other cases, there was fibrous tissue filling the space and in contact with the implant.

6.4 Discussion

In this experiment, HA-coated, partially threaded trans-cortical screws were treated with fibrin or with a combination of autologous or allogeneic BMSCs in fibrin glue and implanted into 1.5 mm tibial defects. In contrast to Chapter 4, when autologous BMSCs suspended in fibrin and sprayed onto HA-coated implant collars enhanced new bone formation in an *in vivo* model, this same system for applying BMSCs to implants did not result in an increase in new bone formation, or in bone-implant contact. Interestingly, in this model, those samples with no treatment demonstrated significantly more bone area within defects than with either fibrin or BMSCs. It is thought that BMSCs have the ability to augment new bone formation when implanted into a model of bone repair either a) by differentiating into bone-forming osteoblasts or b) via the recruitment of cells favourable to bone repair and ossification, either by direct cell-cell interactions or by the secretion of growth factors and/or cytokines, either locally or systemically (See 5.4). As the cells in this model were not marked, it is impossible to make any conclusions as to whether or not the cells had a direct effect on new bone formation in the defects created in the model used in this chapter. It is possible that the use of a semi-occlusive e-PTFE membrane, with possible side effects of using fibrin glue within a sealed bone cavity, may have had a deleterious effect on new bone formation.

It is possible that mechanical factors played a role in the lack of new bone formation in this model. Studies such as those by Nagatomi et al. (2003), Hamilton, Maul and Vorp (2004) and Ignatius et al. (2005) have shown the sensitivity of BMSCs to mechanical forces and that while an application of compressive forces can cause osteoblastic differentiation of BMSCs, shear forces can cause cells to differentiate into mature vascular endothelial cells. Whereas low stress and strain are conducive to intramembranous bone formation, compressive stresses have been shown to induce a chondrogenic response in BMSCs. Ignatius et al. (2005)

demonstrated increasing expression of the master osteoblastic gene CBFA-1 after mechanical stretching of a human osteoblast precursor cell line (hFOB 1.19). It has been proposed that this mechanical effect is regulated by the MAP kinase (MAPK) signalling pathway, using extracellular signal-regulated kinase 1/2 (ERK 1/2) (Simmons et al. 2003). What was interesting about the BMSC group in Chapter 4 was that even with the addition of BMSCs, patterns of bone growth medio-laterally and anterior-posteriorly around mid-shaft tibial replacements were similar to that observed clinically, which has been shown to correlate with patterns of stress and strain (Blunn and Wait 1991; Taylor et al. 1997). It may be the case that in this particular model, strain was not transmitted to the BMSCs as effectively as in the ovine model used in chapter 4. Thus the cells may not have differentiated into osteoblasts or may have differentiated into another cell type such as a fibroblast phenotype. A notable difference between this study and previous studies, that may have affected the contribution of cell dosage to bone growth, is that they used models where the cell construct is mechanically loaded. Petite et al inserted a coral implant loaded with autologous BMSCs in an ovine model, where the defect was stabilised with a rigid plate. Lengthening plates were also used by Arinzeh et al. (2003) to stabilise a canine defect into which a ceramic cylinder loaded with BMSCs was implanted. Perhaps without this stable fixation (Zhim et al. 2005) the implants underwent micromotion in relation to the near cortex, which caused the formation of a fibrous tissue layer. Jasty et al. (1997) implanted porous-coated, cylindrical implants into the distal femoral metaphases of dogs and exposed them to various micrometers of oscillary motion for six weeks. In the groups with lower levels of micromotion (0-40 μm), bone, fibrocartilage and fibrous tissue was found, whereas at the higher level of motion (150 μm), a dense fibrous tissue layer was found surrounding the implants. It may be useful to measure the forces transmitted to the defects, possibly using telemetric analysis (Taylor et al. 1997). Although it may be useful investigate the effects of more rigid fixation on the tibia, Bhumbra

et al. (1998) showed new bone formation in a rabbit femoral model with a 500 µm defect around trans-cortical screws.

In other models of bone tissue engineering, it is possible that cells may have migrated out of the bony site and into the surrounding soft tissues, influencing bone formation from the musculature and vasculature. Marking cells, as well as retrieving bone samples together with surrounding soft tissue, would allow an analysis of MSC migration from the site. Cell fusion has been observed in cases where cells have fused in kidney tissue with host cells (Terada et al. 2002) such as hepatocytes (Wang et al. 2003), causing transdifferentiation or stimulation of new bone formation based on cell fusion and perhaps higher gene expression based on the aneuploidy of the system or the development of chimeric cells with the gene expression and chromosomal organisation of both cell types (Medvinsky and Smith 2003). If such is the case with the osteogenic contribution of BMSCs, a PTFE membrane may have interfered. It is also possible that e-PTFE membrane played a role in the failure of fibrin or BMSCs and fibrin to induce greater amounts of bone formation than the untreated group. It has also been shown that PTFE affects cell cytokine expression (Wakabayashi et al. 1997). Takata, Wang and Miyauchi (2001) showed that cells from an osteoblastic cell line (MC3T3-E1) did not readily attach and proliferate on e-PTFE. Alpar et al. (2000) found downregulated mitochondrial activity in those HPLF and SAOS-2 cultures grown on e-PTFE. It would also be useful to compare the effects of e-PTFE to no e-PTFE with fibrin or BMSCs in a similar large animal model.

Haematoma formation in this model may have resulted in cytotoxic levels of potassium ions. Street et al. (2005) demonstrated that haematoma supernatant prevented endothelial cell proliferation and microtubule formation *in vitro* and that that haematomas contain high levels

of VEGF, which give it the potential to form new blood vessels when transplanted subcutaneously in mice. However this occurs only once the haematoma has been resorbed and its inhibitory effect diminished. If the large numbers of dead cells or fibrin glue kept in the space by e-PTFE triggered a macrophage response, this may have resulted in cells being phagocytosed, as well as possibly triggering osteoclastic activity. This is in contrast to the normal situation in which guided bone generation using a semi-occlusive barrier is normally applied, as in other situations the number of BMSCs/osteoprogenitors migrating from the marrow to the defect site is significantly lower. The percentage of BMSCs in the bone marrow has been estimated as being approximately 0.001 %-0.0001 % of all bone marrow cells (Pittenger et al. 1999).

It is also possible that fibrin itself may have impeded new bone formation in this particular model. This may be in part due to the e-PTFE membrane preventing degradation of BMSCs by migrating cells or due to the attraction of fibroblasts to the site by the fibrin. Fibrin has previously been shown to be conducive to cell proliferation and migration (Becker, Domschke and Pohle 2004). Tisseel[®] contains factor XIIIa, and fibronectin, which encourages cell migration (Cox, Cole and Tawil 2004; Brown 1993), in addition to increasing levels of the angiogenic factor VEGF *in vivo* (Hojo et al. 2003). Lennon et al. (2000) showed that in subcutaneously implanted cell-seeded ceramic cubes, BMSCs were able to produce bone *in vivo* when diluted with dermal fibroblasts, up to a ratio of 50:50, providing evidence that fibroblasts have differential effects on new bone formation *in vivo*.

Also, as fibrin is conducive to fibroblast and vascular smooth-muscle cell migration, it is possible that the fibrin glue encouraged migration of BMSCs from the defect site into the marrow. Although work by many authors has shown that BMSCs can proliferate and

differentiate in fibrin glue (Boo et al. 2002; Lee et al. 2005), as well as ovine BMSCs as shown in Chapter 3 of this thesis, fibrin and fibrin and BMSCs have not previously been tested in this kind of model. Fibrin alone has not been shown in the literature to be osteoinductive unless combined with osteoprogenitor cells, such as BMSCs or an osteoconductive scaffold such as hydroxyapatite (Abiraman et al. 2002; Lee et al. 2005; Yamada et al. 2003). The fibrin glue layer was allowed to set for 3 minutes, after which fibrin may have set around the screw, but not necessarily directly attached to the bone surface. It is a possibility that shear stresses between the fibrin and bone surfaces within the gap caused osteocytes apoptosis via a fluid flow effect (Van der Vis et al. 1998).

One technique that could be used to improve bone is pre-operative osteogenic stimulation of BMSCs. As discussed in Chapter 4, studies have shown an increased angiogenic response of BMSCs after 7 days' treatment with standard osteogenic supplements. It would be interesting to test whether or not osteogenic BMSCs, or fibrin with added growth factors, would show any difference in results.

Regarding the radiological results, the use of radiography in an attempt to measure differences in bone mineral density between groups in this experiment was not a sensitive enough method. Also, the far cortex in most of the radiographs obscured visualisation of the defect. Genant (1998) reported, for example, that radiographs showed bone loss only when the bone mineral density had reduced by 30-50%. A more precise method would be to use dual energy X-ray absorptiometry (DEXA), which can digitally monitor and quantify bone density.

In conclusion, autologous and allogeneic BMSCs were suspended in fibrin glue at different concentrations and sprayed onto HA-coated partially fixed trans-cortical screws within 1.5 mm defects, and compared to fibrin only or untreated controls in an ovine model. It was found that there was no significant effect of varying cell dosage on the amount of new bone formation or bone-implant contact. Thus the proposed hypothesis is invalid. With PTFE, there did not seem to be any benefit in preventing fibrous tissue growth. There was significantly more bone formation in the group with no treatment when compared to all other groups. It may be possible that BMSC-based bone tissue engineering is not beneficial to every clinical scenario and/or in combination with guided bone regeneration.

CHAPTER SEVEN

GENERAL DISCUSSION

The overall hypothesis of my thesis was that **bone marrow stromal cells (BMSCs) could be applied to orthopaedic implants using a fibrin glue-spray system, in order to increase bone growth adjacent to these implants and improve bone-implant contact.** Experimentation to examine this hypothesis has been reported in this thesis (Figure 7.1).

Firstly, in Chapter 2, bone marrow stromal cells were isolated from the iliac crest of sheep and expanded in culture. These cells were characterised by differentiating them down different cell lineages (osteoblastic and adipogenic), using chemical cues. For example, oBMSCs treated with osteogenic supplements had increased ALP activity after 7 to 14 days and were positive for calcium phosphate deposition. Cells treated with adipogenic reagents showed increased lipid content. However, when other cell lines that were not derived from a stromal cell lineage were tested for their osteogenic potential after treatment with the same reagents, they were found to react similarly. These results indicate that these tests are not specific for oBMSCs. Nevertheless, isolated oBMSCs did show an ability to produce a mineralised matrix, indicating that they may also form mineralised tissue if implanted *in vivo*. The rigorous controls used in this chapter have not generally been used by other groups when using osteogenic differentiation to characterise BMSCs (Bruder, Jaiswal and Haynesworth 1997; Declercq et al. 2005; Janssen et al. 2006; Gorustovich, Rosenbusch and Guglielmotti 2002), and this brings into question these commonly - used techniques. There is also a possibility that these cultured cell lines are de-differentiating in culture conditions causing phenotypic instability (Real et al. 2006) and/or trans-differentiating when certain cues are present, or when in contact with other mature cell types. Examples of these are the transdifferentiation of mesenchymal stem cells down the hepatic

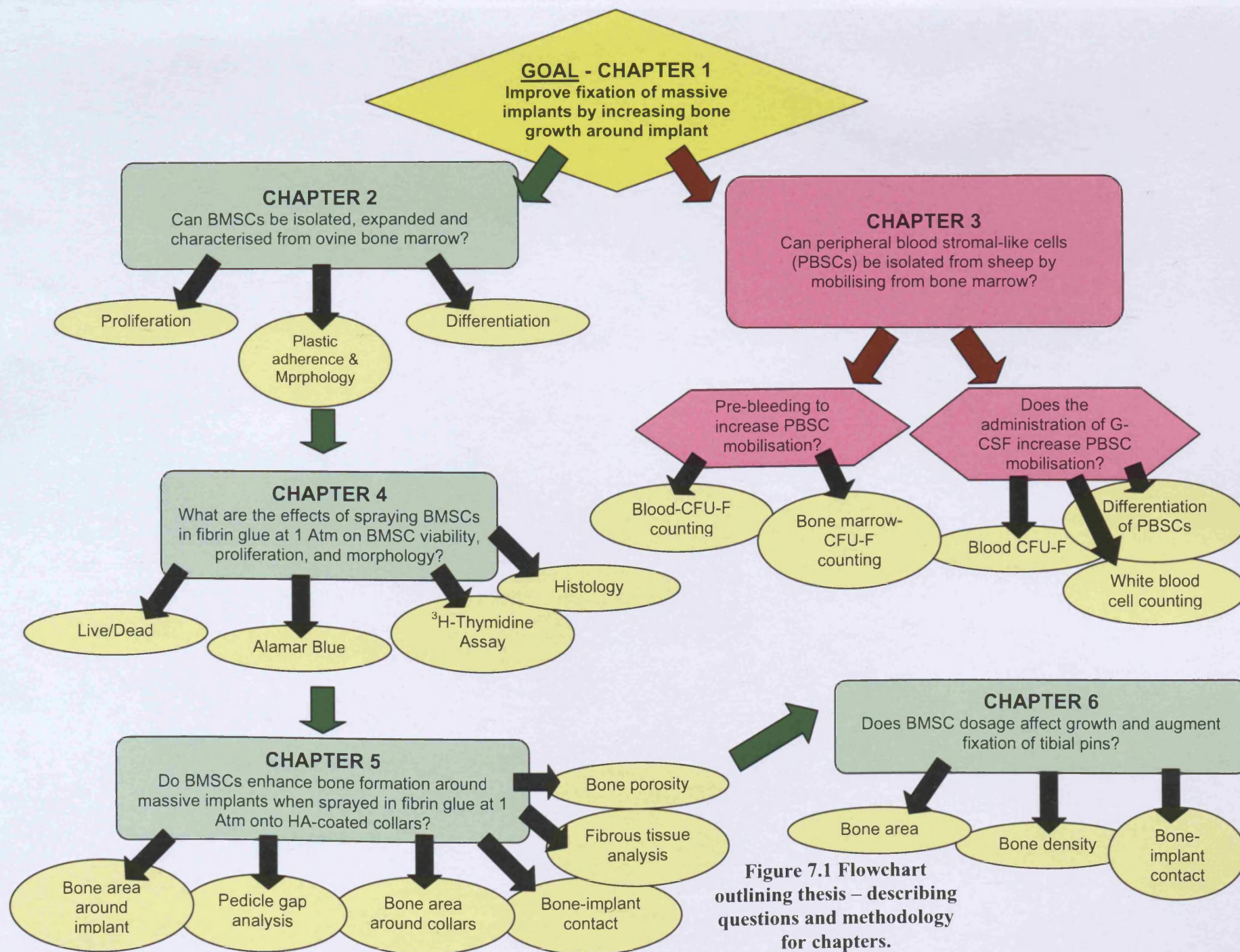


Figure 7.1 Flowchart
outlining thesis – describing
questions and methodology
for chapters.

lineage when serum-deprived and then treated with supplements, or co-cultured with liver cells, as well as the differentiation of BMSCs into neurons using the signalling molecule Sonic hedgehog (Shh) and retinoic acid (Taléns-Visconti et al. 2007; Lange et al. 2005; Kondo et al. 2005).

In order to fully characterise the oBMSCs used in this study and identify them as being the multipotent cells described in the literature (Haynesworth et al. 1992; Jaiswal et al. 1997), more *in vitro* work needs to be done, looking at gene expression after stimulation with supplements for differentiation. Also, surface marker analysis or “gene chip” analysis needs to be done, with a panel of antigens that are known to positively or negatively react with BMSCs, using a FACS or MACS system (Pittenger et al. 1999). “Gene chips” may also provide useful information (Bourne et al. 2004; Hishikawa et al. 2004). As always, a thorough, correct statistical analysis of the results is required. Results from Jiang et al. (2002a; 2002b) have recently been challenged, due to flaws in the analysis of surface marker expression of their special multipotent adult progenitor cells, or MAPCs, as well as the mislabelling and use of their results in more than one ‘original’ publication (Verfaillie and Jiang 2006; Jiang et al. 2007).

BMSCs are thought to undergo osteogenic differentiation via a MAP kinase-mediated mechanism (Jaiswal et al. 2000). Pre-differentiation of these cells into osteoblast precursor cells or osteoblasts may help expedite the bone healing process by skipping stages of differentiation, or the requirement for certain environmental/mechanical cues in order to differentiate and, once integrated into the repair site, could begin bone matrix and matrix mineralisation without delay. Additionally, the applied cells could be genetically modified first to express osteogenic growth factors and cytokines .

The peripheral blood was tested as another source for stromal cells in Chapter 3. Ovine peripheral blood stromal-like cells (oPBSCs) were isolated, expanded and characterised. The aim of pursuing an alternative to BMSCs was to obtain a similar cell population without painful bone marrow aspiration procedures, which usually require a general anaesthetic. In an attempt to increase the BMSC numbers in the blood, and thus the number of cells isolated from the blood, two techniques were tested: 1) pre-induced blood loss and 2) the administration of granulocyte-colony stimulating factor (G-CSF). Whereas blood loss did not appear to have a noticeable effect on the number of oPBSCs isolated from sheep, G-CSF administration resulted in a significant increase in oPBSC number in the blood stream two weeks post-treatment. When expanded in culture and then characterised by differentiation down three cell lineages (osteogenic, chondrogenic, and adipogenic), the oPBSCs showed a response similar to oBMSCs, indicating cell plasticity and the ability to produce calcium phosphate nodules *in vitro*, even without stimulation using osteogenic reagents. Other groups have also demonstrated the *in vitro* osteogenic capacity of PBSCs isolated from circulating peripheral blood (Rocheffort et al. 2006, Kassis et al. 2006). There may be some resulting concern that these cells could ossify in the body and contribute towards heterotopic ossification. However, nodule production only occurred after the cells had been grown in static culture for 28 days. It is a possibility that the cells do not have this capacity when being circulated in the peripheral blood. It may also be possible that these cells home to specific tissues and that their appearance in the bloodstream is only transitory (Devine et al. 2001). The mobilisation of HSCs and BMSCs after G-CSF administration may be a result of changes and/or modifications to the niche environment within the bone marrow. It is known that BMSCs and HSCs interact with each other via cell surface molecules such as VCAM-1 (on BMSCs), VLA-4 and CXCL12 (on HSCs), as well as cytokines such as stromal-derived factor-1 (SDF-1), (Kronenwett, Martin and Haas 2000; Kucia et al. 2004; Levesque et al.

2001), and that both cell types can influence each other in terms of cell proliferation (Baksh, Davies and Zandstra 2005). Further work is required into the niche environment of the bone marrow, including HSC-BMSC interactions, and changes that may induce BMSC mobilisation.

G-CSF has so far been shown to be useful in stimulating the mobilisation of BMSCs from the bone marrow, in order to isolate them from the blood. Besides the potential of these cells for localised application of BMSCs, G-CSF may have other applications. Alternatively, G-CSF has shown some potential for amplifying natural healing responses by mobilising BMSCs for fracture healing (Bozlar et al. 2005), or by mobilising endothelial progenitor cells to promote the repair of cardiac ischemia (Minamino et al. 2005). Also, further study into changes in the microenvironment and HSC-BMSC relationship after cytokine therapy and cell mobilisation may facilitate the application of these techniques in the future.

After two stromal-like cell types were investigated for their potential use in augmenting bone growth adjacent to orthopaedic implants in an *in vivo* model, Chapter 4 investigated oBMSC viability, proliferation, and morphology *in vitro* after being sprayed at 1 atm with fibrin glue. The ultimate goal of such a system was to apply oBMSCs to the surface of orthopaedic implants, in order to increase bone formation at the site of application. The use of such a system would be a much more convenient and translatable method, as the cells are cultured separately and then combined with fibrin per-operatively rather than pre-culture of the cells onto the implant. Both methods have been shown to produce the same amount of new bone *in vivo* when seeded onto ceramic cubes and implanted ectopically (Kruyt et al. 2004). All of the assays showed that oBMSCs were not affected by spraying at 1 atm. Specifically, cell viability was preserved post-spraying, similar to unsprayed samples, and proliferation was

maintained *in vitro* as measured up to 72 hours post-spraying. This chapter provided evidence that oBMSCs, with osteogenic potential, could survive after spraying at 1 atm in a fibrin glue carrier. The next step in my thesis was to test whether oBMSCs applied using this system could improve bone formation and contact adjacent to orthopaedic implants, in an *in vivo* model.

Chapter 5 investigated the ability of oBMSCs to augment new bone formation adjacent to massive orthopaedic implants in an ovine model. OBMSCs suspended in fibrin glue, at two different densities (2×10^6 cells/collar and 10×10^6 cells/collar), were sprayed onto the hydroxyapatite-coated collars of massive implants and implanted into the midshaft of sheep tibiae, and compared to untreated implants. The area of bone adjacent to the implants and to the implant collars was increased when implants were treated with low and high doses of oBMSCs in fibrin glue when compared to untreated implants. When fibrin glue was applied to the collars alone, new bone formation was increased around collars when compared to untreated implants, however levels were not as high as when cells were used. It must be noted, however, that the fibrin-only and high-BMSC dose had a lower number of samples than the other two groups. This will be investigated further in future work. Those implants treated with a higher density of cells showed an increase in new bone formation when compared to those treated with the lower number of cells, although this difference was not statistically significant. Bone-implant contact was also improved and although this result was not statistically significant, more than twice the number of BMSC-treated collars had bone-implant contact when compared to untreated implants. When the presence of radiolucent lines between the new pedicle of bone and implant was evaluated radiographically, there was a significant decrease in the length of these lines in both BMSC-treated groups, when compared to control specimens.

The percentage of fibrous tissue adjacent to implants was found to be significantly reduced when oBMSCs were applied to implant collars when compared to untreated implants (low dose $p=0.02$; high dose $p=0.01$), as measured using histological specimens. The higher dose of oBMSCs also resulted in a significant reduction in fibrous tissue when compared to the lower dose group. Additionally, radiolucent lines between pedicle bone and the implants were reduced in BMSC-treated groups. Regarding bone porosity, bone adjacent to collars in the high-dose BMSC group had half the porosity of the untreated control groups samples ($p=0.018$), and the low-BMSC group about 39% less, although there was no significant difference ($p>0.05$). The reduction in porosity found in the BMSC-treated groups correlates with bone-implant contact and may be related to load transfer from the implant to host bone when BMSCs are applied. Additionally, statistically significant positive correlations were found between bone porosity and bone-implant contact in all groups. Increased extra-cortical bone formation and in-growth fixation to the implant surface will increase implant fixation, improve stress transfer across the bone-prosthesis junction and improve fixation of the prosthesis, thereby improving fixation. The above results showed that BMSCs significantly enhance new bone formation when applied in fibrin glue onto the HA-coated collars of massive implants, improving bone-implant contact.

The autologous oBMSCs isolated and expanded were shown to have beneficial results on new bone formation around massive implants, as shown in Chapter 5. The next steps in this research are: 1) an optimization of the system, looking mainly at cell dosages, and 2) the application of this method in a clinical setting. Patients undergoing bone tumour replacement could have their BMSCs harvested in advance, isolated, expanded, and applied to the HA-

coated collars of their implants, using a fibrin glue spray system. This research will be carried out within the next few years.

One must consider that when using the autologous BMSCs of a bone cancer patient, the theoretical risk of undetected metastatic tumour cells being isolated from the bone marrow in addition to BMSCs. If this is the case, use of donor-derived, allogeneic BMSCs may also be useful (Horwitz et al. 1999). However, one must also consider that all BMSCs, autologous or allogenic, are immunosuppressive and express VEGF, which is essential to tumour growth (Aggarwal and Pittenger 2005; Ferrara and Davis-Smyth 1997). These effects may have negative consequences for tumourogenesis in any patient (Djouad et al. 2003).

Future research looking into the use of BMSCs in conjunction with massive implants could also investigate the use of implant materials with a lower Young's modulus. The use of such a material, with a modulus closer to that of bone, would further promote load transfer from the implant to the host bone. An increased compressive load promote more bone growth, as developed from Wolff's law (Wolff 1892), and BMSCs may also be responsive to such forces (Ignatius et al. 2005), and may also further increase bone formation and bone-implant contact when applied to these implants. Whether a different polymer, metal, or a porous material was used, increased load transfer via this mechanism may be an effective solution.

In future work, cells should be tracked to try and identify their contribution to new bone formation in *in vivo* models. This could be done by genetically modifying the cells to express a gene, such as lacZ, which encodes the bacterial enzyme β -galactosidase, green fluorescent protein (GFP) and Fluc, which encodes firefly luciferase (Zhou et al. 2005).

A further strategy to improve bone formation around the implants could be to incorporate growth factors into the fibrin-cell mixture that is sprayed onto the HA collars. Inclusion of growth factors such as BMP-2 or BMP-7, well documented osteogenic factors, could further increase bone formation, by influencing the differentiation of the cells. Alternatively, these factors could be supplied using a cell therapy approach, where genetically modified BMSCs, expressing BMPs or other relevant genes, could be implanted at the repair site (Tsuchida et al. 2002; Lieberman et al. 1999; Edwards et al. 2004; Mistry and Mikos 2005). Growth factors targeting neo-angiogenesis and revascularisation could also play an important role, such as VEGF (Geiger et al. 2005; Peng et al. 2005) and SDF-1.

Following from the results of Chapter 5, another large animal *in vivo* model was used in order to establish if cell dosage effects bone formation. The purpose of Chapter 6 was to find the optimal dosage when BMSCs were implanted peri-operatively, for use in future bone tissue engineering models. Six groups were compared: 1) no treatment; 2) fibrin glue-only; 3) 1×10^5 autologous oBMSCs/mL; 4) 1×10^6 autologous oBMSCs/mL; 5) 1×10^7 autologous oBMSCs/mL; and 6) 1×10^6 allogeneic oBMSCs/mL. Six HA-coated transcortical screws were coated with one of the six treatments (or not coated, in the case of the untreated control), and implanted into 1.5mm tibial gaps in the mid-shaft of sheep. After a period of six months, bone formation, and bone-implant contact was assessed radiographically and histologically. Radiographically, there was no significant difference in new bone formation between the six groups. When specimens from all six groups were compared histologically, no significant difference was found. Further investigation into altering this model and understanding why oBMSCs were not effective in this part of my thesis, as opposed to the one described in Chapter 5, is required.

7.1 Future Work

The BMSC-fibrin glue spray technique could also be applied to total hip arthroplasty (THAs). Despite the success of cemented and uncemented THAs, they still incur a high revision rate when compared to knee replacements (Kurtz et al. 2005). Approximately 50,000 THAs are performed in the UK every year (1 million per year worldwide; Department of Health 2006). Failures are most often a result of aseptic loosening of the components due to wear debris-associated osteolysis, and revision surgery is costly.

As discussed by Bhumbra et al. (2000) and Coathup et al. (2005), it may be possible to prevent the loosening of implants through this mechanism by improving the fixation between the bone and implant, or promoting the formation of a biological bony seal around the component, in order to prevent the influx of wear particles or pressurised joint fluid. Current *in vivo* work in a goat THA model will hopefully be able to show whether or not BMSCs do improve bone formation and bone-implant contact of uncemented acetabular cups to host bone.

BMSCs were used in the *in vivo* models in this study, rather than PBSCs. BMSCs have been used in other models previously, but there is only one previously described study in the literature utilising PBSCs (Wan, He and Li 2006). Most literature on PBSCs (Rochefort et al. 2006; Mansilla et al. 2006; Khosla and Eghbali-Fatourehchi 2006; Kassis et al. 2006) have been published relatively recently, although they show a similar potential for use in bone tissue engineering applications as BMSCs (Wan, He and Li 2006). One example of this, shown in Chapter 3 of this thesis, is their ability to produce nodules of calcium phosphate even without stimulation with osteogenic supplements. Further *in vivo* studies are required using PBSCs, to test their osteogenic potential *in situ*.

In conclusion, the work described in this thesis has successfully proved the hypothesis, which was that **viable BMSCs could be applied to orthopaedic implants using a fibrin glue-spray system, and increase bone formation adjacent to the implants and improve bone-implant contact.** The successful application of BMSCs in bone tissue engineering has thus been demonstrated. This small step towards understanding which cells facilitate the regeneration of tissues, and in which situations *in vivo*, will hopefully contribute towards directly improving patients' quality of life and reduce implant morbidity, with the clinical application of a BMSC-fibrin spray system; and indirectly, by stimulating the further development of new and innovative approaches to bone tissue engineering and regeneration.

REFERENCES

- Abiraman, S., Varma, H.K., Umashankar, P.R. et al., 2002. Fibrin glue as an osteoinductive protein in a mouse model. *Biomaterials*. 23(14), pp 3023-31.
- Abudu, A., Carter, S.R., and Grimer, R.J., 1996a. The outcome and functional results of diaphyseal endoprostheses after tumour excision. *Journal of Bone & Joint Surgery (Br)*. 78(4), pp 652-7.
- Abudu, A., Sferopoulos, N.K., Tillman, R.M. et al., 1996b. The surgical treatment and outcome of pathological fractures in localised osteosarcoma. *Journal of Bone & Joint Surgery (Br)*. 78(5), pp 694-8.
- Aggarwal, S. and Pittenger, M.F. 2005. Human mesenchymal stem cells modulate allogeneic immune responses. *Blood*. 105(4), pp 1815-22.
- Almeida, M.J., Pereira, L., Milet, C. et al., 2001. Comparative effects of nacre water-soluble matrix and dexamethasone on the alkaline phosphatase activity of MRC-5 fibroblasts. *Journal of Biomedical Materials Research*. 57(2), pp 306-12.
- Alpar, B., Leyhausen, G., Gunay, H. et al., 2000. Compatibility of resorbable and nonresorbable guided tissue regeneration membranes in cultures of primary human periodontal ligament fibroblasts and human osteoblast-like cells. *Clinical Oral Investigations*. 4(4), pp 219-25.
- Améen, C., Strehl, R., Bjorquist, P. et al., 2007. Human embryonic stem cells: current technologies and emerging industrial applications. *Critical Reviews in Oncology/Hematology*. August 3rd, pp 1-27.
- Amstein, C.F. and Hartman, P.A. 1975. Adaptation of plastic surfaces for tissue culture by glow discharge. *Journal of Clinical Microbiology*. 2(1), pp 46-54.
- Andree C., Voigt, M., Wenger, A. et al., 2001. Plasmid gene delivery to human keratinocytes through a fibrin-mediated transfection system. *Tissue Engineering* 7(6), pp 757-66.

Antoniou, E.S., Sund, S., Homsy, E.N. et al., 2004. A theoretical simulation of hematopoietic stem cells during oxygen fluctuations: prediction of bone marrow responses during hemorrhagic shock. *Shock*. 22(5), pp 415-22.

Arinzeh, T.L., Peter, S.J., Archambault, M.P. et al., 2003. Allogeneic mesenchymal stem cells regenerate bone in a critical-sized canine segmental defect. *Journal of Bone and Joint Surgery (Am)*. 85-A(10), pp 1927-35.

Arinzeh, T.L. 2005. Mesenchymal stem cells for bone repair: preclinical studies and potential orthopaedic applications. *Foot and Ankle Clinics*. 10(4), pp 651-55, viii.

Asakura, A. 2003. Stem cells in adult skeletal muscle. *Trends in Cardiovascular Medicine*. 13(3), pp 123-8.

Aubin, J.E. 1998. Bone stem cells. *Journal of Cellular Biochemistry Supplement*. 30-31, pp 73-82.

Bab, I., Ashton, B.A., Gazit, D., Marx, G., Williamson, M.C., and Owen, M.E. 2006. Kinetics and differentiation of marrow stromal cells in diffusion chambers *in vivo*. *Journal of Cell Science*. 84, pp 139-51.

Bacou, F., el Andaloussi, R.B., Daussin, P.A. et al., 2004. Transplantation of adipose tissue-derived stromal cells increases mass and functional capacity of damaged skeletal muscle. *Cell Transplant*. 13(2), pp 103-11.

Baksh, D., Davies, J.E. and Zandstra, P.W. 2003. Adult human bone marrow-derived mesenchymal progenitor cells are capable of adhesion-dependent survival and expansion. *Experimental Hematology*. 31(8), pp 723-32.

Baksh, D., Davies, J.E. and Zandstra, P.W. 2005. Soluble factor cross-talk between human bone marrow-derived hematopoietic and mesenchymal stem cells enhances *in vitro* CFU-F and CFU-O growth and reveals heterogeneity in the mesenchymal progenitor cell compartment. *Blood*. 106(9), pp 3012-9.

Bancroft, J.D. and Stevens, A., 1986. *Theory and Practice of Histological Techniques, Second Edition*. Churchill Livingstone, London, pp 168-9.

Bartholomew, A., Patil, S., Mackay, A. et al., 2001. Baboon mesenchymal stem cells can be genetically modified to secrete human erythropoietin in vivo. *Human Gene Therapy*. 12(12), pp 1527-41.

Bartholomew, A., Sturgeon, C., Siatskas, M. et al., 2002. Mesenchymal stem cells suppress lymphocyte proliferation *in vitro* and prolong skin graft survival *in vivo*. *Experimental Hematology*. 30(1), pp 42-8.

Bartsch, G., Yoo, J.J., De Coppi, P. et al., 2005. Propagation, expansion, and multilineage differentiation of human somatic stem cells from dermal progenitors. *Stem Cells and Development*. 14(3), pp 337-48.

Basu, A. and Haldar, S. 1998. The relationship between Bcl2, Bax and p53: consequences for cell cycle progression and cell death. *Molecular Human Reproduction*. 4(12), pp 1099-109.

Baxter, M.A., Wynn, R.F., Jowitt, S.N. et al., 2004. Study of telomere length reveals rapid aging of human marrow stromal cells following in vitro expansion. *Stem Cells*. 22(5), pp 675-82.

Baxter Bioscience. *Tissue Engineering Guide*. Baxter Bioscience, Deerfield, IL, USA.

Baxter Healthcare. *Tisseel Product Information*, 2000. Baxter Healthcare, Deerfield, IL, USA.

Baxter Healthcare Corporation (2006). *Baxter Tisseel[®] Two-component Fibrin Sealant, Vaport Heated Kit (Package Insert)*. Westlake Village, CA: Baxter Healthcare Corporation.

Beauvais, D.M. and Rapraeger, A.C. 2004. *Reproductive Biology and Endocrinology*. 2, pp 3.

- Becker, J.C., Domschke, W. and Pohle, T. 2004. Biological in vitro effects of fibrin glue: fibroblast proliferation, expression and binding of growth factors. *Scandinavian Journal of Gastroenterology*. 39(10), pp 927-32.
- Belboul, A., Dernevik, L., Aljassim, O. et al., 2004. The effect of autologous fibrin sealant (Vivostat) on morbidity after pulmonary lobectomy: a prospective randomised, blinded study. *European Journal of Cardio-Thoracic Surgery*. 26(6), pp 1187-91.
- Bellamy, N., Buchanan, W.W., Goldsmith, C.H. et al., 1998. Validation study of WOMAC: a health status instrument for measuring clinically important patient relevant outcomes to antirheumatic drug therapy in patients with osteoarthritis of the hip or knee. *The Journal of Rheumatology*. 15(12), pp 1833-40.
- Bellows, C.G., Aubin, J.E., Heersche, J.N. et al., 1986. Mineralized bone nodules formed in vitro from enzymatically released rat calvaria cell populations. *Calcified Tissue International*. 38(3), pp 143-54.
- Bensaid, W., Triffitt, J.T., Blanchat, C. et al., 2003. A biodegradable fibrin scaffold for mesenchymal stem cell transplantation. *Biomaterials*. 24(14), pp 2497-502.
- Bergmann, G., Siraky, J., Rohlmann, A. et al., 1984. A comparison of hip joint forces in sheep, dog and man. *Journal of Biomechanics*. 17(12), pp 907-21.
- Bertani, N., Malatesta, P., Volpi, G. et al., 2005. Neurogenic potential of human mesenchymal stem cells revisited: analysis by immunostaining, time-lapse video and microarray. *Journal of Cell Science*. 118(Pt 17), pp 3925-36.
- Best, S., Sim, B., Kayser, M. et al., 2004. The dependence of the osteoblastic response on variations in the chemical composition and physical properties of hydroxyapatite. *Journal of Materials Science: Materials in Medicine*. 8(2), pp 97-103.

Bhumra, R.S., Walker P.S., Berman A.B. et al., 2000. Prevention of loosening in total hip replacements using guided bone regeneration. 2000. *Clinical Orthopaedics and Related Research*. 372, pp 192-204.

Bhumra, R.S., Berman, A.B., Walker, P.S. et al., 1998. Enhanced bone regeneration and formation around implants using guided bone regeneration. *Journal of Biomedical Materials Research* 43(2), pp 162-7.

Biosource,TM International, Inc., (2003). *Use of Almar BlueTM in the measurement of cell viability and toxicity*.

Bloebaum, R.D., Beeks, D., Dorr, L.D. et al., 1994. Complications with hydroxyapatite particulate separation in total hip arthroplasty. *Clinical Orthopaedics and Related Research*. 298, pp 19-26.

Blunn, G.W., Briggs T.W., Cannon S.R. et al., 2000. Cementless fixation for primary segmental bone tumor endoprostheses. *Clinical Orthopaedics and Related Research*. 372, pp 223-30.

Blunn, G.W. and Wait, M.E. 1991. Remodelling of bone around intramedullary stems in growing patients. *Journal of Orthopaedic Research*. 9(6), 809-19.

Bonucci, E., Marini, E., Valdinucci, F. et al., 1997. Osteogenic response to hydroxyapatite-fibrin implants in maxillofacial bone defects. *European Journal of Oral Sciences*. 105(6), pp 557-61.

Boo, J.S., Yamada, Y., Okazaki, Y. et al., 2002. Tissue-engineered bone using mesenchymal stem cells and a biodegradable scaffold. *Journal of Craniofacial Surgery*. 13(2), pp 231-9.

Bosch, P., Lintner, F., Arbes, H. et al., 1980. Experimental investigations of the effect of the fibrin adhesive on the Kiel heterologous bone graft. *Archives of Orthopaedic and Trauma Surgery*. 96(3), pp 177-85.

- Bosch, P., Pratt, S.L. and Stice, S.L. 2006. Isolation, characterization, gene modification, and nuclear programming of porcine mesenchymal stem cells. *Biology of Reproduction*. 74(1), pp 46-57.
- Bourne, S., Polak, J.M., Hughes, S.P. et al., 2004. Osteogenic differentiation of mouse embryonic stem cells: differential gene expression analysis by cDNA microarray and purification of osteoblasts by cadherin-11 magnetically activated cell sorting. *Tissue Engineerring*. 10(5-6), pp 796-806.
- Boyne, P.J. and Yeager, J.E. 1969. An evaluation of the osteogenic potential of frozen marrow. *Oral Surgery, Oral Medicine, Oral Pathology, Oral Radiology, and Endodontology*. 28(5), pp 764-71.
- Bozdech, M.J. and Bainton, D.F. 1981. Identification of alpha-naphthryl butyrate esterase as a plasma membrane ectoenzyme of monocytes and as a discrete intracellular membrane-bounded organelle in lymphocytes. *Journal of Experimental Medicine*. 153(1), pp 182-95.
- Bozlar, M., Aslan, B., Kalaci, A. et al., 2005. Effects of human granulocyte-colony stimulating factor on fracture healing in rats. *Saudi Medical Journal*. 26(8), pp 1250-4.
- Bradish, C.F., Kemp, H.B., Scales, J.T. et al., 1987. Distal femoral replacement by custom-made prostheses. Clinical follow-up and survivorship analysis. *Journal of Bone and Joint Surgery (Br)*. 69(2), pp 276-84.
- Brazelton, T.R. and Blau, H.M. 2005. Optimizing techniques for tracking transplanted stem cells in vivo. *Stem Cells* 23(9), pp 1251-65.
- Breitbart, A.S., Grande, D.A., Mason, J.M. et al., 1999. Gene-enhanced tissue engineering: applications for bone healing using cultured periosteal cells transduced retrovirally with the BMP-7 gene. *Annals of Plastic Surgery*. 42(5), pp 488-95.

- Brendel, C., Kuklick, L., Hartmann, O. et al., 2005. Distinct gene expression profile of human mesenchymal stem cells in comparison to skin fibroblasts employing cDNA microarray analysis of 9600 genes. *Gene Expressions*. 12(4-6), pp 245-57.
- Brown, L.F. 1993. Fibroblast migration in fibrin gel matrices. *American Journal of Pathology*. 142(1), pp 273-83.
- Bruder, S.P. and Caplan, A.I. 2000. Bone Regeneration Through Cellular Engineering. In *Principles of Tissue Engineering 2nd Edition*. Lanza, R.P., Langer, P. and Vacanti, J., eds. London: Academic Press, 2000, pp 599-618.
- Bruder, S.P. and Caplan, A.I. 1990. A monoclonal antibody against the surface of osteoblasts recognizes alkaline phosphatase isoenzymes in bone, liver, kidney, and intestine. *Bone* 11(2), pp 133-9.
- Bruder, S.P., Jaiswal, N. and Haynesworth, S.E. 1997. Growth kinetics, self-renewal, and the osteogenic potential of purified human mesenchymal stem cells during extensive subcultivation and following cryopreservation. *Journal of Cellular Biochemistry*. 64(2), pp 278-94.
- Bruder, S.P., Kraus, K.H., Goldberg, V.M. et al., 1998. The effect of implants loaded with autologous mesenchymal stem cells on the healing of canine segmental bone defects. *Journal of Bone and Joint Surgery (Am)*. 80(7), pp 985-96.
- Bruland, O.S., Hoifodt, H., Saeter, G. et al., 2005. Hematogenous micrometastases in osteosarcoma patients. *Human Cancer Biology*. 11(13), pp 4666-73.
- Bucala, R., Spiegel, L.A., Chesney, J. et al., 1994. Circulating fibrocytes define a new leukocyte subpopulation that mediates tissue repair. *Molecular Medicine*. 1(1), pp. 71-81.
- Bulte, J.W., Douglas, T., Witwer, B. et al., 2001. Magnetodendrimers allow endosomal magnetic labelling and in vivo tracking of stem cells. *Nature Biotechnology*. 19(12), pp 1141-7.

- Buma, P., Schreurs, W. and Verdonchot N. 2004. Skeletal tissue engineering-from in vitro studies to large animal models. *Biomaterials* 25(9), pp 1487-95.
- Burke, Z.D. and Tosh, D. 2005. Therapeutic potential of transdifferentiated cells. *Clinical Science (Lond)* 108(4), pp 309-21.
- Burkus, J.K., Heim, S.E., Gornet, M.F. et al., 2003. Is INFUSE bone graft superior to autograft bone? An integrated analysis of clinical trials using the LT-CAGE lumbar tapered fusion device. *Journal of Spinal Disorders & Techniques*. 16(2), pp 113-22.
- Byers, B.A., Guldberg, R.E., Hutmacher, D.W. et al., 2006. Effects of Runx2 genetic engineering and in vitro maturation of tissue-engineered constructs on the repair of critical size bone defects. *Journal of Biomedical Materials Research Part A*. 76(3), pp 646-55.
- Calafiori, A.R., Di Marco, G., Martino, G. et al., 2007. Preparation and characterization of calcium phosphate biomaterials. *Journal of Materials Science. Materials in Medicine*. June 14.
- Calvi, L.M., Adams, G.B., Weibrecht, K.W. et al., 2003. Osteoblastic cells regulate the haematopoietic stem cell niche. *Nature*. 425(6960), pp 841-6.
- Campagnoli, C., Roberts, I.A., Kumar, S. et al., 2001. Identification of mesenchymal stem/progenitor cells in human first-trimester fetal blood, liver, and bone marrow. *Blood*. 98(8), pp 2396-402.
- Cannon, S.R. 1997. Massive prostheses for malignant bone tumours of the limbs. *Journal of Bone and Joint Surgery (Br)*. 79(3), pp 497-506.
- Capanna, R., Morris, H.G., Campanacci, D. et al., 1994. Modular uncemented prosthetic reconstruction after resection of tumours of the distal femur. *Journal of Bone and Joint Surgery (Br)*. 76(2), pp 178-86.
- Caplan, A.I. and Dennis J.E. 2006. Mesenchymal stem cells as trophic mediators. *Journal of Cell Biochemistry*. 98(5), pp 1076-84.

Castro-Malaspina, H., Gay, R.E., Resnick, G. et al., 1980. Characterization of human bone marrow fibroblast colony-forming cells (CFU-F) and their progeny. *Blood*. 56(2), pp 289-301.

Catelas, I., Sese, N., Helgersson, S. et al., 2004. Effects of fibrin gel formulation of mesenchymal stem cell proliferation and differentiation. *7th World Biomaterials Congress, Sydney Australia*.

Chan, C., Thompson, I., Robinson, P. et al., 2002. Evaluation of Bioglass/dextran composite as a bone graft substitute. *International Journal of Oral Maxillofacial Surgery*. 31(1), pp 73-7.

Chang, D.J., Ji, C., Kim, K.K. et al., 1998. Reduction in transforming growth factor beta receptor I expression and transcription factors Cbfa1 on bone cells by glucocorticoid. *Journal of Biological Chemistry*. 273(9), pp 4892-6.

Chao, E.Y., Fuchs, B., Rowland, C.M. et al., 2004. Long-term results of segmental prosthesis fixation by extracortical bone-bridging and ingrowth. *Journal of Bone and Joint Surgery (Am)*. 86-A(5), pp 948-55.

Chao, E.Y. and Sim, F.H. 1985. Modular prosthetic system for segmental bone and joint replacements after tumor resection. *Orthopaedics*. 8(5), pp 641-51.

Chaudhary, L.R., Hofmeister, A.M. and Hruska, K.A. 2004. Differential growth factor control of bone formation through osteoprogenitor differentiation. *Bone* 34(3), pp 402-11.

Cheng, S.L., Zhang, S.F. and Avioli, L.V. 1996. Expression of bone matrix proteins during dexamethasone-induced mineralization of human bone marrow stromal cells. *Journal of Cellular Biochemistry*. 61(2), pp 182-93.

Coathup, M.J., Cobb, J.P., Walker, P.S. et al., 2000. Plate fixation of prostheses after segmental resection for bone tumours. *Journal of Orthopaedic Research*. 18(6), pp 865-72.

- Coathup, M.J., Blunn, G.W., Flynn, N. et al., 2001. A comparison of bone remodelling around hydroxyapatite-coated, porous-coated, and grit-blasted hip replacements retrieved at post-mortem. *Journal of Bone and Joint Surgery (Br)*. 83(1), pp 118-23.
- Coathup, M.J., Blackburn, J., Goodship, A.E. et al., 2005. Role of hydroxyapatite coating in resisting wear particle migration and osteolysis around acetabular components. *Biomaterials*. 26(19), pp 4161-9.
- Cobb, J.P. 2002. Distal femoral limb salvage 10 years on. *Clinical Orthopaedics and Related Research*. 405, pp 207-215.
- Cobb, J.P., Ashwood, N., Robbins, G. et al., 2005. Triplate fixation: a new technique in limb-salvage surgery. *Journal of Bone and Joint Surgery (Br)*. 87(4), pp 534-9.
- Cohen, M., Bahoric, A. and Clarke, H.M. 2001. Aerosolization of epidermal cells with fibrin glue for the epithelialization of porcine wounds with unfavourable topography. *Plastic and Reconstructive Surgery*. 107(5), pp 1208-15.
- Corbett, S.A., Hukkanen, M., Batten, J. et al., 1999. Nitric oxide in fracture repair. Differential localisation, expression and activity of nitric oxide synthases. *Journal of Bone and Joint Surgery (Br)*. 81(3), pp 531-7.
- Cottle, T.E., Fier, C.J., Donadieu, J. et al., 2002. Risk and benefit of treatment of severe chronic neutropenia with granulocyte-colony stimulating factor. *Seminars in Hematology*. 39(2), pp 134-40.
- Cottler-Fox M.H., Lapidot, T., Petit, I. et al., 2003. Stem Cell Mobilization. *American Society of Hematology. Education Program*, pp 419-37.
- Cox, S., Cole, M. and Tawil, B. 2004. Behavior of human dermal fibroblasts in three-dimensional fibrin clots: dependence on fibrinogen and thrombin concentration. *Tissue Engineering*. 10(5-6), pp 942-54.

- Currie, L.J., Martin, R., Sharpe, J.R. et al., 2003. A comparison of keratinocyte cell sprays with and without fibrin glue. *Burns*. 29(7), pp 677-85.
- Dahir, G.A., Cui, Q., Anderson, P., Simon, C., Joyner, C., Triffitt, J.T. and Balian, G. 2000. Pluripotential mesenchymal cells repopulate bone marrow and retain osteogenic properties. *Clinical Orthopaedics and Related Research*. 379S, pp S134-145.
- D'Antonio, J.A., Capello, W.N. and Jaffe W.L. 1992. Hydroxyapatite-coated hip implants. Multicenter three-year clinical and roetgenographic results. *Clinical Orthopaedics and Related Research*. 285, pp 102-15.
- Datta, N., Pham, Q.P., Sharma, U. et al., 2006. In vitro generated extracellular matrix and fluid shear stress synergistically enhance 3D osteoblastic differentiation. *Proceedings of the National Academy of Sciences USA*. 103(8), pp 2488-93.
- Davani, S., Marandin, A., Mersin, N. et al., 2003. Mesenchymal progenitor cells differentiate into an endothelial phenotype, enhance vascular density, and improve heart function in a rat cellular cardiomyoplasty model. *Circulation*. 108 (Suppl. 1), pp II253-8.
- Davidson, B.R., Burnett, S., Javed, M.S. et al., 2000. Experimental study of a novel fibrin sealant for achieving haemostasis following partial hepatectomy. *British Journal of Surgery*. 87(6), pp 790-5.
- De Kok, I.J., Peter, S.J., Archambault, M. et al., 2003. Investigation of allogeneic mesenchymal stem cell-based alveolar bone formation: preliminary findings. *Clinical Oral Implants Research*. 14(4), pp 481-9.
- Declercq, H.A., Verbeeck, R.M., De Ridder, L.I. et al., 2005. Calcification as an indicator of osteoinductive capacity of biomaterials in osteoblastic cell cultures. *Biomaterials*. 26(24), pp 4964-74.
- DeGowin, R.L. and Gibson, D.P. 1981. Prostaglandin-mediated enhancement of erythroid colonies by marrow stromal cells (MSC). *Experimental Hematology*. 9(3), pp 274-80.

Dennis, J.E. and Charbord, P. 2002. Origin and differentiation of human and murine stroma. *Stem Cells*. 20(3), pp 205-14.

Department of Health. 2006. *Department of health* [online]. London: Department of Health. Available from: <http://www.dh.gov.uk> [Accessed 17 May 2006]

Desmeules, S., Bergeron, M.J., and Isenring, P. 2003. Acute phosphate nephropathy and renal failure. *The New England Journal of Medicine*. 349(10), pp 1006-7.

Devine, S.M., Bartholomew, A.M., Mahmud, N. et al., 2001a. Mesenchymal stem cells are capable of homing to the bone marrow of non-human primates following system infusion. *Experimental Hematology*. 29(2), pp 244-55.

Devine, S.M., Peter, S., Martin, B.J. et al., 2001b. Mesenchymal stem cells: stealth and suppression. 2001. *The Cancer Journal*. 7 (Suppl. 2), pp S76-82.

Di Martino, A., Sittenger, M. and Risbud, M.V. 2005. Chitosan: a versatile biopolymer for orthopaedic tissue-engineering. *Biomaterials*. 26(30), pp 5983-90.

Diefenderfer, D.L., Osyczka, A.M., Garino, J.P. et al., 2003. Regulation of BMP-induced transcription in cultured human bone marrow stromal cells. *Journal of Bone and Joint Surgery (Am)*. 85-A (Suppl 3.), pp 19-28.

Dimitriou, R., Dahabreh, Z., Katsoulis, E. et al., 2005. Application of recombinant BMP-7 on persistent upper and lower limb non-unions. *Injury*. 36 (Suppl. 4), pp S51-9.

Dixon, T., Shaw, M., Ebrahim, S. et al., 2004. Trends in hip and knee joint replacement: socioeconomic inequalities and projections of need. *Annals of the Rheumatic Diseases*. 63(7), pp 825-30.

Djouad, F., Bony, C., Haupl, T. et al., 2005. Transcriptional profiles discriminate bone marrow-derived and synovium-derived mesenchymal stem cells. *Arthritis Research & Therapy*. 7(6), pp R1304-15.

- Djouad, F., Plence, P., Bony, C. et al., 2003. Immunosuppressive effect of mesenchymal stem cells favors tumor growth in allogeneic animals. 2003. *Blood*. 102(10), pp 3837-44.
- Dobbs, H.S. and Scales, J.T., 1983. Behaviour of commercially pure titanium and Ti-318 (Ti-6Al-4V) in orthopaedic implants. In: *Titanium alloys in surgical implants*, eds. Luckey, H.A. and Kubli, F. American Society for Testing and Materials, pp 173-86.
- Dressler, M.R., Butler, D.L. and Boivin, G.P. 2005. Effects of age on the repair ability of mesenchymal stem cells in rabbit tendon. *Journal of Orthopaedic Research*. 23(2), pp 287-93.
- Eckardt, J.J., Eilber F.R., Rosen, G. et al., 1991. Endoprosthetic replacement for stage IIB osteosarcoma. 1991. *Clinical Orthopaedics and Related Research*. 270, pp 202-13.
- Eckardt, J.J., Matthews, J.G. 2nd and Eilber, F.R. 1991. Endoprosthetic reconstruction after bone tumor resections of the proximal tibia. *The Orthopaedic Clinics of North America*. 22(1), pp 149-60.
- Edwards, P.C., Ruggiero, S., Fantasia, J. et al., 2005. Sonic hedgehog gene-enhanced tissue engineering for bone regeneration. *Gene Therapy*. 12(1), pp 75-86.
- EMS Catalogue. 2007. Thermanox Coverslips, #72274.
- Engstrom, A. and Zetterstrom, R. 1951. Studies on the ultrastructure of bone. *Experimental Cell Research*. 2, pp 268-74.
- International Union of Biochemistry and Molecular Biology. 1992. *Enzyme Nomenclature 1992*. San Diego, CA: Academic Press.
- Evans, M.J., and Kaufman, M.H. 1981. Establishment in culture of pluripotential cells from mouse embryos. *Nature*. 292(5819), pp 154-6.
- Exner, T., Burridge, J., Power, P. et al., 1979. An evaluation of currently available methods for plasma fibrinogen. *American Journal of Clinical Pathology*. 71(5), pp 521-7.

- Fernandez, M., Simon, V., Herrera, G. et al., 1997. Detection of stromal cells in peripheral blood progenitor cell collections from breast cancer patients. *Bone Marrow Transplant.* 20(4), pp 265-71.
- Ferrara, N. and Davis-Smyth, T. 1997. The biology of vascular endothelial growth factor. *Endocrine Reviews.* 18(1), pp 4-25.
- Ferrari, A., Hannouche, D., Oudina, K. et al., 2001. In vivo tracking of bone marrow fibroblasts with fluorescent carbocyanine dye. *Journal of Biomedical Materials Research.* 56(3), pp 361-7.
- Fields, R.D. and Lancaster, M.V. 1993. Dual-attribute continuous monitoring of cell proliferation/cytotoxicity. *American Biotechnology Laboratory.* 11(4), pp 48-50.
- Fischmeister, G. and Gadner, H. 2000. Granulocyte-colony stimulating factor versus granulocyte-macrophage colony-stimulating factor for collection of peripheral blood progenitor cells from healthy donors. *Current Opinion in Hematology.* 7(3), pp 150-5.
- Frangioni, J.V. and Hajjar, R.J. 2004. In vivo tracking of stem cells for clinical trials in cardiovascular disease. *Circulation.* 110(21), pp 3378-83.
- Friedenstein, A.J., Petrakova, K.V., Kurolesova, A.I. et al., 1968. Heterotopic transplants of bone marrow. Analysis of precursor cells for osteogenic and hematopoietic tissues. *Transplantation* 6(2), pp 230-47.
- Friedenstein, A.J., Chailakhjan, R.K. and Lalykina, K.S. 1970. The development of fibroblast colonies in monolayer cultures of guinea-pig bone marrow and spleen cells. *Cell & Tissue Kinetics.* 3(4), pp 393-403.
- Friedenstein, A.J., Gorskaja, J.F. and Kulagina, N.N. 1976. Fibroblast precursors in normal and irradiated mouse hematopoietic organs. *Experimental Hematology.* 4(5), pp 267-74.

- Friedlaender, G.E., Perry C.R., Cole, J.D. et al., 2001. Osteogenic protein-1 (bone morphogenetic protein -7) in the treatment of tibial non-unions. *Journal of Bone and Joint Surgery (Am)*. 83-A Supp 1(2), pp S151-8.
- Friedman, M.S., Long, M.W. and Hankenson, K.D. 2006. Osteogenic differentiation of human mesenchymal stem cells is regulated by bone morphogenetic protein-6. *Journal of Cellular Biochemistry*. 98(3), pp 538-54.
- Frosch, K.H., Drengk, A., Krause, P. et al., 2006. Stem cell-coated titanium implants for the partial joint resurfacing of the knee. *Biomaterials*. 27(12), pp 2542-9.
- Furumatsu, T., Shen Z.N., Kawai, A. et al., 2003. Vascular endothelial growth factor principally acts as the main angiogenic factor in the early stage of human osteoblastogenesis. *The Journal of Biochemistry (Tokyo)*. 133(5), pp 633-9.
- Gailit, J., Clarke, C., Newman, D. et al., 1997. Human fibroblasts bind directly to fibrinogen at RGD sites through integrin $\alpha(v)\beta3$. *Experimental Cell Research*. 232(1), pp 118-26.
- Gangji, V., Hauzeur, J.P., Matos, C., et al., 2004. Treatment of osteonecrosis of the femoral head with implantation of autologous bone-marrow cells. A pilot study. *Journal of Bone and Joint Surgery (Am)*. 86-A(6), pp 1153-60.
- Gavrieli, Y., Sherman, Y. and Ben-Sasson, S.A. 1992. Identification of programmed cell death in situ via specific labelling of nuclear DNA fragmentation. *The Journal of Cell Biology*. 119(3), pp 493-501.
- Gebhardt, M.C., Flugstad, D.I., Springfield, D.S. et al., 1991. The use of bone allografts for limb salvage in high-grade extremity osteosarcoma. *Clinical Orthopaedics and Related Research*. 270, pp 181-96.
- Geesink, R.G., de Groot, K. and Klein, C.P. 1988. Bonding of bone to apatite-coated implants. *Journal of Bone and Joint Surgery (Br)*. 70(1), pp 17-22.

- Geesink, R.G. and Hoefnagels, N.H. 1995. Six-year results of hydroxyapatite-coated total hip replacement. *Journal of Bone and Joint Surgery (Br)*. 77-B(4), pp 534-47.
- Geesink, R.G. 1993. Clinical, radiological and human histological experience with hydroxyapatite coatings in orthopaedic surgery. *Acta Orthopaedica Belgica*. 59 (Suppl. 1), pp 160-4.
- Geiger, F., Bertram, H., Berger, I. et al., 2005. Vascular endothelial growth factor gene-activated matrix (VEGF165-GAM) enhances osteogenesis and angiogenesis in large segmental bone defects. *The Journal of Bone and Mineral Research*. 20(11), pp 2028-35.
- Genant, H.K. 1998. Current state of bone densitometry for osteoporosis. *Radiographics*. 18(4), pp 913-8.
- Giardino, R., Aldini, N.N., Fini, M. et al., 2002. Enhanced guided bone regeneration with a resorbable chamber containing demineralised bone matrix. *The Journal of Trauma: Injury, Infection, and Critical Care*. 52(5), pp 933-7.
- Gorustovich, A., Rosenbusch, M., Guglielmotti, M.B. Characterization of bone around titanium implants and bioactive glass particles: an experimental study in rats. 2002. *The International Journal of Oral and Maxillofacial Implants*. 17(5), pp 644-50.
- Gotz, H.E., Muller, M., Emmel, A. et al., 2004. Effect of surface finish on the osseointegration of laser-treated titanium alloy implants. *Biomaterials*. 25(18), pp 4057-64.
- Grant, I., Warwick, K., Marshall, J. et al., 2002. The co-application of sprayed cultured autologous keratinocytes and autologous fibrin sealant in a porcine wound model. *British Journal of Plastic Surgery*. 55(3), pp 219-27.
- Greco, F., de Palma, L., Specchia, N. et al., 1988. Experimental investigations into reparative osteogenesis with fibrin adhesive. *Archives of Orthopaedic and Trauma Surgery*. 107(2), pp 99-104.

- Grigoriadis, A.E., Heersche, J.N. and Aubin, J.E. 1988. Differentiation of muscle, fat, cartilage, and bone from progenitor cells present in a bone-derived clonal cell population: effect of dexamethasone. *The Journal of Cell Biology*. 106(6), pp 2139-51.
- Grimer, R.J., Carter, S.R. and Sneath, R.S. 1991. Endoprosthetic replacements of the proximal tibia. In: *Limb Salvage – Major Reconstructions in Oncologic and Nontumoral Conditions*, eds. Langlais, F. and Tomeno, B. Springer-Verlag, Berlin, 1991, pp 285-292.
- Grimer, R.J., Carter S.R., Tillman, R.M. et al., 1999. Endoprosthetic replacement of the proximal tibia. *Journal of Bone and Joint Surgery (Br)*. 81(3), pp 488-94.
- Gronthos, S., Graves S.E., Ohta, S. et al., 1994. The STRO-1+ fraction of bone marrow contains the osteogenic precursors. 1994. *Blood*. 84(12), pp 4164-73.
- Gronthos, S. 2003. Molecular and cellular characterisation of highly purified stromal cells derived from human bone marrow. *Journal of Cell Science*. 116(Pt 9), pp 1827-35.
- Gu, Y., Zhang, J. and Qi, L. 2006. Effective autologous bone marrow stem cell dosage for treatment of severe lower limb ischemia. Chinese. *Zhongguo Xiu Fu Chong Jian Wai Ke Za Zhi*. 20(5), pp 504-6.
- Gurevich, O., Vexler A., Marx, G. et al., 2002. Fibrin microbeads for isolating and growing bone marrow-derived progenitor cells capable of forming bone tissue. *Tissue Engineering*. 8(4), pp 661-72.
- Hamilton, D.W., Maul, T.M. and Vorp, D.A. 2004. Characterization of the response of bone marrow-derived progenitor cells to cyclic strain: implications for vascular tissue-engineering applications. *Tissue Engineering*. 10(3-4), pp 361-9.
- Han, C.I., Campbell, G.R. and Campbell, J.H. 2001. Circulating bone marrow cells can contribute to neointimal formation. *Journal of Vascular Research*. 38(2), pp 113-9.

Han, D.K., Kim, C.S., Jung, U.W. et al., 2005. Effect of a fibrin-fibronectin sealing system as a carrier for recombinant human bone morphogenetic protein-4 on bone formation in rat calvarial defects. *Journal of Periodontology*. 76(12), pp 2216-22.

Harris, I.E., Leff, A.R., Gitelis, S. et al., 1990. Function after amputation, arthrodesis, or arthroplasty for tumors about the knee. *The Journal of Bone and Joint Surgery*. 72(10), pp 1477-85.

Hayflick, L. 1965. The limited in vitro lifetime of human diploid cell strains. *Experimental Cell Research*. 37, pp 614-36.

Haynesworth, S.E., Goshima, J., Goldberg, V.M. et al., 1992. Characterization of cells with osteogenic potential from human marrow. *Bone*. 13(1), pp 81-8.

Heins, N., Englund, M.C., Sjoblom, C. et al., 2004. Derivation, characterization, and differentiation of human embryonic stem cells. *Stem Cells*. 22(3), pp 367-76.

Heng, B.C., Liu, H. and Cao, T. 2005. Utilising human embryonic stem cells as “catalysts” for biological repair and regeneration. Challenges and some possible strategies. *Clinical and Experimental Medicine*. 5(1), pp 37-9.

Hishikawa, K., Miura, S., Marumo, T. et al., 2004. Gene expression profile of human mesenchymal stem cells during osteogenesis in three-dimensional thermoreversible gelation polymer. 2004. *Biochemical and Biophysical Research Communications*. 317(4), pp 1103-7.

Hofmann, S., Knecht, S., Langer, R. et al., 2006. Cartilage-like tissue engineering using silk scaffolds and mesenchymal stem cells. *Tissue Engineering*. 12(10), pp 2729-38.

Hojo, M., Inokuchi, S., Kidokoro, M. et al., 2003. Induction of vascular endothelial growth factor by fibrin as a dermal substrate for cultured skin substitute. *Plastic and Reconstructive Surgery*. 111(5), pp 1638-45.

- Hong, S.J., Kim, C.S., Han, D.K. et al., 2006. The effect of a fibrin-fibronectin/beta-tricalcium phosphate/recombinant human bone morphogenetic protein-2 system on bone formation in rat calvarial defects. *Biomaterials*. 27(20), pp 3810-6.
- Horowitz, S.M., Glasser D.B., Lane, J.M. et al., 1993. Prosthetic and extremity survivorship after limb salvage for sarcoma. How long do the reconstructions last? *Clinical Orthopaedics and Related Research*. 293, pp 280-6.
- Horwitz, E.M., Prockop, D.J., Fitzpatrick, L.A. et al., 1999. Transplantability and therapeutic effects of bone marrow-derived mesenchymal stem cells in children with *osteogenesis imperfecta*. *Nature Medicine*. 5(3), pp 309-13.
- Hua, J. and Walker, P.S. 1992. A comparison of cortical strain after cemented and press-fit proximal and distal femoral replacement. *Journal of Orthopaedic Research*. 10(5), pp 739-44.
- Huang, Y.C., Kaigler, D., Rice, K.G. et al., 2005. Combined angiogenic and osteogenic factor delivery enhances bone marrow stromal cell-driven bone regeneration. *The Journal of Bone and Mineral Research*. 20(5), pp 848-57.
- Hubbell, J.A. 2000. Matrix effects. In: *Principles of Tissue Engineering, 2nd Edition*, eds. Lanza, R.P., Langer, R. and Vacanti, J. London, UK: Academic Press, 2000, pp 237-246.
- Huiskes, R. 1990. The various stress patterns of press-fit, ingrown, and cemented femoral stems. *Clinical Orthopaedics and Related Research*. 261, pp 27-38.
- Igarashi, M., Kamiya, N., Hasegawa, M. et al., 2004. Inductive effect of dexamethasone on the gene expression of cbfa1, osterix, and bone matrix proteins during differentiation of cultured primary rat osteoblasts. *Journal of Molecular Histology*. 35(1), pp 3-10.
- Ignatius, A., Blessing, H., Liedert, A. et al., 2005. Tissue engineering of bone: effects of mechanical strain on osteoblastic cells in type I collagen matrices. *Biomaterials*. 26(3), pp 311-8.

- Inglis, A.E., and Walker, P.S. (1989) Long-term radiographic evaluation of massive proximal femoral replacements. In: *Limb Salvage-Major Reconstructions in Oncologic and Nontumoral Conditions*. eds. Langlais, F. and Tomeno, B. Berlin: Springer-Verlag, 1991, pp 257-262.
- Jaiswal, N., Haynesworth, S.E., Caplan, A.I. et al., 1997. Osteogenic differentiation of purified, culture-expanded human mesenchymal stem cells in vitro. *Journal of Cellular Biochemistry*. 64(2), pp 295-312.
- Jaiswal, R.K., Jaiswal, N., Bruder, S.P., et al., 2000. Adult human mesenchymal stem cell differentiation to the osteogenic or adipogenic lineage is regulated by mitogen-activated protein kinase. *Journal of Biological Chemistry*. 275(13), pp 9645-52.
- Janssen, F.W., Oostra, J., Oorschot, A. et al., 2006. A perfusion bioreactor system capable of producing clinically relevant volumes of tissue-engineered bone: in vivo bone formation showing proof of concept. *Biomaterials*. 27(3), pp 315-23.
- Jarcho, M. 1981. Calcium phosphate ceramics as hard tissue prosthetics. *Clinical Orthopaedics and Related Research*. 157, pp 259-78.
- Jasty, M., Bragdon, C., Burke, D. et al., 1997. In vivo skeletal responses to porous-surfaced implants subjected to small induced motions. *Journal of Bone and Joint Surgery (Am)*. 79(5), pp 707-14.
- Jewell, J.H. and Bush, L.F. 1964. "Benign" giant-cell tumor of bone with a solitary pulmonary metastasis. A case report. *Journal of Bone and Joint Surgery (Am)*. 46, pp 848-52.
- Johnstone, B., Hering, T.M., Caplan, A.I. et al., 1998. In vitro chondrogenesis of bone marrow-derived mesenchymal progenitor cells. *Experimental Cell Research*. 238(1), pp 265-72.

Jiang, Y., Vaessen, B., Lenvik, T. et al., 2002. Multipotent progenitor cells can be isolated from postnatal murine bone marrow, muscle, and brain. *Experimental Haematology*. 30, pp 896-904.

Jiang, Y., Jahagirdar, B.N., Reinhardt, R.L. et al., 2002. Pluripotency of mesenchymal stem cells derived from adult marrow. *Nature*. 418, pp 41-9.

Jiang, Y., Jahagirdar, B.N., Reinhardt et al., 2007. Corrigendum – Pluripotency of mesenchymal stem cells derived from adult marrow. *Nature*. 447, pp 879-80.

Joyner, C.J., Bennett, A., and Triffitt, J.T. 1997. Identification and enrichment of human osteoprogenitor cells by using differentiation stage-specific monoclonal antibodies. *Bone*. 21(1), pp 1-6.

Kadiyala, S., Young, R.G., Thiede, M.A. et al., 1997. Culture expanded canine mesenchymal stem cells possess osteochondrogenic potential in vivo and in vitro. *Cell Transplant*. 6(2), pp 125-34.

Kalia, P., Blunn G.W., Miller, J. et al., 2006. Do autologous mesenchymal stem cells augment bone growth and contact to massive bone tumor implants? *Tissue Engineering*. 12(6), pp 1617-26.

Kang, Q., Sun, M.H., Cheng, H. et al., 2004. Characterization of the distinct orthotopic bone-forming activity of 14 BMPs using recombinant adenovirus-mediated gene delivery. *Gene Therapy*. 11(17), pp 1312-20.

Kang, X.Q., Zang W.J., Song, T.S. et al., 2005. Rat bone marrow mesenchymal stem cells differentiate into hepatocytes in vitro. *World Journal of Gastroenterology*. 11(22), pp 3479-84.

Kania, R.E., Meunier, A., Hamadouche, M. et al., 1998. Addition of fibrin sealant to ceramic promotes bone repair: long-term study in rabbit femoral defect model. *Journal of Biomedical Materials Research*. 43(1), pp 38-45.

- Karageorgiou, V. and Kaplan, D. 2005. Porosity of 3D biomaterial scaffolds and osteogenesis. *Biomaterials*. 26, pp 5474-91.
- Kassis, I., Zangi, L., Rivkin, R. et al., 2006. Isolation of mesenchymal stem cells from G-CSF-mobilized human peripheral blood using fibrin microbeads. *Bone Marrow Transplant* 37(10), pp 967-76.
- Kauth, H. and Kapperich, C. 2005. Examination of the dynamic mechanical properties of tissue engineering scaffold. *Materials Research Society Symposium Proceedings*. 844, pp Y1.2.1-Y1.2.6.
- Kavanagh, B.F., Ilstrup, D.M. and Fitzgerald, R.H. Jr. 1985. Revision total hip arthroplasty. *Journal of Bone and Joint Surgery (Am)*. 67(4), pp 517-26.
- Kenan, S., Jones, C. and Lewis, M.M. 1987. Limb-sparing reconstructive surgery in malignant and aggressive benign bone tumours of the extremities. *Surgical Rounds For Orthopaedics*. August, pp 25-36.
- Kern, S., Eichler, H., Stoeve, J. et al., 2006. Comparative analysis of mesenchymal stem cells from bone marrow, umbilical cord blood, or adipose tissue. *Stem Cells*. 24(5), pp 1294-301.
- Khosla, S. and Eghbali-Fatourehchi, G.Z. 2006. Circulating cells with osteogenic potential. *Annals of New York Academy of Sciences*. 1068, pp 489-97.
- Kilpadi, KL, Chang PL, Bellis SL. Hydroxyapatite binds more serum proteins, purified integrins, and osteoblast precursor cells than titanium or steel. 2001. *Journal of Biomedical Materials Research*. 57(2), pp 258-67.
- Kim, C.H., Cheng, S.L. and Kim, G.S. 1999. Effects of dexamethasone on proliferation, activity, and cytokine secretion of normal human bone marrow stromal cells: possible mechanisms of glucocorticoid-induced bone loss. 1999. *Journal of Endocrinology*. 162(3), pp 371-9.

King, V.R., Phillips, J.B., Hunt-Grubbe, H. et al., 2006. Characterization of non-neuronal elements within fibronectin mats implanted into the damaged adult rat spinal cord. *Biomaterials*. 27(3), pp 485-96.

Knapp, D.M., Helou, E.F. and Tranquillo, R.T. 1999. A fibrin or collagen gel assay for tissue cell chemotaxis: assessment of fibroblast chemotaxis to GRGDSP. *Experimental Cell Research*. 247(2), pp 543-53.

Knox, P., Crooks, S. and Rimmer, C.S. 1986. Role of fibronectin in the migration of fibroblasts into plasma clots. *The Journal of Cell Biology*. 102(6), pp 2318-23.

Koc, O.N., Gerson, S.L., Cooper, B.W. et al., 2000. Rapid haematopoietic recovery after coinfusion of autologous-blood stem cells and culture-expanded marrow mesenchymal stem cells in advanced breast cancer patients receiving high-dose chemotherapy. *Journal of Clinical Oncology*. 18(2), pp 307-16.

Kodama, M., Naito, M., Nomura, H. et al., 2002. Role of D and E domains in the migration of vascular smooth muscle cells into fibrin gels. *Life Sciences*. 71(10), pp 1139-48.

Kon, E., Muraglia, A., Corsi, A. et al., 2000. Autologous bone marrow stromal cells loaded onto porous hydroxyapatite ceramic accelerate bone repair in critical-size defects of sheep long bones. *Journal of Biomedical Materials Research*. 49(3), pp 328-37.

Kondo, T., Johnson, S.A., Yoder, M.C. et al., 2005. Sonic hedgehog and retinoic acid synergistically promote sensory fate specification from bone marrow-derived pluripotent stem cells. *Proceedings of the National Academy of Sciences USA*. 102, pp 4789-94.

Korda, M., Blunn, G., Phipps, K. et al., 2006. Can mesenchymal stem cells survive under normal impaction force in revision total hip replacements? *Tissue Engineering*. 12(3), pp 625-30.

- Kostura, L., Kraitchman, D.L., Mackay, A.M. et al., 2004. Feridex labelling of mesenchymal stem cells inhibits chondrogenesis but not adipogenesis or osteogenesis. *NMR in Biomedicine*. 17(7), pp 513-517.
- Kreke, M.R. and Goldstein, A.S. 2004. Hydrodynamic shear stimulates osteocalcin expression but not proliferation of bone marrow stromal cells. *Tissue Engineering*. 10(5-6), pp 780-8.
- Krishnamurthy, A.B., MacDonald, S.J. and Paprosky, W.G. 1997. 5-to 13-year follow-up study on cementless femoral components in revision surgery. *The Journal of Arthroplasty*. 12(8), pp 839-47.
- Krishnan, V., Moore, T.L., Ma, Y.L. et al., 2003. Parathyroid hormone bone anabolic action requires Cbfa/Runx2-dependent signalling. *Molecular Endocrinology*. 17(3), pp 423-35.
- Kronenwett, R., Martin, S. and Haas, R. 2000. The role of cytokines and adhesion molecules for mobilization of peripheral blood stem cells. *Stem Cells*. 18(5), pp 320-30.
- Kruyt, M.C., de Bruijn J.D., Wilson, C.E. et al., 2003. Viable osteogenic cells are obligatory for tissue-engineered ectopic bone formation in goats. *Tissue Engineering*. 9(2), pp 327-36.
- Kruyt, M.C., de Bruijn, J.D., Yuan, H. et al, 2004. Optimization of bone tissue engineering in goats: a peroperative seeding method using cryopreserved cells and localized bone formation in calcium phosphate scaffolds. *Transplantation*. 77(3), pp 359-65.
- Kucia, M., Ratajczak, J., Reza, R. et al., 2004. Tissue-specific muscle, neural and liver stem/progenitor cells reside in the bone marrow, respond to an SDF-1 gradient and are mobilized into peripheral blood during stress and tissue injury. *Blood Cells, Molecules and Diseases*. 32(1), pp 52-7.
- Kumar, U. and Albala, D.M. 2001. Fibrin glue applications in urology. *Current Urology Reports*. 2(1), pp 79-82.

- Kuboki, Y., Jin, Q. and Takita, H. Geometry of carriers controlling phenotypic expression in BMP-induced osteogenesis and chondrogenesis. *Journal of Bone and Joint Surgery (Am)*. 83-A (supplement 1 part 2), pp S105-15.
- Kurioka, K., Umeda, M., Teranobu, O. et al., 1999. Effect of various properties of hydroxyapatite ceramics on osteoconduction and stability. *Kobe Journal of Medical Sciences*. 45(3-4), pp 149-63.
- Kurtz, S., Mowat, F., Ong, K. et al., 2005. Prevalence of primary and revision total hip and knee arthroplasty in the United States from 1990 through 2002. *Journal of Bone and Joint Surgery (Am)*. 87(7), pp 1487-97.
- Kuznetsov, S.A., Mankani, M.H., Gronthos, S. et al., 2001. Circulating skeletal stem cells. *The Journal of Cell Biology*. 153(5), pp 1133-40.
- Lam, A.C., Li, K., Zhang, X.B. et al., 2001. Preclinical ex vivo expansion of cord blood hematopoietic stem and progenitor cells: duration of culture; the media, serum supplements, and growth factors used; and engraftment in NOD/SCID mice. *Transfusion*. 41(12), pp 1567-76.
- Lange, C., Bassler, P., Lioznov, M.V. et al., 2005. Liver-specific gene expression in mesenchymal stem cells is induced by liver cells. *World Journal of Gastroenterology*. 11(29), pp 4497-4504.
- Lapidot, T. and Petit, I. 2002. Current understanding of stem cell mobilization: the roles of chemokines, proteolytic enzymes, adhesion molecules, cytokines, and stromal cells. *Experimental Hematology*. 30(9), pp 973-81.
- Lazarus, H.M., Haynesworth, S.E., Gerson, S.L. et al., 1997. Human bone marrow-derived mesenchymal (stromal) progenitor cells (MPCs) cannot be recovered from peripheral blood progenitor cell collections. *Journal of Hematotherapy*. 6(5), pp 447-55.

- Lazarus, H.M., Koc, O.N., Devine, S.M. et al., 2005. Cotransplantation of HLA-identical sibling culture-expanded mesenchymal stem cells and hematopoietic stem cells in hematologic malignancy patients. *Biology of Blood and Marrow Transplantation*. 11(5), pp 389-98.
- Le Blanc, K., Tammik, C., Rosendahl, K. et al., 2003a. HLA expression and immunologic properties of differentiated and undifferentiated mesenchymal stem cells. *Experimental Hematology*. 31(10), pp 890-6.
- Le Blanc, K., Tammik, L., Sundberg, B. et al, 2003b. Mesenchymal stem cells inhibit and stimulate mixed lymphocyte cultures and mitogenic responses independently of the major histocompatibility complex. *Scandinavian Journal of Immunology*. 57(1), pp 11-20.
- Le Blanc, K. and Pittenger, M. 2005. Mesenchymal stem cells: progress towards promise. *Cytotherapy*. 7(1), pp 36-45.
- Lee, D.A., Assoku, E. and Doyle, V. 1998. A specific quantitative assay for collagen synthesis by cells seeded in collagen-based biomaterials using Sirius Red F3B precipitation. *Journal of Materials Science: Materials in Medicine*. 9(1), pp 47-51.
- Lee, H.J., Choi, B.H., Min, B.H. et al., 2006. Low-intensity ultrasound stimulation enhances chondrogenic differentiation in alginate culture of mesenchymal stem cells. *The International Journal of Artificial Organs*. 30(9), pp 707-15.
- Lee, K.D., Kuo, T.K., Whang-Peng, J. et al., 2004. In vitro hepatic differentiation of human mesenchymal stem cells. *Hepatology*. 40(6), pp 1275-84.
- Lee, K.S., 2002. *Effects of chemotherapy on bone and bone regeneration using tissue engineering techniques*. Phd. University of London.
- Lee, O.K., Kuo, T.K., Chen, W.M. et al., 2004. Isolation of multipotent mesenchymal stem cells from umbilical cord blood. *Blood*. 103(5), pp 1669-75.

- Lee, O.K., Coathup, M.J., Goodship, A.E. et al., 2005. Use of mesenchymal stem cells to facilitate bone regeneration in normal and chemotherapy-treated rats. *Tissue Engineering*. 11(11-12), pp 1727-35.
- Lee, S.T., Chu, K., Jung, K.H. et al., 2005. Granulocyte colony-stimulating factor enhances angiogenesis after focal cerebral ischemia. *Brain Research Reviews*. 1058(1-2), pp 120-128.
- Lennon, D.P., Haynesworth, S.E., Arm, D.M. et al., 2000. Dilution of human mesenchymal stem cells with dermal fibroblasts and the effects on in vitro and in vivo osteochondrogenesis. *Developmental Dynamics*. 219(1), pp 50-62.
- Levesque, J.P., Takamatsu, Y., Nilsson, S.K. et al., 2001. Vascular cell adhesion molecule-1 (CD106) is cleaved by neutrophil proteases in the bone marrow following hematopoietic progenitor cell mobilization by granulocyte colony-stimulating factor. *Blood*. 98(5), pp 1289-97.
- Levesque, J.P., Hendy, J., Takamatsu, Y. et al., 2003. Disruption of the CXCR4/CXCL12 chemotactic interaction during hematopoietic stem cell mobilization induced by GCSF or cyclophosphamide. *The Journal of Clinical Investigation*. 111(2), pp 187-96.
- Lewis, M.M., Kaplan, H., Klein, M.J. et al., 1985. Giant cell tumor of the proximal radius.. *Clinical Orthopaedics and Related Research*. 201, pp 186-9.
- Lieberman, J.R., Daluiski, A., Stevenson, S. et al., 1999. The effect of regional gene therapy with bone morphogenetic protein-2-producing bone-marrow cells on the repair of segmental femoral defects in rats. *Journal of Bone and Joint Surgery (Am)*. 81(7), pp 905-17.
- Liechty, K.W., MacKenzie, T.C., Shaaban, A.F. et al., 2000. Human mesenchymal stem cells engraft and demonstrate site-specific differentiation after in utero transplantation in sheep. *Nature Medicine*. 6(11), pp 1282-6.

Lin, C.Y., Schek, R.M., Mistry, A.S. et al., 2005. Functional bone engineering using ex vivo gene therapy and topology-optimized, biodegradable polymer composite scaffolds. *Tissue Engineering*. 11(9-10), pp 1589-98.

Lisignoli, G., Cristino, S., Piacentini, A. et al., 2006. Chondrogenic differentiation of murine and human mesenchymal stromal cells in a hyaluronic acid scaffold: differences in gene expression and cell morphology. *Journal of Biomedical Materials Research. A* 77(3), pp 497-506.

Molecular Probes. 2001. *LIVE/DEAD Viability/Cytotoxicity Kit Product Information*, Invitrogen Ltd., Paisley, UK.

Loewe, R. et al., 2006. Dimethylfumarate impairs melanoma growth and metastasis. *Cancer Research*. 66(24), pp 11888-1896.

Lopes, C.C., Dietrich, C.P. and Nader, H.B. 2006. Specific structural features of syndecans and heparan sulphate chains are needed for cell signalling. *Brazilian Journal of Medical Biology Research*. 39(2), pp 157-67.

Lucht, U., Bunker, C., Moller, J.T. et al., 1986. Fibrin sealant in bone transplantation. No effects on blood flow and bone formation in dogs. *Acta Orthopaedica Scandinavica*. 57(1), pp 19-24.

Mackay, A.M., Beck, S.C., Murphy, J.M. et al., 1998. Chondrogenic differentiation of cultured human mesenchymal stem cell from marrow. *Tissue Engineering*. 4(4), pp 415-28.

Majumdar, M.K., Thiede, M.A., Haynesworth, S.E. et al., 2000. Human marrow-derived mesenchymal stem cells (MSCs) express haematopoietic cytokines and support long-term haematopoiesis when differentiated toward stromal and osteogenic lineages. *Journal of Hematotherapy and Stem Cell Research*. 9(6), pp 841-8.

- Malawer, M.M. and Chou, L.B. 1995. Prosthetic survival and clinical results with use of large-segment replacements in the treatment of high-grade bone sarcomas. *Journal of Bone and Joint Surgery (Am)*. 77(8), pp 1154-65.
- Malchau, H., Garellick, G., Eisler, T. et al., 2005. Presidential guest address: the Swedish Hip Registry: increasing the sensitivity by patient outcome data. *Clinical Orthopaedics and Related Research*. 441, pp 19-29.
- Maniscalco, P., Gambera, D., Bertone, C. et al., 2002. Healing of fresh tibial fractures with OP-1. A preliminary report. *Acta Biomedica Ateneo Parmense*. 73(1-2), pp 27-33.
- Mansilla, E., Marin, G.H., Drago, H. et al., 2006. Bloodstream cells phenotypically identical to human mesenchymal bone marrow stem cells circulate in large amounts under the influence of acute large skin damage: new evidence for their use in regenerative medicine. *Transplantation Proceedings*. 38(3), pp 967-9.
- Marom, R., Shur, I., Solomon, R. et al., 2005. Characterization of adhesion and differentiation markers of osteogenic marrow stromal cells. *Journal of Cellular Physiology*. 202(1), pp 41-8.
- Martin, D.R., Cox, N.R., Hathcock, T.L. et al., 2002. Isolation and characterization of multipotent mesenchymal stem cells from feline bone marrow. *Experimental Hematology*. 30(8), pp 879-86.
- Martin, J. 2004. Metabolism and Toxicity of Inhaled Anesthetics. In *Miller's Anesthesia Vol I*, ed. Miller, R.D. Churchill Livingstone, pp 165-79.
- Martin, M., Van Hoof, V., Couttenye, M. et al., 1997. Analytical and clinical evaluation of a method to quantify bone alkaline phosphatase, a marker of osteoblastic activity. *Anticancer Research*. 17(4B), pp 3167-70.
- Martini, L., Fini, M., Giavaresi, G. et al., 2001. Sheep model in orthopaedic research: a literature review. 2001. *Comparative Medicine*. 51(4), pp 292-9.

Martins-Green, M. 2000. Dynamics of cell-ECM interactions. In *Principles of Tissue Engineering, 2nd Edition*, eds. RP Lanza, R Langer, and J Vacanti. London, UK: Academic Press, pp 33-57.

Marx, G. and Mou, X. 2002. Characterizing fibrin glue performance as modulated by heparin, aprotinin, and factor XIII. *Journal of Laboratory & Clinical Medicine*. 140(3), pp 152-60.

Mason, J.M., Breitbart, A.S., Barcia, M. et al., 2000. Cartilage and bone regeneration using gene-enhanced tissue engineering. *Clinical Orthopaedics and Related Research*. 379, pp S171-8.

Masuhara, K., Yoshikawa, R., Takaoka, K. et al., 1991. Monoclonal antibody against human bone alkaline phosphatase. *International Orthopaedics*. 15(1), pp 61-4.

Mauck, R.L., Yuan, X. and Tuan, R.S. 2006. Chondrogenic differentiation and functional maturation of bovine mesenchymal stem cells in long-term agarose culture. *Osteoarthritis Cartilage* 14(2), pp 179-89.

Maurer, H.R. 1981. Potential pitfalls of [3H]thymidine techniques to measure cell proliferation. *Cell & Tissue Kinetics*. 14(2), pp 111-20.

Medvinsky, A. and Smith, A. 2003. Stem cells: fusion brings down barriers. *Nature* 422(6934), pp 823-5.

Meinel, L., Fajardo, R., Hofmann, S. et al., 2005. Silk implants for the healing of critical size bone defects. *Bone*. 37(5), pp 688-98.

Meinhart, J.G., Schense, J.C., Schima, H. et al., 2005. Enhanced endothelial cell retention on shear-stressed synthetic vascular grafts precoated with RGD-cross-linked fibrin. *Tissue Engineering*. 11(5-6), pp 887-95.

Memon, I.A., Sawa, Y., Miyagawa, S. et al., 2005. Combined autologous cellular cardiomyoplasty with skeletal myoblasts and bone marrow cells in canine hearts for ischemic cardiomyopathy. *Journal of Thoracic and Cardiovascular Surgery*. 130(5), pp 1333-41.

Minamino, K., Adachi, Y., Okigaki, M. et al., 2005. Macrophage-colony stimulating factor (M-CSF), as well as granulocyte-colony stimulating factor (G-CSF), accelerates neovascularization. 2005. *Stem Cells*. 23(3), pp 347-54.

Misao, Y., Takemura, G., Arai, M. et al., 2006. Importance of recruitment of bone marrow-derived CXCR4⁺ cells in post-infarct cardiac repair mediated by G-CSF. *Cardiovascular Research*. 71(3), pp 455-65.

Mistry, A.S. and Mikos, A.G. 2005. Tissue engineering strategies for bone regeneration. *Advances in Biochemical Engineering Biotechnology*. 94, pp 1-22.

Mizutani, A., Fujita, S., Watanabe, K. et al., 1990. Experiments on antigenicity and osteogenicity in allotransplanted cancellous bone. *International Orthopaedics*. 14(3), pp 243-8.

Moore, M.A. 2002. Putting the neo into neoangiogenesis. *Journal of Clinical Investigations*. 109(3), pp 313-5.

Mori, K., Kitazawa, R., Kondo, T. et al., 2006. Modulation of mouse RANKL gene expression by Runx2 and PKA pathway. 2006. *Journal of Cellular Biochemistry*. 98(6), pp 1629-44.

Morris, H.G., Capanna, R., Del Ben, M. et al., 1995. Prosthetic reconstruction of the proximal femur after resection for bone tumors. *The Journal of Arthroplasty*. 10(3), pp 293-9.

Morris, M.L. 1969. The implantation of human dentin and cementum with autogenous bone and red marrow into the subcutaneous tissues of the rat. *Journal of Periodontology*. 40(5), pp 259-63.

- Mor-Vaknin, N., Punturieri, A., Sitwala, K. et al., 2003. Vimentin is secreted by activated macrophages. *Nature Cell Biology*. 5(1), pp 59-63.
- Moutsatsos, I.K., Turgeman, G., Zhou, S. et al., 2001. Exogenously regulated stem cell-mediated gene therapy for bone regeneration. *Molecular Therapy*. 3(4), pp 449-61.
- Muraglia, A., Cancedda, R. and Quarto, R. 2000. Clonal mesenchymal progenitors from human bone marrow differentiate in vitro according to a hierarchical model. *Journal of Cell Science*. 113, pp 1161-1166.
- Nagatomi, J., Arulanandam, B.P., Metzger, D.W. et al., 2003. Cyclic pressure affects osteoblast functions pertinent to osteogenesis. *Annals of Biomedical Engineering*. 31(8), pp 917-23.
- Nagaya, N., Kangawa, K., Itoh, T., et al., 2005. Transplantation of mesenchymal stem cells improves cardiac function in a rat model of dilated cardiomyopathy. *Circulation*. 112(8), pp 1128-35.
- Nakano, N., Adachi, Y., Minamino, K. et al., 2006. Mechanisms underlying acceleration of blood flow recovery in ischemic limbs by macrophage-colony stimulating factor. *Stem Cells*. 24(5), pp 1274-9.
- Nakayama, M., Gorai, I., Minaguchi, H. et al., 1998. Purification and characterization of bone-specific alkaline phosphatase from a human osteosarcoma cell line. *Calcified Tissue International*. 62(1), pp 67-72.
- Nayar, S., Sinha, M.K., Basu D. et al., 2006. Synthesis and sintering of biomimetic hydroxyapatite nanoparticles for biomedical applications. *Journal of Materials Science: Materials in Medicine*. 17(11), pp 1063-1068.
- Neuss, S., Becher, E., Eblenkamp, M. et al., 2004. Fibrinolytic capacity of human adult mesenchymal stem cells. 7th *World Biomaterials Congress, Sydney, Australia*, pp 379.

- Office of the Medical Director, Washington State Department of Labor and Industries. 2003. *Bone Morphogenetic Protein for the treatment of long bone fractures and for use in spinal fusion procedures*. Report. Olympia, WA, USA: Washington State Department pp 1-32.
- Okada, Y., Suka, T., Sim, F.H., et al., 1988. Comparison of replacement prostheses for segmental defects of bone. Different porous coatings for extracortical fixation. *Journal of Bone and Joint Surgery (Am)*. 70(2), pp 160-72.
- Okamoto, M., Dohi, Y., Ohgushi, H. et al., 2006. Influence of the porosity of hydroxyapatite ceramics on in vitro and in vivo bone formation by cultured rat bone marrow stromal cells. *Journal of Materials Science: Materials in Medicine*. 17(4), pp 327-36.
- Oonishi, H., Kushitani, S., Yasukawa, E. et al., 1997. Particulate bioglass compared with hydroxyapatite as a bone graft substitute. *Clinical Orthopaedics and Related Research*. 334, pp 316-25.
- Oreffo, R.O., Driessens, F.C., Planell, J.A. et al., 1998. Growth and differentiation of human bone marrow osteoprogenitors on novel calcium phosphate cements. *Biomaterials*. 19(20), pp 1845-54.
- Owen, M., Cavé, J., and Joyner, C.J. 1987. Clonal analysis *in vitro* of osteogenic differentiation of marrow CFU-F. *Journal of Cell Science*. 87, pp 731-8.
- Owen, M. and Friedenstein, A.J. 1988. Stromal stem cells: marrow-derived osteogenic precursors. *Ciba Foundation Symposium*. 136, pp 42-60.
- Ozawa, S. and Kasugai, S. 1996. Evaluation of implant materials (hydroxyapatite, glass-ceramics, titanium) in rat bone marrow stromal cell culture. *Biomaterials*. 17(1), pp 23-9.
- Pachence, J.M. and Kohn, J. 2000. Biodegradable polymers. In: *Principles of Tissue Engineering, 2nd Edition*, eds. Lanza, R.P., Langer, R. and Vacanti, J. London, UK: Academic Press, 2000, pp 263-274.

- Paget J. 1854. *Lectures On Surgical Pathology*. Royal College of Surgeons of England; Philadelphia, PA: Lindsay and Blakiston, 1854, pp 446.
- Park, J.B. 1995. Metallic Biomaterials. In: *The Biomedical Engineering Handbook*. ed. Bronzino, J.D. Boca Raton, FL: CRC Press, 1995, pp 537-551.
- Pearson, R.G., Bhandari, R., Quirk, R.A. et al., 2002. Recent advances in tissue engineering. *Journal of Long Term Effects of Medical Implants*. 12(1), pp 1-33.
- Peng, H., Usas, A., Olshanski, A. et al., 2005. VEGF improves, whereas sFlt1 inhibits, BMP-2-induced bone formation and bone healing through modulation of angiogenesis. *The Journal of Bone and Mineral Research*. 20(11), pp 2017-27.
- Petite, H., Viateau, V., Bensaid, W. et al., 2000. Tissue-engineered bone regeneration. *Nature Biotechnology*. 18(9), pp 959-63.
- Phillips, J.L., Hayward, S.W., Wang, Y. et al., 2001. The consequences of chromosomal aneuploidy on gene expression profiles in a cell line model for prostate carcinogenesis. *Cancer Research*. 61(22), pp 8143-9.
- Phinney, D.G., Kopen, G., Isaacson, R.L. et al., 1999. Plastic adherent stromal cells from the bone marrow of commonly used strains of inbred mice: variations in yield, growth, and differentiation. *Journal of Cellular Biochemistry*. 72(4), pp 570-85.
- Pierschbacher, M.D. and Ruoslahti, E. 1984. Cell attachment activity of fibronectin can be duplicated by small synthetic fragments of the molecule. *Nature*. 309(5963), pp 30-3.
- Pittenger, M.F., Mackay, A.M., Beck, S.C. et al., 1999. Multilineage potential of adult human mesenchymal stem cells. *Science*. 284(5411), pp 143-7.
- Posner, A.S. 1969. Crystal chemistry of bone mineral. *Physiological Reviews*. 49(4), pp 760-92.
- Preece A. 1972. *Manual for histologic technicians*. 3rd Ed. Boston, MA: Little Brown and Co., 1972.

- Purpura, K.A., Aubin, J.E. and Zandstra, P.W. 2003. Two-color image analysis discriminates between mineralized and unmineralized bone nodules in vitro. *Biotechniques*. 34(6), pp 1188-92.
- Purpura, K.A., Zandstra, P.W. and Aubin, J.E. 2003. Fluorescence activated cell sorting reveals heterogeneous and cell non-autonomous osteoprogenitor differentiation in fetal rat calvaria cell populations. *Journal of Cellular Biochemistry*. 90(1), pp 109-20.
- Purton, L.E., Mielcarek, M. and Torok-Storb, B. 1998. Monocytes are the likely candidate 'stromal' cell in G-CSF-mobilized peripheral blood. *Bone Marrow Transplantation*. 21(10), pp 1075-6.
- Rago, R., Mitchen, J. and Wilding, G. 1990. DNA fluorometric assay in 96-well tissue culture plates using Hoechst 33258 after cell lysis by freezing in distilled water. *Analytical Biochemistry*. 191(1), pp 31-4.
- Ramsey, W.S., Hertl, W., Nowlan, E.D. et al., 1984. Surface treatments and cell attachment. *In Vitro* 20(10), pp 802-8.
- Rao, J. and Otto, W.R. 1992. Fluorometric DNA assay for cell growth estimation. *Analytical Biochemistry*. 207(1), pp 186-92.
- Rasmusson, I., Ringden, O., Sundberg, B. et al., 2003. Mesenchymal stem cells inhibit the formation of cytotoxic T lymphocytes, but not activated cytotoxic T lymphocytes or natural killer cells. *Transplantation*. 76(8), pp 1208-13.
- Real, C., Glavieux-Pardanaud, C., Le Douarin, N.M. et al., 2006. Clonally cultured differentiated pigment cells can dedifferentiate and generate multipotent progenitors with self-renewing potential. *Developmental Biology*. 300, pp 656-69.
- Reddy, R.L. 2005. Mobilization and collection of peripheral blood progenitor cells for transplantation. *Transfusion and Apheresis Science*. 32(1), pp 63-72.

- Reyes, M., Dudek, A., Jahagirdar, B. et al., 2002. Origin of endothelial progenitors in human postnatal bone marrow. *Journal of Clinical Investigation*. 109(3), pp 337-46.
- Richards, M., Huibregtse, B.A., Caplan, A.I. et al., 1999. Marrow-derived progenitor cell injections enhance new bone formation during distraction. *Journal of Orthopaedic Research*. 17(6), pp 900-8.
- Ripamonti, U. 1996. Osteoinduction in porous hydroxyapatite implanted in heterotopic sites of different animal models. *Biomaterials*. 17(1), pp 31-5.
- Roberts, P., Chan, D., Grimer, R.J. et al., 1991. Prosthetic replacement of the distal femur for primary bone tumours. *Journal of Bone and Joint Surgery (Br)*. 73(5), pp 762-9.
- Rochefort, G.Y., Delome, B., Lopez, A. et al., 2006. Multipotential mesenchymal stem cells are mobilized into peripheral blood by hypoxia. *Stem Cells*. 24(10), pp 2202-8.
- Rodriguez, A.M., Elabd, C., Delteil, F. et al., 2004. Adipocyte differentiation of multipotent cell established from human adipose tissue. *Biochemical and Biophysical Research Communications*. 315(2), pp 255-63.
- Rogers, A.B., Cormier, K.S. and Fox, J.G. 2006. Thiol-reactive compounds prevent non-specific antibody binding in immunohistochemistry. *Laboratory Investigation*. 86, pp 526-33.
- Rougraff, B.T., Simon, M.A., Kneisl, J.S. et al., 1994. Limb salvage compared with amputation for osteosarcoma of the distal end of the femur. A long-term oncological, functional, and quality-of-life study. *Journal of Bone and Joint Surgery (Am)*. 76(5), pp 649-56.
- Roy, R.G., Markel, M.D., Lipowitz, A.J. et al., 1993. Effect of homologous fibrin adhesive on callus formation and extracortical bone bridging around a porous-coated segmental endoprosthesis in dogs. *American Journal of Veterinary Research*. 54(7), pp 1188-96.
- Ruiz de Almodovar, C., Luttun, A. and Carmeliet, P. 2006. An SDF-1 trap for myeloid cells stimulates angiogenesis. 2006. *Cells*. 124(1), pp 18-21.

- Rust, P.A. 2004. *Human Mesenchymal Stem Cells for Tissue Engineering of Bone*. [MD thesis]. London, UK: University of London. pp 1-298.
- Ryden, M., Dicker, R., Gotherstrom, C. et al., 2003. Functional characterization of human mesenchymal stem cell-derived adipocytes. *Biochemical and Biophysical Research Communications*. 311(2), pp 391-7.
- Sanes, J.R., Engvall, E., Butkowski, R. et al., 1990. Molecular heterogeneity of basal laminae: isoforms of laminin and collagen IV at the neuromuscular junction and elsewhere. *The Journal of Cell Biology*. 111(4), pp 1685-99.
- Scales, J.T., Wait, M.E. and Wright, K.W. 1984. Intramedullary fixation of 'custom-made' major endoprostheses with special reference to the bone response. *Engineering in Medicine*. 13(4), pp 185-9.
- Schecroun, N. and Delloye, C. 2003. Bone-like nodules formed by human bone marrow stromal cells: comparative study and characterization. *Bone*. 32(3), pp 252-60.
- Schindler, O.S., Cannon, S.R., Briggs, T.W. et al., 1997. Stanmore custom-made extendible distal femoral replacements. Clinical experience in children with primary malignant bone tumours. *Journal of Bone and Joint Surgery (Br)*. 79(6), pp 927-37.
- Schmoekel, H.G., Weber, F.E., Schense, J.C. et al., 2005. Bone repair with a form of BMP-2 engineered for incorporation into fibrin cell ingrowth matrices. *Biotechnology and Bioengineering*. 89(3), pp 253-62.
- Scholz, W.K. 2003. Cell adhesion and growth on coated or modified glass or plastic surfaces. Nunc Bulletin, number 13.
- Schwarz, N., Redl, H., Zeng, L. et al., 1993. Early osseointegration in rats is not altered by fibrin sealant. *Clinical Orthopaedics and Related Research*. 293, pp 353-9.

- Sekhar, R.V., Culbert, S., Hoots, W.K. et al., 2001. Severe osteopenia in a young boy with Kostmann's congenital neutropenia treated with granulocyte colony-stimulating factor: suggested therapeutic approach. *Pediatrics*. 108(3), pp E54.
- Semerad, C.L., Christopher, M.J., Liu, F. et al., 2005. G-CSF potently inhibits osteoblast activity and CXCL12 mRNA expression in the bone marrow. *Blood*. 106(9), pp 3020-7.
- Shang, Q., Wang, Z., Liu, W., et al., 2001. Tissue-engineered bone repair of sheep cranial defects with autologous bone marrow stromal cells. *The Journal of Craniofacial Surgery*. 12(6), pp 586-93.
- Shenfield, F. 2005. Semantics and ethics of human embryonic stem-cell research. *Lancet*. 365(9477), pp 2071-3.
- Sim, F.H. and Chao, E.Y.S. 1979a. Prosthetic replacement of the knee and a large segment of the femur or tibia. *Journal of Bone and Joint Surgery (Am)*. 61(6A), pp 887-92.
- Sim, F.H., Pritchard, D.J., Ivins, J.C. et al., 1979b. Total joint arthroplasty. Applications in the management of bone tumors. *Mayo Clinic Proceedings*. 54(9), pp 583-9.
- Simmons, C.A., Nikolovski, J., Thornton, A.J. et al., 2004. Mechanical stimulation and mitogen-activated protein kinase signalling independently regulate osteogenic differentiation and mineralization by calcifying vascular cells. *Journal of Biomechanics*. 37(10), pp 1531-41.
- Sinanan, A.C., Hunt, N.P. and Lewis, M.P. 2004. Human adult craniofacial muscle-derived cells: neural-cell adhesion-molecule (NCAM; CD56)-expressing cells appear to contain multipotential stem cells. *Biotechnology and Applied Biochemistry*. 40(Pt 1), pp 25-34.
- Sinclair, E., Hanley, M.B., Carroll, P. et al., 2000. Rapid turnover of bone marrow in both HIV-1 infected and uninfected individuals. *7th Conference of Retroviral Opportunistic Infections, San Francisco, CA, USA, Jan 30-Feb 2*.

- Sotiropoulou, P.A., Perez, S.A., Salagianni, M. et al., 2006. Characterization of the optimal culture conditions for clinical scale production of human mesenchymal stem cells. *Stem Cells*. 24(2), pp 462-71.
- Spotnitz, W.D., Dalton, M.S., Baker, J.W. et al., 1987. Reduction of perioperative hemorrhage by anterior mediastinal spray application of fibrin glue during cardiac operations. *The Annals of Thoracic Surgery*. 44(5), pp 529-31.
- Steinwender, C., Hofmann, R., Kammler, J., et al., 2006. Effects of peripheral blood stem cell mobilization with granulocyte-colony stimulating factor and their transcatheter transplantation after primary stent implantation for acute myocardial infarction. *American Heart Journal*. 151(6), pp 1296.
- Stevens, M.M., Marini, R.P., Schaefer, D. et al., 2005. In vivo engineering of organs: the bone bioreactor. *Proceedings of the National Academy of Sciences USA*. 102(32), pp 11450-5.
- Still, K., Reading, L. and Scutt, A. 2003. Effects of phenol red on CFU-f differentiation and formation. *Calcified Tissue International*. 73(2), pp 173-9.
- Street, J., Winter, D., Wang, J.H. et al., 2000. Is human fracture hematoma inherently angiogenic? *Clinical Orthopaedics and Related Research*. 378, pp 224-37.
- Stuckey, D.J., Carr, C.A., Martin-Rendon, E. et al., 2006. Iron particles for non-invasive monitoring of bone marrow stromal cell engraftment into, and isolation of viable engrafted donor cells from, the heart. *Stem Cells*. 24(8), pp 1968-75.
- Sugarbaker, P.H., Barofsky, I., Rosenberg, S.A. et al., 1982. Quality of life assessment of patients in extremity sarcoma clinical trials. *Surgery*. 91(1), pp 17-23.
- Sugimoto, C., Fujieda, S., Sunaga, H. et al., 2001. Granulocyte colony-stimulating factor (G-CSF)-mediated signalling regulates types IV collagenase activity in head and neck cancer cells. *International Journal of Cancer*. 93(1), pp 42-6.

- Taichman, R.S. and Emerson, S.G. 1998. The role of osteoblasts in the hematopoietic microenvironment. *Stem Cells*. 16(1), pp 7-15.
- Takagi, Y., Yoshiyama, M., Omura, T. et al., 2005. Effects of granulocyte-colony stimulating factor on cardiac remodelling after myocardial infarction. *Osaka City Medical Journal*. 51(2), pp 43-50.
- Takahashi, T., Kalka, C., Masuda, H. et al., 1999. Ischemia- and cytokine-induced mobilization of bone marrow-derived endothelial progenitor cells for neovascularization. *Nature Medicine*. 5(4), pp 434-8.
- Takata, T., Wang, H.L. and Miyauchi, M. 2001. Migration of osteoblastic cells on various guided bone regeneration membranes. *Clinical Oral Implants Research*. 12(4), pp 332-8.
- Takeyama, K. and Ohto, H. 2004. PBSC mobilization. *Transfusion and Apheresis Science*. 31(3), pp 233-43.
- Taléns-Visconti, R., Bonora, A., Jover, R. et al., 2007. Human mesenchymal stem cells from adipose tissue: Differentiation into hepatic lineage. *Toxicology in Vitro*. 21, pp 324-29.
- Tang, Y.L., Zhao, Q., Qin, X. et al., 2005. Paracrine action enhances the effects of autologous mesenchymal stem cell transplantation on vascular regeneration in rat model of myocardial infarction. *The Annals of Thoracic Surgery*. 80(1), pp 229-36.
- Tanzer, M., Turcotte, R., Harvey, E. et al., 2003. Extracortical bone bridging in tumor endoprostheses: Radiographic and Histologic Analysis. *Journal of Bone and Joint Surgery (Am)*. 85-A(12), pp 2365-70.
- Taylor, S.J., Perry, J.S., Meswania, J.M. et al., 1997. Telemetry of forces from proximal femoral replacements and relevance to fixation. *Journal of Biomechanics*. 30(3), pp 225-34.
- Terada, N., Hamazaki, T., Oka, M. et al., 2002. Bone marrow cells adopt the phenotype of other cells by spontaneous cell fusion. *Nature*. 416(6880), pp 542-5.

- Thomson, J.A., Itskovitz-Eldor, J., Shapiro, S.S. et al., 1998. Embryonic stem cell lines derived from human blastocysts. *Science*. 282(5395), pp 1827.
- Till, J.E. and McCulloch, E.A. 1980. Hematopoietic stem cell differentiation. *Biochimica et Biophysica Acta*. 605(4), pp 431-59.
- Ting, V., Sims, C.D., Brecht, L.E. et al., 1998. In vitro prefabrication of human cartilage shapes using fibrin glue and human chondrocytes. *Annals Plastic Surgery*. 40(4), pp 413-20.
- Tondreau, T., Meuleman, N., Delforge, A. et al., 2005. Mesenchymal stem cells derived from CD133-positive cells in mobilized peripheral blood and cord blood: proliferation, Oct4 expression, and plasticity. *Stem Cells*. 23(8), pp 1105-12.
- Troyer, D.L., Weiss, M.L., Mitchell, K.E. et al., 2003. Incorporation of bovine bone marrow cells into porcine foetal tissues after xenotransplantation. *Anatomia, Histologia, Embryologia*. 31(3), pp 129-31.
- Tse, W.T., Pendleton, J.D., Beyer, W.M. et al., 2003. Suppression of allogeneic T-cell proliferation by human marrow stromal cells: implications in transplantation. *Transplantation*. 75(3), pp 389-97.
- Tsuchida, H., Hashimoto, J., Crawford, E. et al., 2003. Engineered allogeneic mesenchymal stem cells repair femoral segmental defect in rats. *Journal of Orthopaedic Research*. 21(1), pp 44-53.
- Tsuruga, E., Takita, H., Itoh, H., Wakisaka, Y., Kuboki, Y. Pore size of porous hydroxyapatite as the cell-substratum controls BMP-induced osteogenesis. *Journal of Biochemistry (Tokyo)*. 121(2), 317-24.
- Tzukerman, M., Rosenberg, T., Ravel, Y. et al., 2003. An experimental platform for studying growth and invasiveness of tumor cells within teratomas derived from human embryonic stem cells. *Proceedings of the National Academy of Sciences USA*. 100(23), pp 13507-12.

- Uchida, A., Myoui, A., Araki, N. et al., 1997. Neoadjuvant chemotherapy for pediatric osteosarcoma patients. *Cancer*. 79(2), pp 411-15.
- Unwin, P., Cannon, S., Carter, S. et al., 2005. The 10 Year Follow-Up of Hydroxyapatite Coated Collared Distal Femoral Replacements. *13th International Symposium on Limb Salvage, Seoul, Korea*. Sept. 7-10, pp 137.
- Unwin, P.S., Cobb, J.P. and Walker, P.S. 1991. Loosening in cemented femoral prostheses A study of 668 tumour cases. *Complications of limb salvage: Prevention, management and outcome. I.S.O.L.S. Meeting, Montreal, Canada*, pp 133-137.
- Unwin P.S., Walker P.S., Blunn G.W., 1995. A radiographic and retrieval study, comparing porous collared and hydroxyapatite coated segmental femoral replacements. *41st Annual Meeting of the Orthopaedic Research Society, Orlando, Florida*. Feb. 13-16.
- Unwin, P.S., Cannon, S.R., Grimer, R.J. et al., 1996. Aseptic loosening in cemented custom-made prosthetic replacements for bone tumours of the lower limb. *Journal of Bone and Joint Surgery (Br)*. 78(1), pp 5-13.
- Unwin, P.S. and Walker, P.S. 1996. Extendible endoprotheses for the skeletally immature. *Clinical Orthopaedics and Related Research*. 322, pp 179-93.
- Vacanti, J.P. and Vacanti, C.A. 2000. The history and scope of tissue engineering. In: *Principles of Tissue Engineering, 2nd Edition*, eds. Lanza, R.P., Langer, R. and Vacanti, J. London, UK: Academic Press, 2000, pp 3-7.
- Vacanti, V., Kong, E., Suzuki, G. et al., 2005. Phenotypic changes of adult porcine mesenchymal stem cells induced by prolonged passaging in culture. *Journal of Cellular Physiology*. 205(2), pp 194-201.
- van der Vis H., Aspenberg, P., de Kleine, R. et al., 1998. Short periods of oscillating fluid pressure directed at titanium-bone interface in rabbits lead to bone lysis. *Acta Orthopaedica Scandinavica*. 69(1), pp 5-10.

Vats, A., Tolley, N.S., Buttery, L.D. et al., 2004. The stem cell in orthopaedic surgery. *Journal of Bone and Joint Surgery (Br)*. 86(2), pp 159-64.

Velders, G.A. and Fibbe, W.E. 2005. Involvement of proteases in cytokine-induced hematopoietic stem cell mobilization. *Annals of New York Academy of Sciences*. 1044, pp 60-9.

Verfaillie, C. and Jiang, Y. 2006. Errata - Multipotent progenitor cells can be isolated from postnatal murine bone marrow, muscle, and brain. *Experimental Hematology*. 34(6), pp 809.

Voet, D. and Voet, J. 1995. *Biochemistry, Second Edition*. Toronto, ON, Canada: John Wiley & Sons, Inc. 2000, pp. 1-1361.

Volk, S.W., Diefenderfer, D.L., Christopher, S.A. et al. 2005. Effects of osteogenic inducers on cultures of canine mesenchymal stem cells. *American Journal of Veterinary Research*. 66(10), pp 1729-37.

Wakabayashi, R.C., Iha, D.K., Niu, J.J. et al., 1997. Cytokine production by cells adherent to regenerative membranes. *Journal of Periodontal Research*. 32(2), pp 215-24.

Wakasugi, S., Noguti, A., Katuda, T. et al., 2002. Potential of ^{99m}Tc-MIBI for detecting bone marrow metastases. *The Journal of Nuclear Medicine*. 43(5), pp 596-602.

Walker, P.S., Greene, D., Reilly, D. et al., 1981. Fixation of tibial components of knee prostheses. *Journal of Bone and Joint Surgery (Am)*. 63(2), pp 258-67.

Wan, C., He, Q. and Li, G. 2006. Allogenic peripheral blood derived mesenchymal stem cells (MSCs) enhance bone regeneration in rabbit ulna critical-sized bone defect model. *Journal of Orthopaedic Research*. 24(4), pp 610-8.

Wang, X., Willenbring, H., Akkari, Y. et al., 2003. Cell fusion is the principal source of bone-marrow-derived hepatocytes. *Nature*. 422(6934), pp 897-901.

- Wang, Y., Huso, D.L., Harrington, J. et al., 2005. Outgrowth of a transformed cell population derived from normal human BM mesenchymal stem cell culture. *Cytotherapy* 7(6), pp 509-19.
- Wang, Y., Li, Y., Mao, K. et al., 2003. Alcohol-induced adipogenesis in bone and marrow: a possible mechanism for osteonecrosis. *Clinical Orthopaedics and Related Research*. 410, pp 213-24.
- Ward, W.G., Eckardt, J.J., Johnston-Jones, K.S. et al., 1991. Five to ten year results of custom endoprosthetic replacement for tumours of distal femur. *Complications of limb salvage: Prevention, management and outcome. I.S.O.L.S. Meeting, Montreal, Canada*. pp 483-91.
- Ward, W.G., Johnston, K.S., Dorey, F.J. et al., 1993. Extramedullary porous coating to prevent diaphyseal osteolysis and radiolucent lines around proximal tibial replacements. A preliminary report. *Journal of Bone and Joint Surgery (Am)*. 75(7), pp 976-87.
- Ward, W.G., Johnston, K.S., Dorey, F.J. et al., 1997. Loosening of massive proximal femoral cemented endoprostheses. Radiographic evidence of loosening mechanism. *The Journal of Arthroplasty*. 12(7), pp 741-50.
- Warnke, P.H., Wiltfang, J., Springer, I. et al., 2006. Man as a living bioreactor: fate of an exogenously prepared customized tissue-engineered mandible. *Biomaterials*. 27(17), pp 3163-7.
- Watt, F.M. and Hogan, B.L. 2000. Out of Eden: stem cells and their niches. *Science*. 287(5457), pp 1427-30.
- Watt, S. 2006. Blueprint of the response of mesenchymal stem cells to hypoxia. *1st UK Mesenchymal Stem Cell Meeting, York, UK, 8th June*.
- Watt, S.M., Buhring, H.J., Rappold, I. et al., 1998. CD164, a novel sialomucin on CD34(+) and erythroid subsets, is located on human chromosome 6q21. *Blood*. 92(3), pp 849-66.

- Watts, M.J., Addison, I., Ings, S.J. et al., 1998. Optimal timing for collection of PBSC after glycosylated G-CSF administration. *Bone Marrow Transplantation*. 21(4), pp 365-8.
- Weddington, W.W. Jr., Segraves, K.B. and Simon, M.A. 1985. Psychological outcome of extremity sarcoma survivors undergoing amputation or limb salvage. *Journal of Clinical Oncology*. 3(10), pp 1393-9.
- Williams, C.G., Kim, T.K., Taboas, A. et al., 2003. In vitro chondrogenesis of bone marrow-derived mesenchymal stem cells in photopolymerizing hydrogel. *Tissue Engineering*. 9(4), pp 679-88.
- Wilson, I.H. and Baskett P.J.F, 1992. The Diagnosis and Treatment of Haemorrhagic Shock. *Practical Procedures*. 1, pp 1-2.
- Wojakowski, W., Tendera. M., Zebzda, A. et al., 2006. Mobilization of CD34(+), CD117(+), CXCR4(+), c-met(+) stem cells is correlated with left ventricular ejection fraction and plasma NT-proBNP levels in patients with acute myocardial infarction. *European Heart Journal*. 27(3), pp 283-9.
- Wolff, J. 1892. *Das Gesetz der Transformation der Knochen* (Berlin; Hirschwald); translated as *The Law of Bone Remodeling* (trans. Maquet, P. & Furlong, R.) 1892.
- Wu, X., Ding, S., Ding, Q. et al., 2002. A small molecule with osteogenesis-inducing activity in multipotent mesenchymal progenitor cells. *Journal of the American Chemical Society*. 124(49), pp 14520-1.
- Wulling, M., Delling, G. and Kaiser, E. 2003. The origin of the neoplastic stromal cell in giant cell tumor of bone. *Human Pathology*. 34(10), pp 983-93.
- Yakisan, E., Schirg, E., Zeidler, C., et al., 1997. High incidence of significant bone loss in patients with severe congenital neutropenia (Kostmann's syndrome). *Journal of Pediatrics*. 131(4), pp 592-7.

- Yamada, Y., Boo, J.S., Ozawa, R. et al., 2003. Bone regeneration following injection of mesenchymal stem cells and fibrin glue with a biodegradable scaffold. *Journal of Cranio-Maxillofacial Surgery*. 31(1), pp 27-33.
- Yamanouchi, K., Satomura, K., Gotoh, Y. et al., 2001. Bone formation by transplanted human osteoblasts cultured within collagen sponge with dexamethasone in vitro. *The Journal of Bone and Mineral Research*. 16(5), pp 857-67.
- Yang, L., Tao, T., Wang, X. et al., 2003. Effects of dexamethasone on proliferation, differentiation and apoptosis of adult human osteoblasts in vitro. *Chinese Medicine Journal (England)*. 116(9), pp 1357-60.
- Yang, W., Wu, B., Asakura, S. et al., 2004. Soluble fibrin augments spreading of fibroblasts by providing RGD sequences of fibrinogen in soluble fibrin. *Thrombosis Research*. 114(4), pp 293-300.
- Ye, Q., Zund, G., Jockenhoevel, S. et al., 2000. Scaffold precoating with human autologous extracellular matrix for improved cell attachment in cardiovascular tissue engineering. 2000. *ASAIO J* 46(6), pp 730-3.
- Yin, L., Li, Y.B. and Wang, Y.S. 2006. Dexamethasone-induced adipogenesis in primary bone marrow stromal cell cultures: mechanism of steroid-induced osteonecrosis. *Chinese Medicine Journal (England)*. 119(7), pp 581-8.
- Yoon, J., Min, B.G., Kim, Y.H. et al., 2005. Differentiation, engraftment and functional effects of pre-treated mesenchymal stem cells in a rat myocardial infarct model. *Annals of Hematology*. 84(11), pp 715-21.
- Young, F.E. 2000. A time for restraint. *Science*. 287(5457), pp 1424.
- Yuan, H., Van Den Doel, M., Li, S. et al., 2002. A comparison of the osteoinductive potential of two calcium phosphate ceramics implanted intramuscularly in goats. *Journal of Materials Science: Materials in Medicine*. 13(12), pp 1271-5.

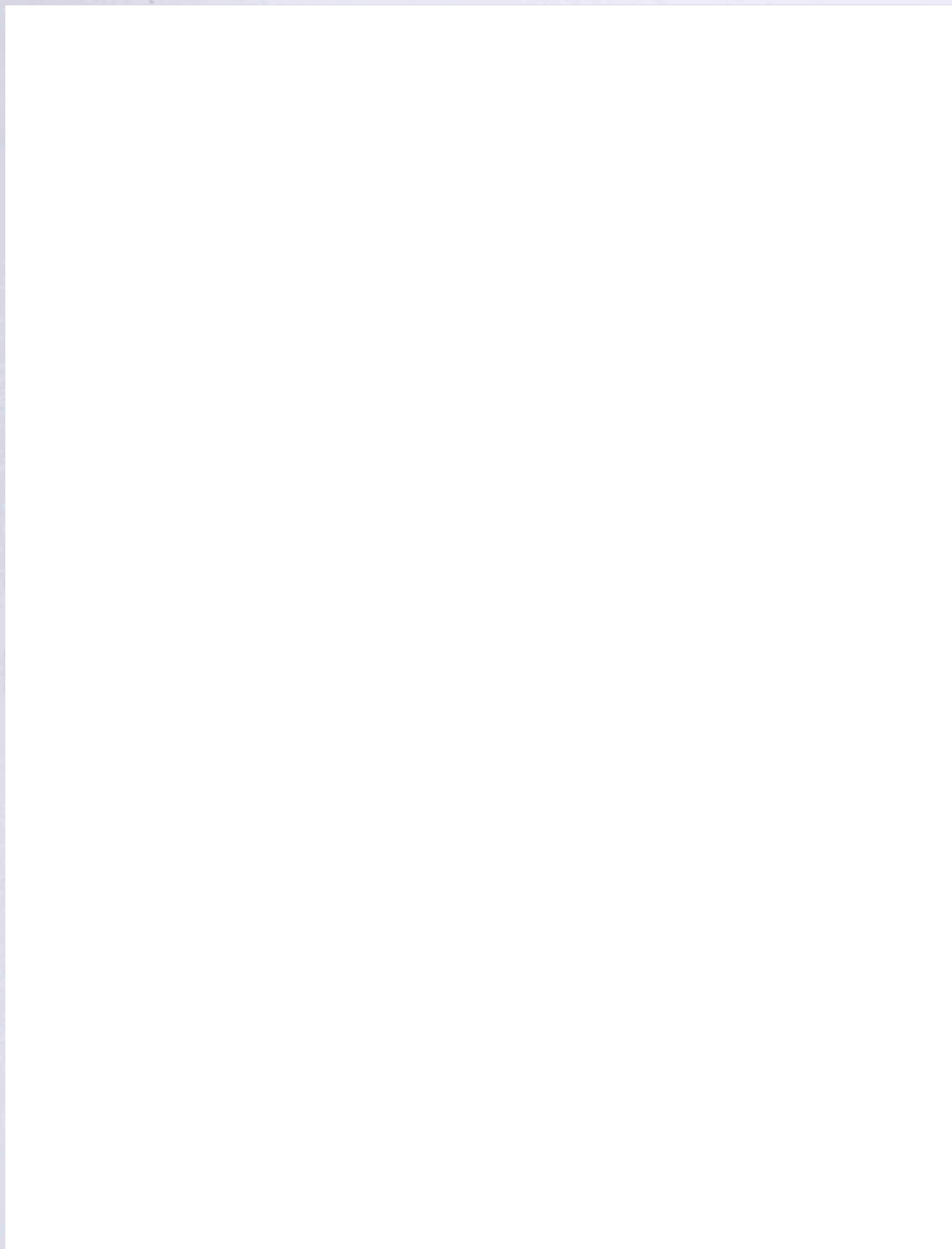
- Yuan, H., Yang, Z., Li, Y. et al., 1998. Osteoinduction by calcium phosphate biomaterials. *Journal of Materials Science: Materials in Medicine*. 9(12), pp 723-6.
- Zandstra, P.W. and Nagy, A. 2001. Stem cell bioengineering. *Annual Review of Biomedical Engineering*. 3, pp 275-305.
- Zannettino, A.C., Buhring, H.J., Niutta, S. et al., 1998. The sialomucin CD164 (MGC-24v) is an adhesive glycoprotein expressed by human hematopoietic progenitors and bone marrow stromal cells that serves as a potent negative regulator of hematopoiesis. *Blood*. 92(8), pp 2613-28.
- Zhim, F., Laflamme, G.Y., Viens, H. et al., 2005. Biomechanical stability of high tibial opening wedge osteotomy: internal fixation versus external fixation. *Clinical Biomechanics (Bristol, Avon)*. 20(8), pp 871-6.
- Zhou, R., Thomas, D.H., Qiao, H. et al., 2005. In vivo detection of stem cells grafted into infarcted rat myocardium. *The Journal of Nuclear Medicine*. 46(5), pp 816-22.
- Zuk, P.A., Zhu, M., Ashjian, P. et al., 2002. Human adipose tissue is a source of multipotent stem cells. *Molecular Biology of the Cell*. 13(12), pp 4279-95.
- Zvaifler, N.J., Marinova-Mutafchieva, L., Adams, G. et al., 2000. Mesenchymal precursor cells in the blood of normal individuals. *Arthritis Research*. 2(6), pp 477-88.

APPENDIX

Publications & Papers

Do Autologous Mesenchymal Stem Cells Augment Bone Growth and Contact to Massive Bone Tumor Implants?

**PRIYA KALIA, B.Sc., GORDON W. BLUNN, Ph.D., JEMIMA MILLER, B.Sc.,
APRAJIT BHALLA, M.D., MICHAEL WISEMAN, Ph.D.,
and MELANIE J. COATHUP, Ph.D.**



Presentation - Orthopaedic Research Society (ORS) Meeting 2005, Washington, D.C., U.S.A.
Mario Boni Prize Winner - European Orthopaedic Research Society (EORS) Meeting 2004
Presentation Prize - British Orthopaedic Research Society (BORS) Meeting 2004

**THE AUGMENTATION OF IMPLANT FIXATION USING MESENCHYMAL
STEM CELLS**

*Kalia, P; Bhalla, A; Coathup, MJ; Miller, J; Goodship AE; Blunn GW

Poster - Orthopaedic Research Society Meeting 2007, San Diego, CA, U.S.A.
Presentation - British Orthopaedic Research Society Meeting 2007, Dundee, Scotland, U.K.

**MOBILIZING MESENCHYMAL STEM CELLS FROM THE BONE MARROW TO THE PERIPHERAL
BLOOD USING GRANULOCYTE-COLONY STIMULATING FACTOR (G-CSF)**

Kalia, P; Singhrao, TK; Coathup, MJ; Gibson, SJ; Blunn, GW

Presentation - British Orthopaedic Research Society Meeting 2007, Dundee, Scotland, U.K.

Sealing the Bone-Implant Interface in Total Hip Arthroplasty Using Bone Marrow Stromal Cells (BMSCs)

P. Kalia, S. Oussedik, S. Konan, M. Dodd, M.J. Coathup, G.W. Blunn